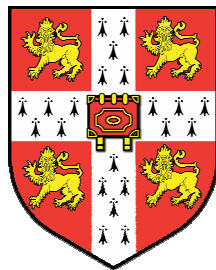


**Murine embryonic stem cells as a route towards exploring
host-pathogen interactions**

**By
Raffaella Rossi**

This dissertation is submitted for the degree of Doctor of Philosophy

September 2008



**Clare Hall College
Cambridge University**



Sanger Institute

Abstract

In the last 20 years embryonic stem (ES) cells have emerged as a new hope for future therapeutic solutions for chronic human diseases such as Alzheimer's, Parkinson's, cancer and cardiovascular disease. They may also pave the way for pharmaceutical drug discovery, minimizing the reliance on animal models. In this study the potential of murine embryonic stem cell technology to probe host-pathogen interactions and infectious diseases is investigated, focusing on the pathogens *Shigella* and *Salmonella* that are able to establish complicated lifestyles within mammalian cells. Murine ES cells were infected independently with *Shigella flexneri* and *Salmonella* Typhimurium and characterized by flow cytometry, microbiology and microscopic observations. It was observed that these pathogens could enter and survive within ES cells in a manner that resembled their interactions with terminally differentiated cells growing in culture. Consequently there is evidence that substantiates the proposal that mouse ES cells could be comparably infected by these bacteria since they also occupied similar intracellular niches. Once the infection protocol was established, the mRNA expression profile of ES cells during infection was investigated, using Affymetrix mouse arrays. The data produced was analyzed by three separate programmes: Bioconductor, GeneSpring and ASCA and they identified a weak immune response. This highlighted the fact that ES cells maintain strict controls on gene expression and that bacterial infection does not induce a characteristic immune response as in specialized cells. Consequently, the potential of ES cells to be differentiated into specific antigen presenting cells like dendritic cell was explored. After differentiation of the ES cells into dendritic cells and their characterization by flow cytometry, the resulting cells were infected with *S.* Typhimurium and purified by FACs sorting in order to perform mRNA expression profiling utilizing Illumina arrays. The expression pattern of surface antigenic markers and the ability of these cells to present antigen and secrete cytokines was also analyzed. The microarray data analysis, cell marker studies and cytokine production profiles emphasized a clear immunological response to bacterial infection in the murine ES derived dendritic cells (esDC). This is the first study of this type performed and further analysis may help to understand both the cell differentiation process and ES cell behavior during infection. In addition, this study revealed the flexibility and the applicability of ES cells as a new *in vitro* model for infectious disease research.

Acknowledgements

Firstly, I would like to thank Professor Gordon Dougan for giving me the opportunity to complete my Ph.D. in his laboratory at the Sanger Institute, for his support and enthusiasm.

I would also like to thank Dr. Hale, Dr. Yu and Dr. Petrovska for their precious experienced tips, to Dr. Lefebvre, Dr. Andrew, Dr. Conesa and Dr. Lynn for helping me with the microarray analyses. A special thank goes to Chris, Linda and Angela for the constructive discussions, suggestions and critical reading of the thesis and to Kat for final proofreading of the thesis and constructive suggestions.

I would like to thank all the members of teams 15 and 100 for keeping the spirit up, the camping trips, the dragon race and evening drinks. I am thankful also to my thesis committee members for suggestions and support. A special thanks goes to all the wonderful people I met during this experience that contributed to making it unforgettable!

A special thank goes to Jim who helped me all through this experience and never doubted that I could do it. His support and positive thinking have been essential.

Un ringraziamento e un pensiero particolare va alla mia famiglia che in questi anni mi ha sostenuto e incoraggiato da lontano e a volte di persona. Il loro supporto e continua fiducia mi hanno aiutato enormemente a raggiungere questo obiettivo.

I would like to dedicate this thesis to my family.

Declaration

I declare that this dissertation is the result of my own work and includes nothing which is the outcome of work done in collaboration, except where specifically indicated in the text.

The gentamicin assays employing wild type *Shigella* were performed in collaboration with Dr. Jun Yu. Guidance with the bone marrow extraction and bone marrow dendritic cells differentiation was provided by Dr. Petrovska. The microarray analyses using Bioconductor were performed by Dr. Lefebvre, Dr. Andrews from the Wellcome Trust Sanger Institute, and the analysis using ASCA was performed by Dr. Conesa from the Centro de Investigación Príncipe Felipe. Synthesis of cDNA, cRNA and hybridizations on Illumina arrays was performed by Peter Ellis from the microarray facility at Wellcome Trust Sanger Institute. Electron microscopy pictures were taken by David Goulding the microscope officer at the Wellcome Trust Sanger Institute.

All the other techniques including tissue cultures, FACS analyses, confocal characterization, Affymetrix hybridization, GeneSpring analysis, RT-PCR, statistical analysis and optimization of invasion protocols were performed by the author.

Raffaella Rossi

September, 2008

Paper

Interaction of Enteric bacteria Pathogens with Murine Embryonic Stem Cells

Jun Yu*ξ, **Raffaella Rossi***, Christine Hale, David Goulding and Gordon Dougan.

Infection and Immunity, Feb. 2009.

Doi:10.1128/IAI.01003-08

Index

1	Introduction.....	19
1.1	General Introduction.....	19
1.2	Host-pathogen interaction.....	21
1.2.1	Infectious diseases today	21
1.2.2	Methods to study host-pathogen interactions	23
1.2.2.1	Historical.....	23
1.2.2.2	The use of genetics	24
1.2.2.3	The use of cell culture.....	25
1.3	<i>Shigella</i>	27
1.3.1	Bacteria and disease.....	27
1.3.2	Mechanism of host invasion	28
1.3.2.1	Type III secretion.....	28
1.3.2.2	Intracellular lifestyle	29
1.4	<i>Salmonella</i>	32
1.4.1	History	32
1.4.2	Bacteria and disease.....	32
1.4.3	Type Three Secretion Systems	33
1.4.4	Mechanism of host invasion	35
1.5	Embryonic stem cells.....	37
1.5.1	History	37
1.5.2	Murine ES cells.....	37
1.5.3	Differentiating ES cells.....	38
1.5.4	ES cell mutants and KO mice	40
1.6	Dendritic Cells	43
1.6.1	What are they?	43
1.6.2	Antigen interaction	44
1.6.3	Antigen processing and presentation by DCs	47
1.6.4	Interaction of DCs with <i>Salmonella</i>	49
1.7	Microarray technology.....	50
1.7.1	Overview.....	50
1.7.2	Microarrays and gene expression	51

1.7.3	Other uses of microarrays	52
1.7.4	Analysis tools.....	53
1.8	Aims of the thesis	55
2	Materials and Methods.....	56
2.1	Materials	56
2.1.1	Bacteria	56
2.1.2	Cell lines	56
2.1.3	Tissue culture.....	57
2.1.4	<i>In vitro</i> infection	58
2.1.5	Flow cytometry	58
2.1.6	Bone marrow extraction materials.....	59
2.1.7	Cytokines	60
2.1.8	Confocal microscopy	60
2.1.9	Antigen presentation assay	60
2.1.10	RNA extraction.....	61
2.1.11	RNA quantification and quality.....	61
2.1.12	Real Time RT-PCR.....	61
2.1.13	Microarrays.....	62
2.1.13.1	Affymetrix array	62
2.1.13.2	Illumina array.....	62
2.1.13.3	Microarray analysis tools.....	63
2.2	Methods	64
2.2.1	<i>In vitro</i> culture of mouse ES cell lines.....	64
2.2.2	<i>In vitro</i> culture of Hep2 and J774A.1 and MF2.2d9.....	64
2.2.3	Bacterial strains.....	65
2.2.3.1	Invasion assay using <i>Shigella flexneri</i>	65
2.2.3.2	Invasion assay with <i>S. Typhimurium</i>	66
2.2.3.3	Viable count analysis or Gentamicin invasion assay.....	67
2.2.4	Flow Cytometric Analyses.....	67
2.2.4.1	<i>In vitro</i> bacterial infection (Gentamicin invasion assay).....	67
2.2.4.2	Murine ES cells characterization	67
2.2.4.3	EsDC and BMDC surface markers.....	68
2.2.4.4	Cell Sorting.....	68
2.2.4.5	Cytometric Bead Array (CBA) Analysis	68

2.2.5	Immunofluorescence labeling.....	69
2.2.5.1	Murine ES cells infected by <i>Shigella flexneri</i> or <i>S. Typhimurium</i>	69
2.2.5.2	EsDC immunofluorescence labeling	69
2.2.6	Total RNA extraction, quantification and Bioanalyzer analysis	70
2.2.7	Affymetrix Microarray	70
2.2.8	Real Time RT-PCR.....	71
2.2.9	Dendritic cell differentiation.....	72
2.2.9.1	Differentiation of murine ES cells into dendritic cells	72
2.2.9.2	Bone marrow extraction and dendritic cells differentiation	72
2.2.9.3	Antigen presentation assay	73
2.2.9.4	Cytometric Bead Array	73
2.2.10	Illumina microarray hybridization	74
3	Characterization of the interaction of <i>S. flexneri</i> and <i>S. Typhimurium</i> with undifferentiated murine embryonic stem cells.....	75
3.1	Introduction.....	75
3.1.1	<i>Salmonella</i> interaction with <i>in vitro</i> models	75
3.2	Results.....	79
3.2.1	The interaction of <i>Shigella flexneri</i> with murine ES cells.....	79
3.2.1.1	The ability of <i>S. flexneri</i> Sh42 to invade Hep2 cells	79
3.2.1.2	Flow Cytometric characterization of AB2.2 murine ES cells	82
3.2.1.3	Gentamicin assay on AB2.2 mouse ES cells exposed to <i>S. flexneri</i> ... 84	
3.2.1.4	Gentamicin assay using wild type <i>S. flexneri</i> M90TS and AB2.2 mouse ES cells	85
3.2.1.5	Flow cytometric analysis of AB2.2 infected by <i>S. flexneri</i>	86
3.2.1.6	Confocal imaging of AB2.2 murine ES cells infected by <i>S. flexneri</i> . 87	
3.2.2	The interaction of <i>S. Typhimurium</i> with murine ES cells	91
3.2.2.1	Gentamicin assay of <i>S. Typhimurium</i> interaction with control J774A.1 cells 91	
3.2.2.2	Flow cytometric analysis of <i>S. Typhimurium</i> infecting mouse J774A.1 cell line 92	
3.2.2.3	Gentamicin assay monitoring the interaction of <i>S. Typhimurium</i> SL1344(p1C/1) with AB2.2 murine ES cells	93
3.2.2.4	Flow cytometric analysis of mouse ES cells infected with <i>S. Typhimurium</i> using a time course of infection.....	94

3.2.2.5	Confocal imaging of <i>S. Typhimurium</i> infecting AB2.2 murine ES cells	97
3.2.3	Role of Type III secretion systems during infection of mouse ES cells	100
3.2.3.1	Gentamicin assay using the <i>S. flexneri mxiD</i> mutant interacting with AB2.2 mouse ES cells	100
3.2.3.2	Gentamicin assay monitoring the levels of invasion of AB2.2 mouse ES cells by a <i>S. Typhimurium sipB</i> mutant	101
3.3	Discussion	102
4	Transcription profiling of murine ES cells infected by <i>S. Typhimurium</i> SL1344	108
4.1	Introduction	108
4.1.1	Microarrays in host-pathogen interactions studies	108
4.2	Experimental design	113
4.3	Results	114
4.3.1	Murine ES cell infection with <i>S. Typhimurium</i> and total RNA extraction	114
4.3.2	Murine ES cell total RNA extraction and analysis	116
4.3.3	cRNA synthesis, labelling and microarray hybridization	118
4.3.4	Microarray data analysis	120
4.3.4.1	Bioconductor analysis	120
4.3.4.1.1	Results from Bioconductor pair-comparison analysis	120
4.3.4.1.2	InnateDB pathways analysis	124
4.3.4.1.3	Real time RT-PCR to confirm Bioconductor analysis	127
4.3.4.1.4	Statistical analysis of RT-PCR data on genes identified by Bioconductor	128
4.3.4.2	GeneSpring analysis	130
4.3.4.2.1	Results from GeneSpring pair-comparison analysis	130
4.3.4.2.2		136
4.3.4.2.3	Gene Ontology analysis of the genes differentially expressed at 4h	136
4.3.4.2.4	Real time RT-PCR to confirm GeneSpring analysis	139
4.3.4.2.5	Statistical analysis of RT-PCR data on genes identified by GeneSpring	140
4.3.4.3	GEPAS: ASCA analysis	141
4.3.4.3.1	Time course analysis using ASCA	141

4.3.4.3.2	Functional category analysis using FatiGO on ASCA results....	148
4.3.4.3.3	Real Time RT-PCR relative quantification on genes derived from ASCA analysis.....	150
4.3.4.3.4	Statistical analysis of RT-PCR data on genes identified by ASCA	151
4.4	Discussion.....	152
5	Procedures for differentiating mouse Embryonic Stem cells into dendritic cell ..	159
5.1	Introduction.....	159
5.1.1	Stem cells and <i>in vitro</i> differentiation.....	159
5.1.2	Dendritic cells and their <i>ex-vivo</i> extraction and research application ..	161
5.2	Results.....	163
5.2.1	Formation of embryoid bodies and differentiation into dendritic cells	163
5.2.2	EsDC characterization by flow cytometric analysis.....	167
5.2.3	Confocal characterization esDCs.....	170
5.2.4	Confocal investigation of esDCs infected with <i>S. Typhimurium</i> SL1344	174
5.2.5	Electron microscopy characterization of esDCs.....	179
5.2.6	Functional assays on esDCs.....	181
5.2.6.1	Cytokine production by esDCs.....	181
5.2.6.2	Antigen presentation assay	183
5.3	Discussion.....	184
6	Messenger RNA expression profile analysis of <i>S. Typhimurium</i> infected esDCs	190
6.1	Introduction.....	190
6.1.1	<i>Salmonella</i> -DC interactions.....	190
6.1.2	Microarray analysis on DCs	191
6.2	Experimental design	194
6.3	Results.....	195
6.3.1	Infection of esDCs by <i>S. Typhimurium</i> SL1344	195
6.3.2	FACS sorting of esDCs infected with <i>S. Typhimurium</i> (p1C/1).....	196
6.3.3	Total RNA extraction, quantification and quality assessment.....	197
6.3.4	cRNA synthesis, labeling and hybridization on Illumina arrays	199
6.3.5	Bioconductor analysis and pathway analysis with InnateDB.....	199
6.3.6	Real time RT-PCR data on genes differentially expressed by esDCs during infection.....	204

6.3.7	Statistical analysis of the RT-PCR data on genes differentially expressed by esDCs during infection	205
6.4	Discussion.....	207
7	Final remarks and future work.....	213
8	Appendix A.....	218
8.1	Affymetrix QC report for Bioconductor analysis.....	218
8.2	Gene Ontology analysis of the top GeneSpring annotated genes.....	220
8.2.1	GO description for cellular component of the top genes deriving from GeneSpring analysis	220
8.2.2	GO description for biological process of the top genes deriving from GeneSpring analysis	221
8.3	Genes analyzed by RT-PCR deriving from ASCA analysis.....	223
9	Appendix B.....	224
9.1	Flow cytometric characterization of murine ES cells AB2.2, esDCs and BMDCs testing the expression of myeloid surface markers.....	224

Figures list

Figure 1.1	<i>Shigella</i> invasion of the gut mucosa	30
Figure 1.2	<i>Salmonella</i> invasion of the gut mucosa	36
Figure 1.3	Genetic manipulation of ES cells and their potential application.....	40
Figure 1.4	Generation of target mutant ES cells	42
Figure 1.5	TLRs and their respective binding products.....	45
Figure 1.6	TLR induced signaling pathways	46
Figure 1.7	Antigen processing and presentation trafficking inside DCs.....	48
Figure 3.1	Bacterial CFUs from gentamicin assay on Hep2 cells with <i>S. flexneri</i> Sh42 at MOI 100.....	80
Figure 3.2	Bacterial CFU counts at 2 and 4h infection of Hep2 with <i>S. flexneri</i> Sh42 harbouring the plasmid pJKD18 (Sh42/18)	81
Figure 3.3	Flow cytometric characterization of AB2.2 murine ES cells	83
Figure 3.4	CFU counts from gentamicin assays performed on AB2.2 with <i>Shigella flexneri</i> Sh42 with and without plasmid pJKD18 at MOI 10 and 100	84
Figure 3.5	CFU counts obtained during a gentamicin assay performed on mouse ES cells AB2.2 using wild type <i>S. flexneri</i> M90TS at MOI 100.....	85
Figure 3.6	Flow cytometric analysis of murine ES AB2.2 cells during infection with <i>S. flexneri</i> Sh42(pJKD18)	86
Figure 3.7	Confocal image of AB2.2 murine ES cells infected with <i>S. flexneri</i> Sh42 (pJKD18) at time point 0	87
Figure 3.8	Confocal image of AB2.2 murine ES cells after 30 minutes infection with <i>S. flexneri</i> Sh42(pJKD18).....	88
Figure 3.9	Confocal image of AB2.2 murine ES cells at 2h infection with <i>S. flexneri</i> Sh42(pJKD18)	89
Figure 3.10	Confocal image of AB2.2 murine ES cells at 2h infection with <i>S. flexneri</i> Sh42(pJKD18)	90
Figure 3.11	Gentamicin assay on mouse J774A.1 cells infected with <i>S. Typhimurium</i> SL1344	91
Figure 3.12	Flow cytometric analysis of murine J774A.1 cells infected with <i>S. Typhimurium</i> SL1344(p1C/1)	92

Figure 3.13	Gentamicin assay of mouse ES cells infected by <i>S. Typhimurium</i> SL1344 with or without the reporter plasmid p1C/1	93
Figure 3.14	Flow cytometric analysis of time course infection of mouse ES cells infected with <i>S. Typhimurium</i> expressing GFP protein	95
Figure 3.15	CFU counts from time course gentamicin assay of <i>S. Typhimurium</i> SL1344 infection of mouse ES cells.....	96
Figure 3.16	Confocal image of AB2.2 cells infected with <i>S. Typhimurium</i> at 30 minutes	97
Figure 3.17	Confocal image of AB2.2 mouse ES cells infected with <i>S. Typhimurium</i> (p1C/1) at 1 h.....	98
Figure 3.18	Confocal image of AB2.2 mouse ES cells infected with <i>S. Typhimurium</i> (p1C/1) at 1 h.....	99
Figure 3.19	Gentamicin assay performed on mouse ES cells using <i>S. flexneri mxiD'</i>	100
Figure 3.20	Levels of <i>S. Typhimurium</i> SL1344 sipB mutant invasion of mouse ES cells AB2.2	101
Figure 4.1	Host-pathogen interactions that can be exploited using microarray technology	112
Figure 4.2	Flow cytometric analysis of murine ES cells infected with <i>S. Typhimurium</i> SL1344.....	115
Figure 4.3	Bioanalyzer analysis of total RNA from infected and uninfected ES cells	117
Figure 4.4	Bioanalyzer analysis of the biotin-labelled cRNA	118
Figure 4.5	RT-PCR results conducted on representative genes identified by the Bioconductor analysis of genes differentially expressed at 4h infection vs. uninfected cells	128
Figure 4.6	Whisker box plot of the RT-PCR results for the Bioconductor-generated differentially expressed genes.....	129
Figure 4.7	Graphical representation of the Gene Ontology analysis for molecular function of genes differentially expressed at 4h.....	138
Figure 4.8	RT-PCR results conducted on a few genes identified by GeneSpring analysis	139
Figure 5.1	Image of a cystic EB.....	164
Figure 5.2	Images of esDCs emerging during differentiation from EBs	165

Figure 5.3	Scheme of the differentiation protocol for transforming murine ES cells into esDCs	166
Figure 5.4	Images of immature esDC stained for the expression of MHC class II	171
Figure 5.5	Confocal image of murine esDC after over night activation with TNF α and stained for MHC II	172
Figure 5.6	Confocal images of esDC incubated with DQ OVA	173
Figure 5.7	Confocal image of esDC infected with <i>S. Typhimurium</i> SL1344 (p1C/1)	175
Figure 5.8	Confocal image of esDC incubated for 3h with <i>S. Typhimurium</i> SL1344 (p1C/1)	176
Figure 5.9	Confocal image of esDCs infected with <i>S. Typhimurium</i> SL1344 (p1C/1)	177
Figure 5.10	Transmission electron microscopic images of undifferentiated murine ES cells AB2.2 and derived esDC during infection with <i>S. Typhimurium</i> SL1344	180
Figure 6.1	FACS analysis of esDCs infected with <i>S. Typhimurium</i> SL1344(p1C/1)	195
Figure 6.2	EsDCs were infected with <i>S. Typhimurium</i> SL1344(p1C/1) and FACS sorted for transcriptome analysis	196
Figure 6.3	Bioanalyzer profile of the total RNA quality extracted from esDCs uninfected and infected with <i>S. Typhimurium</i> SL1344(p1C/1) at 2h and 4h	198
Figure 6.4	Graphical representation of qRT-PCR results	205
Figure 6.5	Whisker-Box plots for RT-PCR results statistical analysis	206
Figure 6.6	This Cytoscape picture represents the IL-12-mediated pathway at 4h.	209
Figure 6.7	Cytoscape representation of the SOCS pathway in esDCs at 4h infection	210
Figure 8.1	Affymetrix QC report	219
Figure 8.2	Pie chart of the GeneSpring data analyzed for GO term Cellular components	221
Figure 9.1	Flow cytometry characterization of murine AB2.2 ES cells	224
Figure 9.2	Murine ES cells characterization for myeloid markers	225
Figure 9.3	Flow cytometric characterization of immature and mature esDCs	226
Figure 9.4	Flow cytometric characterization of immature and mature esDCs, number 2	227
Figure 9.5	Flow cytometric characterization of BMDCs immature and mature	228

Figure 9.6 Flow cytometric characterization of immature and mature BMDCs,
number 2 229

Tables list

Table 2.1	Antibodies for FACS analysis of murine ES and esDC characterization...	59
Table 2.2	Isotype control antibodies for FACS analysis	59
Table 2.3	Antibodies used for confocal analysis	60
Table 2.4	RT-PCR Primers to confirm microarray data from murine ES cells uninfected and infected.....	61
Table 2.5	RT-PCR Primers to confirm microarray data from esDC uninfected and infected	62
Table 4.1	Total RNA concentration of murine ES cells infected by <i>S. Typhimurium</i> (p1C/1) measured with NanoDrop1000 technology.....	116
Table 4.2	Bioconductor analysis of RNA expression profile of murine ES cells at 2h infection	120
Table 4.3	Bioconductor analysis of RNA expression profile of murine ES cells at 4h infection	121
Table 4.4	Bioconductor analysis of RNA expression profile of murine ES cells at 4h infection compared to 2h	122
Table 4.5	InnateDB analysis of genes expressed by murine ES cells at 2h infection with <i>S. Typhimurium</i>	124
Table 4.6	InnateDB pathway analysis of murine ES cells expression profile at 4h infection: up-regulated pathways.....	125
Table 4.7	InnateDB pathway analysis of murine ES cells expression profile at 4h infection: down-regulated pathways.....	125
Table 4.8	InnateDB analysis of genes expressed by murine ES cells at 4h infection with <i>S. Typhimurium</i> compared to 2h: up-regulated pathways.....	126
Table 4.9	InnateDB analysis of genes expressed by murine ES cells at 4h infection with <i>S. Typhimurium</i> compared to 2h: down-regulated pathways.....	126
Table 4.10	GeneSpring analysis of the mRNA expression profile of AB2.2 murine ES cells at 2h infection	131
Table 4.11	GeneSpring analysis of the mRNA expression profile of AB2.2 murine ES cells at 4h infection	132
Table 4.12	GeneSpring analysis of the mRNA expression profile of AB2.2 murine ES cells at 4h vs. 2h infection.....	134

Table 4.13	Gene Ontology results in the molecular-function category for GeneSpring analysis	137
Table 4.14	Gene list derived from ASCA analysis of the genes up-regulated during infection	143
Table 4.15	Gene list derived from ASCA analysis of genes down-regulated during infection	145
Table 4.16	FatiGO analysis of up-regulated genes from ASCA analysis.....	148
Table 4.17	FatiGO analysis of down-regulated genes from ASCA analysis.....	149
Table 5.1	Flow cytometric analysis of surface markers of AB2.2 murine ES cells, esDC and BMDC, immature and matured with LPS, OVA and TNF α	169
Table 5.2	The levels in pg/ml of cytokines produced by AB2.2 murine ES cells and esDCs infected and uninfected with <i>S. Typhimurium</i> SL1344.	181
Table 5.3	Cytokine production by esDCs and BMDCs activated with <i>S. Typhimurium</i> LPS 10 μ g/ml, OVA protein 10 μ g/ml or TNF α 5000 WHOSU/ml.....	182
Table 5.4	Cytokine production by esDCs and BMDCs during antigen presentation assay	182
Table 5.5	IL-2 production by T cells activated during antigen presentation assays involving BMDCs and esDCs.....	183
Table 6.1	Total RNA concentration from esDC uninfected and infected with <i>S. Typhimurium</i> SL1344(p1C/1)	197
Table 8.1	GeneSpring data analyzed for GO term Cellular component.....	220
Table 8.2	GeneSpring pear-comparison data analyzed for GO term Biological Process	221
Table 8.3	Table Gene resulting from ASCA analysis which expression was confirmed by RT-PCR	223

Abbreviations

Ab : Antibody

Ag : Antigen

APC: Antigen Presentation Cell

Amp: Ampicillin

BM: Bone Marrow

BMDC: Bone Marrow derived Dendritic Cells

BSA : Bovine Serum Albumin

CBA: Cytometric Bead Array

CD: Cluster of Differentiation

ConA: Concanavalin A

Ct: Treshold Cycle

DC: Dendritic Cell

DMEM: Dulbecco's Modified Eagle's Medium

ECACC: European Collection of Cell Cultures

ES: Embryonic Stem

esDC: Embryonic stem cells derived Dendritic cell

FCS : Fetal Calf/Bovine Serum

FITC: Fluorescein isothiocyanate

GFP: Green Fluorescent Protein

GM-CSF : Granulocyte/Macrophage-Colony Stimulating Factor

HI-FBS: Heat Inactivated Foetal Bovine Serum

IL: Interleukin

IMDM: Iscove's modified Dulbecco's Medium

M&M: Materials and Methods

LB: Luria Bertani

LIF : Leukemia Inhibitory Factor

LPS: Lipopolysaccharide

MHC: Major Histocompatibility Complex

MOI: Multiplicity of Infection

OD: Optical Density

OVA : Ovalbumin

PAMP: Pathogen-Associated Molecular Pattern

PRR: Pattern Recognition Receptor

PBS: Phosphate Buffered Saline

PE: Phycoerythrin

QC: Quality Control

RT: Room Temperature

RT-PCR: Real Time Polymerase Chain Reaction

S. Typhimurium: *Salmonella enterica* serovar Typhimurium

SPI: Salmonella Pathogenic Island

TISS: Type Three Secretion System

TLR: Toll Like Receptor

TNF α : Tumor Necrosis Factor alpha

WTSI : Wellcome Trust Sanger Institute

WHOSU: World Health Organization Standard Units

1 Introduction

1.1 General Introduction

The Enterobacteriaceae form a large family of rod-shaped, facultative anaerobic, Gram-negative bacteria that are able to ferment sugars to produce lactic acid. Members of the Enterobacteriaceae are found in water, soil and in the gut flora of humans and animals. They include several renowned pathogens such as *Salmonella* and *Shigella* as well as opportunistic commensals such as *Escherichia coli*. Infections associated with the Enterobacteriaceae can be caused by endogenous bacteria that are normally part of the intestinal flora (commensals or opportunistic pathogens) or by exogenous bacteria derived from the environment. In many cases enterobacteria are associated with nosocomial infections that are acquired in hospital. For example, pneumonia, ear, sinus and urinary tract infections can be caused by *Klebsiella* and *Proteus* whereas bacteraemia can be caused by *Enterobacter* and *Serratia*. Enterobacteria-associated diarrhoea is a common problem and can range from minor nuisance to a life-threatening disorder especially in infants, the elderly, HIV infected patients and malnourished persons. The economic and health burdens exerted by enteric disease is enormous, although the exact amount is difficult to estimate (WHO, 2002). Enterobacteriaceae are found worldwide and are one of the leading killers of children in developing countries (Frey, 2002). For this reason it is important to understand the mechanisms of infection employed by these pathogens in order to design better control methods and therapies.

The enteric bacteria have evolved subtle mechanisms for interacting with the tissues of their hosts. For example, they can adhere to or invade eukaryotic cells via specific receptors found on the target cells. Some enteric bacteria harbour novel gene loci that express specific virulence associated factors that can be utilised during infection. Toxins can be produced to disrupt normal cellular processes. Consequently pathogenic enterobacteria can, ironically, be used as powerful probes to explore eukaryotic cell function. Historically, cellular studies on pathogenic bacteria have focused on the use of terminally differentiated cells adapted to long term survival in tissue culture. Some work has also focused on primary cells obtained directly from the host. Both these approaches have proved to be extremely productive and informative. However recent

work on pluripotent stem cells has shown their versatility as tools to explore biology but little has been done with these cells in terms of exploring pathogen interactions.

One of the aims of this project was to initiate studies on interactions between pathogens and murine stem cells with a view to gauging their potential as research tools.

1.2 Host-pathogen interaction

1.2.1 Infectious diseases today

The presence of infectious disease in our society is a sentinel of civilization (Gershon, 2000) and humanity has made great progress in the knowledge and defeat of transmitted disease. However in the world today, with an increasing number of people able to move easily from one continent to another together with the ability of the pioneers to reach unexplored ecosystems, society is facing increasing challenges from fast-tracking diseases and new potential pathogens. Technological progress has not completely eliminated the risk of disease transmitted from live stock animals which are nowadays often exchanged between countries and the emergence of zoonotic disease is still a front row factor in today's battle against infectious disease. For example in 1989 a new influenza strain (H3N2) was isolated in China and within 16 months was reported in Europe and North America (Meslin *et al.*, 1998). Moreover new technology can bring potential new sources of infection, for example xeno-transplantation practice could induce transmission of infectious agents originating in animals to human recipients (Domenech *et al.*, 2006). It may be possible to find a common denominator to these problems: globalization, a process bringing challenges to both industrialized and developing countries. Currently sanitary and phyto-sanitary control measures are a high priority in intercontinental travelling as well as in international trade. However it is not possible to reach a global high standard of precautionary measures, especially in developing countries where populations are still facing high rates of death from diseases commonly cured in industrialized countries. In fact more than 90% of the deaths from infectious diseases are caused by a few widely spread infections: lower respiratory infections, human immunodeficiency virus (HIV), diarrhoeal diseases, tuberculosis, malaria and measles (Coloma & Harris, 2008). In 2008 malaria, measles, lower respiratory infections and diarrhoeal illness are still causes of high mortality in infants and children in developing countries (Kaler, 2008). Malaria is an anopheline mosquito-borne parasitic disease; the most acute form is due to *Plasmodium falciparum*. The common symptoms of this disease are high fever, chill, vomiting and severe headache. A global estimation of 300 to 500 million clinical cases per year with more than 1 million paediatric deaths per year makes this disease one of the principal health

concerns. Measles is caused by a negative-strand RNA virus, specifically a *paramyxovirus* of the genus *morbillivirus*. The virus is transmitted by aerosol through the respiratory tract and induces high fever, cough, runny nose, conjunctivitis and characteristic skin rash. Measles represents one of the principal causes of vaccine-preventable childhood mortality and after a vaccination campaign measles deaths in Africa dropped by 60% in 2005 from 873,000 to 345,000 (UNICEF, 2005). Pneumonia is an acute lower respiratory tract infection caused by bacteria such as *Streptococcus pneumoniae*, several viruses or even fungi (Nascimento-Carvalho *et al.*, 2008). In children the majority of deaths occur in the newborn with about 1.6 million deaths in infants and children per year, of which 90% occur in developing countries. Many of the deaths caused by *S. pneumoniae* are 'vaccine preventable' and a clinical trial using a conjugated vaccine against 13 serotypes demonstrated an efficacy of between 50-80% of all paediatric deaths (Kaler, 2008). Diarrhoeal infections are caused by ingestion of virus, bacteria or parasites present in the water or food. Infection can spread easily into the population through contaminated utensils, hands or vectors such as flies. About 1.8 million children younger than 5 years die of diarrhoeal infections annually. Here, vaccination can have an impact but these are not available for some of the more common forms of diarrhoeal infection. Consequently, vaccines cannot substitute for the preventive practice of providing drinkable water to the population and following proper hygiene procedures (Kaler, 2008).

The incidence of these high burden diseases is enhanced by malnutrition, particularly associated with anaemia, and the spread of HIV (Pasquali, 2004). In Africa, the years of HIV pandemic have been superimposed on an enduring malaria pandemic. In Eastern and Southern Africa nearly 30% of the population is affected by the HIV virus and it is estimated that almost a quarter of clinical malaria occurs in HIV infected adults. HIV infection increases the incidence and severity of clinical malaria, however malaria seems to slow the effects of HIV. The enhancement and the interference of different combinations of infection is still under investigation and requires more emphasis (UNICEF, 2003). In developed countries many infectious diseases have been controlled or nearly eliminated as the main cause of mortality by the use of vaccines. Although vaccines have proved to be efficacious in the battle to control infectious disease the vaccine sector represents less than 2% of the world wide pharmaceutical market

(Editorial, 2008). Less than 10% of global applied research funding is directed to investigating the diseases that affect 90% of the population (Abbasi, 2001).

Projections for 2002 to 2030 predict that the risk of death in children younger than 5 years will fall by only 50% and global deaths due to HIV will rise from 2.8 million in 2002 to 6.5 million in 2030 (assuming that antiviral drug coverage will reach 80% by 2012). In an optimistic scenario, which takes into consideration improved preventive measures, HIV deaths are projected to increase to 3.7 million in 2030 (Mathers & Loncar, 2006). Taken together, these sorts of statistics highlight the requirement for more focused and effective research in this area.

1.2.2 Methods to study host-pathogen interactions

1.2.2.1 Historical

Koch's postulates are famous as a pioneering vision into infectious diseases. In 1890 Koch had already recognized the importance of the host as a key part of the pathogen survival, reproduction and persistence (Walker *et al.*, 2006). After all, there is no pathogen without a host. One of the first attempts to develop *in vitro* techniques to examine host/pathogen interactions was made in 1902 by the German botanist Haberlandt. He advanced the idea of cultivating artificial embryos from vegetative cells and demonstrated the totipotency of plant cells to produce a whole new plant. Haberlandt reported for the first time the *in vitro* culture of isolated palisade cells, pith cells, stamen hairs and stomatal guard cells in enriched medium containing glucose (Werbrouck *et al.*, 1998). However in his efforts to demonstrate totipotency the cells grown under these conditions did not divide but they did survive for a few weeks. In 1934, White was the first to obtain indefinite cultures with plant roots but Bonner in 1937 discovered that yeast extract components were fundamental to cell survival (Werbrouck *et al.*, 1998). Pioneering work on animal cells was done by Walther Flemming in the late 19th century and he initiated the science of cytology (Singer, 1989). The major contribution of *in vitro* culture of animal cells to infectious diseases has been to enable the growth of infectious agents that can't grow on agar or broth (Buehring, 1996). Animal cell culture, now referred to as tissue culture, became a routine laboratory technique in the 1950s. Major epidemics of polio in the 1940s and

1950s promoted efforts to develop effective vaccines and the need for cell culture became evident with the search for viral vaccines. The polio vaccine produced from deactivated virus became one of the first commercial products from cultured animal cells (Chaudry, 2004).

1.2.2.2 The use of genetics

The use of genetically modified organisms is common nowadays in many fields of research. Genome manipulation can help to characterize the role of genes in the ability of a micro-organism to infect and cause disease. On the other hand the manipulation of the host genome can indicate if a gene is involved in susceptibility or resistance to infections. In 1988 Professor Falkow proposed a revised version of the Koch's postulates adapted to molecular genetic studies on microbial pathogenesis that could help to identify genes related to pathogenicity. He proposed that genetic manipulation was almost a prerequisite for success and called this Molecular Koch's Postulates (Falkow, 1988). Molecular Koch's Postulates can be even more true for the host cell. Nevertheless, there is no doubt that this postulate contributed to the design of work leading to the identification of virulence factors that enable a bacteria to be pathogenic, or host 'factors' that permit a microbe to be virulent.

With the advance of research in this field it became more obvious that genetic manipulation has to be applied to both parties in infection and only in this way is it possible to obtain a complete picture of the complex interactions between host and pathogen. For example, the SipB protein encoded on the Salmonella Pathogenicity Island 1 (SPI-1) and secreted via a Type III secretion system (TIISS) in *Salmonella* was suspected to interact with the host protein Caspase-1. When the gene encoding this protein was mutated, the bacteria were unable to express a functional SPI-1 and could not be used to confirm any interaction with Caspase-1. In this case the use of caspase-1 knockout mice, together with biochemical interaction assays, helped to define the role of SipB and the relationships with Caspase (Jarvelainen *et al.*, 2003; Lara-Tejero *et al.*, 2006; Monack *et al.*, 2000). Macrophages were subsequently harvested from mutant mice and these were used to further explore the biology of these interactions.

Mutagenesis of the host genome is now really in vogue and new mutagenesis techniques have been developed to investigate this complex system. Lengeling *et al.* recognize

three main approaches that are already in place: 1) target mutations of candidate loci to disrupt specific immune-responses; 2) identification of new loci involved in host response through induced or spontaneous mutation; 3) induction of new inbred mouse strains that are susceptible or resistant to specific pathogens, this will permit the tracing of complex gene interactions using quantitative trait loci (QTL) mapping (Lengeling *et al.*, 2001). The combination of host and pathogen genetic manipulation has been referred to as “genetics-squared” (Persson & Vance, 2007).

1.2.2.3 The use of cell culture

Models have played an important role in the study of infectious disease particularly as it is not ethical to expose humans to potentially lethal pathogens in order to study disease progression (Wiles *et al.*, 2006). *In vivo* animal models have also contributed in a great way to advances in infectious disease research although there are also ethical issues here. Consequently, the use of *in vitro* models has proved to be of great value in this field. Both *in vivo* and *in vitro* models cover different aspects of host-pathogen interactions and they complement each other. On one hand animal models can give insight into the complex interactions that a biological system exhibits during infection, including synergic responses between different components of the body. On the other hand *in vitro* models offer the possibility of investigating host-pathogen interactions at the cellular level and examine the cellular reaction to pathogen invasion. Both of these approaches have pros and cons and they cannot fully replace the natural host. *In vitro* models are advantageous in many ways, they can be well controlled, they are comparatively inexpensive and they have limited ethical issues. Further, human cells can be employed. The examination of host-pathogen interaction *in vitro* can be conducted under well controlled conditions and close observation is possible. The use of live animals in experimentation is associated with ethical responsibilities and substantial administrative costs. Many countries participate in the three Rs: replacement, refinement and reduction. However, it is not always possible to eliminate *in vivo* models.

In vitro models can be classified into three major types: non-polarized cell layers, polarized cell layers and ‘organoids’. The immortalised properties of non-polarized cell models raise some concern about their ‘normal’ behaviour during infection. Polarized

cells are regarded as being generally more closely related to the *in vivo* situation, however aberrant genomic composition and properties can effect the outcomes of host-pathogen interactions. The third class of *in vitro* model ‘organoids’ represent the only three dimensional *in vitro* model and are perhaps the closest to *in vivo* structures (Wiles *et al.*, 2006). ES cells may represent a revolutionary *in vitro* model that can avoid some of the pitfalls of existing *in vitro* cell culture models. One important characteristic of ES cells is that they have and retain a normal karyotype. Further, human ES cells can be used to investigate species-specific pathogens that cannot be effectively used in other models. Additionally, the pluripotency and flexibility of these cells can provide the opportunity to develop three dimensional *in vitro* models that might reproduce more closely *ex-vivo* structures.

If ES cells are to be exploited as novel cells for investigating host-pathogen interactions it is worth considering which pathogens might be exploited in such systems. Some pathogens such as *Salmonella* and *Shigella* can actively invade human and murine cells using specialised genetic systems encoded in their genomes. Also, unlike viruses, intracellular growth is not intimately linked to viability as bacteria can readily survive outside of cells. Hence *Shigella* and *Salmonella* can be considered as potentially ideal probes for investigating pathogen interactions with ES cells. Mutant bacteria, as well as mutant ES cells, are available and the interaction of *Shigella* and *Salmonella* with differentiated cells has been well described. Consequently, it is worth looking here in some detail at the pathogenic properties of these bacteria.

1.3 *Shigella*

1.3.1 Bacteria and disease

Shigella, members of the Enterobacteriaceae, are unencapsulated, non-motile bacteria responsible for a significant global human health problem. *Shigella* can be classified in four species *S. dysenteriae*, *S. flexneri*, *S. boydii* and *S. sonnei*, these species are further subdivided into serotypes on the basis of the surface O-specific polysaccharide LPS. *Shigella dysenteriae* type 1 was the first *Shigella* species to be isolated in 1896 by Kiyoshi Shiga (Niyogi, 2005). *Shigella* genomes are very similar to *Escherichia coli* although comparatively they have significant chromosomal rearrangements and unique genetic islands called *Shigella*-specific islands (Sis). Many Sis have the classical characteristics of pathogenicity islands. In addition *Shigella* can harbour different plasmids, some of which are associated with invasiveness. *Shigella* can be found in the environment and they can survive for weeks in cool and humid locations or for up to 46 days when dried on linen (Altwegg & Bockemuhl, 1998). Moreover, *Shigella* survive and divide in humans, the only natural host, causing shigellosis or dysentery. They have a low infectious dose and consequently they can easily spread from person to person and be transmitted via the environment. The principal form of transmission is by the faecal-oral route. Shigellosis symptoms include dysentery with frequent mucoid bloody stools, abdominal cramps and tenesmus. It has been estimated that there are 163 million episodes of shigellosis per year with more than one million deaths (Kweon, 2008). No definite groups of individuals are immune to shigellosis but certain individuals are at higher risk. Most episodes of shigellosis in healthy individuals are self-limited and resolve within 5-7 days without consequences. The incidence of shigellosis is elevated among children of 1 to 4 years old and in those that suffer from malnutrition the disease can be quite harsh and induce further growth retardation. *S. sonnei* and *S. flexneri* are linked to the endemic form of the disease which occurs worldwide. *S. flexneri* is the hyper-endemic type in developing countries and is accountable for 10% of all diarrhoeal episodes among children younger than five years (Niyogi, 2005). *S. dysenteriae* 1, which expresses the potent Shiga toxin, is responsible for the epidemic form of the disease which accounts for deadly outbreaks in developing countries. Shigellosis diagnosis requires laboratory growth of stool sample on differential/selective media and

aerobic incubation to inhibit the growth of anaerobic normal flora. This clearly makes diagnosis quite a challenge in developing countries. Vaccines effective against *Shigella* are not available despite the international community efforts in this direction. There is need for a multivalent vaccine covering the prevalent species and serotypes. One of the major obstacles to vaccine development is the unsuitability of animal models. For a comprehensive review refer to Kweon (Kweon, 2008).

1.3.2 Mechanism of host invasion

1.3.2.1 Type III secretion

Shigella are able to invade and multiply within colonic epithelial cells and the rectal mucosa, causing cell death while spreading laterally through the epithelial layers (Niyogi, 2005). Before the development of dysentery symptoms include early inflammatory lesions of the colorectal mucosa, comparable to aphthoid ulcers, with the presence of lymphoid follicles (Sansonetti, 2002). *Shigella* predominantly invades the colonic epithelium through M cells in the Peyer's patches, which do not bear a microvillae brush border (Jepson & Clark, 2001). Also, *Shigella* can be phagocytosed by dendritic cells (DC) and macrophages resident in the dome. Subsequently, intracellular *Shigella* are able to induce macrophage apoptosis involving caspase-1 activation and consequent secretion of two cytokines, IL-1 β and IL-18 (Sansonetti, 2002).

Shigella species harbour plasmids that confer the 'invasive phenotype'. The plasmid pWR100 (214kb) from *S. flexneri* serotype 5a strain M90T has been fully sequenced and it contains a pathogenicity island of 30kb encoding the *ipa/mxi-spa* operons which direct the expression of Ipa or invasin proteins delivered inside the host cell through the TIISS apparatus formed by the *mxi* and *spa* products (Buchrieser *et al.*, 2000). The primary function of the TIISS is to transport proteins from the bacterial cytoplasm into the host cell. The TIISS molecular structure was described as a 'needle complex' (NC) by Kubori and coworkers in 1998 (Kubori *et al.*, 1998) and even though *Shigella* is a non-motile bacterium the structure resembles flagellar basal bodies (Blocker *et al.*, 2001). Three parts of this secretion system were described: an external needle, a transmembrane complex or neck and a large bulb-like structure internal to the bacterial membrane. The needle complex is formed by at least five proteins: MxiD, MxiG, MxiJ,

MxiH, and MxiI (Blocker *et al.*, 2001). The secreted proteins remain in the bacterial cytoplasm until the secretion machinery is activated by host contact or external signals such as serum or the small amphipathic dye molecule Congo red (Bahrani *et al.*, 1997; Menard *et al.*, 1994). Then at least three invasion proteins are injected inside the host cells (IpaB, IpaC and IpaD) through a channel within the structure (Blocker *et al.*, 1999). The Ipas are able to catalyze the formation of a localized actin rich macropinocytic-like ruffle of the host cell membrane which mediates bacterial internalization (Bourdet-Sicard *et al.*, 1999; Niebuhr *et al.*, 2000; Tran Van Nhieu *et al.*, 1999). Once inside the cell the *Shigella* bacterium is able to escape the vacuole and start a cycle of intra- and inter-cellular spreading.

1.3.2.2 Intracellular lifestyle

Shigella is an invasive bacterium able to induce its own phagocytosis and survive and spread from cell to cell disrupting the colonic epithelial structure and inducing inflammation and dysentery. It has been established that the *Shigella* internal-cell growth rate is not dependent on the Shiga toxin but on the plasmid-mediated dynamic lysis of the phagocytic membrane soon after endocytosis (Sansone *et al.*, 1986). The endosomal membrane lysis is mediated by Ipa proteins injected into the host cell (High *et al.*, 1992). IpaB seems to play the main role and a *Shigella ipaB* mutant showed cell entry but no lysis of the phagocytic vacuole. This *Shigella* mutant did not induce the contact mediated haemolytic activity characteristic of this bacterium. Once free inside the host cytoplasm the bacteria move via the formation of an F-actin tail. The bacterial movements are random and quick and the catalyst for this movement is the polymerization of actin at the base of the bacteria. The actin polymerization is due to the IcsA protein which is encoded on the large virulent plasmid pWR100 (Bernardini *et al.*, 1989). IcsA distribution on the bacteria surface is asymmetric and accumulates at the bacterial pole. This polar localization is also accentuated by the action of a protease, SopA, which seems to regulate the asymmetric distribution of IcsA. *Shigella sopA* mutants do not show intracellular motility (Egile *et al.*, 1997). The random propulsion of the bacteria inside the host cell cytosol ultimately causes a contact with the inner face of the cytoplasmic membrane and the bacteria protrude into the adjacent cell until they are eventually phagocytosed. It has been speculated that the bacteria establish contact with components of the cellular junction and that the passage is an active actin-driven

protrusion. However, the interaction with cellular cadherins is a prerequisite to inter-cellular spreading of *Shigella* (Sansonetti *et al.*, 1994). Once engulfed in the neighbouring cell, *Shigella* is surrounded by a double membrane vesicle and in this case liberation into the cytosol is due to IcsB, which is encoded just up-stream of the Ipa genes in the locus encoding the effectors for the entry (Allaoui *et al.*, 1992).

All this happens in epithelial cells. *Shigella* follows a different behaviour once inside macrophage cells located just underneath the Peyer's patches. Once inside macrophage cells, *Shigella* induces host-cell apoptosis through the action of IpaB protein which activates caspase-1 (Hilbi *et al.*, 1998). Caspase-1 activation mediates the cleavage of the pro-inflammatory cytokines, IL-1 β and IL-18, triggering the inflammation reaction probably through the production of IFN γ . Once outside the host-cell the bacteria are more vulnerable to host defences. Neutrophils can produce elastase which actively degrades virulence factors and prevents the escape of *Shigella* from the phagocyte (Weinrauch *et al.*, 2002). Also the intracellular bacteria can be trapped in intertwined filamentous structures known as neutrophil extracellular traps preventing infection of intact cells (Brinkmann *et al.*, 2004). In this condition the bacteria can be kept under control and the host immune system can take action against the pathogen.

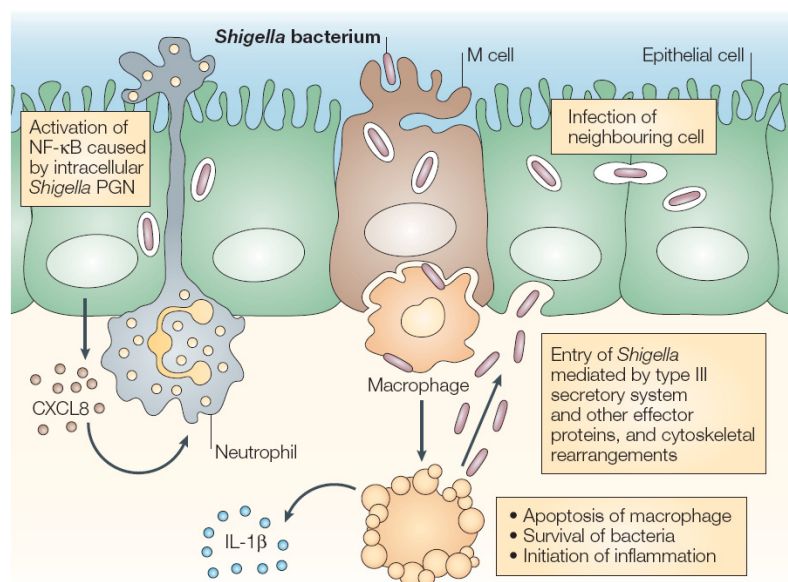


Figure 1.1 *Shigella* invasion of the gut mucosa

Shigella invades the gut epithelium preferentially targeting M-cells associated with the follicle-associated epithelium above the lymph node. Bacteria can spread laterally invading epithelial cells or phagocytic

cells present beneath the follicle associated epithelium (FAE). In macrophages apoptosis can be induced through the activation of caspase 1 and the release of mature IL-1 β and IL-18 and CXC-chemokine ligand 8 can then initiate the inflammation response. (Sansonetti, 2004)

1.4 *Salmonella*

1.4.1 History

Salmonella was named after Daniel Elmer Salmon, an American veterinary pathologist who first discovered the *Salmonella* bacterium in pigs in 1885. However typhoid fever was first described by the French physician Pierre Charles Alexandre Louis who first proposed the name "typhoid fever" as early as 1827. Interestingly, it is believed that several historical figures were killed by Salmonellosis, including Alexander the Great. He mysteriously died in 323 B.C. and in 1998 a group from the University of Maryland School of Medicine reported that his death was likely due to typhoid fever (Oldach *et al.*, 1998). In recent years many cases of Salmonellosis have been reported throughout the western world, where *Salmonella* outbreaks are associated not only with eggs and cow milk but with canned products like peanut butter and tomatoes (<http://www.salmonellablog.com/articles/salmonella-outbreaks/>).

For example consumeraffairs.com reported three outbreaks of Salmonellosis in February 2007 in the US, Canada and UK respectively. It is difficult to generate a true global picture of outbreaks in developing countries where *Salmonella* overlaps with other diseases but the problem is significant.

1.4.2 Bacteria and disease

The *Salmonella* genus is divided in two species: *Salmonella bongori* and *Salmonella enterica* which is further subdivided into five subspecies: I - enterica, II – salamae, IIIa – arizonae, IIIb – diarizonae, IV – houtenae, V – obsolete , VI – indica. *Salmonella* are today classified according to the serological techniques developed by Kauffman and White, which uses antisera to determine the taxonomical characteristic of the surface O antigen which is the polysaccharide associated with the lipopolysaccharide of the bacterial outer membrane. Antisera to the flagellar antigen H is also used and this can be further divided into phase 1 and phase 2. These phase antigens reflect the ability of *Salmonella* to live in different phases: a motile phase and a non-motile phase or flagellated and non-flagellated phases (sometimes additional flagella are also expressed). *Salmonella* serovar Typhi expresses an additional polysaccharide antigen,

Vi, associated with the bacterial capsule. When expressed this antigen causes enhanced virulence as determined by a lower infective dose in human volunteers (Parry, 2006).

Salmonella Typhimurium has been recognised as a common cause of disease throughout the world and was first isolated in late 19th century (Forsyth, 1998). *S. enterica* serovar Typhimurium (*S. Typhimurium*) is an etiological cause of salmonellosis in humans and animals and is adapted to a life-style in the gastrointestinal tract. *S. Typhimurium* is normally contracted by ingestion of contaminated food of animal origin like eggs and milk or from water. For this reason it is more commonly found in developing countries where water supply systems can be cross-contaminated by animal and human waste. This pathogen is able to escape the hostile stomach environment to attack the intestinal epithelium normally causing localised gastroenteritis in humans and systemic typhoid fever in mice. However, strains of *S. Typhimurium* (Non-typhoidal salmonellae or NTS) can cause invasive disease in humans in some regions of the world, particularly Africa. The symptoms of *S. Typhimurium* appear 12-72 hours post infection and include fever, abdominal pain, diarrhoea, nausea and sometimes vomiting. The illness normally lasts 4-7 days and most people recover without treatment, but in very young and elderly people the bacteria can enter the blood stream and antibiotic therapy may be needed (WHO, Fact Sheet N 139 Revised April 2005). In developing countries as in Africa, salmonellosis is more common during the rainy season but also can reflect seasonal patterns of diseases such as malnutrition and malaria. The incidence of sepsis caused by NTS is very high in African children. In 1987 a study was conducted on NTS bacteraemia in Rwanda where 72% of children with NTS bacteraemia were sick enough to require hospitalization and a 12% fatality rate was reported. Also, cases of NTS meningitis were reported in Malawi between 1996-1997 with a fatality rate of 57% (Graham *et al.*, 2000).

1.4.3 Type Three Secretion Systems

S. enterica has received the most attention since it is responsible for most human disease and contains many serovars associated with disease. *S. enterica* serovar Typhi is a human restricted serovar associated with systemic typhoid disease. *S. Typhimurium* causes systemic disease in the mouse and is often used as a surrogate model of typhoid fever. These two serovars exhibit significant genome homology. However, *S. Typhi* has

a high number of pseudogenes, 204, compared to *S. Typhimurium* and these mutations may contribute to host restriction. Genome comparisons with other enteric bacteria facilitate the identification of genetic insertions and deletions. Many of the larger insertions encode for virulence determinants that are named *Salmonella* pathogenicity islands (SPIs). Some SPIs are shared between all or few *Salmonella* serovars but a few are restricted to particular serovars. The TIISS encoded on SPI-1 has a significantly lower GC content than the chromosome and is flanked by IS-3-like elements (Sukhan, 2000). TIISSs have been found in many animal and plant pathogens and the fact that both animals and plants can be invaded by pathogens carrying this type of secretion system highlights their versatility (Sukhan, 2000). The horizontal insertion of these elements has been supported by three observations: different GC content compared to the rest of the bacterial chromosome; flanking genes that are contiguous in closely related non pathogenic bacteria; transposons or bacteriophage sequence close to SPIs suggesting mechanisms of acquisition (Ohl & Miller, 2001).

S. enterica encode at least two TIISSs associated with the invasion process, located in SPI-1 and 2 respectively. SPI-1 encodes a system required for entry into epithelial cells and at least 13 known effector proteins, several of which are involved in the host cytoskeleton remodelling inducing bacteria phagocytosis, are secreted directly into host cells (Pascale Cossart, Second Edition 2005). SPI-2 encodes genes essential for intracellular replication and this locus is necessary for the establishment of systemic infections. Different TIISS share common features such as the absence of a cleavable amino-terminal signal sequence on the secreted proteins, the need for specific chaperones for the secretion of effector proteins and the requirement of an activation signal involving contact with the host cells. Contact is required for the full formation of the system and delivery of proteins into the cytosol of host cells. Sequence comparisons have highlighted similarities between components of the TIISS and the proteins involved in their export (Sukhan, 2000). Also electron microscopy has revealed an elongated structure spanning the inner and the outer membranes called the needle complex for both these systems. The TIISS encoded on SPI-1 can be distinguished into structural components including a basal structure that resembles the flagellar basal body and an outer membrane structure named the needle complex (Kubori *et al.*, 1998). In addition there are a number of cytoplasmic proteins that are thought to help the assembly of the secretion apparatus. At least five proteins have been described that

make up part of the inner cell structure. These are InvA, SpaP, SpaQ, SpaR and SpaS (Hensel, 2006). Homologs of these proteins are found to play key roles in the flagellar assembly systems in various bacteria (Ohnishi *et al.*, 1997). *Salmonella* InvA is homologous to MxiA of *Shigella* (Ginocchio & Galan, 1995). Whereas many different effector proteins such as SipA, SipB, SipC, SptP are encoded by genes located within SPI-1, SopA, SopB, SopD, SopE and SopE2 are encoded in loci outside the island (Miroid *et al.*, 2001). Also, other proteins, such as those involved in iron uptake, are encoded on the locus (Zhou *et al.*, 1999).

The TIISS encoded on SPI-2 is essential for *Salmonella* to proliferate within the host cell. The structure of this TIISS has not been fully determined but needle like structures were determined to be present on *Salmonella* inside the SCV (Chakravortty *et al.*, 2005). SPI-2 encodes several translocator proteins including SseB, SseC and SseD and maybe SpiC (Freeman *et al.*, 2002), and a few effector proteins SseF, SseG (Kuhle & Hensel, 2002). Others such as SifA, SifB, SspH1, SspH2, SlrP, SseI, SesJ, PipB, PipB2 and SopD2 are encoded outside the SPI-2 locus (Hensel, 2006).

1.4.4 Mechanism of host invasion

Salmonella TIISSs are responsible for both invasion and bacterial survival in the host cells. *Salmonella* invasion of non-phagocytic cells is mediated by the TIISS encoded on SPI-1 whose secreted effector proteins induce cytoskeletal rearrangements that lead to membrane ruffling facilitating bacterial internalization. *Salmonella* invade the gut epithelium preferentially through M-cells. These cells are generally targeted by pathogens since they have a reduced amount of mucus on their surface and present irregular microvilli. M-cells are located in regions of follicle-associated epithelium (FAE) which are organized mucosa-associated lymphoid tissues such as the intestinal Peyer's patches (Jepson & Clark, 2001). The first effectors proteins to be translocated inside the host cells are SopE, SopE2 and SptP which target the monomeric GTP-binding proteins of the Rho family. Members of the Rho family include cdc42, rac and rho and they play a central role in regulating the actin cytoskeleton. SopE activates these GTP-ases inducing a reorganization of the cytoskeleton F-actin filaments. These form ruffles by activation of JNK kinase which ultimately regulates transcription factors (Patel & Galan, 2006). Also the SPI-1 TIISS induces transmembrane fluid and

electrolyte fluxes in addition to the synthesis of cytokines and prostaglandin mediator factors of inflammation. Once inside the host cell, the pH change inside the endosome induces the expression of the SPI-2 TIISS which is involved in bacterial survival and persistence inside the host cell. One effector protein playing an important role is SifA, which is responsible for the maintenance of the integrity of the SCV during intracellular survival (Beuzon *et al.*, 2000). Another protein secreted by SPI-2 TIISS is SpiC that appears to interfere with normal cellular trafficking (Uchiya *et al.*, 1999)

In phagocytic cells *Salmonella* can induce rapid apoptosis, stimulated in part by the delivery of cytosolic flagellin through the assembly of the IpaF inflammasome leading to activation of caspase-1 and finally resulting in the activation of IL-1 β and IL-18 (Franchi *et al.*, 2006; Miao *et al.*, 2006). *Salmonella* associated phagocytic cells produce and release antimicrobial products such as reactive oxygen species (ROS) and reactive nitrogen species (RNS) inducing local inflammation (Abrahams & Hensel, 2006).

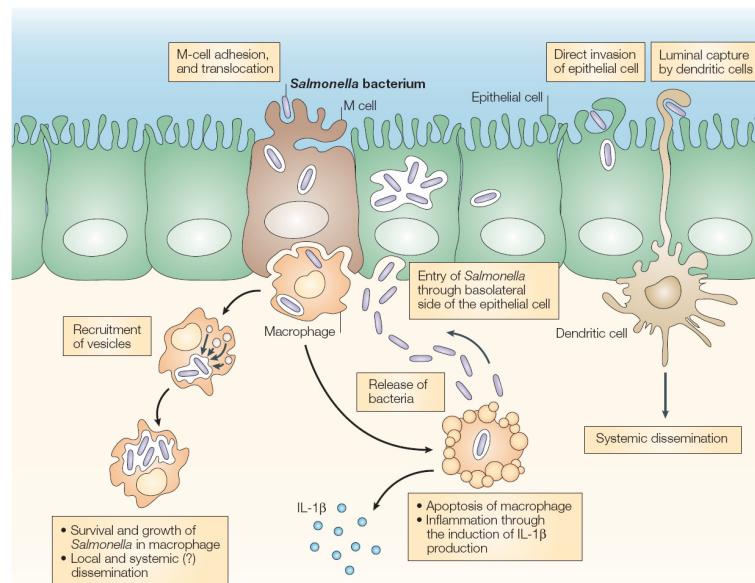


Figure 1.2 *Salmonella* invasion of the gut mucosa

Salmonella invade the gut epithelium through M-cells and reach the underlying lymph nodes where phagocytic cells take up the bacteria. *Salmonella* is able to induce apoptosis of macrophages and DCs with consequent secretion of IL-1 β and IL-18. In this representation DCs are shown protruding through the epithelial cells to sample the lumen content (Sansone, 2004).

1.5 Embryonic stem cells

1.5.1 History

The first documented suggestion that cells had pluripotency goes back as far as 1902 when Haberlandt suspected that plant cells could produce a whole organism. However it proved to be more challenging to establish the same concept in animal cells due to the complicated pattern of functions and tissues found in the animal body. Nevertheless, the concept that cells can be pluripotent was not abandoned by researchers. The first reports of the formation of a mosaic mouse were in 1961 (Tarkowski, 1961) followed in 1981 by the description of the first establishment of an *in vitro* culture of pluripotent cells. Two laboratories obtained pluripotent cells isolated directly from the inner cell mass (ICM) of late blastocysts cultured in medium conditioned by established teratocarcinoma stem cell masses (Evans & Kaufman, 1981; Martin, 1981). The ES cultures were initially maintained in undifferentiated status by co-culture with mouse embryonic feeder cells. Later a factor produced by the feeder cells that contributed to ES cell growth was recognized to be the Leukaemia Inhibitory Factor (LIF) which is a chemokine of the IL-6 family that acts by activating STAT pathways (Smith *et al.*, 1988; Williams *et al.*, 1988). More recently other factors have been recognized as playing a pivotal role in maintaining the undifferentiated state of ES cells including the bone morphogenetic proteins (BMPs) and transcription factors such as Oct3/4 and nanog (Chambers & Smith, 2004). These discoveries were important in advancing the understanding of how ES cells maintain their self-renewal status and enabled researchers to grow ES cells in FCS free medium.

1.5.2 Murine ES cells

ES cells derive from the ICM of an embryo at the pre-implantation stage or blastocyst. The mouse embryo is in the blastula stage when it harbours between 50-250 cells or is at 3-4 days of growth. Two types of embryonic cells can be observed in the blastocyst, namely the ICM and the trophectoderm (TE). The TE is formed by large polar cells organized in an epithelium of single cells compactly connected by tight junctions, desmosomes and gap junctions whereas the ICM is formed by smaller, apolar cells

compacted to form the epiblast (Ducibella *et al.*, 1975; Ducibella & Anderson, 1975; Magnuson *et al.*, 1977). In later foetus development the TE descendant cells develop into extra-embryonic structures such as the placenta that makes contact with the mother body. The ICM grow into the three germinal layers: ectoderm, endoderm and mesoderm as well as into other external structures such as visceral yolk sac, amnion and the allantois that will form the umbilical cord (Lopez & Mummery, 2004). For this reason the cells that compose the blastocyst are identified as pluripotent because they can differentiate into multiple lineage cells.

ES cells have the characteristic of being self-renewing. This means that they are able to divide and create a copy of the original cell and progenitor cells are able to generate certain lineages of differentiated cells. In this latter case the differentiation capacity of the cell is restricted (Smith, 2001). Totipotent cells are typical of the embryo at the cleavage stage. As the embryo divides the blastomers lose the ability to differentiate into all cell types present in the foetus and in the adult. Three types of cell lines deriving from embryonic cells are currently available as cellular models. They are: Embryonal Carcinoma (EC) cells, Embryonic Stem (ES) cells and Embryonic Germ (EG) cells. All of these have pluripotent traits and a distinct ability to differentiate.

The term ‘Stemness’ refers to the transcriptional profile underlying the molecular process of the stem cell properties of self-renewal and the generation of differentiated progeny. Although stem cells in different cellular environments or niches will have different physiological demands and therefore distinct molecular programs, it is believed that a certain genetic profile is shared by all (Melton & Cowan, 2004). Some characteristic transduction pathways have been identified as active in stem cells (Clark *et al.*, 2004) and additional studies have been conducted in this direction (Ivanova *et al.*, 2002; Ramalho-Santos *et al.*, 2002)

1.5.3 Differentiating ES cells

The main feature of embryonic stem cells is the ability to differentiate into any kind of somatic cell present in the adult body. Their ability to ‘produce’ any type of cell is likely to find application in therapeutic treatment to cure organ failure or dysfunction. Thirty years after their initial *in vitro* culture, ES cells have been exploited in a vast

number of differentiation protocols. They can undergo spontaneous differentiation *in vitro*, by forming embryoid bodies (EBs) that contain different types of cells (Abe *et al.*, 1996) and *in vivo*, following their injection into immunodeficient mice, form differentiated tumors known as teratocarcinomas (Stevens, 1984). *In vitro* differentiation methods can be distinguished in three different approaches. In the first approach the ES cells are grown in single-cell-suspension and dividing, they form three-dimensional structures called embryoid bodies (EBs) (Doetschman *et al.*, 1985; Keller, 1995). In the second method the ES cells are grown on a stromal cell layer and the differentiation occurs in contact with these cells (Nakano *et al.*, 1994). The most widely used stromal cells for the last method are OP9 which were derived from a CSF-1 deficient *op/op* mouse (Yoshida *et al.*, 1990). The third protocol involves ES cells grown in a monolayer on extra-cellular matrix proteins (Nishikawa *et al.*, 1998). The three different protocols have pros and cons and not all of these methods are optimized for all types of differentiation processes that can be performed. The first two methods listed have been described as efficient protocols. However the third is the most appealing for therapeutic application since it can deliver pure populations of differentiated cells without any need for screening different type of cells. However, this methodology still needs to be optimized for most applications. One of the main factors that stand between the *in vitro* differentiation and the *in vivo* implantation is the use of FCS in the differentiation protocols. FCS has an uncertain composition and is subjected to composition variability from batch-to-batch. Also, human re-implantation of cells differentiated in FCS can present some immunological and ethical issues. Nevertheless the research on *in vitro* differentiation protocols has made huge progress in the past 10-15 years. Differentiated cells deriving from *in vitro* cultured ES cells can be distinguished based on the germinal layer they are derived from. Among the mesoderm-derived lineages that have been explored, protocols to obtain haematopoietic, vascular and cardiac cells appear to be the easiest to perform but skeletal muscle, osteogenic and adipogenic cell protocols have also been described. Research on lineages with endoderm origins is concentrated especially on pancreatic β -cells and hepatocytes, with the hope of their clinical applicability to treat type I diabetes and liver diseases. The ectoderm differentiation of mouse ES cells is well established and many studies have reported the characterization of neural differentiation. Although these are interesting subjects, a detailed discussion of the different differentiation protocols and clinical

applications goes beyond the scope of this study so for an extensive review on the subject please refer to Keller (Keller, 2005).

1.5.4 ES cell mutants and KO mice

Many researchers have documented the importance of ES cells and the many advantages they present for clinical applications as well as for basic scientific research. Indeed, perhaps the biggest advantages of ES cells versus immortalized cell lines is that they maintain a normal karyotype following extensive passaging in culture and have the propensity to be genetically manipulated (Austin *et al.*, 2004). The genetic manipulation of a specific gene in ES cells can be exploited to investigate function during development, if expression is followed during embryoid body formation or if the mutant cell is employed to generate chimeric mice. Also, the gene mutation can be investigated during lineage differentiation or in studies of cell homeostasis. Many of the methods that can be used to induce gene mutations in ES cells are summarized in Figure 1.3.

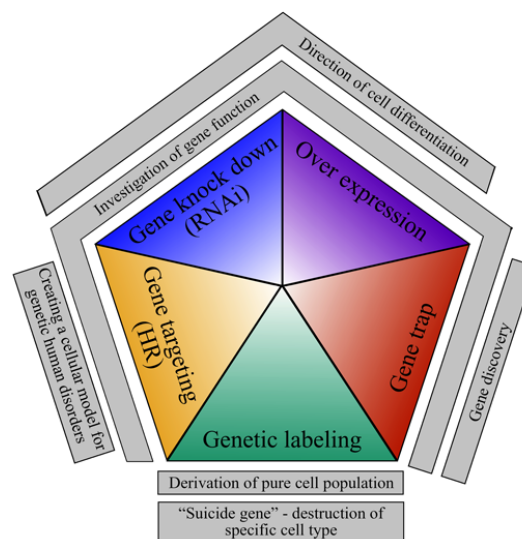


Figure 1.3 Genetic manipulation of ES cells and their potential application

This cartoon summarizes the genetic approaches that can be used to obtain mutant ES cells. The more traditional approaches, like transfection and the use of viral vectors can be more difficult to use especially on human ES cells. Transfection is the introduction of foreign DNA into the cultured cells by physical or biochemical methods (electroporation or LipofectAMINA Pulse, FuGENE). Infection using viral vectors, especially lentiviruses, have shown to provide a high level of stable integrants. However, the long terminal repeats (LTRs) may effect expression of the transgene, the vector size can be a limiting factor in addition to non-specific integration and potential effect of the virus genome in clinical studies. However, these methods still find use in mouse studies. Genetic tagging can be used to track transplanted cells or

the expression of a mutated gene. RNAi techniques use RNA to interfere with the gene expression through mRNA degradation. In this case researchers talk of knock-down expression by transfection of small RNA or of a plasmid that directs the production of interfering molecules (Kopper & Benvenisty, 2005). Gene trap is a random introduction of the mutagenic agent into the promoter, enhancer or the polyadenylation (poly-A) of a gene and is meant to disrupt the gene function. For an extensive review on gene-trapping please refer to Stanford, 2001 (Stanford *et al.*, 2001).

Of all the techniques reported in Figure 1.3 the main approach used to create ES cells mutants and mouse knockouts is Gene Targeting (Figure 1.4). The remarkable importance of this process has been underlined by the award of the 2007 Nobel Prize in physiology or medicine to three researchers, Mario R. Capecchi, Martin J. Evans and Oliver Smithies, for their discover of “principles for introducing specific gene modifications into mice by the use of embryonic stem cells” (The Nobel Prize Assembly, Press Release 2007-10-08). This was a milestone of modern research. In 1986 Capecchi and Smithies proved that it was possible to target specific genes by homologous recombination in cultured cells and Evans contributed by providing the necessary vehicle to target the mouse germ line to transmit the mutation from generation to generation, mouse ES cells. In 1989 the first knockout mice using gene targeting were produced. By 2004 about 10% of all mouse genes were targeted in the form of knockout mutant mice (Austin *et al.*, 2004).

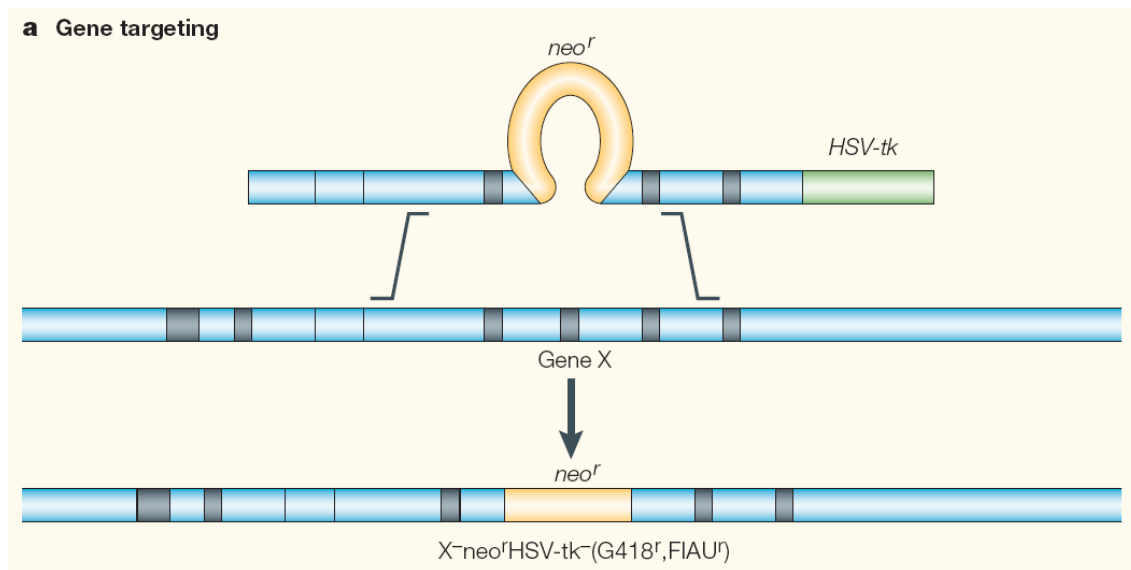


Figure 1.4 Generation of target mutant ES cells

The target vector is introduced by electroporation into ES cells and the desired mutant cells are selected by positive selection. The vector contains a neomycin resistance (neo^r) gene in an exon of the target gene and a linked herpes virus thymidine kinase ($HSV-tk$) gene at the other end. The vector pairs with the chromosomal target gene and after homologous recombination the resistance to neomycin is inserted into the gene, disrupting one copy of it. The cells in which this event occurs will be of $X^{+/-}$, neo^{r+} and $HSV-tk^{-}$ genotype and will be resistant both to G418 and FIAU (Capecchi, 2005).

Ambitious programmes for more efficient and effective production of mouse knockouts were announced in 2004 bringing together international efforts to achieve this ambitious and important goal for the research and social community (Auwerx *et al.*, 2004). In the last 10 years a new mutagenesis technique has been introduced that utilizes a bacterial artificial chromosome (BAC) to introduce mutagenesis into the mouse genome with more efficiency and less labour. Nowadays this technique is used to produce ‘mutant libraries’ that can be employed for the *in vivo* and *in vitro* study of specific genes in different mice backgrounds, for an example refer to Adams *et al.* (Adams *et al.*, 2005).

1.6 Dendritic Cells

1.6.1 What are they?

Dendritic cells (DCs) are professional antigen presenting cells that were described for the first time in 1973 by Steinman (Steinman & Cohn, 1973; Steinman & Cohn, 1974; Steinman *et al.*, 1974). However, it is more appropriate to talk of a ‘family’ of DCs because several different types of DCs have been described and they form a heterogeneous population of single cells found in different sites of the body. However, all DCs perform a similar important role, the processing and presentation of antigens leading to the activation of naïve T lymphocytes. Steinman showed in 1974 that DCs are at least 100-fold better activators of T cell responses in a mixed leukocyte reaction when compared to other antigen presenting cells such as macrophages and B cells (Steinman & Witmer, 1978). Later on it was demonstrated that DCs are able to induce a T cell antigen specific response both *in vitro* (Nussenzweig *et al.*, 1980) and *in vivo* (Inaba *et al.*, 1990). DCs are also involved in the establishment self-tolerance. Tolerance is mediated by DCs in two ways, by the stimulation of clonal deletion of T cells during antigen presentation in a steady state (Bennett & Clausen, 2007; Hawiger *et al.*, 2001) and by modulating regulatory T cell differentiation (Luo *et al.*, 2007). DCs have an essential function in the immune system participating in the immediate response to pathogens through innate immune activation as well as in the induction of antigen specific immune responses.

DCs are located in lymphoid organs such as the spleen and lymph nodes and in non-lymphoid organs such as the skin or liver. They can be generally classified into two categories: conventional DCs which are blood-borne, and plasmacytoid DC which are differentiated from bone marrow (Ardavin, 2007). Conventional DCs are present as immature or mature APCs, resident in lymphoid organs such as the thymus, spleen, lymph nodes, lymphoid tissues and the intestinal and respiratory tracts. They can be separated into subpopulations based on their differential expression of the surface markers CD8, CD11b, CD4. Conventional immature DCs that are located within non-lymphoid organs are able to migrate to the lymph nodes upon contact with external antigens, where they interact with antigen specific T cells and other cells of the immune

system like NK cells, B cells and other DCs. This DC population include Langerhans cells and are also called tissue-resident DCs. Similar DCs are also present in the parenchyma of the liver and kidney. These cells are strategically located in intimate connection with epithelial surfaces that are exposed to external pathogens. Tissue-DCs form a subpopulation expressing specialized endocytic and phagocytic receptors that permit proficient uptake and procession of pathogen-specific antigens. However, in the last few years it has been established that the involvement of tissue-derived DC in priming antigen-specific T cells after microbial infection of the skin or mucosa is limited. The arrival of dermal DC in the draining lymph nodes coincides with antigen presentation by lymph node-resident DC, suggesting that dermal DC transport the antigen cargo to resident DC in the lymph node, which in turn activates specific T cell responses (Allan *et al.*, 2006). Plasmacytoid DCs are specialized in producing large quantities of type I IFN, particularly during viral infection. They are non-conventional DCs with low expression levels of CD11c, CD11b and MHC class II markers but they are B220⁺. In the steady state, they resemble plasma cells and upon encounter with antigen they assume a DC characteristic morphology with weak property of antigen presentation (Liu, 2005).

Exploiting the functions of different DC subsets *in vivo* is challenging since the depletion of only one type of DC at a time can present technical problems due to subtle differences in marker expression and overlapping functions between subsets. However, a recent report investigating DC-ablated mice highlighted the crucial role of DC in generating anti-microbial T cell immunity (Bennett & Clausen, 2007).

1.6.2 Antigen interaction

Pathogens are recognized by specific pattern recognition receptors (PRRs) which include transmembrane toll-like receptors (TLRs), cytosolic nucleotide oligomerisation domain (NOD)-like receptors (NLRs), RIG-1-like receptors (RLRs) and C-type lectin receptors (CLRs). Innate immune cells such as macrophages and DCs sense the pathogens through TLRs, phagocytose them and evoke immune responses. The recognition of pathogen-associated molecular patterns (PAMPs) is crucial to the host in order to avoid the activation of innate immunity against self (Takeuchi & Akira, 2007). To date ~13 different TLRs have been described in mice and ~11 in humans. Each TLR

recognizes distinct PAMPs derived from bacteria, viruses, protozoa and fungi (Figure 1.5). TLR1, 2, 4 and 6, which are expressed on the cellular membrane, recognize a broad range of microbe-derived lipid structures; TLR5 and 11 are specialized in protein recognition; TLR3, 7, 8 and 9 are localized intra-cellularly in the endoplasmic reticulum (ER) or endosomal membrane where they detect nucleic acids from viruses or bacteria (Akira *et al.*, 2006).

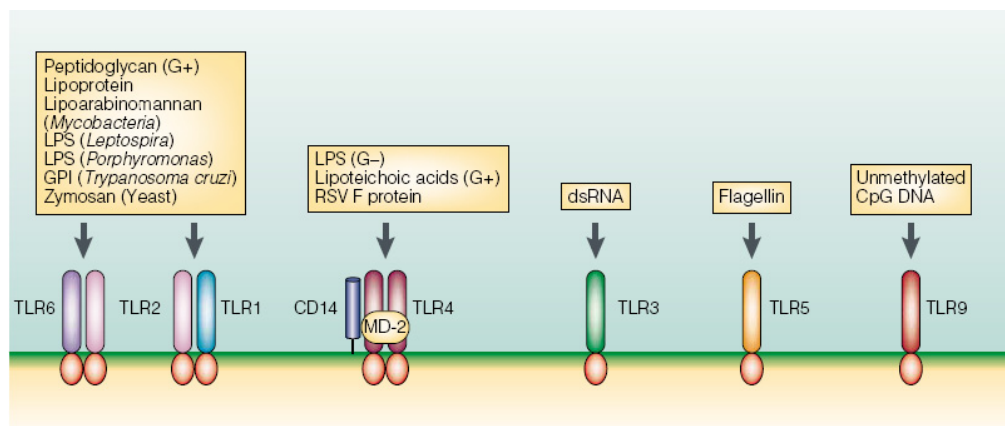


Figure 1.5 TLRs and their respective binding products

This image summarizes some of the TLRs found in mice and the respective PAMPs that they recognize. The best characterised of the TLRs is perhaps TLR4 which recognizes and binds to LPS with the help of two accessory proteins CD14 and MD-2; TLR2 binds a broad range of structurally and functionally unrelated ligands as hetero-dimers with other TLRs like TLR1 and 6; TLR3 recognizes unfamiliar double-stranded DNA; TLR5 specifically binds to bacterial flagellin and TLR9 reacts with unmethylated CpG motifs. G+, gram-positive, G-, gram-negative, GPI, glycosphosphoinositol, RSV, respiratory syncytial virus (Medzhitov, 2001).

TLRs are normally expressed as homo- or heterodimers of transmembrane proteins. The extracellular domain is composed of leucine rich repeats that participate in the recognition of PAMPs. The intracellular domains initiate the signaling response through the Toll/interleukin-1 receptor (TIR) domain that interacts with TIR-domains containing adaptor molecules. Four principally different adaptor proteins have been described so far, myeloid differentiation primary response gene 88 (MyD88) is utilized by all the TLRs except TLR3 which transduces a signal through TRIF. Some TLRs use the adaptors Mal or TRAM to bind to MyD88 or TRIF. The majority of TLRs signal through the MyD88 adaptor protein leading to a pathway that involves the molecule

TIR-domain containing adaptor protein (TRIF or TICAM1). These complexes interact with IRAK members and TRAF6 leading to the activation of MAP-kinases and nuclear factor- κ B (NF- κ B)-dependent cytokine secretion. These events can result in the production of pro-inflammatory cytokines such as TNF, IL-1 and IL-6. In the same pathway inhibitors of NF- κ B kinase (IKK) complex can be induced (Trinchieri & Sher, 2007). Figure 1.6 reports a few examples of the pathways triggered by TLRs.

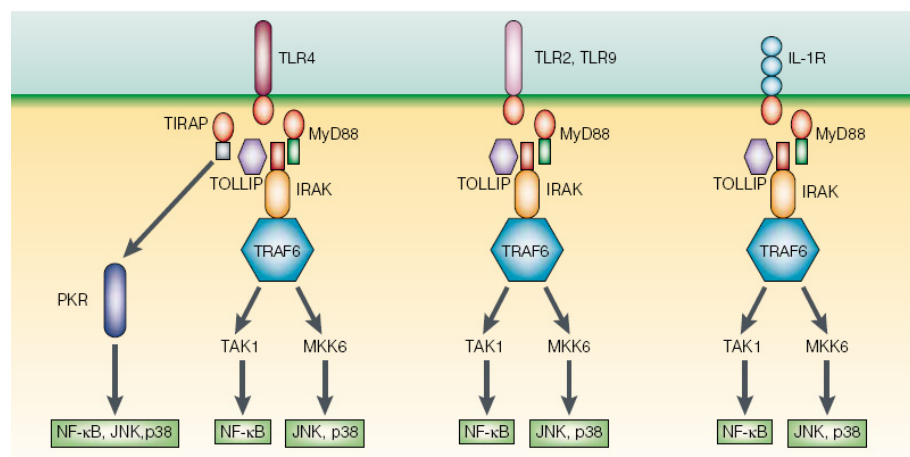


Figure 1.6 TLR induced signaling pathways

This image illustrates examples of the pathways triggered by TLRs. The TLR and the IL-1 receptor family members share signaling machinery such as the adaptor MyD88; Toll-like interacting protein (TOLLIP) has a down-regulating effect on TLR pathway activation; the protein kinase IRAK (IL-1R associated kinase) and TRAF6 (TNF receptor associated factor 6) (Medzhitov, 2001).

Among the non-TLR PAMP binding receptors the NLR family has ~30 members in humans and is characterized by the presence of a NATCH domain and leucine-rich repeats. Only two members of this family have been characterized, NOD1 and NOD2, which bind to two different substructures of bacterial peptidoglycan leading to the activation of NF- κ B. Ligand recognition of NLRs, IpaF and NALP3 promotes the assembly of the inflammasome and subsequent caspase-1 mediated activation of the active form of IL-1 β and IL-18 and IL-33 (Franchi *et al.*, 2008). Other PRRs include RLRs (RIG-1-like receptors), which are located in the cytoplasm, and some members of this family like TIG-1 and MDA5 mediate the detection of viral RNA resulting in the production of type I IFN (Bowie & Fitzgerald, 2007). Finally the CLR family represents surface expressed PRRs that recognize glycans.

1.6.3 Antigen processing and presentation by DCs

DCs are crucially required for the priming of antigen specific T cell responses, whereas the major histo-compatibility complex (MHC) class I and II presentation pathways are responsible for the priming of CD8⁺ and CD4⁺ T cells respectively. These pathways represent major check points for promoting the induction of adaptive immunity directed against intracellular and extracellular pathogens. Pathogens, including some bacteria, can induce host cell apoptosis and in such cases their antigens can engage with DCs upon the phagocytosis of apoptotic bodies (Albert *et al.*, 1998a; Albert *et al.*, 1998b).

MHC class I is responsible for the processing and presentation on the cell surface of antigens derived from endogenous proteins found in the cytosol. MHC class I presents peptide antigens of ten amino acids to CD8⁺ T lymphocytes. This mechanism seems to be always active in the cell and almost all cells express an MHC class I complex. Cytosolic proteins are ubiquitinated to mark them for proteolytic degradation in the proteasome complex or by cytosolic enzymes. Once the immune response is activated, three proteosomal subunits are replaced by the 'immunological' homologues LMP2 and LMP7 and MECL1, forming the immunoproteasome complex. The trafficked peptides are translocated into the ER lumen by transporter proteins involved in the antigen processing (TAP). In the ER lumen the peptides undergo N-terminal trimming by aminopeptidases such as endoplasmic reticulum aminopeptidases (ERAP)-1 and ERAP-2. Eventually, the optimal length peptide is associated with the presentation groove of MHC class I. This involves the intervention of specific chaperone proteins that coordinate the assembly of a trimeric complex containing MHC class I heavy chain, β 2-microglobulin and antigenic peptide. Consequently the MHC class I-peptide complex moves along the secretory pathway to the cell surface (Jensen, 2007).

The MHC class II complex presents exogenous peptide to CD4⁺ T cells. The association of the MHC class II complex with the peptide antigen is linked to the endocytic route and endosome/lysosome proteolysis. The formation of the MHC class II complex take place in the ER lumen where the α and β MHC class II chains assemble with a transmembrane protein called the invariant chain (Ii) that directs the formation of large complexes of three MHC dimers and three Ii proteins. Ii is also responsible for the trafficking of the complexes from the ER to the endocytic pathway through the Trans-

Golgi Network (TGN). Newly synthesized MHC class II-Ii complexes accumulate in the late endosome and lysosome. Once fused with the endosome/lysosome the Ii chain is degraded and peptide exchange is catalyzed by the chaperone H2-DM whose activity is triggered by acidic pH. Subsequently, Ii is completely degraded by the cysteine protease Cathepsin S, permitting the MHC class II complexes to reach the cell surface through tubulo-vesicular structures present in mature DCs.

Figure 1.7 reports a simple schematic representation of the events leading to antigen presentation.

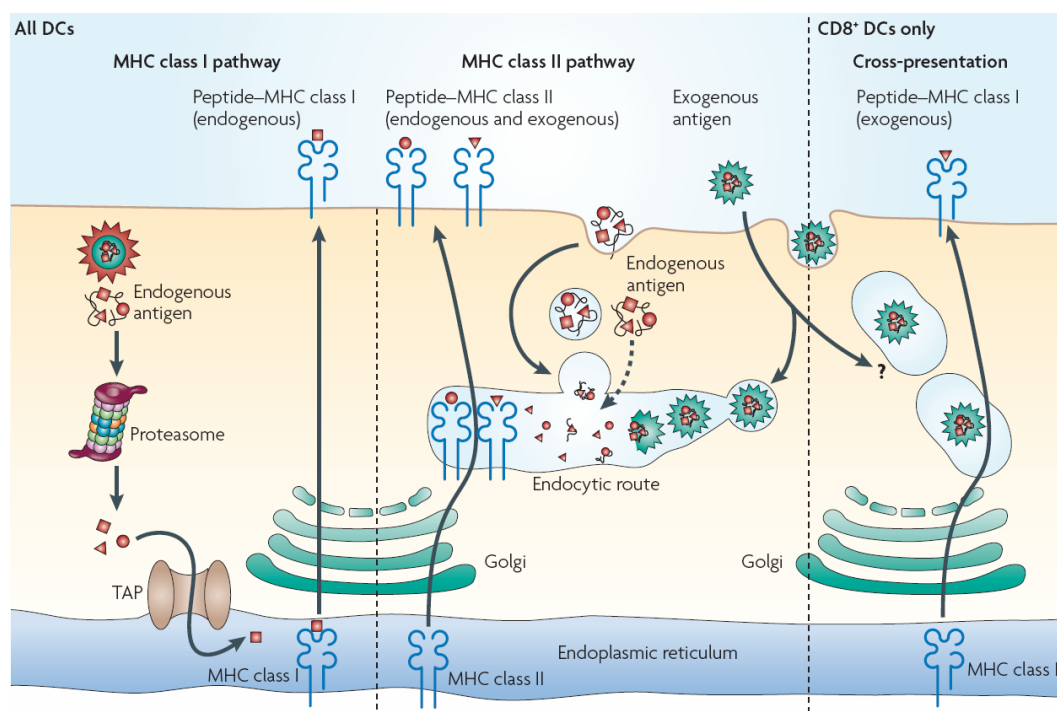


Figure 1.7 Antigen processing and presentation trafficking inside DCs (Villadangos & Schnorrer, 2007).

MHC class I complexes can present exogenous proteins to CD8+ T cells in a mechanism called cross-presentation. It is not totally clear how this pathway works but it may involve both TAP-dependent and independent mechanisms. The TAP-independent mechanism appears to involve peptide exchange on recycling MHC class I molecules in endosomes or on the cell surface involving Cathepsin S (Shen *et al.*, 2004). The TAP-dependent pathway involves the transport of antigens from endosomes to the cytoplasm and cross-presentation is suggested to result from an adaptation of

retrotranslocation mechanisms dependent on Sec61, involving the degradation of misfolded proteins in the ER (Ackerman *et al.*, 2006). However this antigen presentation pathway has not been fully elucidated yet. Whatever, the exposure of antigen peptide on the MHC class I and II is not sufficient to activate T cells. The co-expression of co-factors is required and T cell activation depends upon their presence. Such co-factors include B7-1 and B7-2 on the DC and on the T cell the CD28, CD4 or CD8 molecule together with the T cell receptor (TCR) (Green, 2000; Greenwald *et al.*, 2005; Yang & Wilson, 1996).

1.6.4 Interaction of DCs with *Salmonella*

Bacteria infecting the gut epithelium preferentially pass through M-cells. However, the ability of DCs to elongate between the epithelial cells and sample the lumen content can facilitate the uptake of bacteria. In this way DCs are suspected to facilitate the penetration of bacteria and if the cell is not able to kill the pathogens they inadvertently become transporters through the epithelial barrier (Rescigno *et al.*, 2001). DCs also contribute to 'immune correspondence' with the lymph node and more DCs are recruited as the infection progresses (Sundquist & Wick, 2005). Generally DCs have some capacity to kill micro-organisms and they express on their cell surface specific antigens such as MHC class I and class II that participate in the initiation of adaptive immune responses. Potential interaction between *Shigella* and DCs has not been well investigated whereas *Salmonella*-DC interaction has been used as a model to study the interaction between invasive pathogens and antigen presenting cells. *Salmonella* demonstrate unusual intracellular behaviour inside bone marrow derived DCs (BMDCs). *Salmonella* reside inside DCs in a static, non replicating form even though SPI-2 expression is detected (Jantsch *et al.*, 2003). In addition, intracellular *Salmonella* reduce the ability of BMDCs to present model proteins and stimulate the proliferation of antigen specific T cells (Cheminay *et al.*, 2005). There is also reduced expression of MHC class II on the surface of DCs during *Salmonella* infection (Mitchell *et al.*, 2004). These studies have reported interference by the SPI-2 TIISS on the ability of DCs to present antigen on their surface and advanced the hypothesis that SifA may be interfering with cell vacuole trafficking.

1.7 Microarray technology

1.7.1 Overview

The microarray is a key component of an *in vitro* platform technology that facilitates the simultaneous expression analysis of tens of thousands of genes. Using microarrays, in a few days it is possible to know which genes are differentially expressed under different growth conditions or within tissues, for example comparing normal to cancerous cells. Microarray analysis requires some knowledge of the DNA sequence of the target organism and is dependent upon sequence-specific probes representative of each gene. DNA templates are reproduced and bound to a surface (this can be glass, beads or other substrates) generating a genome array. Many copies of the same probes are spotted in an ordinate position and in the size order of less than a micron. This makes it possible to have tens of thousands of spots on the same small matrix. Then, RNA extracted from a target biological sample is labelled using various biochemical tags that can be detected by fluorescence (cyanine dyes), colorimetric detection (biotin/enzyme) or radioactivity. The labelled-RNA is incubated with the microarray slide under conditions where individual RNA molecules will bind to complementary single strands spotted on the array. Any un-bound labelled-RNA is then washed away and bound RNA is revealed by a scanning procedure that senses and records the signal emitted by the labelled-RNA. The intensity of the hybridized probes is measured to estimate the abundance of each target transcript.

The concept of DNA arrays was already in use in the 1970s in the form of dot and slot blots, where radioactive labelling was used to measure the relative expression of a few genes in a target sample (Kafatos *et al.*, 1979). However, the development of microarrays as we know them today has been strongly improved by the automation of PCR, sequencing technologies, progress in robotics, imaging systems and in computational biology (Ewis *et al.*, 2005). The development of new technologies promises to introduce more powerful expression analysis tools. For example, high throughput sequencing machines, that has a reported accuracy of over 99.9%, will improve the precision of interrogation of transcript levels (Margulies *et al.*, 2005). Moreover the development of nanoarrays promises to overcome the microarray

technical problems of ‘point-of-care’ and ‘field applications’. Nanoarrays are already proposed to be suitable for label-free nucleic acid analysis, for protein detection and for enzymatic-based assays with further potential applications in drug discovery, medical diagnosis, genetic testing, environmental monitoring and food safety inspection (Chen & Li, 2007).

1.7.2 Microarrays and gene expression

DNA microarray technology has been mainly applied to quantify mRNA expression or determine single nucleotide polymorphisms (SNPs). In biomedical applications, microarrays are providing enormous amounts of information on genotype-phenotype relationships, gene-environment interactions, helping to understand diseases, aging, mental illness, diet, drug and hormone effects. It is possible to infer molecular phenotyping of diseases through gene expression profiling revealing genes up- or down-regulated in a given physiological state. This can provide diagnostic, prognostic and mechanistic insights that improve our understanding of human diseases. Microarray analysis offers the opportunity to investigate complex diseases where multiple factors are affecting the illness outcome, like in cancer. Microarrays provided invaluable tools to classify and understand the mechanisms of induction and progression of different forms of cancer. The use of microarray in cancer studies highlighted that different clinical cancer phenotypes can correlate with different genetic characteristics and the analysis of expression profiles can give an indication of the disease grade, clinical course and response to treatment or the propensity to metastasis formation. All these factors come together to provide useful information for cancer prognosis.

Microarray technology is finding applications in drug discovery, investigating the impact of a medication on general genome expression patterns and defining potential side effects. An important goal of modern medicine is to achieve a personalized drug dose for each person depending on their responsiveness to the drug. More importantly, microarrays can give insight into the molecular profile of different cell types under normal functioning conditions. For example, such analysis can help in the understanding of developmental events, or highlight genes specifically expressed in a tissue. This perhaps will help to understand different physiological mechanisms and identify specific genes expressed in different loci of the body. For example, Ewins

reported in 2005 a study of expression patterns in 10 different human tissues (Ewis *et al.*, 2005). Microarrays will also find future application in proteomic research, looking at key interactions between proteins and elucidating complicated pathways involved in the different biological processes. In summary, microarray are being applied in many different fields. However, a future bottleneck may be in data analysis and interpretation. Moreover microarray technology is still facing strong criticism from some quarters. A general lack of standardization of methods and procedures makes it difficult to confirm and correlate observations by different groups. For an exhaustive report of the subject please refer to Ewis 2005 (Ewis *et al.*, 2005).

1.7.3 Other uses of microarrays

Microarray technology is currently utilized in many different areas of research from applied to basic study and from medical diagnostics to prognostics. Microarrays have also been applied in genome wide association studies to identify SNP variation associated with complex disorders. The International Haplotype Mapping Project and Perlegen Science reported more than 2 million SNP markers (Syvanen, 2005). However, it has been estimated that the human genome includes ~10 million hot spots of variation and to map genes associated with diseases can require the genotyping of hundreds or thousands of SNPs. Many commercial microarrays are available for this type of study and they differ in terms of the number of SNPs analyzed and the number of samples that can be loaded per chip (Syvanen, 2005). Also microarray based techniques are available for genome wide mapping of protein-DNA interactions and epigenetic markers. In order to identify protein-DNA binding sites a frequently applied technique is chromatin immuno-precipitation (ChIP) combined with microarray analysis (ChIP-chip). An example of microarrays applied to the investigation of methylation sites is the use of the McrBC enzyme that cuts only methylated DNA. Several variations to this approach are available (van Steensel, 2005). Such research will help to discover mechanisms of gene expression regulation and will provide the knowledge to intervene in deregulated systems. Also, microarrays are finding applications in research on small-RNAs and RNAi cell microarrays are being employed in 'loss-of-function' analyses (Wheeler *et al.*, 2005)

1.7.4 Analysis tools

Microarrays representing whole genomes can produce massive amounts of data and the nature of the analysis is crucial to the questions the researcher is aiming to address. The same data can be analyzed with different programs and different aspects of cell homeostasis can be investigated. Usually microarray expression studies are carried out to compare two or more samples with one used as control sample representing the 'normal status' (a reference sample). The control or reference sample is normally compared to a 'treated' or 'different' sample in order to comparatively investigate any differences in the gene expression. Data from replicate samples is combined and the output depends on gene annotation of the specific genome and statistical tools used in the analysis.

As a prelude to any analysis the recorded signals from each single array must be normalized before any comparisons are made. This practice is called data pre-processing and includes imputing missing values, normalization and necessary actions are specified depending on the analysis tools used. Normalization is performed in order to minimise systematic technical errors that are a risk of variability in the microarray employed. All 'microarray chips' have a background signal to which all the single spot signals need to be normalized. Further, chips need to be normalized to each other before they are compared. The normalization of the signal intensities can be done using different methods. In this study GCRMA was used for array normalization, which stands for Robust Multi-array Average with GC-content background correction taking into account the background of the chip and the intensity recorded for the perfect match (PM) and the mismatch (MM) probes based on their sequence information (Wu *et al.*, 2004). Once the normalization is performed the arrays can be compared using different statistical packages.

Pair-comparison analysis highlights genes that are repressed or activated in one sample compared to the other giving fold changes in expression. The differential list can be further filtered utilising statistical analysis of the samples based on significant p-values. For this reason it is important to run at least three biological replicates otherwise a robust statistical analysis cannot be performed. The data can be filtered with different statistical formulae, for example Benjamini-Hochberg False Discovery Rate or

ANOVA. The data analysis can be performed using computer programming language like R or using graphical user interface packages for non-bioinformaticians like GeneSpring or GEPAS (Montaner *et al.*, 2006). Gene lists can be further analyzed by clustering or pathway analysis. Clustering can be a powerful approach to identify gene expression ‘signatures’ associated with a certain disease or cancer. This method analyses individual genes taking into consideration only those genes differentially expressed above or below a certain threshold. Pathway analysis aims to identify pathways affected during treatment. All these steps will produce different data sets and this must be taken in consideration during their interpretation. Methodologies should be appropriate for the samples under consideration and the biological question addressed.

1.8 Aims of the thesis

The aims of this study were to investigate new approaches to studying host-pathogen interactions using *in vitro* models. This study focused on the host response to two Enteropathogenic bacteria, *Shigella flexneri* and *Salmonella enterica* serovar Typhimurium. In the first part of the thesis a new *in vitro* cell model was employed, mouse embryonic stem cells. Since this *in vitro* model is new to the investigation of pathogenic bacteria firstly it was investigated ES cell's interactions with the pathogens. This enabled to identify if the bacteria behave as previously described in studies using *in vitro* differentiated cells. Subsequently, transcriptomic profiling of murine ES cells during *S. Typhimurium* infection at 2h and 4h incubation was performed. Whole genome arrays were employed in order to investigate the cells' reaction to the bacterial invasion with the view to highlighting patterns of interaction. Additionally, murine ES cells were driven to differentiate into antigen presenting or dendritic cells. The differentiation protocol was optimized for the murine ES cell line used in the first part of the study and the derived esDC were characterized for surface markers and in functional assays. Lastly, the esDC transcriptome active during *S. Typhimurium* infection was investigated revealing novel insights into host-pathogen interactions.

2 Materials and Methods

2.1 Materials

2.1.1 Bacteria

Strains

Shigella flexneri wild type M90T serotype 5a.

Shigella flexneri M90T mutant Sh42 *dsbA33G* Str^r (Yu *et al.*, 2000) and harboring the plasmid pJKD18 expressing GFP constitutively, produced by Dr. Yu.

Shigella flexneri M90T mutant Δ MxiD (MxiD⁻) kindly donated by Professor Sansonetti's laboratory.

Salmonella enterica serovar Typhimurium virulent wild type SL1344 and expressing GFP on p1C/1 vector (SL1344/p1C/1) under the control of the promoter *ssaG* (McKelvie *et al.*, 2004).

S. Typhimurium SL1344 Mutant *SipB* obtained by insertion of a Kanamycin (Kan) resistance cassette, produced by Dr. Yu.

Bacterial Medium

Luria-Bertani (LB) broth: in 1L of water, 10g of Tryptone/Peptone, 5gr Yeast Extract, 10gr Sodium Chloride (NaCl);

LB agar plate, 15gr/L of Agar in LB broth;

Congo red (SIGMA) 1% stock solution;

Ampicillin (Roche) 100 μ g/ml final concentration;

Kanamycin (Roche) 50 μ g/ml final concentration.

2.1.2 Cell lines

AB2.2 murine embryonic stem cells, from mouse 129/Sv/EvBRD-Hprt^b-m2, a gift from Professor Allan Bradley's Laboratory (WTSI);

J774A.1, mouse hybridoma macrophages-like cells ECACC number 91051511;

Hep2, human hybridoma epithelial cell line ECACC number 86030501;

MF2.2d9 T cell hybridoma recognizing OVA₂₆₅₋₂₈₀ peptide presented on I-A^b, a gift from Dr. Kenneth L. Rock (University of Massachusetts Medical School);
STO's/SNL76/7 murine embryonic feeder cells, a gift from Professor Allan Bradley's Laboratory (WTSI).

2.1.3 Tissue culture

Dimethyl Sulphoxide Biotechnology performance certified (DMSO) (SIGMA);
Dulbecco's Phosphate buffered saline solution (DPBS) CaCl₂·MgCl₂ (GIBCO);
Gelatin 2% Solution Type B: from bovine skin (SIGMA);
Cell Dissociation Solution (1x) non-enzymatic (SIGMA);
Trypan blue solution (0.4%) (SIGMA);
25cm², 75cm² Culture Flasks (Corning);
Cell Culture Dishes, 100mmx20mm (Corning);
EDTA tetrasodium salt (SIGMA);
Trypsin 2.5% solution (Invitrogen);
Chicken serum (Invitrogen);
Glasgow's Minimum Essential Medium (GMEM) (SIGMA);
Knockout Dulbecco's Modified Eagle's Medium (DMEM) Optimized for ES cells 1X (+4.5g/L D-Glucose, +Sodium Pyruvate, GIBCO);
Eagle's Minimum Essential Medium (EMEM) (SIGMA);
Iscove's Modified Dulbecco's Medium (IMDM) (GIBCO);
Foetal Bovine Serum (FBS) (Hyclone);
Foetal Calf Serum (FCS) (SIGMA);
L-Glutamine 200mM (GIBCO);
Sodium Pyruvate 100mM (GIBCO);
MEM-NEAA 100x (GIBCO);
2-Mercaptoethanol (2-ME) 99% (SIGMA);
Penicillin/streptomycin solution 100x (SIGMA);
Leucocyte Inhibitory Factor (LIF) produced in house.

2.1.4 *In vitro* infection

Gentamicin solution 10mg/ml (SIGMA), TRITON-X100 (SIGMA), DPBS CaCl₂⁺ MgCl₂⁺ (SIGMA), LB-agar plates.

2.1.5 Flow cytometry

Becton Dickinson FACSAria Cell-Sorting System operated by DIVA software v4.

Buffers were all made in DPBS CaCl₂⁻ MgCl₂⁻ (GIBCO).

Calibride beads (BD Biosciences).

- Staining Buffer: 5% Heat Inactivated (HI) (56°C for 30min) Fetal Calf Serum (SIGMA), 0.1% Sodium Azide (SIGMA), sterile-filtered;
- Sorting Buffer: 5% HI-FCS filtered sterile;
- Fixing Buffer: 1% Para-formaldehyde (SIGMA) sterile-filtered;
- Saponin Buffer: 0.5% Saponin (SIGMA), 1% Bovine Serum Albumin (BSA) (SIGMA), 0.1% Sodium Azide (SIGMA), sterile-filtered.
- RNAlater® solution (Ambion)
- BD Cytometric Bead Array for cytokine quantification: Mouse/Rat soluble protein master buffer kit (BD Biosciences); BD CBA Mouse Inflammation kit (BD Biosciences); BD CBA Mouse IL-2 Flex Set (BD Biosciences).

For antibodies used see Table 2.1 and Table 2.2 for relative isotype antibodies.

Table 2.1 Antibodies for FACS analysis of murine ES and esDC characterization

Target Antigen	Source	Isotype	Conjugated to	Manufacture
h/b/m Integrin $\alpha 6$ (CD49f)	Rat	IgG2a	allophycocyanin	R&D Systems
hOct 3/4	Rat	IgG2b	phycoerythrin	R&D Systems
CD11b	Rat	IgG2b	allophycocyanin	BD Pharmingen
CD11c	Hamster	IgG1	phycoerythrin	BD Pharmingen
H-2K ^b	Mouse	IgG2a	fluorescein isothiocyanate	BD Pharmingen
I-A/I-E	Rat	IgG2a	fluorescein isothiocyanate	BD Pharmingen
CD40	Hamster	IgM	fluorescein isothiocyanate	BD Pharmingen
CD44	Rat	IgG2b	phycoerythrin-Cy5	BD Pharmingen
CD45	Rat	IgG2b	phycoerythrin	BD Pharmingen
CD54	Hamster	IgG1	fluorescein isothiocyanate	BD Pharmingen
CD80	Hamster	IgG2	phycoerythrin	BD Pharmingen
CD86	Rat	IgG2a	fluorescein isothiocyanate	BD Pharmingen
F4/80	Rat	IgG2b	fluorescein isothiocyanate	AbDserotec
DC-SIGN	Rat	IgG2a	phycoerythrin	eBioscience
CD205	Rat	IgG2a	allophycocyanin	MACS
Ly-6C (GR1)	Rat	IgG2b	phycoerythrin	BD Pharmingen
CD4	Rat	IgG2a	allophycocyanin	BD Pharmingen
CD8	Rat	IgG2a	phycoerythrin	BD Pharmingen
TLR2	Rat	IgG2b	fluorescein isothiocyanate	Santa Cruz Biotechnology
TLR4	Rat	IgG2a	phycoerythrin	AbCam
TLR5	Mouse	IgG2a	fluorescein isothiocyanate	AbCam
TLR9	Mouse	IgG2a	fluorescein isothiocyanate	AbCam

Table 2.2 Isotype control antibodies for FACS analysis

These antibodies were tested on the mouse ES cells AB2.2. The isotype controls showed not cross reaction and specificity.

Target Antigen	Source	Isotype	Conjugated to	Manufacture
Isotype control	Hamster	IgG1	phycoerythrin	BD Pharmingen
Isotype control	Hamster	IgG1	fluorescein isothiocyanate	BD Pharmingen
Isotype control	Hamster	IgG2	phycoerythrin	BD Pharmingen
Isotype control	Hamster	IgM	fluorescein isothiocyanate	BD Pharmingen
Isotype control	Mouse	IgG2a	fluorescein isothiocyanate	BD Pharmingen
Isotype control	Rat	IgG2a	allophycocyanin	BD Pharmingen
Isotype control	Rat	IgG2a	fluorescein isothiocyanate	BD Pharmingen
Isotype control	Rat	IgG2a	phycoerythrin	BD Pharmingen
Isotype control	Rat	IgG2b	allophycocyanin	BD Pharmingen
Isotype control	Rat	IgG2b	phycoerythrin-Cy5	BD Pharmingen
Isotype control	Rat	IgG2b	phycoerythrin	BD Pharmingen
Isotype control	Rat	IgG2b	fluorescein isothiocyanate	BD Pharmingen

2.1.6 Bone marrow extraction materials

70% ethanol in water, 2 Petri dishes, 1ml syringes, 25 gauge needles, scissors and forceps, 25cm² flasks, RPMI-1640 (SIGMA), 100x penicillin/streptomycin solution

(SIGMA), HI-FCS, Iscove's Modified Dulbecco's Medium (IMDM (SIGMA)), 2-ME 99% (SIGMA), rmGM-CSF (R&D Systems), rmIL-4 (R&D Systems).

2.1.7 Cytokines

Recombinant Mouse Granulocyte-Macrophage Colony Stimulating Factor (rmGM-CSF) (R&D Systems), Recombinant Mouse Interleukin Mouse (rmIL-3) (R&D Systems), Recombinant Mouse Tumor Necrosis Factor alpha (rmTNF α)/TNFSF1A (R&D Systems), Recombinant Mouse Interleukin 4 (rmIL-4) (R&D Systems).

2.1.8 Confocal microscopy

Confocal ZEISS LSM-510;

Phalloidin TexasRedX (Invitrogen);

ProLong Gold antifade reagent with DAPI (Invitrogen);

Poly-L Lysine 0.01% solution (SIGMA);

DQ-OVA (Invitrogen).

For antibodies used see Table 2.3.

Table 2.3 Antibodies used for confocal analysis

Target Antigen	Source	Type	Conjugated to	Manufacture
EEA-1	Rabbit	polyclonal	primary antibody	AbCam
LAMP-1	Rat	monoclonal	primary antibody	AbCam
LAMP-2	Rat	monoclonal	primary antibody	AbCam
Rabbit IgG, F(ab') ₂	Goat	NA	APC-Cy7	Santa Cruz Biotechnology
Rat IgG, F(ab') ₂	Goat	NA	APC-Cy7	Santa Cruz Biotechnology

2.1.9 Antigen presentation assay

Concanavalin A from *Canavalia ensiformis* (SIGMA); *Salmonella* LPS (SIGMA); rmTNF α (R&D Systems), whole OVA (SIGMA); DQ-OVA (Invitrogen); Mitomycin C (SIGMA).

Cells employed esDC, BMDC and MF2.2d9.

2.1.10 RNA extraction

RNeasy Midi kit (QIAGEN); RNeasy Mini kit (QIAGEN).

2.1.11 RNA quantification and quality

Agilent RNA 6000 Nano Reagents (Agilent)

Agilent 2100 Bioanalyzer

NanoDrop1000 (Thermo Scientific)

2.1.12 Real Time RT-PCR

Stratagene Mx3000P Real-Time machine and system software version 2;

QuantiTect Reverse Transcription kit (QIAGEN);

SensiMix Plus SYBR[®] plus Fluorescein (QUANTACE);

For primers used see Tables 2.4 and 2.5.

Table 2.4 RT-PCR Primers to confirm microarray data from murine ES cells uninfected and infected

Gene Symbol	Forward primer	Reverse primer
β -act	CCGTGAAAAGATGACCCAGATC	CACAGCCTGGATGGCTACGT
Lrpap1	CAGGAGTACAATGTGCTGCTAGAC	CAGGAGTACAATGTGCTGCTAGAC
Ccng2	GTGAAAGTGAGGACTCTGGTGAAGA	CAAAGAAGAAGGTGCACTCCTGAT
Cyp1b1	CCTTTCCTTGCCACTGATC	CTGGAAAACGTCGCCATAGC
Xbp1	AAGAACACGCTTGGGAATGG	CCGGCCACCAGCCTTACT
Herpud1	GGAGTGTGAGTCGCCTCAA	CAACAGCAGCTTCCCAGAAT
Ier3	CGGCGCCAGCTACCA	GATGGCGAACAGGAGAAAGAG
Lyst	CCAGTGCACTCGCCTTCTG	TGCGAGAACCAGCAATGCT
Pou4f2	GGCGATGCGGAGAGCTT	GCACGGGCCAGCAGACT
Socs3	CCACCCTCCAGCATCTTTGT	TCCAGGAACTCCCGAATGG
SpiC	CACGTCAGAGGCAACGCTAA	GGATTGGTGAAGCCTCCTT
Stat2	GAACCGCTTGGAGAATTGGA	GGCTGTCAAGGTTCTGCAACA
Apaf1	GGCTGCTTTCTTTCGATTATCA	ATGACGAGCAACAGGATGTG
Bfar	TGCAGAGAAAAATGGGAAGG	TGAATGTCTTCAACTCGCATTG
Fst	GGCTGGATGGGAAAACCTAC	TTGGTCTGATCCACCACACA
Lamp2	CCTGACTCCTGTCGTTCAGA	GTAGTCGACGGGGCAGTG
RhoD	ACAACCTGCGGAAGAAAAGA	AGCCGAGCTGAACACTCAAG
Socs3*	CCTCGGGGACCATAGGAG	AACTTGCTGTGGGTGACCAT

* used in ASCA confirmation RT-PCR

Table 2.5 RT-PCR Primers to confirm microarray data from esDC uninfected and infected

Gene Symbol	Forward primer	Reverse primer
S18	GAACACCGAAAAATCGAGGA	CGGTTGAGCTTGGGTTTATC
Tyki	ATCTCGTGGCTTCTGAAATAGC	ACCTCAGTAGCTATGGCGTAGG
Oasl1	AGCGAAACTTCGTGAAGCA	GCTTCCCAGGCATAGACAGT
Cxcr4	ACGGCTGTAGAGCGAGTGTT	AGGGTTCCTTGTTGGAGTCA
H2-DMa	TGACAAAAGCTTCTGCGAGAT	GCTGATGAAACAGACCAACG
Lypla3	TGGCCTCCTGTTACCTCTGT	GTCCGTCTTCTGGAGCAA
IL6	GAGCCCACCAAGAACGATAG	GTGGTTGTCACCAGCATCAG
H2-T9	ACAGCTGTCTGAAAGGAATCTG	CTCCACATCGCAGCCTTG

2.1.13 Microarrays

2.1.13.1 Affymetrix array

GeneChip[®] Expression 3'-Amplification One-Cycle cDNA Synthesis kit (Affymetrix);
GeneChip[®] Expression 3'-Amplification Reagents for IVT labeling (Affymetrix);
RNeasy Mini Kit (QIAGEN);
Affymetrix GeneChip[®] Eukariotic Poly-A RNA Control Kit (Ambion for Affymetrix);
Sheared Salmon Sperm DNA (Ambion);
Bovine Serum Albumin (Invitrogen);
GeneChip[®] Mouse Genome 430 2.0 Array (Affymetrix);
GeneChip[®] IVT cRNA Clean up kit (QIAGEN for Affymetrix);
Non-stick RNase Free 1.5 and 2 ml Microfuge tubes (Ambion);
Nuclease-free water (Ambion);
DEPC-treated water (Ambion);
5M NaCl (Ambion);
Tween20 (SIGMA);
MES hydrate Sigma Ultra >99.5% titration (SIGMA) ;
20x SSPE Buffer (Ambion);
Affymetrix GeneChip Scanner 3000.

2.1.13.2 Illumina array

Illumina TotalPrep -96 RNA Amplification Kit (Ambion);
Whole-Genome Expression kit containing Mouse WG-6 v1.1 expression BeadChip with
45,000 spot of 50bp mer probes (Illumina);

Illumina Bead Scanner.

2.1.13.3 Microarray analysis tools

Bioconductor [www.bioconductor.org];

GeneSpring;

GEPAS: ASCA [www.gepas.bioinfo.cipf.es].

2.2 Methods

2.2.1 *In vitro* culture of mouse ES cell lines

Murine ES cell line AB2.2 (129/Sv/EvBRD-Hprt^b-m2) produced by Professor Allan Bradley from the mouse strain 129/Sv/EvBrd was employed in this study. A description of this murine ES cell line can be found in these references (Adams *et al.*, 2005; Bradley *et al.*, 1984; Ramirez-Solis *et al.*, 1995). The cells were maintained in GMEM media with 10% HI-FBS (Hyclone), 2mM L-Glutamine, 1mM Sodium Pyruvate, 1x MEM-NEAA, 1:1000 of 2-ME stock solution (70µl of 2-ME 99% in 20ml water) and 500-1000U/ml Leukocyte Inhibitory Factor (LIF) (Williams *et al.*, 1988) produced in house, unfiltered. The ES cells were grown on a layer of 0.1% gelatin in DPBS. To split the culture, the cells were first washed with warm DPBS and then trypsinized. The trypsin solution was made with 100mg EDTA tetrasodium salt in 500 ml DPBS containing 10ml 2.5% trypsin solution and 5ml chicken serum and stored at -20°C. The cells were sub-cultured every two days at about 1:5 dilution. To freeze murine ES cells, culture medium was mixed with 10% DMSO and filtered.

2.2.2 *In vitro* culture of Hep2 and J774A.1 and MF2.2d9

The Hep2 cell line is a HeLa derived cell line (human cervix carcinoma). They are considered similar to human epithelial cells. They grow in EMEM media supplemented with 10% HI-FCS (SIGMA), 2mM L-Glutamine and 1x MEM-NEAA, filtered. These cells are adherent forming a monolayer on culture flasks, to passage them they were washed with warm DPBS and trypsinized and sub-cultured 1:3 every two days.

The J774A.1 cell line was cultured in DMEM with 10% HI-FCS, 2mM L-Glutamine, 1mM Sodium Pyruvate, 1x MEM-NEAA, 1:1000 of 2-ME stock solution prepared (70µl of 2-ME 99% in 20ml water), filtered. J774A.1 cells adhere to the culture plastic and they were sub-cultured 1:3 every two days and detached by scraping.

The MF2.2d9 cell line grows in suspension in the same media used for J774A.1. They were sub-cultured 1:5 every 5 days.

2.2.3 Bacterial strains

This study utilised the mutant strain *Shigella flexneri* Sh42 derived from the wild type M90TS, serotype 5a. This strain is attenuated as a result of a substitution at A33G of the active site of the protein DsbA, a periplasmic disulfide bond catalyst (Yu *et al.*, 2000). This strain also harbours the plasmid pJKD18 expressing constitutively the GFP protein and Ampicillin resistance. The plasmid pJKD18 (constructed by Dr. Derek Pickard, Team 15, WTSI) was introduced by electroporation into the mutant strain *Shigella flexneri* Sh42 *dsbA33G*. Also a *Shigella flexneri mxiD* mutant was employed in this study (a gift from Prof. Sansonetti laboratory) carrying a Kanamycin resistance (Allaoui *et al.*, 1993). These strains were grown on LB-agar plates containing 0.01% Congo Red with or without 100µg/ml Ampicillin or 50µg/ml of Kanamycin, at 37°C and in liquid culture in LB broth supplemented with or without Ampicillin or Kanamycin at 37°C shaken at 225 rpm/min.

Salmonella Typhimurium strains employed in this study are all derived from the virulent strain SL1344. The wild type strain SL1344 carrying the plasmid pJKD10 integrated with 166bp of the *ssaG* promoter and cloned into a GFP/LacZ reporter Vector p1C/1 is referred to as SL1344/p1C/1 (McKelvie *et al.*, 2004). *SsaG* is a gene from SPI-2 and therefore is activated once inside the host cell to generate expression of GFP. Also, a SL1344 *SipB* mutant was employed and it was constructed by Dr. Yu (Strathclyde University) by insertion of a Kanamycin resistance cassette disrupting the gene. The *Salmonella* strains were grown from frozen stocks on LB-agar plates and a few single colonies were grown in suspension at 37°C shaking at 225rpm/min for 4½-5h and then a 1:50 diluted subculture was grown overnight at 37°C in static conditions.

2.2.3.1 Invasion assay using *Shigella flexneri*

Human Hep2 cells were grown adherent on 24 wells plate whilst murine ES cell line AB2.2 was grown in 6 well plates coated with 0.1% gelatin solution in DPBS, to optimal condition. On the day of infection, the over night bacterial culture was diluted 1:100 in LB broth and grown until log phase ($OD_{600} \sim 0.3$) at 37°C with shaking at 225 rpm in an Innova 44 Incubator Shaker (New Brunswick Scientific). The bacteria were then inoculated into the 6 well plate, containing ES cells, at the MOI (Multiplicity of Infection) of 10 or 100 per well. In order to reach MOI 10, 100µl of bacterial culture

was used per well. In order to reach MOI 100, 1ml of bacteria culture was pelleted at maximum speed on a top bench microcentrifuge (Eppendorf), re-suspended in tissue culture medium and inoculated. Half the volumes were used to infect Hep2 cells in 24 well plates. The plate was centrifuged at 2000 rpm (671g) in a Sorvall Legend RT centrifuge rotor 75006445 (Sorvall Heraeus, Thermo Fisher Scientific) for 10 min at room temperature in order to assist/coordinate bacterial contact with the cells. After incubation for 30 min at 37°C, 5% CO₂ the cells were washed with warm DPBS three times and incubated for 2 or 4 hours in complete media supplemented with 50µg/ml of Gentamicin.

The infected cells were then used either for viable count analysis (colony forming units CFU), immunohistochemistry or flow cytometric analysis. To confirm the MOI the seeded bacteria were serially diluted and each dilution was plated in triplicate on LB-agar plates.

2.2.3.2 Invasion assay with *S. Typhimurium*

Mouse J774A.1 macrophage-like cells and murine AB2.2 ES cells were seeded at 2.5×10^5 and 2×10^5 respectively in 6 well plates and grown until 90% confluent and in uncontaminated conditions. *Salmonella* SL1344, SL1344/p1C/1 or mutant *SipB*, were grown for 4½-5 hours in 5ml LB, with or without Ampicillin selection, at 37°C in shaking condition (225rpm/min) from a few single colonies. A further 1:50 dilution was cultured over night at 37°C in static conditions. The overnight culture was diluted to have an OD₆₀₀ of ~ 0.6, a further 1:10 dilution in culture medium was used to seed the murine cells. MOI ~ 10 was reached using 100µl and MOI 100 was achieved by seeding 1ml of the bacterial suspension. The cells were then incubated at 37°C 5% CO₂ for 30 minutes before being washed with warm DPBS twice and incubated for 2 or 4 hours with complete medium containing 50µg/ml of Gentamicin antibiotic. After incubation the cells were washed with warm DPBS before being used for flow cytometric analysis, immunohistochemistry, colony forming units (CFUs) count or total RNA extraction. In order to confirm the MOI, the seeded bacterial suspension was serially diluted in DPBS and three replicates for each dilution were plated on LB-agar plates.

2.2.3.3 Viable count analysis or Gentamicin invasion assay

Infected human Hep2, mouse J774A.1 and murine AB2.2 ES cells, after incubation with Gentamicin, were washed twice with warm DPBS and lysed with either 500µl per well 0.1% TRITON-X100 solution in water or DPBS with shaking (110mov/min) for 5 min. To count *Shigella* or *Salmonella* CFUs, cell suspension lysates were serially diluted in DPBS and each dilution was plated in triplicate onto LB-agar plated with or without 100µl/ml Ampicillin or Kanamycin and incubated at 37°C over night. Inoculated bacteria were also plated in serial dilution to confirm the MOI applied to the cells.

2.2.4 Flow Cytometric Analyses

2.2.4.1 *In vitro* bacterial infection (Gentamicin invasion assay)

In vitro infection with *Shigella flexneri* M90T mutant Sh42/pJKD18 or *S. Typhimurium* SL1344/p1C/1 was followed by flow cytometric analysis monitoring the production of GFP using the 488nm Argon laser and recording in the FITC channel. Cultured J774A.1, AB2.2 ES cells, and esDCs once infected and incubated under Gentamicin selection for the indicated times, were washed twice with DPBS, fixed with 1% paraformaldehyde in DPBS for 20 min on ice, trypsinized and analyzed on a BD FACS Aria (fluorescence-activated cell sorter) machine. Uninfected cells were used as negative control.

2.2.4.2 Murine ES cells characterization

Murine ES cells were washed with warm DPBS and trypsinized for 2min at 37°C, complete medium was added and the cells were centrifuged at 1200rpm (424g) in a Sorvall Legend RT centrifuge rotor 75006445 (Sorvall Heraeus, Thermo Fisher Scientific) for 7 min, washed with DPBS, pelleted and fixed with Fixing Buffer for 20min on ice. The cells were divided in aliquots and incubated with the chosen antibody at the dilution suggested by the manufacturer, either in FACS Staining Buffer or Saponin Buffer if the marker was exposed on the surface or intracellularly respectively. The cells were washed twice before a final wash with DPBS and read on the FACS Aria.

2.2.4.3 EsDC and BMDC surface markers

EsDCs or BMDCs were collected and seeded in 96 well plates at 10^4 cells per well and incubated over night with or without activation supplements, LPS $10\mu\text{g/ml}$, OVA $10\mu\text{g/ml}$ or $\text{rmTNF}\alpha$ 5000WHOSU/ml , spun for 5 min at 2000rpm (671g) before aspirating the supernatant, washed with $100\mu\text{l}$ of DPBS Mg^+Ca^+ , treated with cell dissociation buffer for 10min at 37°C , pelleted and fixed with 1% paraformaldehyde in DPBS for 20 min on ice. The cells were pelleted once more, washed once with DPBS and stained in FACS Staining Buffer using the suggested manufacturers concentrations of antibody. See antibodies table 2.1.

2.2.4.4 Cell Sorting

In order to sort infected cells from uninfected cells, the FACS Aria was first sterilized, washed and aligned as per the manual. Sorting was performed in sorting buffer at low pressure 30phi using a $100\mu\text{m}$ nozzle and the sorting mask 16-16-0. The uninfected and infected cells were sorted into sterile 15ml Falcon tubes containing 2ml of *RNAlater*[®] solution from Ambion. The cells were pelleted at 671g or 2000rpm in a Sorvall Legend RT centrifuge rotor 75006445 (Sorvall Heraeus, Thermo Fisher Scientific) for 10min and total RNA was extracted using a QIAGEN RNeasy Mini kit. Also an uninfected sample of cells was sorted as negative control.

2.2.4.5 Cytometric Bead Array (CBA) Analysis

EsDC or BMDC were seeded in 96 well flat bottom plates at 1×10^5 with 1:5, 5:1 and 1:1 ratios (each one in triplicate) of MF2.2d9 T cells. Whole OVA protein was added at $10\mu\text{g/ml}$ and incubated over night; as negative control DCs were seeded either alone or with T cells 1:1 without antigen and with $\text{rmTNF}\alpha$ 5000WHOSU/ml .

The concentrations of cytokines produced were measured utilising CBA kits and manufacturer's instructions were followed. Briefly, the standard curve dilutions, prepared freshly for each experiment, and the experimental culture supernatants were incubated with cytokine specific beads. After incubation, the beads were washed and incubated with the detection antibody, washed again and read on the FACS Aria. The data obtained was processed with BD FCAP Array software which extrapolates the concentration of the sample in relation to the standard curve for each cytokine.

2.2.5 Immunofluorescence labeling

2.2.5.1 Murine ES cells infected by *Shigella flexneri* or *S. Typhimurium*

To observe *Shigella* Sh42 *dsbA33C* mutant or *S. Typhimurium* infection of murine AB2.2 ES cells, the latter were grown in 24 well plates for two days on sterile glass cover-slips pretreated with acetone and coated with 0.1% gelatin solution. The Gentamicin invasion assay was performed and the infected ES cells washed with warm DPBS and fixed in 1% paraformaldehyde solution (20 min) on ice. After one rinse with DPBS, the ES cells were permeabilised with Saponin Buffer for 2 min at RT and stained with primary antibodies rabbit anti-mouse EAA-1, rat anti-mouse LAMP1 or LAMP2 at the concentration suggested by the manufacturer and incubated for 30-40 min at RT. Following two washes with Saponin Buffer, the cells were further stained with secondary antibody, goat anti-rabbit or goat anti-rat APC-Cy7 conjugate, at the concentration suggested by the manufacturer and the cells were incubated for 30-40 min in the dark. Next, the infected ES cells were washed with Saponin solution twice before one last wash in DPBS and they were mounted on a glass slide with ProLong Gold antifade reagent with DAPI. To stain actin filaments the cells were permeabilised and incubated with TexasRed-X phalloidin in the dark before been washed with Saponin Buffer and mounted on the glass slide.

2.2.5.2 EsDC immunofluorescence labeling

To observe antigen processing, esDCs were grown for two days on glass cover-slips treated with Poly-L-Lysine solution, then treated with DQ-OVA for 2 hours, washed with Hanks' Balanced Salt Solution (HBSS, SIGMA), followed by the addition of mitomycin-C 25µg/ml for 30 min before 4 hours incubation, they were then washed with DPBS, fixed and mounted on glass slides ready for imaging. Alternatively, esDCs were incubated with OVA, LPS or rmTNF α overnight, washed with DPBS, fixed and permeabilised with Saponin Buffer or not as indicated, before been stained with MHC class II antibody FITC conjugated.

To track bacterial cellular location, infected esDCs were treated as ES cells and at the indicated time the cells were washed and fixed with paraformaldehyde buffer. They were then washed, permeabilised with Saponin buffer and stained with primary antibodies against endosomal and lysosomal components EEA-1, LAMP-1 or LAMP-2 respectively, at the manufacturer's recommended dilutions, for 30-40 min, prior to being washed again. Finally they were stained with secondary antibodies goat anti-rabbit or goat anti-rat conjugated to APC-Cy7 at the manufacturer's recommended dilution. After washing they were mounted on glass slides with ProLong Gold containing DAPI.

2.2.6 Total RNA extraction, quantification and Bioanalyzer analysis

The RNA from uninfected and infected ES cells line AB2.2 was extracted following the QIAGEN RNeasy Midi kit instructions.

The RNA from esDCs uninfected and infected with *S. Typhimurium* was extracted with the QIAGEN RNeasy Mini Kit.

The total RNA quantity was measured by Spectrophotometer NanoDrop-1000 v 3.1.0 and the RNA quality was analyzed using an Agilent 2100 Bioanalyzer following manufacturer's instructions.

2.2.7 Affymetrix Microarray

Affymetrix technical manual instructions for GeneChip[®] expression analysis were followed.

Five µg of total RNA extracted from murine ES cells uninfected and infected were employed for cRNA synthesis. First, double stranded cDNA was synthesized and cleaned using the eukaryotic One-Cycle cDNA Synthesis Affymetrix protocol. This was used as the template to synthesize Biotin-Labeled cRNA using the GeneChip IVT Labeling Kit following the Affymetrix protocol. The cRNA was cleaned, quantified (NanoDrop1000) and analyzed by Bioanalyzer (Agilent) before being fragmented (GeneChip Expression Analysis, Technical Manual Rev. 5, AFFYMETRIX, 2004). Then 15µg of fragmented biotin-labeled cRNA was hybridized onto Affymetrix GeneChip[®] Mouse Genome 430 2.0 arrays at 45°C in a rotator mixer at 60rpm, overnight. The chips were washed with Non-Stringent wash buffer and stained with

SAPE Stain Solution and the Antibody solution automatically by the Fluidics Station 450. Also, the fluidics station automatically washed the chips before they were scanned on the GeneChip Scanner 3000, both supported by the software GCOS. Affymetrix Mouse GeneChip[®] 430 2.0 array comprises 45,000 probe sets representing over 34,000 well-substantiated mouse genes.

2.2.8 Real Time RT-PCR

RT-PCR was performed to confirm the microarray expression data obtained by bioinformatics analysis. cDNA was produced using the same total RNA samples used in the microarray analysis. For cDNA synthesis, QuantiTect Rev. Transcription kit was used and 1µg of total RNA from murine AB2.2 cells uninfected and infected and 30ng of total RNA obtained from esDCs uninfected and infected was transcribed. Manufacturers instructions were used and basically, sample RNA was mixed with water in the presence of RNase and incubated at 42°C for 2 minutes, this was followed by the addition of polymerase and nucleotide mix plus 10x buffer. The cocktail was incubated for a further 20 min at 42 °C.

Primers were designed using the primer3 website [<http://frodo.wi.mit.edu/primer3>] in a way such that they would overlap between two consecutive exons, they would have GC content > 45% and result in a product size between 150 and 200bp. The primers were ordered from SIGMA at 100µM concentration. The RT-PCR reactions were performed using SYBR green dye from Quantace SensiMixPlus SYBR kit. SYBR green binds to double stranded DNA and absorbs light at 488 nm and emits green light at 522nm. A STRATAGENE Mx3000P RT-PCR machine was used. The RT-PCRs were performed following the manufacturers instructions using temperatures and cycle times as indicated i.e. one cycle of 95°C 10min, followed by 40/45 cycles of 95°C 15 sec, 58/60°C 30sec, 72°C 30sec and then one cycle of each 95°C 60sec, 55°C 60sec, 95°C 60sec.

Each sample was run in triplicate for each biological replicate. To test the primers for specificity and quality, efficiency curves were performed and dissociation products were obtained.

The Ct (threshold cycle) values obtained were analyzed for relative quantification. The method employed uses $\Delta\Delta C_t$ value to compare the Ct value of a target gene to the Ct value of the control gene.

2.2.9 Dendritic cell differentiation

2.2.9.1 Differentiation of murine ES cells into dendritic cells

Murine AB2.2 ES cells were induced to differentiate into dendritic cells following the protocol published by Dr. Fairchild (Fairchild *et al.*, 2000; Fairchild *et al.*, 2003; Fairchild *et al.*, 2007). AB2.2 (Bradley *et al.*, 1984) mouse ES cell line at passage 9 were grown with Knockout Dulbecco's Modified Eagle's Medium (DMEM) optimized for ES cells, 15% HI-FBS (Hyclone # CPC0285), 2mM L-Glutamine; 1mM Sodium Pyruvate, 1x MEM-NEAA, 1:1000 of 2-ME stock solution (70 μ l of 2-ME 99% in 20ml water), unfiltered. After thawing, the cells were grown for 2 passages on irradiated feeder cells STO's/SNL 76/7 and then for two passages in media containing 500-1000U/ml LIF in order to eliminate the feeder cells from the culture. ES cells were then seeded at 4×10^5 cells in 20ml medium without LIF in Petri dishes and grown for 14 days until Embryoid Bodies (EBs) were formed. Fourteen day old EBs were seeded in 20 ml of medium containing recombinant mouse GM-CSF 25ng/ml and recombinant mouse IL-3 200WHOSU/ml in culture dishes. EBs appeared as cystic or non-cystic floating cluster of cells. After 48 hours on culture dishes, the EBs attached to the culture plastic and some of them started to beat as a sign of 'good health', some did not attach and were discarded during subsequent medium change. In the presence of rmGM-CSF and rmIL3, EBs started to produce, from the edge of the attached site, DC-like cells that looked lightly attached to the plastic named here esDC. EsDCs were harvested by gently rinsing the surface of the EBs with media.

2.2.9.2 Bone marrow extraction and dendritic cells differentiation

Mice 129/Sv were killed at 5-10 week of age and sprayed with 70% ethanol, the back legs were freed by cutting the skin and the femur and the tibia bones were cleaned from the muscle. The bone marrow was extracted from these bones. In a new Petri dish containing 10ml of RPMI-1640 media supplemented with 1x penicillin/ streptomycin

antibiotic and 2% HI-FCS, a 25g needle was inserted inside the bone and the cavity flushed with about one ml of media. The resulting threads of bone marrow were broken by flushing with a 5ml syringe minus a needle. Finally, the 10 ml of media containing isolated cells was transferred into a 15ml tube and allowed to settle for 5min. The supernatant was aspirated without touching the bottom of the tube and transferred into a 50ml falcon tube and the cells were centrifuged at 1200rpm (242g) for 10min. The cells were resuspended in filtered IMDM media containing 10% HI-FCS, 2mM L-Glutamine, 1mM Sodium Pyruvate, 1x MEM-NEAA, 1:1000 of 2-ME stock solution prepared (70µl of 2-ME 99% in 20ml tissue culture water) and 1x of penicillin/streptomycin and counted. The volume was adjusted to give $\sim 2 \times 10^6$ cells in 10ml of media per 25cm² flask. To the media was added rmGM-CSF 500 WHO Standard Units/ml and rmIL-4 at 150 WHOSU/ml. The cells were incubated for two days at 37°C prior to changing 75% of the medium. Another incubation period of 4 days at 37°C without disturbing led to the development of BMDC which were harvested from day 6 to 9 of incubation.

2.2.9.3 Antigen presentation assay

Murine esDCs and BMDCs were seeded at 1×10^5 cells per well in 96 well plates with flat bottoms with ratios of 1:5, 5:1 or 1:1 (each one in triplicate) of T cell line MF2.2d9 cells in 150µl of medium specific for each DC cell. Whole OVA protein was added at 10µg/ml and incubated over night. As a negative control, either DCs were seeded alone or with T cells 1:1 either without specific antigen or with TNF α 5000 WHOSU/ml. As positive control 3×10^5 MF2.2d9 T cells were incubated with 5µg/ml of ConA. All cells were incubated for 24 or 48 hours at 37°C and the supernatants obtained without disturbing the cells were stored at -20°C.

2.2.9.4 Cytometric Bead Array

The concentration of cytokines was measured with Cytometric Bead Array (CBA) Mouse inflammation kits which detects the cytokines IL-6, IL-10, IL-12, TNF, MCP-1 and IFN γ . The detection limits are different for each cytokine and they are 5pg/ml, 17.5pg/ml, 10.7pg/ml, 7.3pg/ml, 52.5pg/ml and 2.5pg/ml respectively. Also, Mouse CBA IL-2 Flex Kits were used to measure T cell activation. Manufacturer's instructions were followed. Briefly, standard curves for each cytokine were prepared and then the

control dilutions of experimental supernatants were incubated with cytokine specific beads. After washing and incubation with detection Antibody, the beads were washed once more and read on the FACSaria. The data obtained was processed with FCAP Array software which quantifies the concentration of the sample in relation to the standard curve of each cytokine.

2.2.10 Illumina microarray hybridization

Manual instructions were followed. Briefly, Biotin-labeled cRNA was synthesized from 300ng total RNA with the TotalPrep RNA Amplification kit (Ambion, Foster City, CA, USA). The hybridization mix containing 1500ng of labeled cRNA was prepared according to the Illumina BeadStation500x System Manual (Illumina, San Diego, CA, USA). The hybridization of Illumina MouseWG-6 v1.1 Expression BeadChip array was done incubating the chips at 58°C over night on the BeadChip Hyb Wheel. The BeadChips were washed with E1BC solution for 15 min, then washed in 100% Ethanol for 10 min and a final wash in E1BC for 2min. The blocking reaction was performed using Block Buffer E1 on a rocker mixer for 10 min. The staining reaction was performed using 2ml of buffer E1 with 1µg/ml of Cy3-streptavidin followed by a 5min wash with buffer E1BC. The BeadChips were then dried by centrifugation and scanned using the Illumina BeadStation 500 platform operated by Illumina BeadArray Reader software.

3 Characterization of the interaction of *S. flexneri* and *S. Typhimurium* with undifferentiated murine embryonic stem cells

3.1 Introduction

3.1.1 *Salmonella* interaction with *in vitro* models

In vitro models are important tools for studying biology at the cellular level. Cell-based systems have been applied successfully in many areas of basic and applied research such as the evaluation of novel drugs, for example in target identification. They are also used routinely in the assessment of the safety of new chemical compounds with therapeutic potential. “Compounds can be flagged or classified earlier in drug development and consequently this can save time, money and animals in pre-clinical toxicity studies,” writes Silvio Albertini from La Roche (Albertini *et al.*, 2006).

Infectious disease studies utilising *in vitro* cellular models have been largely exploited to investigate the intimate interactions between pathogen and host cells, and such approaches have contributed to our understanding of how pathogens are able to interact with a single cell or groups of related cells. Although host tissues are inevitably much more complex than the *in vitro* systems, the latter give us the opportunity to closely observe host-pathogen interactions in a controlled environment. A further important consideration is the easy availability of *in vitro* systems and their economic accessibility compared to the costs of setting up and maintaining animal facilities, not to mention the ethical issues that *in vivo* animal experimentation pose. Both primary and transformed cells can be examined during *in vitro* studies. However, over the years, certain transformed cell types have emerged as favoured options for cellular studies involving pathogens. This is, in part, because the ease of handling of such cells and the favourable exploitation of a particular cell type stimulates further studies as researchers become familiar with these cell lines. Examples of transformed cell types frequently used to

study host cell-pathogen interactions include HeLa, CaCo, Henle, MHO, and Hep2 cell lines.

Murine embryonic stem (ES) cells have been the subject of intense investigation, as they are readily culturable *in vitro* but retain pluripotency and can be driven down different differentiation pathways using simple stimuli. Indeed, stem cells are potentially exploitable in many areas of biology both in murine and human systems. Mouse ES cells are a ‘young’ model of investigation and relatively little is understood about them but the expectations in medical applications are quite high. In fact it seems from recent research that ES cells are promising to contribute to curing diseases as far ranging as cancer (Lisowski & Sadelain, 2008), Alzheimer’s (Korecka *et al.*, 2007), diabetes (Santana *et al.*, 2006) and Parkinson’s (Lindvall, 2003). Stem cells have the potential to play an important role in infectious disease research but their role in basic research and studies on pathogen-host interactions still needs to be explored.

ES cells can be driven to differentiate into cell types which are either challenging to isolate from the body, difficult to maintain *in vitro* or the limiting factor in their application. In fact, primary cells are difficult to produce in sufficient quantity and can be prone to batch-to-batch variability in quality, depending on the source (Thomson, 2007). ES cells are attractive because they can be subjected to gene targeting or random mutagenesis to investigate the impact of a particular genetic alteration or mutation (Brault *et al.*, 2006). Moreover, ES cells are the only truly immortal stem cells and most importantly usually maintain a normal diploid karyotype, which renders them a suitable model for developmental studies. They can also be implanted into female mice and used to generate transgenic or knock out mouse lines (Gorba & Allsopp, 2003).

This chapter reports on investigations into the ability of murine ES cells to be infected by Enterobacteria such as *S. flexneri* and *S. Typhimurium*, and compares these interactions to those observed with ‘traditionally’ exploited cell lines such as human epithelial cell derived Hep2 cells or J774A.1, a mouse macrophage-like hybridoma cell line. The murine ES cells predominantly used in this study are AB2.2, male (XY) cells derived from the inbred mouse line 129Sv/Ev (Adams *et al.*, 2005; Ramirez-Solis *et al.*, 1995). The cells were originally derived from *hprt*-deficient cells using cre recombination across *loxP* sites embedded in two complementary but non-functional

fragments of the hypoxanthine phosphoribosyl transferase (*hprt*) gene (Ramirez-Solis *et al.*, 1995). For experimental purposes, AB2.2 ES cells were maintained in feeder free culture in medium containing leukaemia inhibitory factor (LIF), a member of the IL-6 family, which maintains the cells in a self-renewing state through interactions with the gp130 receptor and via JAK/STAT pathway activation.

Other cell lines utilised here were Hep2 and J774A.1, which are laboratory adapted and are widely used in the study of infectious disease (Finlay & Falkow, 1988). However, their real karyotype is somewhat dubious and controversial. The Hep2 cell line, for example, was first derived from a laryngeal carcinoma but it seems that it later became 'contaminated' with HeLa cells, giving them an unknown profile that cannot safely be related to any other cells in the body (Nelson-Rees *et al.*, 1981). Nevertheless *in vitro* studies exploiting these cells have proved to be very important in revealing aspects of the complex intracellular survival mechanisms of both *Shigella* and *Salmonella* bacteria (Finlay & Falkow, 1988). It is experimentally well established that *Shigella* can induce an active form of self-phagocytosis through the actions of a (plasmid encoded) Type III Secretion System (TIISS) (Ohya *et al.*, 2005). Once inside the cell, *Shigella* frequently escape from the endosomal vacuole in Hep2 and other cells to live freely inside the cell cytoplasm (Sansonetti *et al.*, 1986). Here the bacteria can propel themselves through the cell via the synthesis and exploitation of a 'comet' like actin tail (Suzuki *et al.*, 1996). *Salmonella* uses a very similar technique of cell invasion whereby a TIISS present on Salmonella pathogenicity island-1 (SPI-1) induces active ruffling of the cell membrane and phagocytosis. However, in contrast to *Shigella*, *Salmonella* normally reside inside the cells in a vacuole-limited area called the Salmonella Containing Vacuole (SCV) and replicate through the actions of proteins carried on a second TIISS present on SPI-2 (Kuhle *et al.*, 2006). *Salmonella* and *Shigella* are able to resist the killing activity of host cells using a number of additional systems (Ohl & Miller, 2001). *Shigella* can induce apoptosis of eukaryotic cells and can mediate cell to cell spread (Hilbi *et al.*, 1998). However, it is still not clear how *Salmonella* escape the eukaryotic intracellular environment and spread inside the host body, although macrophage trafficking does play a key role (Sukhan, 2000). An important reason for studying these pathogens is found in their broad distribution and high disease burden within developing countries and elsewhere. *Shigella* is now more common in developing countries where it is responsible for the death of young children (Sansonetti, 2006). On the other hand,

Salmonella has remained a significant problem in the USA, Japan, and Europe due to transmission in the food chain. In developing countries the incidence has increased thanks to the occurrence of other infectious diseases like HIV and malaria (WHO, 2002).

The attractiveness of any new *in vitro* model will be dependent on the experimental techniques, tools, and reagents available to the research community. Here, a new *in vitro* model based on murine ES cells was investigated for its potential in studies on host-pathogen interactions. Initially, ES cells were examined for their susceptibility to bacterial infections to discover if they could sustain the intracellular survival of invasive bacteria.

3.2 Results

3.2.1 The interaction of *Shigella flexneri* with murine ES cells

3.2.1.1 The ability of *S. flexneri* Sh42 to invade Hep2 cells

In order to optimize cell based invasion assays, Hep2 cells were exploited as a control cell line with known susceptibility to *S. flexneri* infection. Hep2 cells are a human epithelium cell line originally derived from a laryngeal carcinoma. Initially Hep2 cells were infected independently at a multiplicity of infection (MOI) of ~ 100 with *S. flexneri* Sh42 with or without the plasmid pJKD18 which directs the expression of the green fluorescent protein (GFP) constitutively. *S. flexneri* Sh42 is derived from the virulent wild type strain M90TS serotype 5 and harbours a point mutation of A to G in the gene encoding the protein disulfide bond catalyst DsbA at position 33 in the open reading frame (Yu *et al.*, 2000). The attenuated *S. flexneri* Sh42 was used in all preliminary experiments for safety reasons because wild type *S. flexneri* M90TS is highly infectious. The colony forming units (CFUs) shown in Figures 3.1 and 3.2 are the means of triplicate counts from each of three replicate wells. *S. flexneri* Sh42 was readily able to invade Hep2 cells as deduced by the classical gentamicin susceptibility assay, although the levels of invasion were likely to be reduced compared to wild type *Shigella* due to the impact of the *dsbA* mutation (Figure 3.1). This is most probably due to the defective ability of this mutant to spread from cell to cell as described by Yu *et al* (Yu *et al.*, 2000). Also, the observed reduction in bacterial cell count after 2 hours compared to 4 hours could be due to the heavily infected cells dying by some mechanism releasing bacteria into the media containing 50µg/ml of gentamicin antibiotic .

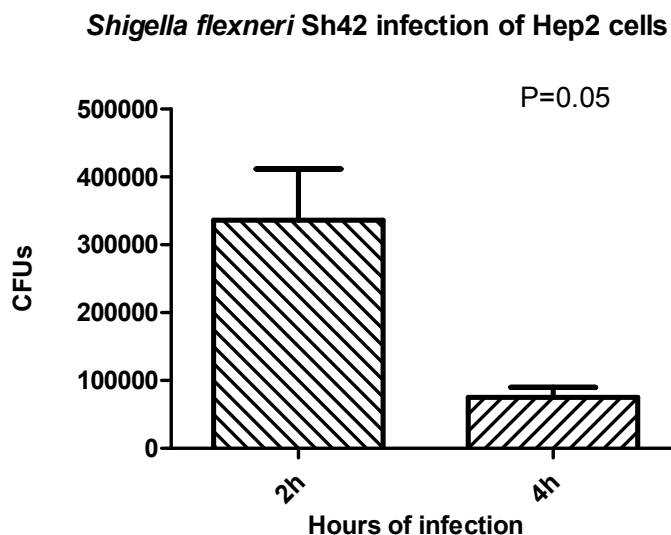


Figure 3.1 Bacterial CFUs from gentamicin assay on Hep2 cells with *S. flexneri* Sh42 at MOI 100

The CFUs are reported as the arithmetic mean of triplicate counts per three wells of a 24 well plate at each time point. The bacteria counts are significantly reduced at 4h infection. This mutant does not exhibit the infection trend expected with the wild type M90TS. The error bars represent 1 standard deviation (SD) and the P value is obtained from a non-parametric Mann-Whitney test.

Figure 3.2 reports the CFU counts resulting from the gentamicin assay performed using *S. flexneri* Sh42 harbouring the plasmid pJKD18 (Sh42/18). These experiments were performed to investigate if the presence of the plasmid significantly affects the behaviour of the *Shigella* bacteria during *in vitro* infection and invasion process. The data indicates that the plasmid does not have a dramatic impact on bacterial behaviour during Hep2 infection.

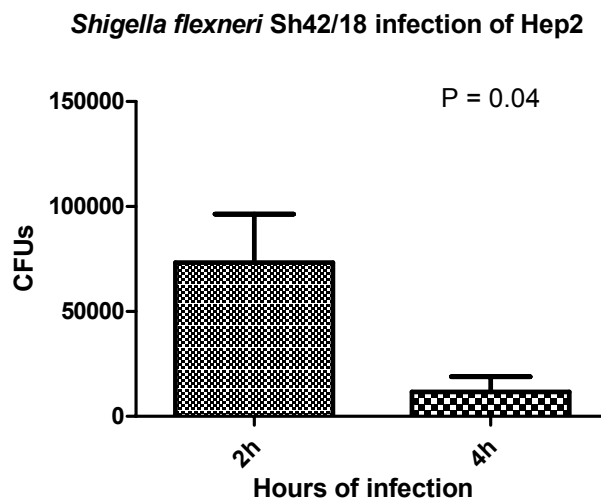


Figure 3.2 Bacterial CFU counts at 2 and 4h infection of Hep2 with *S. flexneri* Sh42 harbouring the plasmid pJKD18 (Sh42/18)

The CFUs are reported as the arithmetic mean of three triplicate counts per three wells of a 24 well plate at each time point. This experiment confirms that the expression of the plasmid pJKD18 does not further attenuate the strain significantly and that the plasmid driving the expression of GFP can be used in flow cytometry and confocal analysis. The error bars represent 1 SD and the P value is obtained from a non-parametric Mann-Whitney test.

These preliminary experiments demonstrate that, under the experimental conditions employed, the behavior of *S. flexneri* Sh42 during *in-vitro* invasion was equivalent to that reported by Yu 2000, who found that this strain is unable to spread from cell to cell and is attenuated (Yu *et al.*, 2000). *S. flexneri* Sh42 harbours a mutation in DsbA a protein involved in disulphide bond formation (Yu, 1998). Although this strain behave differently from the wildtype strains, it was chosen for safety reasons and because it was previously described. Indeed, it was of particular importance to establish how the techniques and strains used in this study worked in well characterised *in vitro* model cells. Such comparative studies would enable the identification of any differences observed during the infection of a new *in vitro* cellular model such as ES cells. Consequently it should be more feasible and reliable to assign any observed phenotypic differences to the nature of the cell line instead of the experimental design.

3.2.1.2 Flow Cytometric characterization of AB2.2 murine ES cells

Due to an unfamiliarity of working with ES cells and before starting bacterial invasion experiments, AB2.2 ES cells were characterised by a number of methods including flow cytometry and microscopy. AB2.2 ES cells originate from 129Sv/Ev mice as previously described (Bradley *et al.*, 1984). The cells were routinely cultured in GMEM complete medium containing 1000 U/ml of LIF on gelatin coated culture flasks. The cells were passaged less than 35 times by routine enzymatic treatment every two days. After ES cells had been successfully propagated and shown to be intact and uncontaminated they were analysed using FACS analysis, monitoring the expression of well documented typical ES cell markers (Figure 3.3). The ES cells were stained with labelled antibody directed against surface markers such as Integrin $\alpha 6$ (Cooper *et al.*, 1991) conjugated with the fluorochrome APC, Stage Specific Embryonic Antigen-1 (SSEA-1) (Solter & Knowles, 1978) conjugated to PE fluorochrome and with the internal marker Oct3/4 also conjugated to PE. For the latter intracellular marker, ES cells were reversibly permeabilised with saponin buffer before incubation with the antibody and washed twice with the same buffer after staining. ES cells were also analysed for the expression of CD44, a protein that has been reported to interact with pathogens during eukaryotic cell invasion (Garcia-del Portillo *et al.*, 1994; Skoudy *et al.*, 2000). The cells were analyzed on a Becton Dickinson FACSAria Sorter using DIVA software for the data analysis.

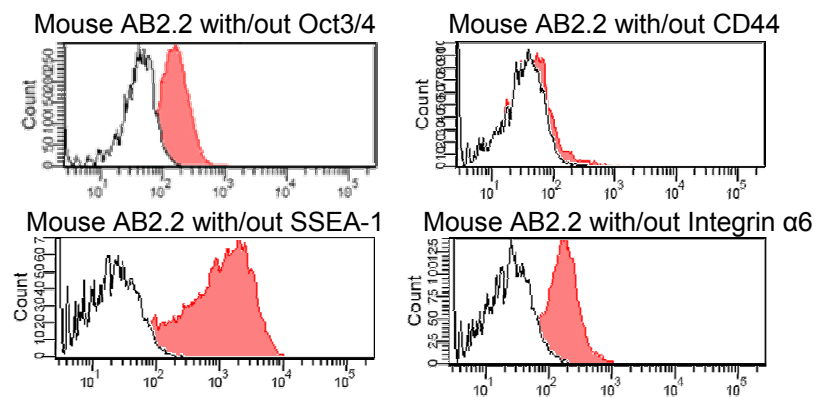


Figure 3.3 Flow cytometric characterization of AB2.2 murine ES cells

AB2.2 murine ES cells, passage 12 (p12) were characterized by flow cytometry using antibodies to the surface markers Integrin α 6, SSEA-1, CD44 as well as the intracellular marker, Oct3/4 (red peaks) compared to their relative isotype controls (white peaks). The data clearly indicate that under the growth conditions used the mouse cell line AB2.2 expressed markers characteristic of pluripotent and self-renewing ES cells whilst being negative for CD44.

3.2.1.3 Gentamicin assay on AB2.2 mouse ES cells exposed to *S. flexneri*

AB2.2 murine ES cells were exposed to *S. flexneri* Sh42 with or without pJKD18 at an MOI of ~ 10 or 100 and subjected to a standard gentamicin assay. In Figure 3.4 it can be observed that the CFU counts are lower after 4h infection and are significantly lower if the infection was performed at MOI 100. This is probably due to the fact that at MOI 10 lower numbers of bacteria enter each single cell.

Murine ES cells AB2.2 infected with *Shigella flexneri* mutant Sh42

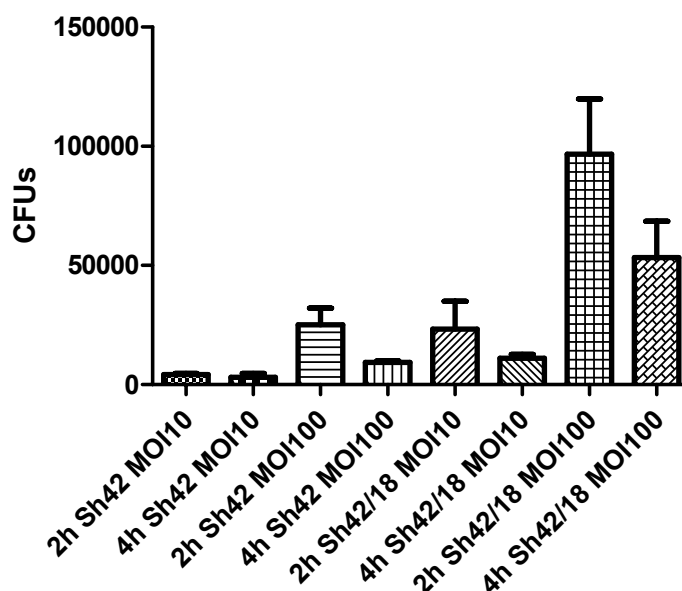


Figure 3.4 CFU counts from gentamicin assays performed on AB2.2 with *Shigella flexneri* Sh42 with and without plasmid pJKD18 at MOI 10 and 100

The histograms show the levels of *S. flexneri* Sh42 and Sh42(pJKD18) CFUs detected after an invasion assay performed on AB2.2 murine ES cells at MOI 10 and 100 after 2 and 4 h incubation time. The data in this histogram demonstrates a difference in the CFUs recovered from Sh42 and Sh42/18 infected cells. This data suggest that the Sh42/18 mutant is more invasive or it is more viable after incubation with ES cells than Sh42. The reasons for these differences were not investigated further. The error bars represent 1 SD and the P value is obtained from a non-parametric Mann-Whitney U-test performed on triplicate wells.

3.2.1.4 Gentamicin assay using wild type *S. flexneri* M90TS and AB2.2 mouse ES cells

Wild type *S. flexneri* serotype 5a strain M90TS was used for these experiments, which were performed in a CL3 containment laboratory under the supervision of Dr. Jun Yu. Although *S. flexneri* is a CL2 pathogen in the UK it was deemed prudent to keep these bacteria in a higher containment environment to avoid potentially exposing other workers to this highly infectious pathogen. Mouse ES cells were grown and then moved inside the CL3 facility for the assay. *S. flexneri* M90TS was grown as previously described but, due to the absence of a spectrophotometer, the bacterial culture OD₆₀₀ was not checked before the assay. During this experiment ES cells were maintained in medium without foetal calf serum (FCS) and no antibiotic selection was used other than the gentamicin selection during the last 2 or 4 hours of incubation. The arithmetic mean of CFU counts resulting from three independent experiments is represented in Figure 3.5.

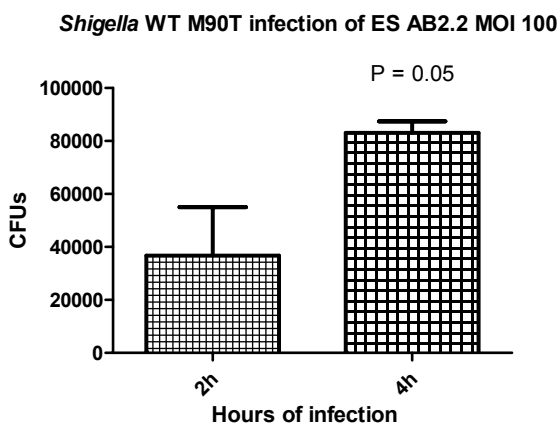


Figure 3.5 CFU counts obtained during a gentamicin assay performed on mouse ES cells AB2.2 using wild type *S. flexneri* M90TS at MOI 100

From this histogram it is clear that, in contrast to the *S. flexneri* Sh42 mutant, the wildtype bacteria are able to enter, replicate, and accumulate inside mouse ES cells as reported before in other cell lines (Yu *et al.*, 2000). The CFUs reported in this histogram are the means of three independent experiments, the error bars represent one SD and the P value is calculated with non-parametric Mann-Whitney test using data from three independent experiments.

3.2.1.5 Flow cytometric analysis of AB2.2 infected by *S. flexneri*

Gentamicin assays are very practical and have been used for many years as a method to quantify and detect bacterial invasion into cells during *in vitro* cellular infections. However gentamicin assays do not provide information on how many eukaryotic cells are infected and how many bacteria are in each cell. In order to have an idea of the dynamics of the *in vitro* infection, parallel flow cytometric analysis of infected cells was performed. For this purpose, *S. flexneri* Sh42/18(pJKD18), expressing GFP, was utilised as this approach permits tracking the intracellular or cell-associated bacteria, giving an estimation of the percentage of infected ES cells.

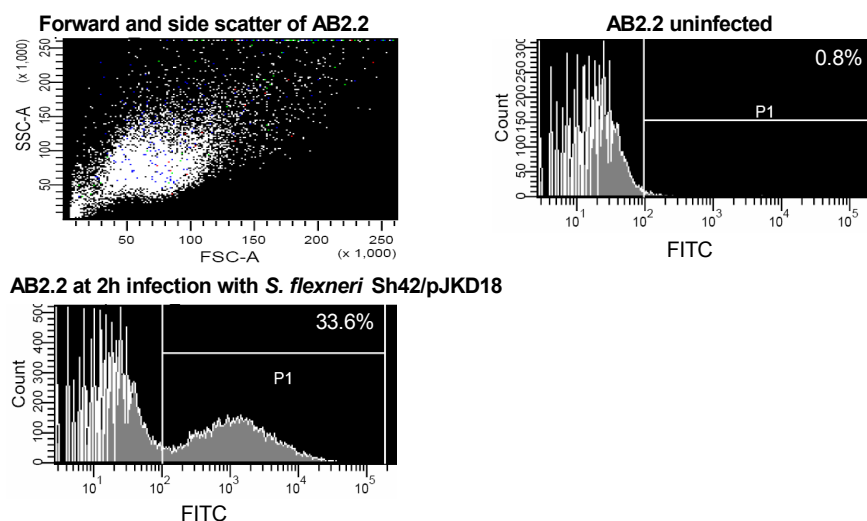


Figure 3.6 Flow cytometric analysis of murine ES AB2.2 cells during infection with *S. flexneri* Sh42(pJKD18)

Mouse ES cells were infected with *S. flexneri* Sh42(pJKD18) constitutively expressing GFP protein as described above. After 2h incubation with medium containing 50 μ g/ml gentamicin the cells were washed with warm PBS, trypsinized, and fixed with 1% paraformaldehyde. The top right dot-plot histogram represents the side and forward scatter of uninfected murine ES cells. The top left histogram represents the uninfected ES cell profile in the FITC channel. The bottom histogram represents the murine ES cells infected with Sh42(pJKD18) at 2h post-infection, the P1 selection on the right represents the emission of the GFP protein expressed by the internalised bacteria. No light emission was recorded in the FITC channel by cells infected with bacteria no-expressing GFP protein (data no shown).

3.2.1.6 Confocal imaging of AB2.2 murine ES cells infected by *S. flexneri*

Confocal microscopy was used to further observe the behaviour of *S. flexneri* bacteria inside ES cells. *S. flexneri* Sh42(pJKD18) expressing GFP facilitated viewing the bacteria under the microscope. Murine ES cells were grown on glass cover slips pre-treated with acetone and coated with 0.1% gelatin solution for two days to assure cell adhesion. AB2.2 cells adhere very gently to glass cover slips forming clusters of cells. Several well known internal eukaryotic cell vesicle markers were analysed using labelled probes. Actin filaments were stained with Texas red phalloidin and the early endosome marker EEA-1 was also visualized, together with late lysosome markers LAMP-1 and LAMP-2. After staining, the cover slips were mounted in Prolong gold containing DAPI and observed with a ZEISS laser scanning microscope (LSM-510) with 63x optical magnification.

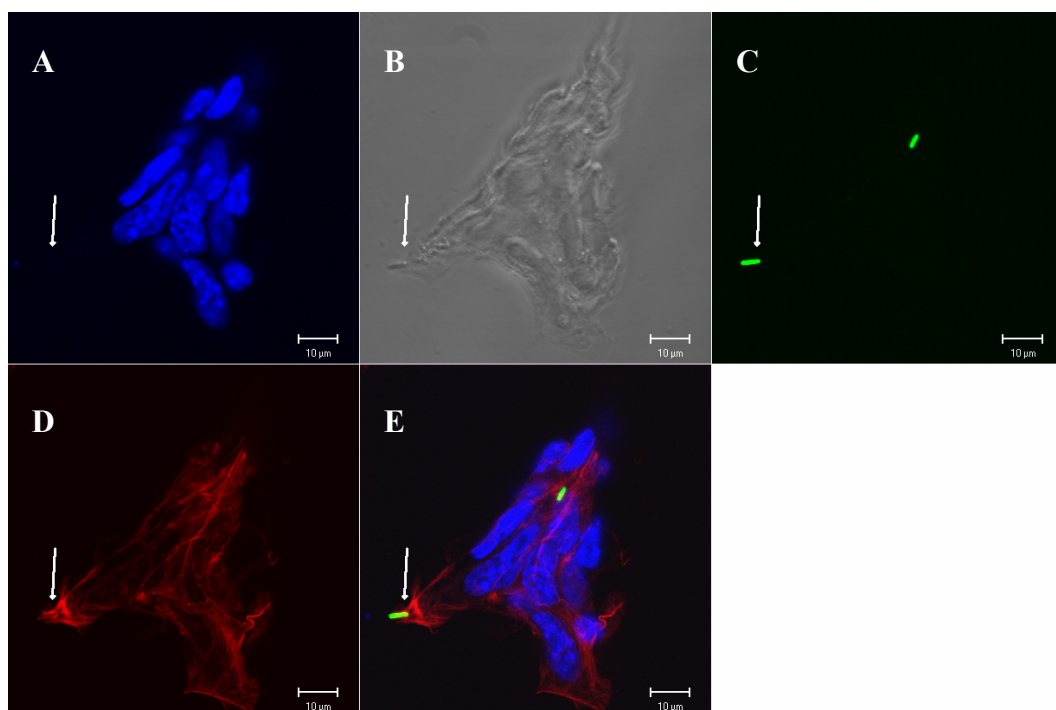


Figure 3.7 Confocal image of AB2.2 murine ES cells infected with *S. flexneri* Sh42 (pJKD18) at time point 0

From confocal observation at time 0 it can be seen that the bacteria preferentially enter cells located at the periphery of the clusters and that the initial interaction between bacteria and ES cells induces actin rearrangements around the entrance point. In this image (63x magnification) can be observed the nuclei stained with DAPI (blue) panel A, the cell cluster shape can be visualized in the phase contrast channel,

panel B; the bacteria *Shigella flexneri* expressing GFP (green) is reported in panel C; the actin filaments were stained with phalloidin TexasRedX (red) panel D; the combination of all the channel can be observed in panel E.

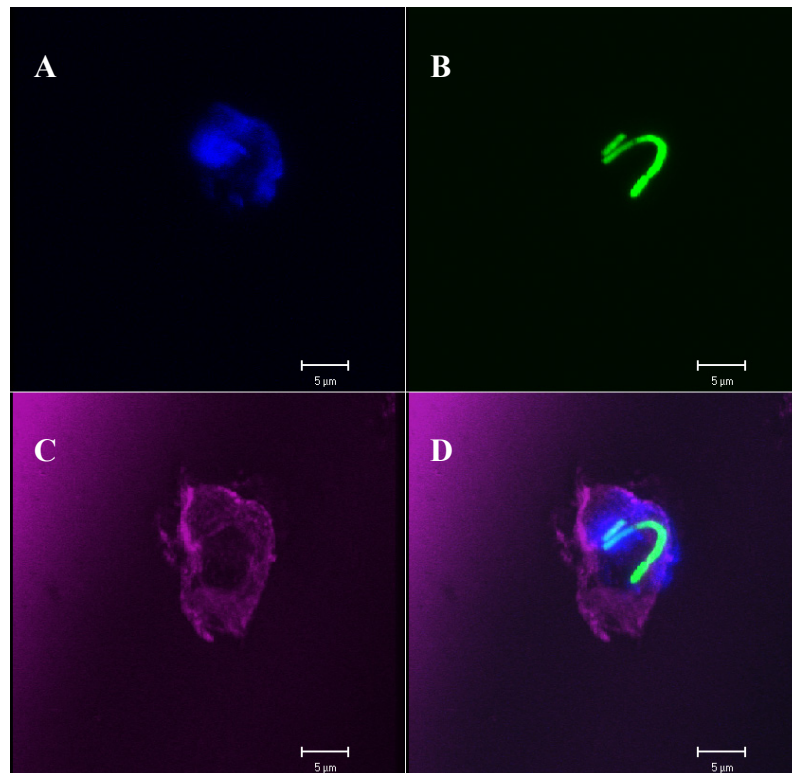


Figure 3.8 Confocal image of AB2.2 murine ES cells after 30 minutes infection with *S. flexneri* Sh42(pJKD18)

AB2.2 murine ES cells were infected with *S. flexneri* Sh42(pJKD18). This image (63x magnification) was obtained after 30 min incubation in media containing 50 μ g/ml of gentamicin from a Z-stack projection. It can be observed that after 30 min the bacteria have already escaped the vacuole and are multiplying inside the cell cytoplasm. The nuclei were stained with DAPI (blue) panel A, the bacterial express constitutively GFP (green) panel B, the early endosome marker EEA-1 with APC-Cy7 conjugated secondary antibody (purple) panel C; the combination of all the channels can be observed in panel D.

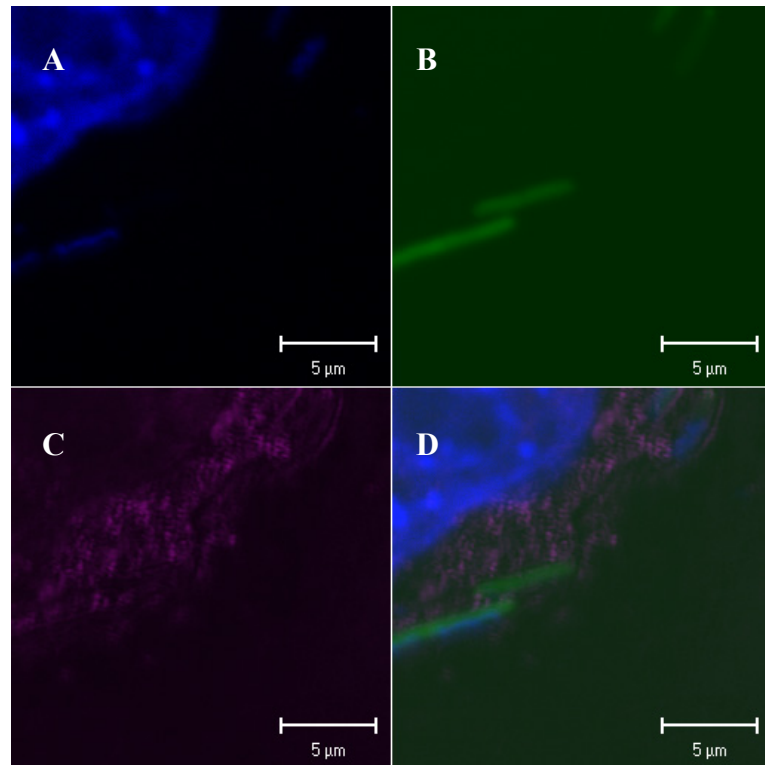


Figure 3.9 Confocal image of AB2.2 murine ES cells at 2h infection with *S. flexneri* Sh42(pJKD18)

After 2h infection of mouse ES cells with *S. flexneri* Sh42(pJKD18), the ES cells were stained with the lysosome marker LAMP-1 then with APC-Cy7 secondary antibody. This experiment investigated whether *Shigella* has the same behaviour inside mouse ES cells as inside other differentiated cells. From the confocal investigation (63x magnification), It is apparent that there is no obvious overlap of the LAMP-1 marker with the green bacteria (GFP). The nuclei are stained blue with DAPI. Panel A, nuclei blue, panel B green bacteria, panel C LAMP-1, panel D overlapping of all the channels.

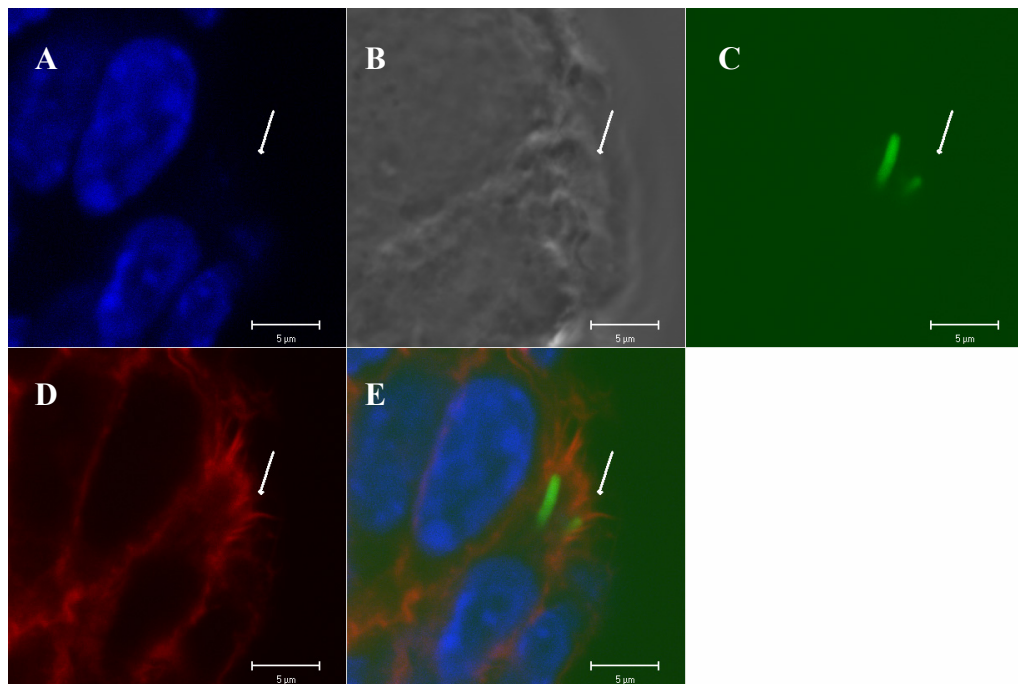


Figure 3.10 Confocal image of AB2.2 murine ES cells at 2h infection with *S. flexneri* Sh42(pJKD18)

ES cells were infected as described with *S. flexneri* Sh42(pJKD18) expressing GFP protein and incubated for 2h with medium containing 50 μ g/ml of gentamicin. From this image (63x magnification) it can be observed how *Shigella* is able to organize an actin tail even in the limited cytoplasm of mouse ES cells. The nuclei are stained with DAPI (blue) panel A, phase-contrast view in panel B, GFP expressing bacteria (panel C), phalloidin Texas Red stains the actin in red panel D and overlap of the channels is in panel E.

3.2.2 The interaction of *S. Typhimurium* with murine ES cells

3.2.2.1 Gentamicin assay of *S. Typhimurium* interaction with control J774A.1 cells

In order to validate the *in vitro* cellular infection conditions, the mouse J774A.1 hybridoma cell line was initially used as a control. J774A.1 is derived from J774.1 and is a mouse BALB/c monocyte macrophage-like cell line that grows in a semi-adherent manner to the culture flask plastic, predominantly as a monolayer. The cells were grown in 24 well plates until 90% confluent and infected with either wild type *S. Typhimurium* SL1344 or SL1344 harbouring the plasmid vector p1C/1. The vector p1C/1 is described in the reference (McKelvie *et al.*, 2004) and carries the gene for GFP protein expressed under the control of 166bp of the *ssaG*'s promoter. SsaG is normally encoded on SPI-2, a TIISS involved in pathogen intra-vacuole survival. The gentamicin assay was performed as described in M&M using an MOI of ~ 100. Here are reported the CFU counts as the arithmetic mean of three counts per dilution; the CFU of a representative assay are shown in Figure 3.11.

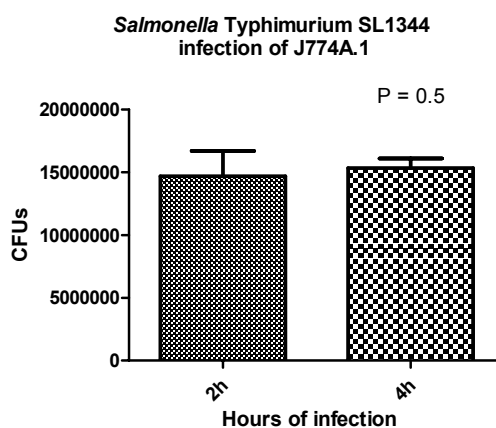


Figure 3.11 Gentamicin assay on mouse J774A.1 cells infected with *S. Typhimurium* SL1344

This histogram reports the mean CFU calculated from three wells during infection with *S. Typhimurium* SL1344 on the mouse J774A.1 macrophage cell line at an MOI of ~100. The CFUs were counted at 2h and 4h post-infection. The histogram shows that the bacteria enter the cells in great numbers and the bacterial counts are similar at 2h and 4h post-infection. J774A.1 cells are able to phagocytose both particles and external pathogens, thus facilitating bacterial entrance. The error bars represent 1 SD of triplicate experiments and the P value was calculated with non-parametric Mann-Whitney U-test.

3.2.2.2 Flow cytometric analysis of *S. Typhimurium* infecting mouse J774A.1 cell line

In order to perform flow cytometric analysis, J774A.1 cells were infected with *S. Typhimurium* expressing GFP under control of the *ssaG* promoter. The protein *ssaG* is part of the TIISS present on SPI-2 which is necessary for bacterial survival inside the vacuole and is predominantly expressed by *S. Typhimurium* only after the bacteria have entered host cells. After infection and subsequent incubation with gentamicin, cells were analysed on a Becton Dickinson FACS Aria Sorter utilising DIVA software. The GFP expressing bacteria were detected in the FITC channel excited by the Argon laser.

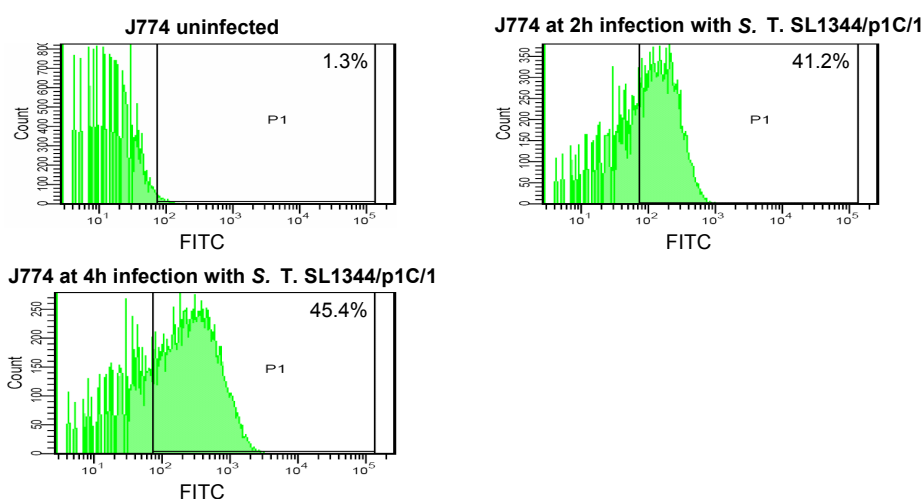


Figure 3.12 Flow cytometric analysis of murine J774A.1 cells infected with *S. Typhimurium* SL1344(p1C/1)

Infection of the mouse J774A.1 macrophage cell line with *S. Typhimurium* SL1344(p1C/1) expressing GFP protein under the control of *ssaG* promoter. The green bacteria infecting the ES cells can be followed by flow cytometry. The histograms show an increase in the percentage of infected cells between 2h and 4h post-infection. However, this apparent discrepancy with the CFU counts reported in Figure 3.11 could be due to the fact that the CFU counts give the total number of bacteria without taking in account how many cells are actually infected and the number of bacteria per cell. Also, GFP can be very stable protein once expressed and its presence does not necessarily reflect bacterial viability. Also cells infected with bacteria no-expressing GFP protein were investigated for light emission in the FITC channel.

3.2.2.3 Gentamicin assay monitoring the interaction of *S. Typhimurium* SL1344(p1C/1) with AB2.2 murine ES cells

AB2.2 ES cells were grown on 6 well plates coated with 0.1% gelatin solution and infected with either *S. Typhimurium* SL1344 or SL1344(p1C/1) at an MOI of ~ 100 in standard gentamicin assays. CFUs were enumerated and a representative histogram of these experiments is reported in Figure 3.13. In these experiments the bacterial numbers increase significantly during infection.

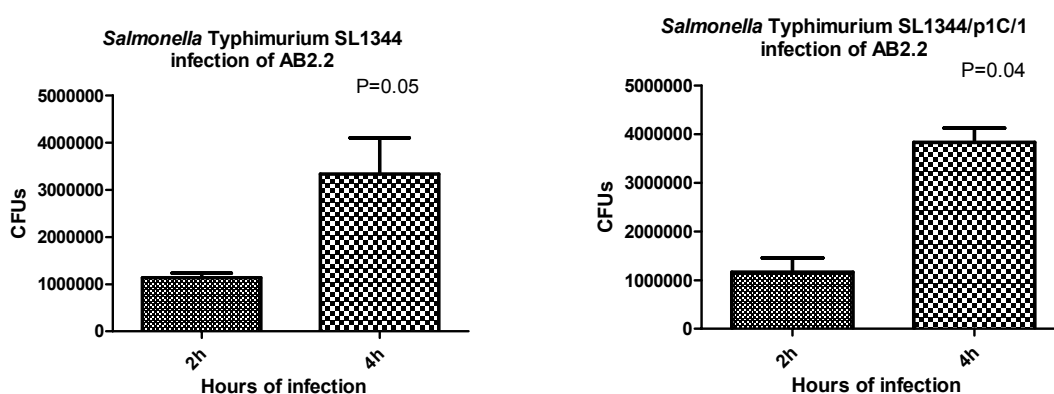


Figure 3.13 Gentamicin assay of mouse ES cells infected by *S. Typhimurium* SL1344 with or without the reporter plasmid p1C/1

The CFU counts reported in these histograms are the arithmetic mean of bacterial numbers counted in three wells detected during the infection of mouse ES cells with *S. Typhimurium* SL1344 or SL1344(p1C/1). The histograms show that *Salmonella* is able to enter and replicate inside mouse ES cells. The presence of the plasmid p1C/1 does not appear to influence the bacterial capacity to infect the cultured cells. The error bars represent 1 SD and the P value is calculated using a non parametric, one tail distribution and the Mann-Whitney test.

3.2.2.4 Flow cytometric analysis of mouse ES cells infected with *S. Typhimurium* using a time course of infection

To investigate the time progression of *S. Typhimurium* infection of AB2.2 murine ES cells, gentamicin assays were performed using the bacteria carrying the plasmid p1C/1 expressing GFP. At each hour up to 5 hours, the cells were analyzed in parallel by FACS (Figure 3.14) and by taking CFU counts (Figure 3.15). The invasion assay was carried out as described in M&M. The aim of this experiment was to investigate the rate of the bacterial entrance, replication and spread between cells. This experiment was repeated 3 times and it was always observed a steady increase of infected cells and CFU counts. The results show how *Salmonella* enter the cells and establish a significant intracellular infection within 2 hours. These results clearly demonstrate that these two techniques are complementary and together they give a more complete understanding of the *in vitro* infection profile.

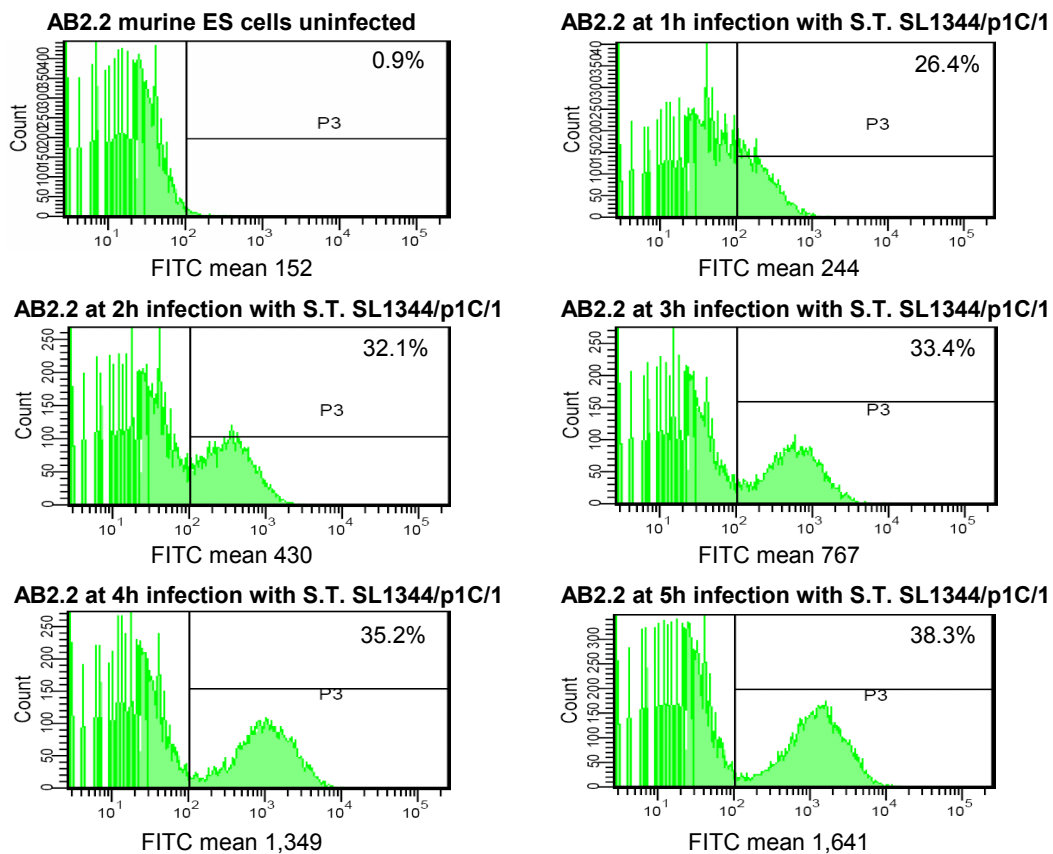


Figure 3.14 Flow cytometric analysis of time course infection of mouse ES cells infected with *S. Typhimurium* expressing GFP protein

Mouse ES cells AB2.2 were infected with *S. Typhimurium* SL1344(p1C/1) expressing the GFP protein under the control of the *ssaG* promoter. The protein *ssaG* is normally encoded in the SPI-2 locus and is expressed optimally once the bacteria are inside the host cell. The infected cells can thus be tracked by flow cytometric analysis using the 488nm Argon laser which excites GFP. The histograms presented here show the increasing percentage of infected AB2.2 cells during a 5 h post-infection assay. The mean intensity of the FITC channel emission increased over time reflecting the increasing number of bacteria inside the cells.

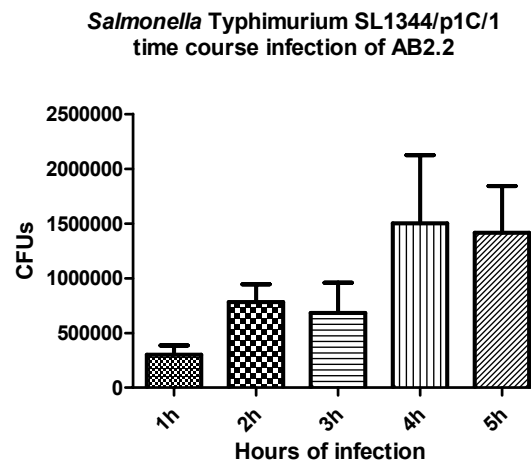


Figure 3.15 CFU counts from time course gentamicin assay of *S. Typhimurium* SL1344 infection of mouse ES cells

The histogram shows the CFUs detected during a 5h infection of ES cells with SL1344(p1C/1). The CFU counts reflect quite closely the FACS data showing a clear increase in numbers of bacteria between 2h and 4h of infection. The CFUs shown are the result of triplicate counts for three wells per time point. The error bars are 1 SD.

3.2.2.5 Confocal imaging of *S. Typhimurium* infecting AB2.2 murine ES cells

To track bacterial intra-cellular localisation, mouse ES cells were grown for two days on glass cover-slips pre-treated with acetone and coated with 0.1% gelatin solution and then infected with *S. Typhimurium* SL1344(p1C/1). After fixation at 30minutes and 1hour after infection, antibodies including rabbit anti-EEA-1, rat anti-LAMP-1 and rat anti-LAMP-2 were utilised as primary reagents on saponin permeabilised cells. Species specific secondary antibodies used were anti-rat APC-Cy7 and anti-rabbit APC-Cy7. The cover-slips were mounted in Prolong Gold containing DAPI and images were captured with the ZEISS LSM510 at 63x magnification.

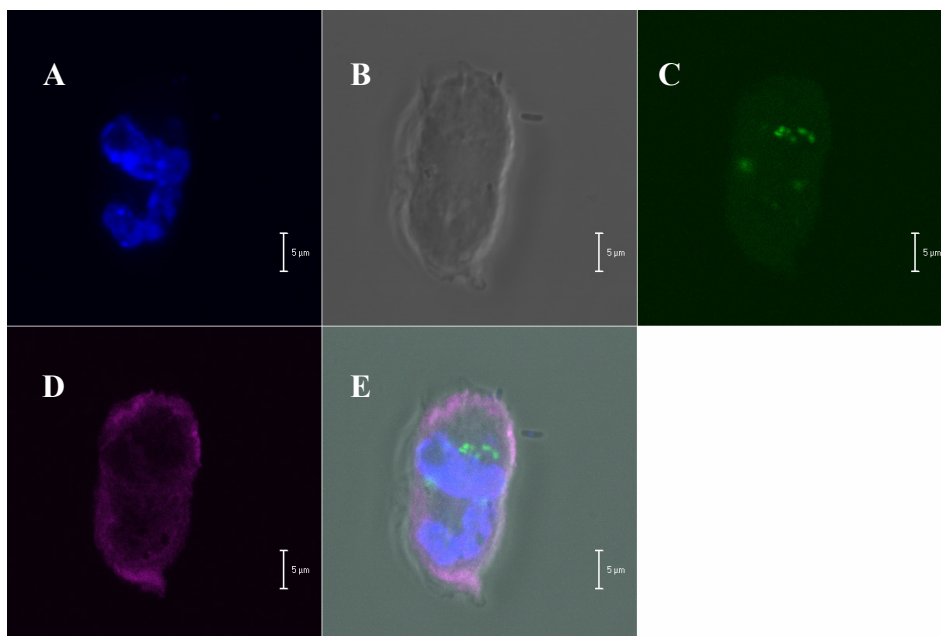


Figure 3.16 Confocal image of AB2.2 cells infected with *S. Typhimurium* at 30 minutes

Murine ES cells were infected with *S. Typhimurium*(p1C/1) detectably expressing GFP protein only when bacteria are inside the host cell. From the picture at 30 min infection, EEA1 has a sub-membrane distribution and an apparent lack of association with bacteria. Note the presence of as few bacteria outside the ES cells which are not expressing GFP. We can observe the nuclei stained with DAPI panel A, a phase contrast panel B, *S. Typhimurium*(p1C/1) in green (GFP), panel C, early endosome marker EEA1 in purple (APC-Cy7) panel D and all the channels overlapped in panel E.

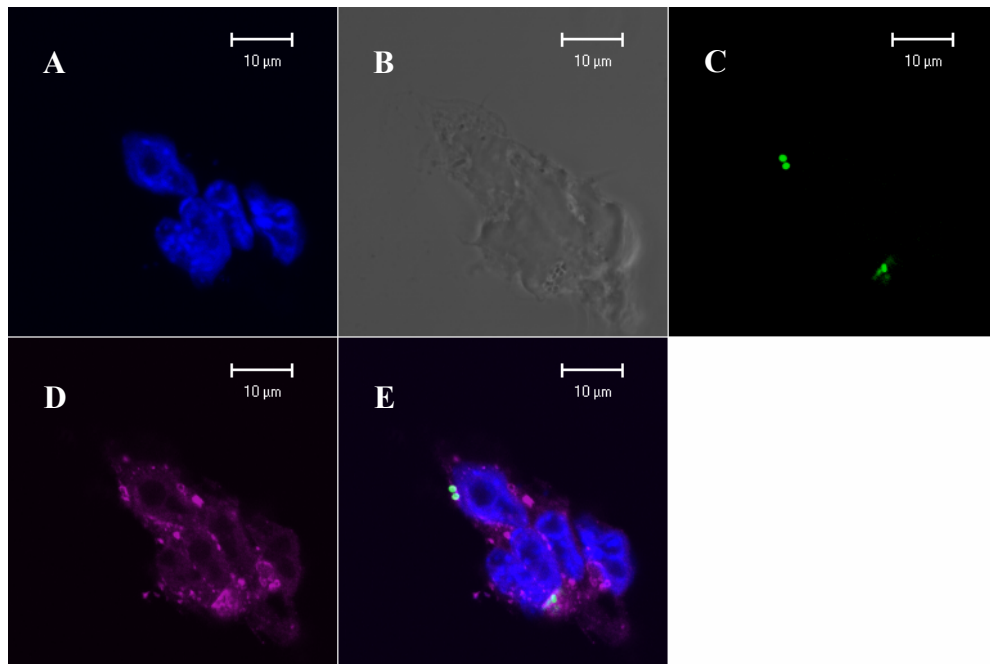


Figure 3.17 Confocal image of AB2.2 mouse ES cells infected with *S. Typhimurium*(p1C/1) at 1 h

After 1 h incubation with ES cells, the bacteria can be clearly seen co-localizing with the LAMP-1 antibody. Here the nuclei are stained in blue panel A, the phase contrast highlights the shape of the cluster panel B, the green *S. Typhimurium*(p1C/1) in panel C, the late lysosomal marker LAMP-1 in purple panel D, and all the channels combined in panel E.

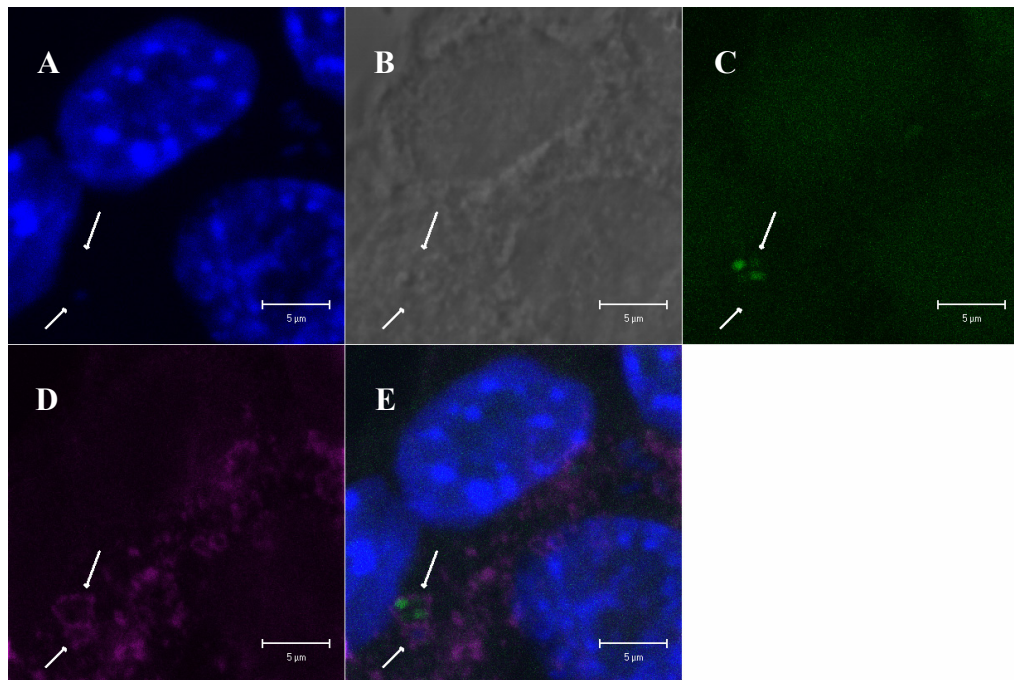


Figure 3.18 Confocal image of AB2.2 mouse ES cells infected with *S. Typhimurium*(p1C/1) at 1 h

After 1 h incubation the cells were washed, fixed and after saponin permeabilisation, stained with rat anti-LAMP-2 and anti-rat APC-Cy7 secondary antibody. LAMP-2 was visible but at an apparently lower level than LAMP-1 staining. In panel A can be observed the nuclei stained with DAPI, panel B report the phase contrast channel, panel C show the green *S. Typhimurium*(p1C/1) bacteria, panel D report late the lysosome marker-2 LAMP-2 (purple), panel E report all the channel combined. Note next to the green bacteria, a blue bacteria also inside a vacuole (white arrows).

3.2.3 Role of Type III secretion systems during infection of mouse ES cells

3.2.3.1 Gentamicin assay using the *S. flexneri mxiD* mutant interacting with AB2.2 mouse ES cells

Shigella invasion of eukaryotic cells requires the expression of a functional type III secretion system, commonly referred to as Mxi-Spa, and a cognate set of secreted Ipa invasins (Schuch *et al.*, 1999). MxiD is an outer membrane protein required for the secretion of the Ipa invasins (Allaoui *et al.*, 1993). Here, a *mxiD* mutant was used to investigate if the *S. flexneri* invasion of mouse ES cells observed in the above studies was dependent on a TIISS.

***Shigella flexneri* MxiD⁻ invasion of mouse ES cells**

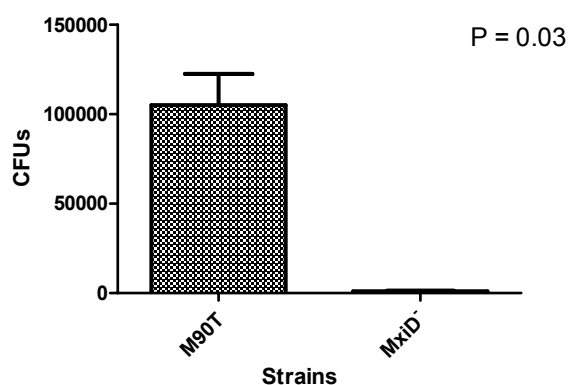


Figure 3.19 Gentamicin assay performed on mouse ES cells using *S. flexneri mxiD*⁻

CFU detected during exposure of mouse ES cells to potential invasion by the wild type *Shigella flexneri* M90TS on the left and the derived mutant *mxiD*⁻ on the right. This result highlights that *S. flexneri* utilizes a TIISS during the invasion of mouse ES cells (as *Shigella* does during the invasion of epithelial cells). The bars represent the mean of the CFUs from three replicate and the error bars represent 1 SD. This experiment was conducted with Dr. Jun Yu.

3.2.3.2 Gentamicin assay monitoring the levels of invasion of AB2.2 mouse ES cells by a *S. Typhimurium sipB* mutant

The *Salmonella* pathogenicity island 1 (SPI-1) is a complex chromosomal locus required for the productive invasion of eukaryotic cells by *S. enterica*. SPI-1 encodes a group of invasion effectors including the Sips (*Salmonella* invasion proteins A-D) that upon contact with the target cell undergo type III export from the bacterial cytoplasm and translocation into the eukaryotic cell membrane or cytosol (Hayward *et al.*, 2000a). Here, the contribution of SPI-1 to *S. Typhimurium* invasion of mouse ES cells was investigated using a TIISS associated *sipB* mutant. Gentamicin assays was performed and the CFU counts are reported in Figure 3.20.

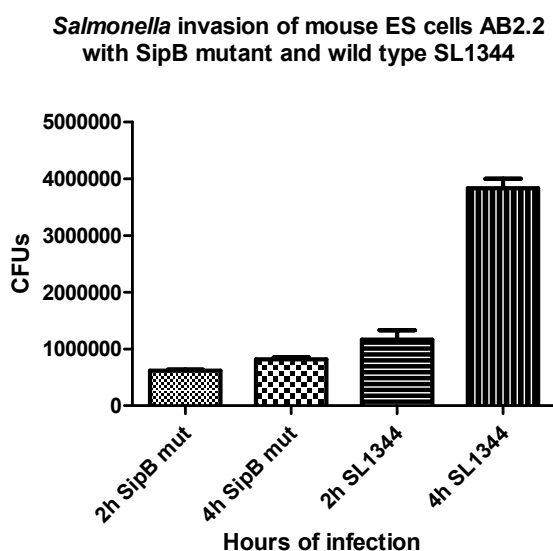


Figure 3.20 Levels of *S. Typhimurium* SL1344 *sipB* mutant invasion of mouse ES cells AB2.2 CFU counts of *S. Typhimurium* SL1344 *sipB* mutant compared to the levels detected with wild type SL1344 at 2h and 4h after infection of AB2.2 mouse ES cells. The histogram indicates that the mutant *Salmonella* enters the cells in lower numbers even though the difference with the wild type at 2h is not statistically significant using one way ANOVA (non-parametric) and Tukey's multiple comparison test. The CFU counts are reported as the arithmetic mean of triplicate count per time point and the error bars are 1 SD.

3.3 Discussion

This chapter reports data that demonstrate how ES cells can be infected by isolates of the enteropathogenic bacteria *S. flexneri* and *S. Typhimurium* using classical gentamicin assays, flow cytometric analyses, and confocal microscopic observations. Infections with *Shigella* and *Salmonella* derivatives harbouring mutations in specific TIISS were also analysed to confirm their involvement in the pathogens ability to enter during ES cells. These data confirmed aspects of the theory that mouse ES cells have the potential to be used as an alternative *in vitro* cellular model to study host-pathogen interactions.

Mouse ES cells are immortal cell lines that grow out from the inner cell mass of cultured pre-implantation mouse embryos. They can maintain the potential to support normal development of embryonic and extra-embryonic structures when re injected into blastocysts and implanted into pseudo-pregnant female mice (Cooper *et al.*, 1991). Currently, we know that these cells have specific surface and internal markers that define their nature. At the beginning of the study a few markers were selected to characterize the murine ES cell line used. The ES cells were characterized by flow cytometric analysis using conjugated antibodies specific for pluripotent cells. Two external markers were used: Integrin $\alpha 6$ /CD49f and stage-specific mouse embryonic antigen (SSEA-1), and one internal marker: Oct3/4. Integrin $\alpha 6$ is one of the first extracellular matrix proteins expressed in the developing mammalian embryo and is present throughout the embryonic tissues thereafter (Cooper *et al.*, 1991). SSEA-1 is important in the regulation of cell interactions, cell sorting development and differentiation (Solter & Knowles, 1978). Oct3/4 is a POU transcription factor involved in the regulation of pluripotent and germline cells. Oct3/4 is essential for the development of the mammalian embryo (Loh *et al.*, 2006). As shown in Figure 3.3, 90% of the AB2.2 cells cultured in LIF were positive for the integrin $\alpha 6$ /CD49f and for Oct3/4 markers, and 70% of the cells were positive for SSEA-1 markers. In contrast, ES cells were found to be negative for a differentiation marker, CD44, that can play a role in bacterial binding and internalization (Garcia-del Portillo *et al.*, 1994; Skoudy *et al.*, 2000). One of the first theories to be investigated as part of this project, was that mouse ES cells lose their pluripotent characteristics on exposure to bacteria and for this purpose Oct3/4 expression was investigated during infection (data not shown). The

experiment showed that loss of Oct3/4 does not detectably occur during infection, possibly as a consequence of the short time window of infection over which the investigations are taking place, i.e. up to several hours after infection.

The first part of this chapter reported how *S. flexneri* is able to invade murine ES cells in a manner comparable to previously described cellular models. *S. flexneri* Sh42 was described previously by Yu *et al.* 2000. The mutant Sh42 harbours a point mutation in the gene encoding DsbA protein which is required for the oxidative folding of Spa32. Spa32 is an outer membrane protein and is part of the TIISS involved in eukaryotic cell invasion. However, DsbA also has an intracellular role in Ipa secretion and in the formation of the Mxi-Spa secretion system required for intracellular spread (Allaoui *et al.*, 1993). All together it was possible to observe facets of how Sh42 interacts with the control cell line Hep2 (Figures 3.1 and 3.2) and the target cell line AB2.2 (Figure 3.4). In both cases after 4 hours incubation the CFU counted were significantly lower than the 2 hours time point. This implies that the bacteria die between 2 and 4 hours post infection. This behaviour was previously observed and reported by Dr. Yu in his paper in 1998 describing a polar *dsbA* mutant (Yu, 1998) in which he documented that this mutant was barely able to grow inside HeLa cells. As Sh42 lacks the ability to spread from cell to cell, it can be postulated that the bacteria, after intracellular proliferation, are released into the extracellular milieu as a consequence of disruption of bacterial or host cell function and are then killed by the gentamicin. Alternatively, the bacteria may be killed by other undefined mechanisms. From these experiments it can be inferred that the bacteria behave in a similar manner in Hep2 and AB2.2 ES cells in the decreased number of recovered bacteria at 4h versus 2h infection, although SH42/pJKD18 gave generally higher CFUs counts during mouse ES cells infection. Moreover, when wild type *S. flexneri* M90TS was used, an increase in CFU counts between 2 and 4 hours incubation during gentamicin selection (Figure 3.5) was observed. This observation reflects the higher infectivity of the wild-type bacteria.

Usually a plaque assay is performed to measure the entrance, growth, and spread of *Shigella* in cultured cells. Unfortunately, due to the physiology of ES cells, this was not possible since they grow in clusters and they don't form regular monolayers. Instead, in order to monitor entry, invasion and the spread of *Shigella* within ES cells, flow cytometric analysis was used to detect GFP expressing bacteria. *S. flexneri* Sh42

harbouring the plasmid pJKD18 which constitutively directs the expression of GFP protein was used in these studies. Initially, the impact of the plasmid on the behaviour of *S. flexneri* in gentamicin invasion assays was assessed. The CFU counts indicated that the bacteria carrying the plasmid pJKD18 behaved in a similar way to the original mutant strain. The results from these experiments are shown in Figures 3.2 and 3.4 panels 3 and 4. It has been reported that *Shigella* is able to infect Henle cells up to levels as high as 97% (Purdy *et al.*, 2002), such levels of invasion were not observed in our laboratory. However, it was noted that mouse ES cells became very delicate during infection and they detached quite easily from the slides or wells and even the washes with DPBS could affect the outcome of the assay. Flow cytometric analyses indicated that up to 33% and sometimes up to 42% of ES cells were infected by the mutant *S. flexneri* Sh42(pJKD18), see figure 3.6.

Confocal microscope observations were made of *S. flexneri* Sh42(pJKD18) infecting murine ES cell line AB2.2. Generally, it was observed that *Shigella* invades cells that are in a peripheral position on the cluster of cells (Figure 3.7). *Shigella* is able to routinely escape the endocytic vacuole and survive freely inside the cell cytoplasm of epithelial cells. Consequently, a serial staining experiment using antibody against the early endosome marker EEA-1 and the late lysosome markers LAMP-1 was performed. Sh42(pJKD18) did not obviously colocalize with the early endosome marker EEA-1 30 minutes post-infection (Figure 3.8). Also, Sh42(pJKD18) infected mouse ES cells staining with LAMP-1 after 1 hour (not shown) and 2 hours, revealed no obvious overlap of the cellular marker with the green bacteria (Figure 3.9). Nevertheless, mouse ES cells stained for actin with phalloidin Texas Red revealed a clear actin rearrangement during bacterial infection (Figure 3.7). Also, by 2 hours after infection it was noticed that the *Shigella* bacteria were often associated with an actin 'comet' tail of polymerised protein (Figure 3.10). It is also obvious from these observations that *S. flexneri* Sh42 bacteria have some kind of deficit in their ability to divide, as they were frequently seen as long strings of bacteria.

S. Typhimurium was subsequently used to further evaluate bacterial interactions with murine ES cells. *S. Typhimurium* is a promiscuous pathogen that can cause gastroenteritis in cattle and establishes a systemic disease in mice that mimics some aspects of typhoid fever. For this reason wild type SL1344 was used in the *in vitro*

cellular experiments. A control mouse macrophage-like cell line J774A.1 was first used to optimize the *in vitro* infection conditions. From the results of gentamicin assays it was concluded that *S. Typhimurium* SL1344 was able to invade macrophage cell line J774A.1 (Figure 3.11) and that the CFU counts at 2 hours and 4 hours infection were very similar. These data were supported by flow cytometry observations wherein SL1344 harbouring the plasmid p1C/1 expressing GFP under the control of a 166bp DNA fragment encoding the *ssaG* promoter region (McKelvie *et al.*, 2004) was employed. In *Salmonella* bacteria harbouring this plasmid, GFP is expressed optimally only once the bacteria are inside the SCV. Consequently, ES cells containing *S. Typhimurium* bacteria were detected by FACS with a 488nm Argon laser in the FITC channel. Figure 3.12 shows that at 2 hours 41% and at 4 hours 45% of the J774A.1 cells were infected, confirming that the *Salmonella* bacteria is most likely able to replicate inside the macrophage cells.

S. Typhimurium SL1344 *in vitro* infection of mouse ES cells displayed some distinct characteristics. The CFU counts from gentamicin assays doubled between 2 and 4 hours infection ($P = 0.05$). Moreover, there seems to be no difference in the invasive ability between wild type SL1344 and the bacteria carrying the plasmid p1C/1, whose CFUs also doubled between 2 and 4 hours (P value = 0.04) (Figure 3.13). Some of the difference in CFU counts observed in the *Salmonella* gentamicin assay between J774A.1 and AB2.2 cell lines could be due to the phagocytotic nature of J774A.1. This possibility was not investigated further.

In order to determine if *Salmonella* was actually invading and replicating inside mouse ES cells, a time course infection was performed and the data were analysed in parallel by both flow cytometry and CFU counts. The data illustrated in Figures 3.14 and 3.15 revealed that *Salmonella* start to enter the cells within 1 hour, during which time relatively low levels of GFP are produced. The GFP intensity increased at 2 hours post infection and the percent of infected cells increased in parallel with the CFU counts. At 3 hours after infection there was an apparent static phase, reflected also by the CFU counts. Here the bacteria might be spreading from cell to cell prior to re-growth in the new cell environment, as indicated by the increase of CFU at 4 hours. The attempt to extend the observation time of these experiments encountered technical difficulties because after a few hours of infection mouse ES cells began to detach from the culture

plate and it became difficult to obtain a reliable estimate of the percentage of infected cells because they were readily washed away.

To observe the complicated intracellular lifestyle of *S. Typhimurium* during infection of mouse ES cells, confocal observations were performed using antibodies to the early endosome antigen EEA-1, and the late lysosome markers LAMP-1 and LAMP-2. Infected AB2.2 ES cells were stained for EEA-1 at 30 minutes and 1 hour post-infection. No obvious co-localization was observed between the internalized GFP expressing bacteria and the early endosome marker, which was clearly localized under the cellular membrane (Figure 3.16). In order to investigate any potential bacterial fusion with lysosomes, lysosome markers such as LAMP-1 and LAMP-2 were used to stain AB2.2 ES cells infected with *S. Typhimurium* SL1344(p1C/1) at 1 hour. As Figures 3.17 and 3.18 show, some co-localization of these two markers with the bacteria was detected. These observations confirm that during infection of murine ES cells, *Salmonella* follow a pathway with similarities to the previously reported route through internal vacuole membranes (Ramsden *et al.*, 2007).

An important aspect of bacteria-host interaction studies is the assessment of how host cells became infected. Host cell infection (or invasion) can involve two distinct but interacting processes. The host cell can actively phagocytose the pathogen or alternatively the pathogen can actively infect the host cell. Indeed, the two processes can occur at the same time. Both *Shigella* and *Salmonella* are able to invade non-phagocytic cells, such as epithelial cells, using a protein structures present on the pathogen surface called TIISSs (Hermant *et al.*, 1995). In order to determine if murine ES cells invasion was due to an active process involving the SPI1 TIISS, mutant bacteria were employed in this study. In particular the CFUs from a gentamicin assay performed using a *S. flexneri mxiD* mutant (Figure 3.14) and a *S. Typhimurium sipB* mutant (Figure 3.15). These experiments revealed that both *S. flexneri* and *S. Typhimurium* actively infected/invaded murine ES cells using TIISS. The invasion of *S. flexneri mxiD* was significantly reduced by the lack of the MxiD protein, which is involved in the formation of the TIISS basal body. In contrast, the *Salmonella* SipB mutant exhibited a relatively small drop in relative CFUs at 2 hours post-infection, possibly due to compensation for the lack of SipB protein function by other Sip proteins. Interestingly, murine ES cells are unable to phagocytose 1 μ m latex beads (our data, not shown) further

supporting the concept that bacterial invasion into ES cells is an active process induced by the pathogen.

In conclusion, this chapter demonstrates how mouse ES cells interact with two representative Gram negative pathogenic bacteria; *S. flexneri* and *S. Typhimurium*. The data confirm that the bacteria invade ES cells at a similar level to terminally differentiate epithelial and macrophage cell lines. This observation partially confirms *in vivo* observation of how these two pathogens are able to interact with different cell types resident on the intestine epithelium and highlight some of the advantages and disadvantages of using *in vitro* cell models. Moreover, the data here generated give hope that in the future ES cells will have a role to play in infectious disease research.

4 Transcription profiling of murine ES cells infected by *S. Typhimurium* SL1344

4.1 Introduction

4.1.1 Microarrays in host-pathogen interactions studies

Microarray analysis was introduced in the mid-1990s and since then this approach has been the method of choice for large-scale gene expression studies. Microarrays provide an efficient and rapid method to investigate the entire transcriptome of a cell or cell population. Perhaps no research field has benefited more from microarray technology than the study of the interplay between pathogens and their hosts (McGuire & Glass, 2005). Figure 4.1 summarize examples of the applications that microarrays can have in infectious diseases and host-pathogen interactions studies (Bryant *et al.*, 2004). The expansion of this technology takes advantage of the recent escalation in DNA sequence resources. In fact the complete genome of a large number of pathogens has now been fully sequenced in addition to the human and mouse genomes, permitting an exhaustive investigation of host-pathogen interactions.

Host-pathogen interactions can be investigated from either the perspective of the host or from that of the pathogen. Microarrays have been designed for a large range of pathogens including *Escherichia coli*, *Leishmania* species, *Bordetella pertussis*, *Yersinia pestis* and *S. Typhimurium* (McGuire & Glass, 2005). Even without the whole genome level of sequence knowledge, shotgun microarrays can be constructed from genomic DNA libraries (Hayward *et al.*, 2000b). One intriguing feature of pathogen microarray studies is the differential expression patterns observed in a large number of genes with no known function. This is the case even in the extensively genetically mapped bacteria *S. Typhimurium* where the function of many genes has been determined. *S. Typhimurium* has been the subject of expression profile studies looking at the bacterial SCV transcriptome profile during infection of macrophages (Clements *et al.*, 2002; Eriksson *et al.*, 2003).

Microarray studies performed on host RNA responses have exploited a variety of *in vivo* and *in vitro* models of human, mouse and other species. These studies can now exploit commercial species-specific arrays such as the Affymetrix porcine GeneChip, specific for pig. A few groups have conducted investigations on the host response to *Salmonella*, both on *ex-vivo* tissues or on *in vitro* models. One of the first reports to be published was in 2000 by Rosenberger *et al.*, who reported changes in gene expression in mouse macrophages during *S. Typhimurium* infection and the effects of LPS as a bacterial virulence factor (Rosenberger *et al.*, 2000). In this study Atlas mouse cDNA expression arrays were employed. These arrays contained duplicate spots of 588 mouse partial cDNAs. Murine macrophages RAW 264.7 were infected with *S. Typhimurium* SL1344 or stimulated with 100ng/ml of LPS, and at 4 hours post infection (pi) total RNA was isolated. At 4 hours post-infection the expression levels of 77 out of 588 genes represented on the array were detectably altered by two-fold or more in the RAW 264.7 macrophages. Among the up-regulated genes were LIF, CD40, IL-1 β , ICAM-1, TGF β 2, MIP-1(α , β and 2 α) and iNOS, and among the down-regulated genes were the IL-6 receptor and a few cyclins. Many of these genes are involved in the immune response. Also a number of transcription factors were regulated by *S. Typhimurium* infection; Egr-1, NF-E2, IRF-1 and c-rel were induced whereas Ski, B-myb, Fli-1 and c-Fes were suppressed. This study highlighted a remarkable overlap of genes induced by *S. Typhimurium* and purified *S. Typhimurium* LPS suggesting a ‘redundancy’ in host response to bacteria and some of their products (Rosenberger *et al.*, 2000).

In a second study on the *in vitro* host response to *S. Typhimurium*, Detweiler *et al.* investigated the response of U-937 human macrophages to wild-type SL1344 and a *phoP* mutant using an in-house human spotted array with 22,571 cDNA. This study reported 68 genes with a two-fold or greater difference in expression level between uninfected and infected macrophages. Among the genes reported to be induced were IL-8, MIP-1 α and β , IL1 β , IL-23p19, NF- κ B and a several transcription factors. However they did not present any data on genes that were down regulated, although genes that were unregulated in the cells infected with the wild-type compared to the *phoP* mutant bacteria were included. Among these genes were CD9, cathepsin D, SSI-3 and contactin 1. The *phoP::Tn10* mutant strain elicited many of the same mRNA transcripts as the wild-type bacteria and overall the inflammatory response in U-937 macrophages to

wild-type *Salmonella* and the *phoP::Tn10* mutant strain were similar. Nevertheless, this report identified 34 mRNAs with expression levels 1.9 times lower in *phoP::Tn10* infected macrophages than in wild-type infected macrophages. Of these about a third of the twenty-one with known function were involved in cell death. In this study, microarray analysis provided a tool to identify host molecular pathways influenced by a virulence determinant (Detweiler *et al.*, 2001). In fact as a long-term survival strategy, pathogens can alter host gene transcription to maintain a hospitable niche and prevent detection and clearance by the immune system (Rosenberger *et al.*, 2001).

In another study conducted in 2002, Nau *et al.* investigated the macrophage response to different bacterial pathogens in the hope of improving our understanding of host defenses and discovering the theme that defines the innate immune responses of the macrophage to bacteria (Nau *et al.*, 2002). With this purpose in mind they infected human monocytes with *Staphylococcus aureus* strain ISP794, *Listeria monocytogenes* strain EGD, *Mycobacterium tuberculosis* Erdam strain, *M. bovis* BCG, *S. Typhi* Quail strain, *S. Typhimurium* (ATCC no. 14028), *E. coli* strain sd-4, and enterohaemorrhagic *E. coli* O157:H7. Human macrophages derived from primary monocytes were exposed to bacteria and bacterial components and the resulting expression levels of 6,800 genes were monitored over 24 hours. The researchers were able to highlight a common core of genes differentially expressed during the infection of all the bacteria: 132 genes were induced and 59 genes were suppressed. The up-regulated genes were listed in the following categories: cytokines, chemokine, proliferation, tissue remodelling, adhesion, receptors, transcription, transporters, enzymes, pro-inflammatory, anti-apoptotic, stress response and signaling; the down-regulated genes were organized in the categories: anti-inflammatory, pro-inflammatory, adhesion, receptors, signaling, transcription, transporters, tissue remodelling, and enzymes (Nau *et al.*, 2002).

These studies were conducted on macrophages but *Salmonella* is also able to invade epithelial cells and in 2000, Eckmann *et al.* reported the response of human HT-29 colorectal epithelial cells and T84 human colon epithelial cells to *S. dublin*. In their studies they utilised two different cDNA arrays: GF211 Human “Named genes” GeneFiltered Release I from Research Genetics Inc. (Huntsville, AL) and the Atlas Cytokine/Receptor cDNA Expression Array from CLONTECH Laboratories (Palo Alto, CA) (Eckmann *et al.*, 2000). In the first experiments they employed the GF211 array

(which incorporated 4000 human cDNAs). They analysed mRNA extracted from epithelial cells at 3, 8 and 20 hours, post-infection and reported that the vast majority of the genes (~95%) showed relatively little change. They postulated that the up-regulated genes may be more important than those down-regulated so they concentrated their attention on the former. Among the genes differentially expressed at 3 hours infection were IL-12p40, IL-8 and MHC Class I heavy chain, LI-cadherin and ubiquitin-conjugating enzyme E2. Subsequently, they investigated the RNA expression profile of similar epithelial cells during *S. dublin* infection using the Atlas Human Cytokines/Receptor array (CLONTECH) (with 277 cDNAs from cytokines and receptors). They reported the top 25 differentially expressed genes, which included ubiquitin, LIF, insulin receptor along with IL-8, IL-17 and G-CSF (Eckmann *et al.*, 2000).

It is somewhat surprising that cyclins were not differentially expressed in this study because others have reported differences in similar assays (Nau *et al.*, 2002). Possibly, these researchers were very much interested in looking at the immune response and not at the events at the cellular level in reaction to the pathogen. It can be concluded from these studies that many variables are potentially present in this type of research (cell type, pathogen type, time of infection, type of array platform and data analysis methods) and they can influence the outcome of the analysis and the subsequent conclusions. These studies also reveal the complexity of the models employed. Perhaps it might be useful to interpret host-pathogen interactions on three levels: immunological response, usually predominant; the pathogen orchestration of the host genome, that is not very easy to discern; and the cellular reaction to invasion.

The experimental results reported in Chapter 3 suggested that mouse ES cells could be a promising model to study host-pathogen interactions and to further confirm this hypothesis experiments were performed to explore ES cell mRNA expression profiles during bacterial infection by microarray analysis. These data could advance the understanding of mouse ES cell gene regulation and other characteristics in addition to providing insight into host-pathogen interactions. The results from microarray expression profiling of AB2.2 murine embryonic stem (ES) cells infected with *S. Typhimurium* SL1344 at 2 and 4 hours are reported in this chapter. The rationale for these studies was to provide insight into the response of ES cells to pathogen invasion,

helping us to understand how this new *in vitro* model compares to those previously characterized. This is part of the planned investigation of the feasibility of using murine ES cells to study infectious diseases. It is hoped that the results obtained here will help to direct future investigations involving genetically mutated ES cells or differentiated cells.

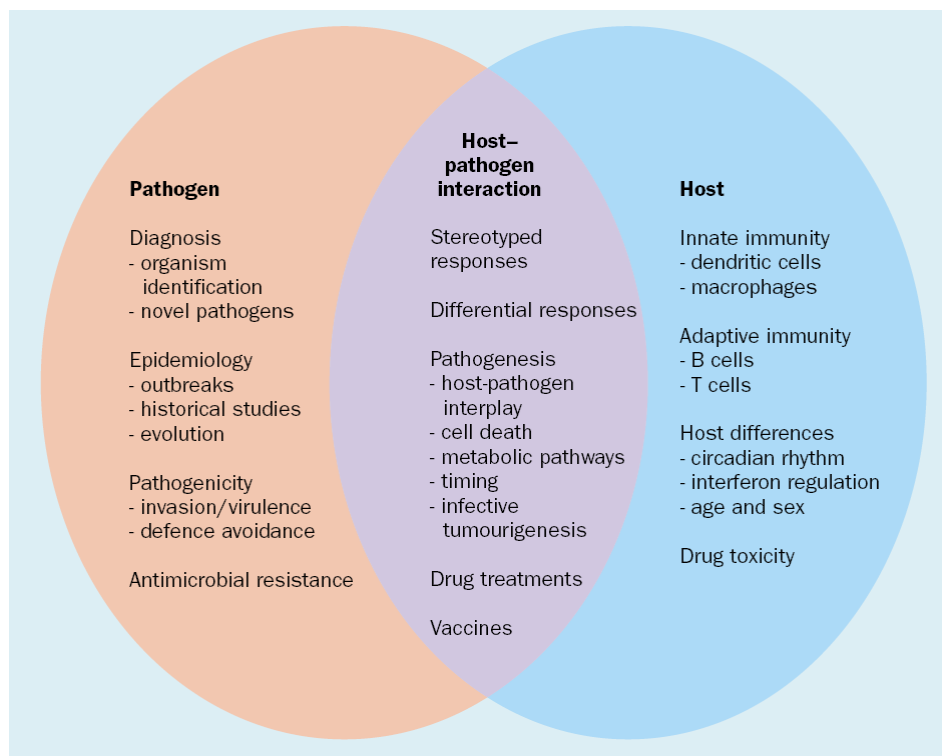


Figure 4.1 Host-pathogen interactions that can be exploited using microarray technology

Microarray technology has a great potential in infectious disease research, helping to explore the complex interactions between host and pathogen and reveal new routes for treatments (Bryant et al., 2004).

4.2 Experimental design

Three independent biological replicates of AB2.2 murine ES cells were infected for 2 hours and 4 hours with *S. Typhimurium* SL1344. Each biological replicate was treated in the same way and total RNA was extracted at time zero from uninfected cells and at 2 hours and 4 hours infection after 30 minutes incubation with the bacterial suspension. Samples of the cells infected at each time point were analyzed by FACS in order to establish the percentage of infected cells. For this reason *S. Typhimurium* SL1344 (p1C/1) expressing GFP was used in these experiments. Three time points (0h, 2h, 4h) were chosen for each of the three biological replicates, giving a total of nine RNA samples for analysis. Also, for each time point three technical replicates were performed for a total of 27 arrays. For each technical replicate an independent cDNA synthesis and cRNA labelling was performed and analyzed by Agilent Bioanalyzer before being hybridized on Affymetrix GenChip[®] Mouse 430.20 arrays (Affymetrix, 2004). The expression data were then analyzed using three different packages: Bioconductor and GeneSpring were used to compare the gene expression profile at 2h and 4h infection to the uninfected cells' mRNA profile and between each other; and ANOVA Simultaneous Component Analysis (ASCA) platform was used to carry out a time course analysis where the time was counted as a variable.

4.3 Results

4.3.1 Murine ES cell infection with *S. Typhimurium* and total RNA extraction

AB2.2 mouse ES cells were maintained undifferentiated in culture media with 1000U/ml of LIF, at 37°C and 5% CO₂. The cells were seeded at 2.5x10⁵ cells per well in 6-well plates and grown for 2 days until 90% confluent. *S. Typhimurium*(p1C/1) expressing GFP was used in these experiments in order to perform parallel flow cytometric examination of the percent of infected cells. *Salmonella* was grown as described in M&M and was seeded into cell culture at MOI ~ 100. After 30 minutes incubation at 37°C the cells were washed with warm Dulbecco's PBS Ca²⁺Mg²⁺ and incubated for 2 hours or 4 hours with complete DMEM medium containing 50µg/ml of gentamicin antibiotic. The cells were then washed and the cells from three wells were trypsinized and analyzed by FACS, whereas the cells in the other three wells were scraped and frozen at -80°C.

Only those cells in which the infection rate was above 30%, as determined by cytometric analysis, were further used for total RNA extraction with the QIAGEN RNeasy Midi kit. The first biological replicate of AB2.2 murine ES cells (passage 33) was infected with *S. Typhimurium* and it was established by flow cytometric analysis that at 2 hours and 4 hours, 30% and 32% of the cells were infected respectively. In the second biological replicate AB2.2 murine ES cells were infected at passage 27 and flow cytometric analysis established that at 2 hours and 4 hours, 42% and 36% of the cells were infected respectively. The third replicate AB2.2 murine ES cells were infected at passage 26 and at 2 hours and 4 hours, 34% and 30% of the cells were infected respectively. An example of the FACS analysis of these cells can be found in Figure 4.2.

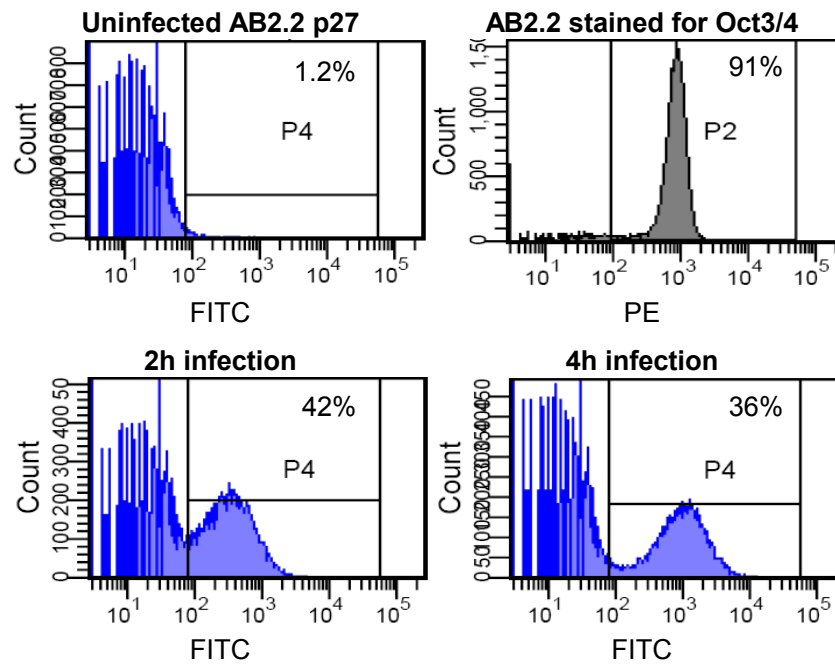


Figure 4.2 Flow cytometric analysis of murine ES cells infected with *S. Typhimurium* SL1344. The AB2.2 murine ES cells were analyzed in parallel by FACS in order to investigate the percentage of infected cells prior to RNA extraction. For this reason *S. Typhimurium*(pC1/1) expressing GFP protein was used for these experiments. In addition Oct3/4 analysis was performed on uninfected cells in order to confirm their pluripotency characteristic.

4.3.2 Murine ES cell total RNA extraction and analysis

The total RNA was extracted using the QIAGEN RNeasy Midi Kit following the manufacturer's instructions. The concentration of total RNA extracted was measured using the NanoDrop1000 (Thermo) spectrophotometer. NanoDrop1000 is a full-spectrum UV/Visible (220-750nm) spectrophotometer used to quantify nucleic acids in a small volume as little as 1µl. The technology used exploits surface tension of small volumes [www.nanodrop.com]. The final concentrations obtained for each sample are reported in Table 4.1.

Table 4.1 Total RNA concentration of murine ES cells infected by *S. Typhimurium*(p1C/1) measured with NanoDrop1000 technology

Sample ID	Description	ng/µl	260/280 Ratio
1	AB2.2 First Biological Replicate	718	2.12
2	AB2.2 First Biological Replicate Infected with SL1344/p1C/1 2h	642	2.12
3	AB2.2 First Biological Replicate Infected with SL1344/p1C/1 4h	830	2.12
4	AB2.2 Second Biological Replicate	914	2.12
5	AB2.2 Second Biological Replicate Infected with SL1344/p1C/1 2h	792	2.12
6	AB2.2 Second Biological Replicate Infected with SL1344/p1C/1 4h	855	2.13
7	AB2.2 Third Biological Replicate	909	2.12
8	AB2.2 Third Biological Replicate Infected with SL1344/p1C/1 2h	707	2.04
9	AB2.2 Third Biological Replicate Infected with SL1344/p1C/1 4h	892	2.12

To test the RNA quality, the samples were analyzed using the Agilent 2100 Bioanalyzer (Agilent Technologies, Palo Alto, CA, USA). The Bioanalyzer is an automated bio-analytical device using microfluidics technology that provides electrophoretic separation in an automated and reproducible manner (Schroeder *et al.*, 2006). Bioanalyzer was used in this study to evaluate the quality of the total RNA extracted from mouse ES cells uninfected and infected by *S. Typhimurium*. Figure 4.3 reports an example of the quality of the total RNA obtained from AB2.2 murine ES cells uninfected and infected at 2 hours and 4 hours with *S. Typhimurium* SL1344(p1C/1).

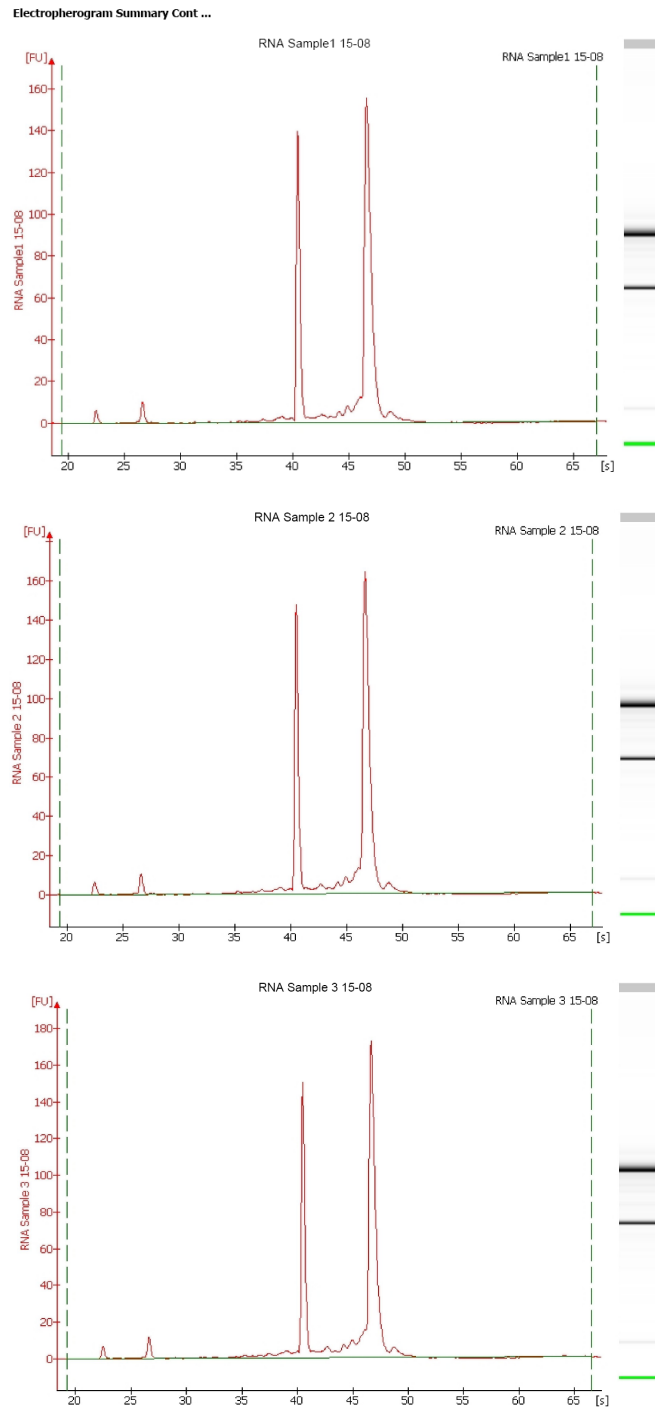


Figure 4.3 Bioanalyzer analysis of total RNA from infected and uninfected ES cells

The quality of the total RNA extracted from each sample was analyzed by Bioanalyzer before microarray analysis.. Representative histograms of the RNA quality from AB2.2 murine ES cells uninfected (top) or infected with *S. Typhimurium* SL1344(p1C/1) at the 2h (middle) and 4h invasion (bottom histogram) with the respective virtual gel, are represented. The histograms reveal two peaks representing the ribosomal RNA 18S and the 28S, from the left. The intensity of the gel band of 28S ribosomal RNA should be about twice that of the 18S ribosomal band.

4.3.3 cRNA synthesis, labelling and microarray hybridization

In order to analyze the expression profile of murine ES cells, the total RNA extracted was hybridized on the Affymetrix GeneChip[®] Mouse 430 2.0 Array following the manufacturer's instructions. Briefly, the 5 μ g of total RNA was used to synthesize double stranded cDNA using the One-Cycle cDNA Synthesis Kit which use poly-T primers. This was 'cleaned' from traces of RNA and used as template for the synthesis of Biotin-Labeled cRNA with the One-cycle Target Labelling Assay kit, following the manufacturer's directions. Then cRNA was cleaned and quantified and its quality was analyzed by Bioanalyzer before hybridization (Figure 4.4). An independent cDNA synthesis and cRNA labelling reaction was carried out for each technical replicate. The cRNA was first fragmented before hybridization and 15 μ g of cRNA per chip was used for hybridization at 45°C in constant rotation (60 rpm) overnight. The chips were washed and scanned at the Fluidics Station 450 operated using GCOS/Microarray Suite software.

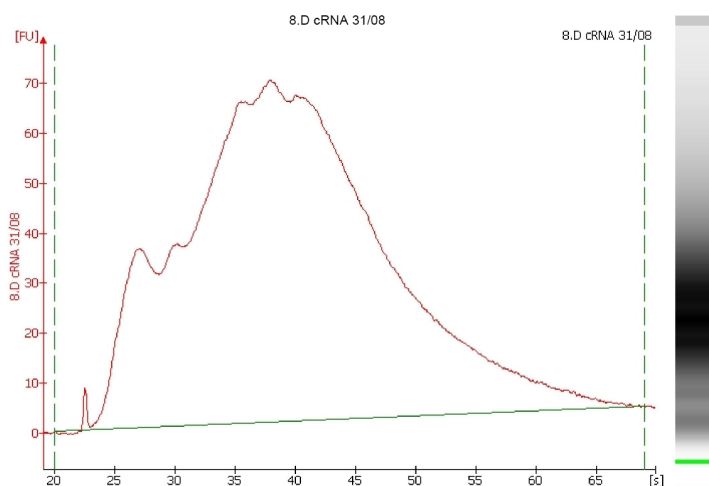


Figure 4.4 Bioanalyzer analysis of the biotin-labelled cRNA

As the Affymetrix manual reports, the cRNA quality needs to be confirmed by Bioanalyzer to prove that the cRNA amplification reaction worked. The optimum is to obtain cRNA fragments between 500-1500 nucleotides, which corresponds to 35 and 40 seconds, respectively. This picture reports an example of the cRNA obtained in this study.

The Affymetrix GeneChip[®] Mouse Genome 430 2.0 Array used harbours 45,000 probes representing transcripts and variants from over 34,000 well characterized mouse genes (Affymetrix, 2004). The Affymetrix expression array uses a set of features (spots), each designed to recognize a molecule of interest. Each feature consists of millions of identical single-stranded 25-mer nucleotide probes designed to hybridize to a specific transcript. The probes are defined Perfect-Match (PM) features and each is accompanied by an adjacent Mis-Match (MM) feature in which the middle residue is changed. Hybridization conditions are designed to maximize binding to the PM feature while minimizing binding to the MM ones. The MM signal can be used to provide a measure of probe specific background for its PM partner. Multiple PM/MM pairs are used for each transcript (Okoniewski & Miller, 2008).

4.3.4 Microarray data analysis

4.3.4.1 Bioconductor analysis

4.3.4.1.1 Results from Bioconductor pair-comparison analysis

Microarray expression profile analysis was initially conducted using Bioconductor [Bioconductor: <http://www.bioconductor.org>] (Gentleman *et al.*, 2004). Bioconductor is a collection of open source software packages designed to support the analysis of biological data. Bioconductor is written using the programming language R, which itself provides access to a wide range of tools for statistical analysis, data presentation, and visualization (Okoniewski & Miller, 2008). In this analysis the mouse ES cell microarray profiles at 2 hours and 4 hours post-infection were compared with the profile of uninfected cells (0h). The arrays were first subjected to quality control and the report can be seen in Appendix A. Normalization using GCRMA (Wu *et al.*, 2004) was then performed and this includes background adjustment, quantile normalization, and median-polish summarization at the probe level. The data were then further analyzed using the Limma package and applying a linear model to estimate the effect of each factor on the variance of the data [limma : <http://bioinf.wehi.edu.au/limma/>]. The results from this analysis are reported in Tables 4.2, 4.3 and 4.4

Table 4.2 Bioconductor analysis of RNA expression profile of murine ES cells at 2h infection

The mRNA expression profile of uninfected AB2.2 murine ES cells and that obtained following 2h infection with *S. Typhimurium* were compared and analyzed using the Bioconductor package; significantly differentially expressed genes are reported (p-value <0.05 and fold change +/- 1.5).

Fold Change	Adj.p-value	Gene Symbol	Gene Title	Process and Functions
10.63	0.0007	Cyp1b1	cytochrome P450, family 1, subfamily b, polypeptide 1	oxidation reduction// monoxygenase activity// iron ion binding// electron carrier activity// ER membrane
4.38	0.0147	Cyp1a1	cytochrome P450, family 1, subfamily a, polypeptide 1	dibenzo-p-dioxin metabolic process // oxidation reduction// monoxygenase activity// iron ion binding// ER membrane

Table 4.3 Bioconductor analysis of RNA expression profile of murine ES cells at 4h infection

Genes determined to be differentially expressed following Bioconductor analysis of arrays hybridized with mRNA from uninfected AB2.2 ES cells and infected with *S. Typhimurium* for 4h. The 30 genes reported are significantly differentially expressed at 4h infection compared to uninfected cells (0h) (p value < 0.05 and fold change +/- 1.5; * = gene reported twice; ** = gene reported three times)

Fold Change	Adj. p value	Gene symbol	Gene Name	Process and Functions
2.32	0.0327	Banp	Btg3 associated nuclear protein	Transcription/ cell cycle/ DNA binding
2.25	0.0002	Hspa1b**	Heat shock protein1B	DNA repair//anti-apoptotic//response to stress
2.01	0.0053	Pdxp	Pyridoxal (vitB6) phosphatase	Magnesium ion binding//catalytic activity
2	0.0065	Zbtb40	Zinc finger and BTB domain containing 40	Nucleic acid binding//zinc binding// prot. binding
1.88	0.0464	Ccng2	Cyclin G2	Cyclin-dependent protein kinase regulator activity
1.84	0.002	Herpud1	Homocystein-inducible, ER stress-inducible, ubiquitin-like domain member 1	Response to stress// response to unfolded protein
1.64	0.0011	Tbl2	Transducin(beta)-like 2	//
1.62	0.0211	Ankrd37	Ankyrin repeat domain 37	//
1.6	0.0336	Aof1	Amine oxidase, flavin containing 1	Zinc binding // electron carrier activity
1.55	0.0016	Clk2	CDC-like kinase 2	Nucleotide binding// protein kinase activity// ATP binding
1.55	0.017	Pex11a	Peroxisomal biogenesis factor 11a	Peroxisome organization and biogenesis
1.54	0.0125	Ccdc117	Coiled-coil domain containing 117	//
1.53	0.0049	Luc7l	Luc7 homolog (<i>S. cerevisiae</i>)-like	Zinc ion binding// metal ion binding
1.53	0.017	Xbp1	X-box binding protein 1	Transcription factor activity
1.51	0.0334	C430002E04Rik	RIKEN cDNA C430002E04 gene	//
-1.51	0	Sfrs5	Splicing factor arginine/serine-rich 5 (SRp40, HRS)	Nucleic acid binding
-1.52	0.0336	LOC100044766	Similar tow domain-containing adapter protein with coiled-coil	Protein binding
-1.55	0.0334	Msc	Musculin	Transcription regulator activity
-1.55	0.0052	Chic2	Cysteine-rich hydrophobic domain 2	Golgi to plasma membrane transport
-1.57	0.0129	1810013L24Rik	RIKEN cDNA 1819913L24gene	//
-1.65	0.0039	Lrpap1*	Low density lipoprotein receptor-related protein associated protein 1	Receptor activity// low-density lipoprotein receptor binding
-1.65	0.0084	Slc7a1	Soluble carrier family 7 member 1	Receptor activity// amino acid transmembrane transporter activity
-1.78	0.0001	LOC100046855	Similar to BKLF	Nucleic acid binding// zinc ion binding
-1.86	0.0003	Foxp1	Forkhead box P1	Nucleic acid binding// transcription factor activity// zinc ion binding
-1.98	0.0341	Luc7l2	LUC7-like 2 (<i>S. cerevisiae</i>)	Protein binding// zinc ion binding
-2.41	0.0403	LOC100045546	Similar to Id4	//
-3	0.0336	Cyp1b1	Cytochrome P450, family 1 subfamily b, polypeptide 1	Monooxygenase activity// iron ion binding// electron carrier activity

Table 4.4 Bioconductor analysis of RNA expression profile of murine ES cells at 4h infection compared to 2h

Gene list resulting from the Bioconductor analysis comparing the expression profiles of murine ES cells at 2h and 4h infection. This analysis identified 39 differentially expressed genes, of which 33 have been annotated and therefore reported here. (* = gene reported twice; ** = gene reported three times)

Fold Change	Adj. p value	Gene Symbol	Gene Name	Process and Functions
2.11	0.00	Hspa1b**	heat shock protein 1B	DNA repair /// anti-apoptosis /// response to stress /// response to heat /// negative regulation of caspase activity
1.98	0.02	Ccng2	cyclin G2	cell cycle /// mitosis /// cell division /// regulation of cell cycle
1.97	0.01	LOC638050 /// Zbtb40	zinc finger and BTB domain containing 40 /// similar to zinc finger and BTB domain containing 40	nucleic acid binding /// protein binding /// zinc ion binding /// metal ion binding
1.78	0.00	Herpud1*	homocysteine-inducible, endoplasmic reticulum stress-inducible, ubiquitin-like domain member 1	protein modification process /// response to stress /// response to unfolded protein /// response to unfolded protein
1.75	0.00	Ankrd37	ankyrin repeat domain 37	---
1.69	0.00	Xbp1**	X-box binding protein 1	transcription /// regulation of transcription, DNA-dependent
1.55	0.02	C430002E04 Rik	RIKEN cDNA C430002E04 gene	---
1.50	0.05	Gdap10	ganglioside-induced differentiation-associated-protein 10	---
-1.52	0.04	Klf10	Kruppel-like factor 10	regulation of transcription, DNA-dependent /// positive regulation of osteoclast differentiation /// zinc-metal ion binding
-1.52	0.01	Zbtb7a	zinc finger and BTB domain containing 7a	negative regulation of transcription from RNA polymerase II promoter /// negative regulation of transcription, DNA-dependent /// zinc ion binding
-1.52	0.04	Gm505	Gene model 505, (NCBI)	---
-1.54	0.04	Lrpap1*	low density lipoprotein receptor-related protein associated protein 1	receptor activity /// heparin binding /// low-density lipoprotein receptor binding /// membrane protein
-1.56	0.01	1810013L24 Rik	RIKEN cDNA 1810013L24 gene	---
-1.56	0.00	Nodal	nodal	negative regulation of transcription from RNA polymerase II promoter // positive regulation of cell proliferation // anterior/posterior pattern formation // stem cell maintenance // negative regulation of cell differentiation /// cytokine activity // growth factor activity
-1.58	0.00	Snai1	snail homolog 1 (Drosophila)	multicellular organismal development // nucleic acid binding // zinc ion binding
-1.58	0.04	Sesn2	sestrin 2	cell cycle arrest

-1.59	0.02	Elf3	E74-like factor 3	regulation of transcription, DNA-dependent /// inflammatory response /// embryonic development /// cell differentiation /// epithelial cell differentiation /// transcription factor activity/// protein binding
-1.61	0.02	Pcmt1	protein-L-isoaspartate (D-aspartate) O-methyltransferase domain containing 1	protein modification process /// methyltransferase activity
-1.68	0.00	Slc7a1	solute carrier family 7 (cationic amino acid transporter, y+ system), member 1	receptor activity /// amino acid transmembrane transporter activity /// arginine transmembrane transporter activity
-1.70	0.00	Foxp1	forkhead box P1	negative regulation of transcription from RNA polymerase II promoter /// pre-B cell differentiation /// positive regulation of immunoglobulin production /// regulation of transcription, DNA-dependent ///embryonic development /// immunoglobulin V(D)J recombination /// positive regulation of epithelial cell proliferation
-1.71	0.03	Rnase4	ribonuclease, RNase A family 4	positive regulation of endothelial cell proliferation /// activation of phospholipase C activity /// multicellular organismal development actin filament polymerization /// activation of phospholipase A2 /// positive regulation of protein secretion/// nucleic acid binding/// receptor binding/// basal lamina
-1.78	0.04	Arl4a	ADP-ribosylation factor-like 4A	small GTPase mediated signal transduction/// GTPase activity
-1.80	0.00	Aff1	AF4/FMR2 family, member 1	transcription /// positive regulation of transcription, DNA-dependent
-1.97	0.02	Ndr1	N-myc downstream regulated gene 1	mast cell activation
-2.06	0.00	Cdkn1a	cyclin-dependent kinase inhibitor 1A (P21)	G1/S and G2/M transition of mitotic cell cycle /// response to DNA damage stimulus /// cell cycle arrest /// positive regulation of B cell proliferation /// cellular response to extracellular stimulus /// negative regulation of apoptosis /// positive regulation of fibroblast proliferation /// protein kinase inhibitor activity
-2.10	0.00	Zfp296	zinc finger protein 296	nucleic acid binding /// zinc ion binding
-2.35	0.00	Klf3 /// LOC100046855	Kruppel-like factor 3 (basic) /// similar to BKLF	transcription /// regulation of transcription, DNA-dependent
-2.49	0.00	LOC100046855	similar to BKLF	nucleic acid binding /// zinc ion binding
-2.60	0.02	LOC100045546	similar to Id4	---
-13.13	0.00	Cyp1b1*	cytochrome P450, family 1, subfamily b, polypeptide 1	monooxygenase activity/// iron ion binding /// oxidoreductase activity aromatic compound metabolic process /// metal ion binding
-22.66	0.00	Cyp1a1	cytochrome P450, family 1, subfamily a, polypeptide 1	oxidation reduction /// monooxidoreductase activity/// electron carrier activity /// metal ion binding

4.3.4.1.2 InnateDB pathways analysis

InnateDB has been developed to facilitate systems-level investigations of the innate immune response in human and mice. Its goal is to provide a manually-curated database of the genes, proteins and, particularly, the interactions and signaling responses involved in the mammalian innate immune response. InnateDB is freely available to the public as a tool for innate immunity research where users can search for particular genes or proteins of interest and their relative interactions and pathways [InnateDB: <http://innatedb.ca/index.jsp>] (Lynn *et al.*, 2008). For this analysis the corresponding human ortholog genes were used since more than 3 quarters of the interactions reported in InnateDB are for *Homo sapiens*. The list of all probes with their respective p-value and the expression fold change determined by pair-comparison of mouse ES cell mRNA expressed at 4h post-infection with *S. Typhimurium* versus uninfected cells, were uploaded and analyzed using InnateDB. The gene expression values obtained at 2 hours infection and those obtained comparing 4 hours to 2 hours were also analyzed with InnateDB. The pathways obtained were further ‘enriched’ using the ‘over-representation’ analysis which uses the genes’ fold expression (± 1.5) and p-value (<0.1) in order to evaluate the proportion of differentially expressed genes for each pathway (using the default settings for the analysis algorithm: Hypergeometric and the correction method: Benjamini Hochberg).

Table 4.5 InnateDB analysis of genes expressed by murine ES cells at 2h infection with *S. Typhimurium*

The analysis reported only up-regulated pathways at 2h infection of AB2.2 murine ES cells with *S. Typhimurium* SL1344, although they are not statistically significant (corrected p-value).

Name of Pathway up-regulated at 2h infection of AB2.2	Source Name	Pathway uploaded gene count	Pathway up-regulated genes count	Pathway up-regulated p-value	Pathway up-regulated p-value (corrected)
P450 Epoxidations	REACTOME	3	1	0.000602	0.790329
Metabolism of xenobiotics by cytochrome P450	KEGG	28	1	0.005618	1.000000
Tryptophan metabolism	KEGG	52	1	0.010433	1.000000

Table 4.6 InnateDB pathway analysis of murine ES cells expression profile at 4h infection: up-regulated pathways

The whole gene list derived from Bioconductor analysis of the expression data at 4h infection with *S. Typhimurium* SL1344 versus uninfected AB2.2 murine ES cells (0h) was used for this analysis. The analysis did not reveal significantly up-regulated pathways according to adjusted p-values.

Name of pathway up-regulated at 4h infection of AB2.2	Source Name	Pathway uploaded gene count	Pathway up-regulated genes count	Pathway up-regulated p-value	Pathway up-regulated p-value (corrected)
Lipoic acid metabolism	KEGG	3	1	0.006008	1
Ubiquitin mediated proteolysis	KEGG	127	2	0.025359	1
Circadian rhythm	KEGG	13	1	0.025802	1
Sprouty regulation of tyrosine kinase signals	PID BIOCARTA	17	1	0.033620	1
Er associated degradation (erad) pathway	PID BIOCARTA	18	1	0.035566	1
Pkc-catalyzed phosphorylation of inhibitory phosphoprotein of myosin phosphatase	PID BIOCARTA	20	1	0.039446	1
EGFR downregulation	REACTOME	22	1	0.043313	1
Maturity onset diabetes of the young	KEGG	23	1	0.045241	1
Rho cell motility signaling pathway	PID BIOCARTA	31	1	0.060540	1
Rac1 cell motility signaling pathway	PID BIOCARTA	35	1	0.068106	1
N-Glycan biosynthesis	KEGG	38	1	0.073745	1

Table 4.7 InnateDB pathway analysis of murine ES cells expression profile at 4h infection: down-regulated pathways

The genes resulting from the analysis of gene expression at 4h infection compared to uninfected AB2.2 murine ES cells were analyzed with InnateDB. The pathway analysis did not reveal any statistically significantly for down regulated pathway after p-value adjustment.

Name of Pathway down-regulated at 4h infection of AB2.2	Source Name	GO term uploaded gene count	GO term down-regulated genes count	GO term down-regulated p-value	GO term down-regulated p-value (corrected)
P450 Epoxidations	REACTOME	3	1	0.003007	1
Gene expression of IL2 by AP-1	INOH	5	1	0.005008	1
TGF-beta Receptor Signaling Pathway	NETPATH	130	2	0.006412	1
Pertussis toxin-insensitive ccr5 signaling in macrophage	PID BIOCARTA	7	1	0.007006	1
Tsp-1 induced apoptosis in microvascular endothelial cell	PID BIOCARTA	7	1	0.007006	1
Il 3 signaling pathway	PID BIOCARTA	8	1	0.008003	1
JNK cascade	INOH	10	1	0.009996	1

Table 4.8 InnateDB analysis of genes expressed by murine ES cells at 4h infection with *S. Typhimurium* compared to 2h: up-regulated pathways

The analysis reported one up-regulated pathway at 4h versus 2h infection of AB2.2 murine ES cells with *S. Typhimurium* SL1344, although the corrected p-value is not statistically significant.

Name of Pathway up-regulated at 4h vs.2h	Source Name	Pathway uploaded gene count	Pathway up-regulated genes count	Pathway up-regulated p-value	Pathway up-regulated p-value (corrected)
Lipoic acid metabolism	KEGG	3	1	0.000602	0.790329

Table 4.9 InnateDB analysis of genes expressed by murine ES cells at 4h infection with *S. Typhimurium* compared to 2h: down-regulated pathways

The analysis reported a few down-regulated pathways at 4h versus 2h infection of AB2.2 murine ES cells with *S. Typhimurium* SL1344, although the corrected p-value is not statistically significant.

Name of Pathway down-regulated at 4h vs. 2h	Source Name	Pathway uploaded gene count	Pathway up-regulated genes count	Pathway down-regulated p-value	Pathway down-regulated p-value (corrected)
P450 Epoxidations	REACTOME	3	1	0.002406	1
Downregulated of mta-3 in er-negative breast tumors	PID BIOCARTA	15	1	0.011988	1
Metabolism of xenobiotics by cytochrome P450	KEGG	28	1	0.022290	1
Tryptophan metabolism	KEGG	52	1	0.041097	1
Viral Messenger RNA Synthesis	REACTOME	59	1	0.046531	1
Adherens junction	KEGG	70	1	0.055023	1
TGF-beta signaling pathway	KEGG	76	1	0.059632	1

4.3.4.1.3 Real time RT-PCR to confirm Bioconductor analysis

Real time Reverse Transcription (RT) followed by polymerase chain reaction (PCR) is a powerful tool for the detection and quantification of mRNA. It is important to confirm bioinformatics analysis with an alternative method although this has been the centre of debate in the scientific community (Allison *et al.*, 2006; Rajeevan *et al.*, 2001). The total RNA extracted from the *S. Typhimurium* infected cells and uninfected controls was subjected to RT-PCR analysis in order to confirm the data obtained from the microarray study and subsequent Bioconductor analysis. The total RNA was reverse transcribed using QuantiTect (QIAGEN). A SYBR Green-based detection reaction was used and the data were analysed using the $\Delta\Delta C_t$ value method developed by Perkin Elmer (Applied Biosystems) to measure the relative quantification of a target gene in comparison to a reference gene. This method is an approximation of the RNA quantity assuming that RT-PCR reaction efficiencies are all equal to 2 (i.e. that each cycle of PCR results in two-fold increase in the number of RNA species). The fold change of the target genes were then calculated in relation to the expression of the internal control gene chosen, β -actin in this study, using the equation “ratio= $2^{\Delta\Delta C_t}$ ” where C_t is the thermo cycle at which the green fluorescence dye is first detectable and 2 represents the reaction efficiency. A few genes determined to be significantly up- or down-regulated by microarray analysis were chosen to be confirmed by semi-quantitative RT-PCR. The genes were selected in order to cover a representative set of genes or pathways exhibiting differential expression. These genes were involved in cholesterol metabolism, cell-cycle regulation, stress responses, apoptosis regulation and transcription factors. For a more detailed description of each gene please refer to Table 4.3.

RT-PCR confirming Bioconductor analysis
of expression data from murine ES infected with *S. Typhimurium* at 4h

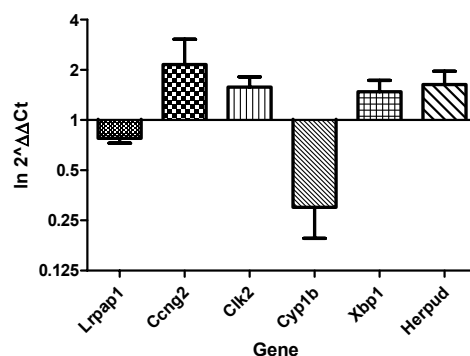


Figure 4.5 RT-PCR results conducted on representative genes identified by the Bioconductor analysis of genes differentially expressed at 4h infection vs. uninfected cells

A few genes with high fold change and significantly differentially expressed during infection, revealed through Bioconductor analysis, were chosen for relative quantification using RT-PCR. In this analysis the Ct values of the target genes were compared to the Ct value of an internal control gene, β -actin, and the ratios calculated and plotted as $\ln 2^{-\Delta\Delta Ct}$. The reactions were carried out in triplicate for each biological replicate at 0h and 4h infection and are reported here as the mean values. The error bars represent the standard error for each replicate. The initial amount of template cDNA is inversely proportional to the parameter measured for each reaction, which is the threshold cycle (Ct).

4.3.4.1.4 Statistical analysis of RT-PCR data on genes identified by Bioconductor

Statistical analysis of the RT-PCR results was carried out using the online Relative expression software tool (REST[©]), and the results can be found in Figure 4.6. This mathematical model compares two groups with up to 16 data points in a sample and 16 in a control group, and is based on the PCR efficiencies and the mean Ct deviation between the sample and the control group (Herrmann & Pfaffl, 2005). Subsequently, the expression ratio results of the investigated transcripts are tested for significance using a randomization test. Permutation or randomization tests are a useful alternative to more standard parametric tests for analysing experimental data. They have the advantage of making no distributional assumptions about the data, while remaining as powerful as parametric tests (Pfaffl *et al.*, 2002).

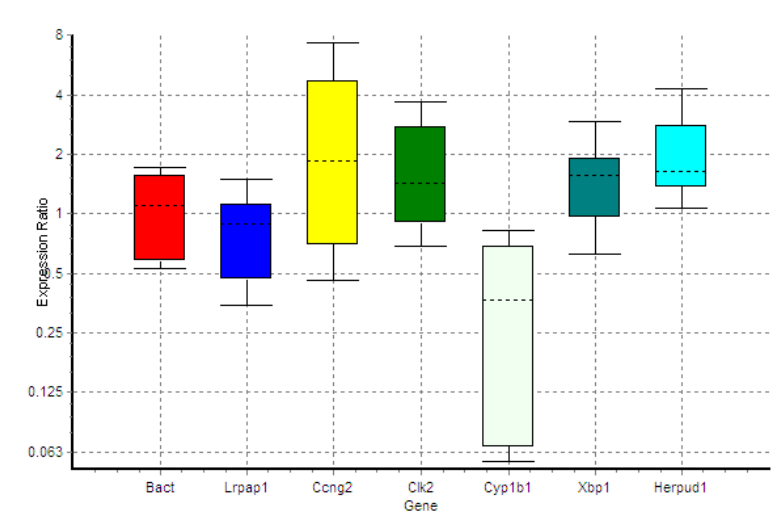


Figure 4.6 Whisker box plot of the RT-PCR results for the Bioconductor-generated differentially expressed genes

The Ct values obtained from RT-PCR for a few of the genes that were identified Bioconductor analysis as differentially expressed in AB2.2 mouse ES cells at 4h invasion with *S. Typhimurium* were statistically investigated by REST©. The random statistical analysis was performed using the triplicate mean values from three different biological replicates; however none of the genes' expression was significantly different in comparison to the internal control gene β -actin.

RT-PCR meant to confirm the results obtained by bioinformatics analysis of up- or down-regulated genes. In this case the genes chosen to be confirmed showed the higher difference in fold expression at 4h infection. However, statistical analysis didn't highlight a significant difference between the level of expression of the genes at 0h and at 4h.

4.3.4.2 GeneSpring analysis

4.3.4.2.1 Results from GeneSpring pair-comparison analysis

In our laboratory microarray data were historically analyzed by GeneSpring. The Agilent GeneSpring version 7.3.1 platform is an expression analysis tool. Here it was used to analyse the Affymetrix Mouse GeneChip[®] 430 2.0 Array used to investigate the murine AB2.2 ES cell RNA expression profile during *S. Typhimurium* infection at 2h and 4h post-infection.

The array QC is shown in Appendix A. The data were first normalized using GCRMA (Wu *et al.*, 2004), which takes into consideration GC content, and then the data was then filtered using the Benjamini-Hochberg false discovery rate (FDH) method, which assumes independent p-values across genes; the genes were filtered for confidence p-value < 0.05. This procedure provides a good balance between discovery of significant genes and protection against false positives, since the occurrence of the latter is confined to a small proportion of the list, and it is the best choice of multiple-testing correction for most analyses (GeneSpring Manual).

Table 4.10 GeneSpring analysis of the mRNA expression profile of AB2.2 murine ES cells at 2h infection

This comparative analysis revealed 26 genes significantly differentially regulated for p-value < 0.05 and fold expression change of +/- 1.5. 19 annotated genes are reported here. (* = reported twice; ** = reported three times)

Genes selected from condition Time 2.0 that have Normalised Data values that are greater or less than those in condition(s) Time 0.0 by a factor of 1.5 fold. Starting gene list: Filter for confidence t-test p-value 0 - 0.05, Benj and Hoch FDR, 1 cond of 3.			
Fold Change	Common	Description	Biological Process and or Molecular Function
8.91	Cyp1a1	cytochrome P450, family 1, subfamily a, polypeptide 1	electron transport// monoxygenase activity; oxidoreductase activity// ER
3.52	Cyp1b1*	cytochrome P450, family 1, subfamily b, polypeptide 1	oxidation reduction /// electron carrier /// ER
1.97	Nfkbiz	nuclear factor of kappa light polypeptide gene enhancer in B-cells inhibitor, zeta	inflammatory response // regulation of transcription // DNA binding
1.66	Clstn3	calsyntenin 3	cell adhesion // ER // Golgi apparatus // calcium ion binding // protein binding
1.65	Anpep	alanyl (membrane) aminopeptidase	proteolysis and peptidolysis // zinc ion binding
1.65	Map3k3	mitogen-activated protein kinase kinase kinase 3	protein amino acid autophosphorylation // ATP binding // kinase activity
1.64	Mark2	MAP/microtubule affinity-regulating kinase 2	cell differentiation // ATP binding // kinase activity
1.59	Slc6a6	solute carrier family 6 (neurotransmitter transporter, taurine), member 6	beta-alanine transport // integral to plasma membrane
1.59	Lpp	LIM domain containing preferred translocation partner in lipoma	cell adhesion // cell junction // metal ion binding // protein binding
1.56	Klf3*	Kruppel-like factor 3 (basic)	regulation of transcription // zinc ion binding
1.55	Zfp296	zinc finger protein 296	//
1.55	Snai1	snail homolog 1 (Drosophila)	development // DNA binding // zinc ion binding
1.54	Inf2	inverted formin, FH2 and WH2 domain containing	actin cytoskeleton organization and biogenesis // actin binding // Rho GTPase binding
1.53	Pdpk1	3-phosphoinositide dependent protein kinase-1	ATP binding // protein serine/threonine kinase activity // signal transduction // cytoplasmic vesicle //
1.52	Synj1	Synaptojanin 1	endocytosis // clathrin coat // cytoplasm // hydrolase activity // inositol or phosphatidylinositol phosphatase activity
1.51	Mint	Msx2 interacting nuclear target protein	regulation of transcription from Pol II promoter // binds G/T-rich dsDNA and ssDNA // mitochondrial inner membrane // nucleus
-1.59	Xist	inactive X specific transcripts	dosage compensation by inactivation of X chromosome
-1.62	Tpd52l2	tumor protein D52-like 2	//

Table 4.11 GeneSpring analysis of the mRNA expression profile of AB2.2 murine ES cells at 4h infection

A total of 89 genes were revealed to be differentially expressed by murine AB2.2 ES cells at 4h infection with *S. Typhimurium* SL1344. 56 annotated genes are reported here. The genes were filtered for p-value < 0.05 and fold change +/- 1.5. A few genes are repeated, as indicated by asterisks, and this is a sign that a gene is particularly relevant (* = reported twice; ** = reported three times).

Genes selected from condition Time 4.0 that have Normalised Data values that are greater or less than those in condition(s) Time 0.0 by a factor of 1.5 fold. Starting gene list: Filter for confidence t-test p-value 0 - 0.05, Benj and Hoch FDR, 1 cond of 3.

Fold Change	Common	Description	Biological Process and or Molecular Function
2.43	Banp	Btg3 associated nuclear protein	protein binding
2.17	Hspa1b**	heat shock protein 1A	anti-apoptosis; inhibition of caspase activation; ATP binding
2.03	Ccng2*	cyclin G2	cell cycle regulation
1.83	Pdpx	pyridoxal (pyridoxine, vitamin B6) phosphatase	catalytic activity // metabolic process
1.82	Stat2	signal transducer and activator of transcription 2	involved in signal transduction and transcription for type I interferon signaling
1.73	AA408868	expressed sequence AA408868	inflammatory response; regulation of transcription, DNA-dependent
1.71	Ier3	immediate early response 3	integral membrane
1.69	Herpud1*	homocysteine-inducible, endoplasmic reticulum stress-inducible, ubiquitin-like domain member 1	response to stress // response to unfolded protein // ER membrane
1.66	Mrpl29/1200010C09Rik	mitochondrial ribosomal protein L49	translation /// structural component of ribosome
1.59	Cnm3*	cyclin M3	ion transport // integral to membrane
1.57	Sel1h	Sel1 (suppressor of lin-12) 1 homolog (<i>C. elegans</i>)	Notch signaling pathway // endoplasmic reticulum // extracellular space
1.56	Socs3	suppressor of cytokine signaling 3	intracellular signaling cascade; regulation of cell growth; signal transduction
1.56	Meg3	maternally expressed 3	
1.54	Lyst	lysosomal trafficking regulator	cellular defense response // response to bacterium // cytoplasm
1.54	1200010C09Rik	RIKEN cDNA 1200010C09 gene	response to unfolded protein// ubiquitin-protein ligase activity
1.54	BC018601	cDNA sequence BC018601	
1.54	Aof1	amine oxidase, flavin containing 1	oxidation reduction // electron carrier // metal ion binding
1.53	Xbp1	X-box binding protein 1	regulation of transcription DNA-dependent
1.52	Eif2ak3	eukaryotic translation initiation factor 2 alpha kinase 3	eIF2a kinase // electron transport// kinase activity // ATP binding
1.52	Cebpd	CCAAT/enhancer binding protein (C/EBP), delta	transcription regulation // DNA binding
1.52	Tbl2	transducin (beta)-like 2	extracellular space
1.52	Zc3h10	zinc finger CCCH type containing 10	metal ion binding // nucleic acid binding
1.51	Mkx	mohawk homeobox	multicellular organismal development // DNA binding
1.51	Irf2bp1	interferon regulatory factor 2 binding protein 1	negative regulation of transcription from Pol II promoter
1.5	Clk2	CDC-like kinase 2	autophosphorylation; protein amino acid phosphorylation// ATP binding; kinase activity
1.5	Hspa1a	heat shock protein 1A	DNA repair // response to heat // ATP binding

-1.5	Spic	Spi-C transcription factor (Spi-1/PU.1 related)	DNA binding; transcription factor activity
-1.5	Sfrs5	splicing factor, arginine/serine-rich 5 (SRp40, HRS)	splicesome // mRNA splice site selection // nucleic acid binding
-1.51	Cphx	cytoplasmic polyadenylated homeobox	transcription regulation // DNA binding
-1.52	Chic2	platelet derived growth factor receptor, alpha polypeptide	Golgi to plasma membrane transport // Golgi-associated vesicle
-1.52	Plaur	urokinase plasminogen activator receptor	binding of urokinase// cell surface receptor// kinase activity
-1.52	Plxdc1	plexin domain containing 1	receptor activity // integral to membrane
-1.54	Foxd3	forkhead box D3	DNA binding // transcription factor activity
-1.54	Mllt6	myeloid/lymphoid or mixed lineage-leukemia translocation to 6 homolog (Drosophila)	transcription regulation // DNA binding // metal ion binding
-1.54	Txnip	thioredoxin interacting protein	response to oxidative stress// anzyme inhibitor activity
-1.56	Cirbp	cold inducible RNA binding protein	RNA binding // nucleic acid binding
-1.56	Lrpap1*	low density lipoprotein receptor-related protein associated protein 1	heparin binding // low-density lipoprotein receptor binding // cytoplasm // ER// contain alpha-2-macroglobulin RAP domain
-1.57	Idb2	inhibitor of DNA binding 2	protein binding // transcription regulation
-1.58	Luc7l2	LUC7-like 2 (S. cerevisiae)	
-1.58	Rpl27a	ribosomal protein L27a	translaction // cytosolic ribosome
-1.59	Arl4a	ADP-ribosylation factor-like 4	small-GTPase mediate signal transduction // GTP binding
-1.64	Rnpc2	RNA-binding region (RNP1, RRM) containing 2	mRNA processing // nuclear mRNA splicing via spliceosome // regulation of transcription
-1.64	Idb3	inhibitor of DNA binding 3	negative regulation of transcription from Pol II promoter
-1.67	Ndrp1*	N-myc downstream regulated 1	mast cell activation // cytoplasm-nucleus
-1.7	Wac	WW domain containing adaptor with coiled-coil	spliceosome // protein binding
-1.76	Foxp1	forkhead box P1	cell differentiation // DNA binding // metal ion binding
-1.76	Klf3	Kruppel-like factor 3 (basic)	transcription regulation // DNA binding // metal ion binding
-1.81	Nab2	Ngfi-A binding protein 2	negative regulation of transcription // regulation of transcription DNA-dependent
-1.82	Slc30a1	solute carrier family 30 (zinc transporter), member 1	cation transport; zinc ion transport
-1.9	Tiparp	TCDD-inducible poly(ADP-ribose) polymerase	NAD + ADP ribosiltransferase activity // metal ion binding // nucleus
-1.94	Luc7l2	LUC7-like 2 (S. cerevisiae)	metal ion binding // protein binding
-2	Cyp1a1	cytochrome P450, family 1, subfamily a, polypeptide 1	electron transport// monooxygenase activity; oxidoreductase activity// ER
-2.18	Idb4**	inhibitor of DNA binding 4	cell proliferation // protein binding // transcription regulation
-2.29	Slc30a1	solute carrier family 30 (zinc transporter), member 1	cation transport // cellular zinc ion homeostasis // integral to membrane
-2.32	Pou4f2	POU domain, class 4, transcription factor 2	axon extension involved in development // chromatin binding
-2.82	Cyp1b1*	cytochrome P450, family 1, subfamily b, polypeptide 1	oxidation reduction // electron carrier // ER

Table 4.12 GeneSpring analysis of the mRNA expression profile of AB2.2 murine ES cells at 4h vs. 2h infection

GeneSpring analysis results of murine ES cell genes differentially expressed at 4h infection vs. 2h infection with *S. Typhimurium*. The genes were filtered for p-value < 0.05 and fold change +/- 1.5. Genes reported more than once are indicated by asterisks (* = reported twice; ** = reported three times).

Genes selected from condition Time 4.0 that have Normalised Data values that are greater or less than those in condition(s) Time 2.0 by a factor of 1.5 fold. Starting gene list: Filter for confidence t-test p-value 0 - 0.05, Benj and Hoch FDR, 1 cond of 3. In total 87 genes were differentially expressed of which 63 were previously annotated

Fold Change	Common	Description	Biological Process and or Molecular Function
2.02	Hspa1b**	heat shock protein 1A	anti-apoptosis // inhibition of caspase activation // response to heat // ATP binding // chaperon activity
1.85	Banp	Btg3 associated nuclear protein	protein binding
1.78	Ccng2	cyclin G2	cell cycle regulation // cyclin-dependent protein kinase regulator activity
1.72	Ier3	immediate early response 3	integral to membrane
1.7	Zbtb40	zinc finger and BTB domain containing 40	nucleus// metal ion binding // zinc ion binding
1.69	Cebpd	CCAAT/enhancer binding protein (C/EBP), delta	regulation of transcription// DNA binding // protein dimerization activity // nucleus
1.68	Gadd45g	growth arrest and DNA-damage-inducible 45 gamma	T-helper 1 cell differentiation // activation of MAPKK // apoptosis // interferon-gamma biosynthesis // negative regulation of protein kinase activity // protein biosynthesis // regulation of cell cycle // nucleus // structural constituent of ribosome
1.65	Ankrd37	ankirin repeat domain 37	cytoplasm // nucleus
1.64	Herpud1*	homocysteine-inducible, endoplasmic reticulum stress-inducible, ubiquitin-like domain member 1	protein modification // response to stress // ER membrane
1.64	Mkx	mohawk homeobox	multicellular organismal development // DNA binding
1.64	Xbp1**	X-box binding protein 1	regulation of transcription DNA-dependent
1.59	Tnfsf11	tumor necrosis factor (ligand) superfamily, member 11	regulates osteoclast differentiation and activation // immune response // cytokine activity // protein binding // tumor necrosis factor receptor binding // integral to membrane
1.58	Pdpx	pyridoxal (pyridoxine, vitamin B6) phosphatase	catalytic activity // metabolic process
1.52	Purg	purine-rich element binding protein G	nucleus // DNA binding
1.52	L3mbtl3	l(3)mbt-like 3 (Drosophila)	regulation of transcription // nucleus
1.5	Ccng2	cyclin G2	cell cycle regulation
-1.5	Lamp2	lysosomal membrane glycoprotein 2	tRNA aminoacylation for protein translation // integral to membrane; lysosome // ATP binding; tRNA ligase activity
-1.5	Syt11	synaptotagmin 11	transport // cell junction //cytoplasmic vesicle // calcium ion binding
-1.5	Sesn2	sestrin 2	cell cycle arrest // nucleus
-1.51	Spic	Spi-C transcription factor (Spi-1/PU.1 related)	regulation of transcription// transcription factor complex // DNA binding // nucleus
-1.51	Tieg1	TGFB inducible early growth response 1	transcription factor
-1.52	Hist1h1c	histone 1, H1c	chromosome organization and biogenesis // nucleosome // DNA binding // protein binding
-1.52	Frm4a	FERM domain containing 4A	cytoplasm // cytoskeleton // binding
-1.52	Idb4	inhibitor of DNA binding 4	cell proliferation // protein binding // transcription regulation
-1.52	Gpr160	G protein-coupled receptor 160	G-protein coupled receptor protein signaling pathway // signaling transduction // integral to

			membrane // receptor activity
-1.53	Luc7l2	LUC7-like 2 (S. cerevisiae)	metal ion binding // protein binding
-1.53	Bcor	Bcl6 interacting corepressor	chromatin modification // regulation of transcription // DNA binding
-1.55	Daf1	decay accelerating factor 1	complement activation, classical pathway // integral to membrane
-1.56	Flnb	filamin beta	skeletal muscle development // cytoplasm// cytoskeleton // actin binding // protein binding
-1.56	Pwwp2b	PWWP domain containing 2B	//
-1.57	Slc7a1	solute carrier family 7 (cationic amino acid transporter, y + system), number 1	amino acid transport// arginine transport // integral to membrane
-1.57	Trak1	trafficking protein, kinesin binding 1	GABA receptor binding
-1.57	Mapk4	mitogen-activated protein kinase 4	cell cycle // protein amino acid phosphorylation // ATP binding // kinase activity
-1.57	Nodal*	nodal	cytokine activity // growth factor activity // determination of left/right symmetry // development
-1.58	Zbtb7*	zinc finger and BTB domain containing 7	cartilage development // negative regulation of transcription from RNA polymerase II promoter // DNA binding // histone acetyltransferase binding
-1.59	Idb1	inhibitor of DNA binding 1	development // negative regulation of transcription from Pol II promoter // regulation of angiogenesis // nucleus
-1.6	Zmat4	zinc finger, matrin type 4	intracellular // nucleus // DNA binding// metal ion binding
-1.61	Spry4	sprouty homolog 4 (Drosophila)	multicellular organismal development // negative regulation of MAP kinase activity // cytoplasm // membrane // protein binding
-1.63	Foxp1	forkhead box P1	cell differentiation // DNA binding // metal ion binding
-1.63	Socs2	suppressor of cytokine signaling 2	intracellular signaling cascade // negative regulation of multicellular organism growth // growth hormone receptor binding // protein binding
-1.67	Rnase4	ribonuclease, Rnase A family 4	endonuclease activity; hydrolase activity; nucleic acid binding; pancreatic ribonuclease activity
-1.68	Plxdc1	plexin domain containing 1	receptor activity // integral to membrane
-1.69	Nab2	Ngfi-A binding protein 2	transcriptional repressor activity //
-1.69	Cyp2s1	cytochrome P450, family 2, subfamily s, polypeptide 1	monooxygenase activity; oxidoreductase activity // integral to membrane
-1.72	Arl4	ADP-ribosylation factor-like 4	small GTPase mediated signal transduction // intracellular // GTP binding // GTPase activity
-1.73	Mllt2h	homolog of human MLLT2 unidentified gene	transcription factor activity // cell growth and/or maintenance
-1.74	Snai1	snail homolog 1 (Drosophila)	DNA binding; nucleic acid binding; zinc ion binding
-1.76	Mllt6	myeloid/lymphoid or mixed lineage-leukemia translocation to 6 homolog (Drosophila)	regulation of transcription // metal ion binding // DNA binding
-1.8	Pqlc1	PQ loop repeat containing 1	integral to membrane
-1.8	Nr4a1	nuclear receptor subfamily 4, group A, member 1	inhibition of caspase activation // regulation of transcription // steroid hormone receptor activity // nucleus
-1.81	Ccno	cyclin O	DNA repair // hydrolase activity // nucleus
-1.89	Slc30a1	solute carrier family 30 (zinc transporter), member 1	cation transporter activity; zinc ion transporter activity // integral to membrane
-1.95	Ndrp1***	N-myc downstream regulated 1	mast cell activation // cytoplasm // nucleus
-1.96	Cdkn1a	cyclin-dependent kinase inhibitor 1A (P21)	cell cycle arrest // negative regulation of apoptosis // positive regulation of B-cell proliferation // positive regulation of non-apoptotic programmed cell death // response to DNA damage stimulus
-2.06	Zfp296	zinc finger protein 296	//
-2.33	Idb4*	inhibitor of DNA binding 4	//
-2.38	Pou4f2	POU domain, class 4, transcription factor 2	axon extension involved in development // chromatin binding

-2.44	Slc30a1	solute carrier family 30 (zinc transporter), member 1	cation transporter activity // zinc ion transporter activity // integral to membrane
-2.48	Klf3***	Kruppel-like factor 3 (basic)	transcription regulation // DNA binding // metal ion binding
-9.9	Cyp1b1*	cytochrome P450, family 1, subfamily b, polypeptide 1	oxidation reduction // electron carrier // ER
-17.79	Cyp1a1	cytochrome P450, family 1, subfamily a, polypeptide 1	electron transport// monooxygenase activity; oxidoreductase activity // ER

4.3.4.2.2

4.3.4.2.3 Gene Ontology analysis of the genes differentially expressed at 4h

The Gene Ontology (GO) Consortium [<http://geneontology.org>], maintains a database of controlled vocabularies for the description of molecular functions, biological processes and cellular components of gene products. A gene product can have one or more molecular functions, be used in one or more biological processes, and may be associated with one or more cellular components. The results from GO analysis can provide insights into the biology of the systems being studied.

GO analysis for molecular functions is performed on the genes significantly differentially expressed at 4h infection as determined by GeneSpring analysis. The genes are filtered for p-value < 0.05 and expression fold change greater than +/- 1.5. The GO results appear as a spreadsheet in Table 4.15 that reports the number and the percentage of genes annotated in each category, the number of analyzed genes and a p-value also known as ‘enrichment score’ per category. The p-value reported indicates the relative importance or significance of the GO term among the entities in the selection compared to the entities in the whole dataset (Ashburner *et al.*, 2000).

The lists of GO analysis for biological processes and cellular components are available in Appendix A.

Table 4.13 Gene Ontology results in the molecular-function category for GeneSpring analysis

The 58 annotated genes, out of 89 total, differentially expressed following 4h of *S. Typhimurium* infection (p-value < 0.05, fold change +/- 1.5) are analyzed.

Filter on 1.5 fold change 4-0h (89 genes, 58 annotated) selected with GO:3674:molecular_function					
GO Category	Genes in Category	% of Genes in Category	Genes in List in Category	% of Genes in List in Category	p-Value
GO:4497: monooxygenase activity	152	0.666	3	5.172	0.00683
GO:16712: oxidoreductase activity	18	0.0789	1	1.724	0.0448
GO:30377: U-plasminogen activator receptor activity	1	0.00438	1	1.724	0.00254
GO:15082: di-, tri-valent inorganic cation transporter activity	44	0.193	2	3.448	0.0056
GO:5385: zinc ion transporter activity	10	0.0438	2	3.448	0.000282
GO:46873: metal ion transporter activity	77	0.337	2	3.448	0.0164
GO:46915: transition metal ion transporter activity	39	0.171	2	3.448	0.00443
GO:1871: pattern binding	125	0.548	2	3.448	0.0403
GO:30247: polysaccharide binding	121	0.53	2	3.448	0.038
GO:5539: glycosaminoglycan binding	119	0.521	2	3.448	0.0369
GO:8201: heparin binding	86	0.377	2	3.448	0.0202
GO:3676: nucleic acid binding	4624	20.26	18	31.03	0.0346
GO:3743: translation initiation factor activity	135	0.591	2	3.448	0.0463
GO:19207: kinase regulator activity	82	0.359	2	3.448	0.0185
GO:19887: protein kinase regulator activity	80	0.35	2	3.448	0.0177
GO:16538: cyclin-dependent protein kinase regulator activity	24	0.105	2	3.448	0.00169
GO:30528: transcription regulator activity	1800	7.885	10	17.24	0.0145
GO:16564: transcriptional repressor activity	164	0.718	3	5.172	0.00841

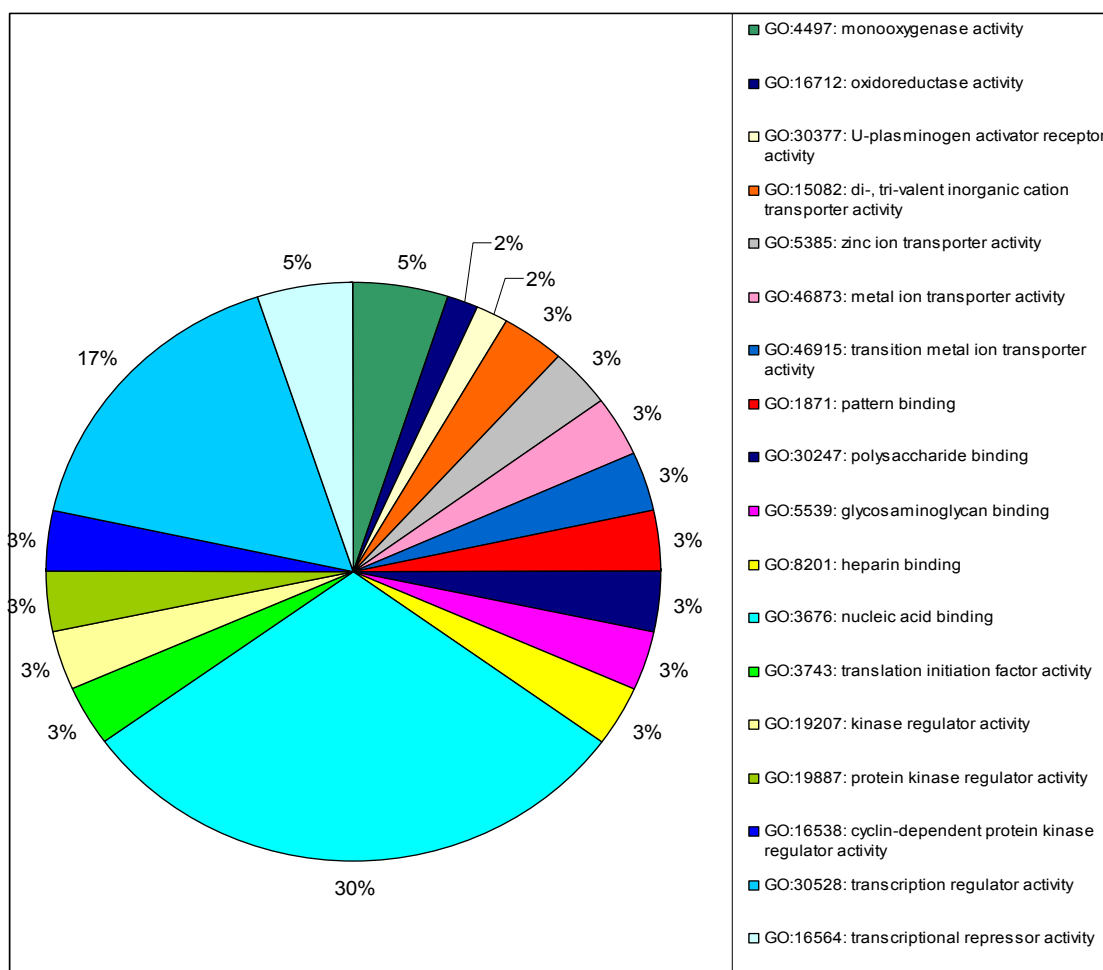


Figure 4.7 Graphical representation of the Gene Ontology analysis for molecular function of genes differentially expressed at 4h

The 89 genes determined to be significantly differentially expressed by GeneSpring analysis of murine AB2.2 ES cells at 4h infection with *S. Typhimurium*, (compared to uninfected controls) were further examined for Gene Ontology annotation describing the molecular function. This analysis highlighted that about a third of the listed genes have ‘nucleic acid binding’ ability and about a quarter have ‘transcription regulator activity’.

4.3.4.2.4 Real time RT-PCR to confirm GeneSpring analysis

The conditions used are the same as previously described for RT-PCR. Briefly, cDNAs were amplified using the QuantiTect QIAGEN kit and the real time RT-PCRs were carried out using the Quantum SYBR Green kit on a Stratagene real time machine. . It is important to validate the results of the bioinformatic analysis and a few genes reported to be significantly up- or down-regulated were selected to be confirmed using the relative quantification method, $\Delta\Delta C_t$. Gene selection was based on their potential relevance to *Salmonella*-host interaction studies suggested by close reading of the literature. These genes were distinct from those identified by Bioconductor analysis. Genes involved in early response, cellular trafficking regulation, cytokine signaling and anti-inflammatory response were included. For a more detailed description of each gene please refer to Table 4.11. The resulting fold changes are reported in Figure 4.8.

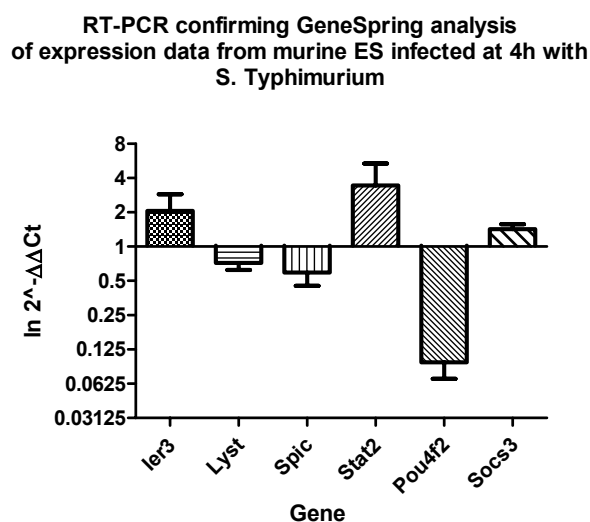


Figure 4.8 RT-PCR results conducted on a few genes identified by GeneSpring analysis

Some of the genes determined by GeneSpring analysis to be up- or down- regulated and with a significant p-value during infection were tested for relative quantification by RT-PCR. In this analysis the Ct values of target genes were compared to the Ct value of an internal control β -actin and the ratios were calculated and plotted as $\ln 2^{-\Delta\Delta C_t}$. The reactions were carried out in triplicate for each biological replicate at 0h and at 4h infection and reported here are the mean values. The error bars represent the standard error for each replicate. The initial amount of template cDNA is inversely proportional to the parameter measured for each reaction, the Ct.

Semi-quantitative RT-PCR confirms the results obtained by bioinformatics analysis of up- or down-regulated genes. In this case the genes chosen to be confirmed were identified by Gene Spring analysis as differentially expressed at 4h infection. The RT-PCR results confirmed that those genes reported to be up- or down-regulated by bioinformatics analysis were really up- or down-regulated.

4.3.4.2.5 Statistical analysis of RT-PCR data on genes identified by GeneSpring

Statistical analysis was conducted on the Ct values obtained from the real time RT-PCR conducted on a few genes identified by GeneSpring analysis. The REST[©] statistical program was used as described before. This analysis indicated that the Ct values of target genes were not significantly (p -value < 0.05) different to the Ct value of the target gene β actin (Figure 4.9). Nevertheless one gene, Pou4f2 reported a p -value < 0.1 . This gene contributes to the maintenance of the stemness characteristic. This result suggests that ES cells may be initiating a differentiation process during infection or that bacterial infection induce cell differentiation. However, further supporting evidence would be required to confirm this possibility.

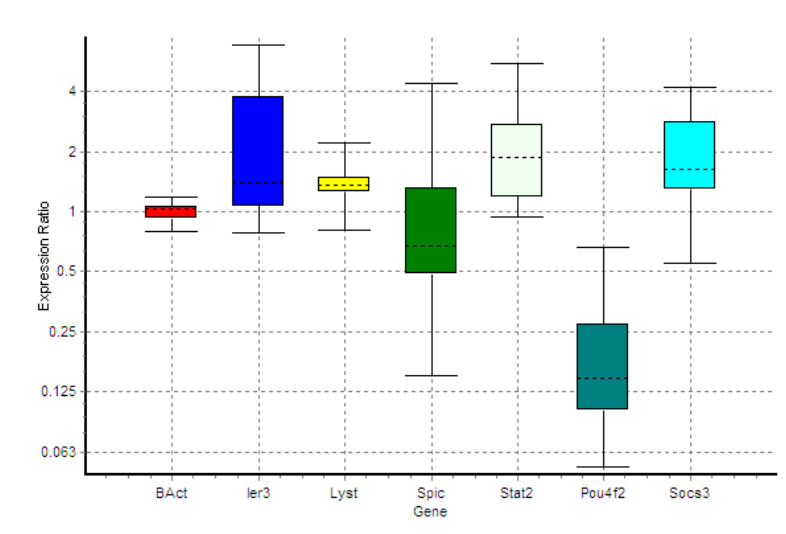


Figure 4.9 Whisker box plot of RT-PCR reaction conducted on genes identified by GeneSpring

This figure represents the Ct mean of three replicate reactions conducted on each gene. The genes were identified by GeneSpring analysis and the expression level of each one was compared to the expression level of an internal control gene: β -actin. In this experiment total RNA extracted from AB2.2 mouse ES cells uninfected and infected at 4h with *S. Typhimurium* SL1344 were used.

4.3.4.3 GEPAS: ASCA analysis

4.3.4.3.1 Time course analysis using ASCA

The mRNA profile of murine ES cells infected with *S. Typhimurium* SL1344 was further examined in a time course analysis. The analysis using time as a variable was carried out in order to highlight interesting expression patterns in gene expression during infection. A similar expression pattern might indicate co-regulation by a common transcription factor. For this purpose the Gene Expression Profile Analysis Suite (GEPAS) [<http://www.gepas.org>], which has been designed to provide an intuitive web-based interface (Montaner *et al.*, 2006), was employed. The ANOVA-simultaneous component analysis (ASCA) was proposed in order to analyze metabolomics data, and in this study was used in order to take into consideration the ‘time’ as a variable over the experiment (Smilde *et al.*, 2005). Basically ASCA fits an ANOVA model for each gene. In this case the ANOVA model has two factors, one is the time, which will give the temporal gene expression change related upon treatment, and the other is the individual. This method looks for different expression profile models that a gene can follow during treatment, and can detect if a gene follows the trend very well, but does not necessarily reach a sufficient significance in the traditional way. For a gene to be selected by ASCA, it must follow the trend of the majority of the changing genes (of the 2-3 major patterns). (Dr. Conesa personal communication)

ASCA analysis reported 943 genes, which were grouped into nine arbitrary clusters according to how their expression changed over time during the infection. The trend in each group is reported in Figure 4.10. Each graph reports the expression of the genes contained in each group represented as the mean log₂ for each gene’s expression divided by its expression at time zero. The three lines represent the three biological replicates. A value of 1 on the y axis represents two-fold up-regulation and a value of -1 represents two-fold down-regulation.

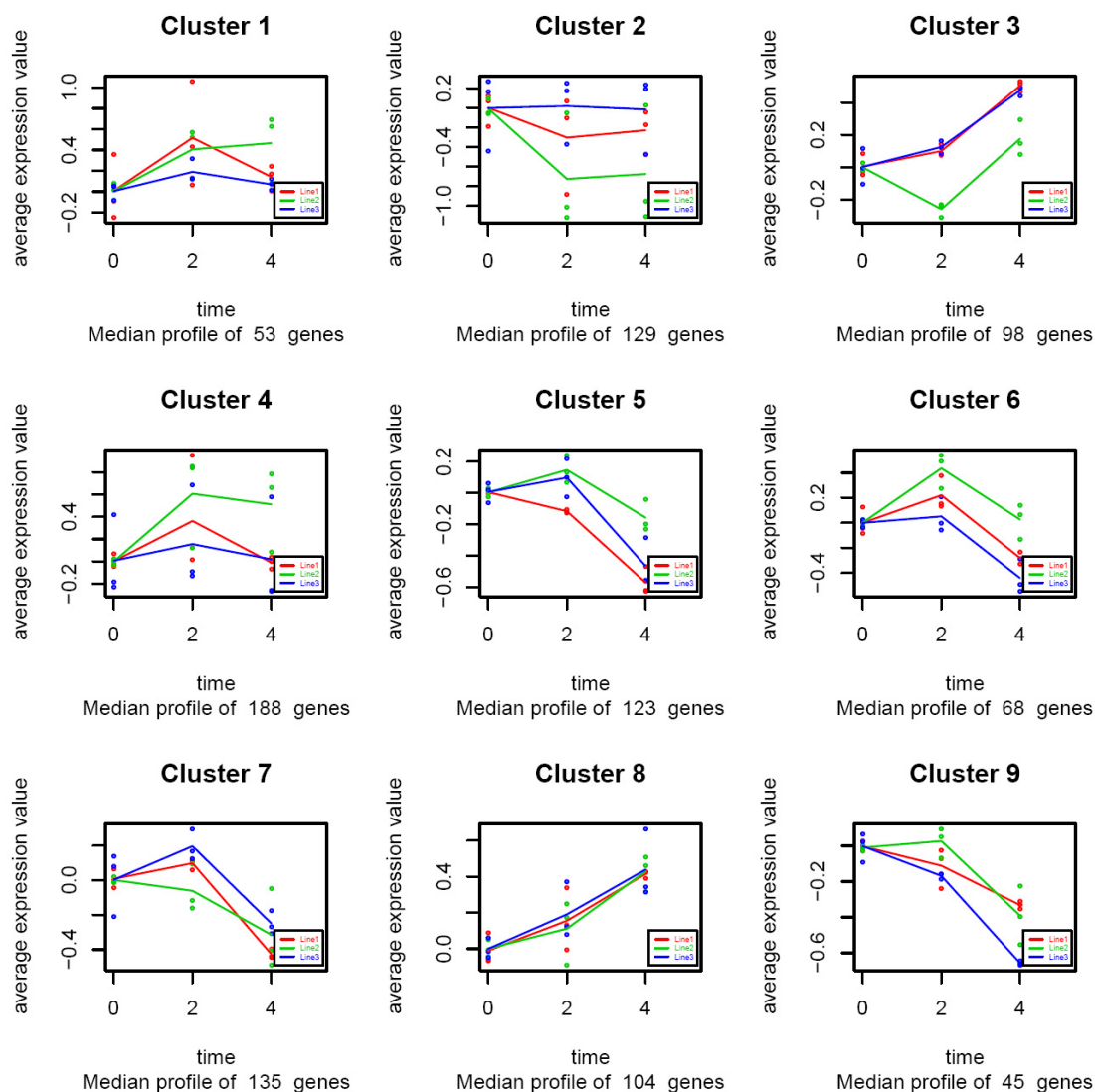


Figure 4.10 Gene clusters derived from ASCA analysis

ASCA analysis was used to investigate the data using time as a variable, and the genes whose expression profile changed during infection are reported. The 953 genes initially listed were then divided into nine arbitrary clusters and only those that best fit each trend were further analyzed.

This study included groups 3 and 8 for up-regulated genes and groups 5, 6, 7 and 9 for down-regulated genes. This analysis revealed 152 genes positively expressed during infection and 271 genes negatively expressed during infection. Tables 4.14 and 4.15 report some of the positively and the negatively regulated genes derived from this analysis, divided in categories that I think are relevant to this study based on current literature. For this reason the genes were organized into six groups: Cyclins, Ubiquitins, Mitochondrion, ER and Golgi apparatus, Cytokines and Chemokines, Cytoskeleton, Immune response and General interest.

Table 4.14 Gene list derived from ASCA analysis of the genes up-regulated during infection

Of the 153 genes found to be up-regulated during infection by ASCA analysis 45 are reported here. The genes are divided in categories that I think are interesting and relevant to this study based on close reading of the literature.

Gene Symbol	Gene Title	Biological and molecular functions
Cyclins		
Ccng2	cyclin G2	regulation of progression through cell cycle /// cell cycle /// mitosis /// cell division/// kinase regularoty activity
Ccnj1	cyclin J-like	regulation of progression through cell cycle
Cnm3	cyclin M3	biological_process
Ubiquitin		
Herpud1	homocysteine-inducible, endoplasmic reticulum stress-inducible, ubiquitin-like domain member 1	response to stress /// response to unfolded protein /// ER membrane // circadian regulation
Shprh	SNF2 histone linker PHD RING helicase	DNA repair /// nucleosome assembly /// transcription /// ubiquitin cycle /// ATP-binding /// zinc ion binding
Syv1	synovial apoptosis inhibitor 1, synoviolin	in utero embryonic development /// ubiquitin cycle /// anti-apoptosis /// response to unfolded protein /// multicellular organismal development /// integral to membrane /// ER membrane
Trim32	tripartite motif protein 32	ubiquitin cycle /// nucleic acid binding /// zinc ion binding
Usp26	ubiquitin specific peptidase 26	ubiquitin-dependent protein catabolic process /// ubiquitin cycle
Vps37a	vacuolar protein sorting 37A (yeast)	protein modification process /// ubiquitin cycle /// transport /// protein transport
Armet	arginine-rich, mutated in early stage tumors	ubiquitin cycle /// biological_process
Mitochondrion, ER, Golgi		
Gls	glutaminase	glutamine metabolic process/// mitochondrial inner membrane
Mtus1	mitochondrial tumor suppressor 1	ATP synthesis coupled proton transport /// receptor activity /// proton-transporting two-sector ATPase complex
Bfar	bifunctional apoptosis regulator	anti-apoptosis /// protein binding /// ER
Dhcr7	7-dehydrocholesterol reductase	blood vessel development /// steroid biosynthetic process /// cholesterol biosynthetic process /// lipid biosynthetic process /// regulation of cell proliferation /// nuclear outer membrane and ER
Eif2ak3	eukaryotic translation initiation factor 2 alpha kinase 3	skeletal development /// electron transport /// translation /// protein amino acid phosphorylation /// caspase activation /// virus-infected cell apoptosis /// ER overload response /// response to unfolded protein /// calcium-mediated signaling /// insulin secretion /// protein kinase activity
Ero1b	ERO1-like beta (S. cerevisiae)	electron transport /// oxidoreductase activity// ER
Gcs1	glucosidase 1	metabolic process /// oligosaccharide metabolic process /// ER /// integral to membrane
Hspa5	heat shock 70kD protein 5 (glucose-regulated protein)	anti-apoptosis /// ER overload response /// negative regulation of caspase activity /// ATP binding /// ribosome binding
Pigc	phosphatidylinositol glycan anchor biosynthesis, class C	GPI anchor biosynthetic process /// transferase activity /// ER membrane
Gopc	golgi associated PDZ and coiled-coil motif containing	transport /// autophagy /// protein transport /// protein homooligomerization /// small GTPase regulator activity /// membrane fraction/// trans-Golgi network transport vescicle
Slc35a5	solute carrier family 35, member A5	carbohydrate transport /// nucleotide-sugar transport /// Golgi membrane
Kif1b	kinesin family member 1B	microtubule-based process /// microtubule-based movement /// nerve-nerve synaptic transmission /// anterograde axon cargo transport /// embryonic development /// cytoskeleton-dependent intracellular transport /// mitochondrion transport along microtubule /// microtubule associated complex/// ATPase activity
Acbd3	acyl-Coenzyme A binding domain containing 3	steroid biosynthetic process /// transport /// acyl-CoA binding /// mitochondrion
EG623661	predicted gene, EG623661	protein modification process /// catalytic activity /// mitochondrion

Cytokine & Chemokine		
Nfat5	nuclear factor of activated T-cells 5	cytokine production /// transcription /// positive regulation of transcription from RNA polymerase II promoter /// protein binding
Tnfsf11	tumor necrosis factor (ligand) superfamily, member 11	immune response /// multicellular organismal development /// lymph node development /// protein homooligomerization /// receptor activity /// cytokine activity /// tumor necrosis factor binding
Cytoskeleton		
Taok2	TAO kinase 2	activation of MAPKK activity /// protein amino acid phosphorylation /// response to stress /// regulation of cell shape /// actin cytoskeleton organization and biogenesis /// positive regulation of JNK cascade /// focal adhesion formation
Actr1b	ARP1 actin-related protein 1 homolog B (yeast)	nucleotide binding /// structural constituent of cytoskeleton /// microtubule associated complex /// actin filament
Elmo2	engulfment and cell motility 2, ced-12 homolog (C. elegans)	phagocytosis /// apoptosis /// cytoskeleton
Enc1	ectodermal-neural cortex 1	proteolysis /// multicellular organismal development /// actin binding /// cysteine-type endopeptidase activity /// cytoskeleton
Hook1	hook homolog 1 (Drosophila)	microtubule cytoskeleton organization and biogenesis /// multicellular organismal development /// actin binding /// microtubule binding /// cytoskeleton
Lyst	lysosomal trafficking regulator	transport /// cellular defense response /// signal transduction /// endosome to lysosome transport /// protein transport /// endosome-microtubule-cytoskeleton
Nisch	nischarin	cell communication /// Rac protein signal transduction /// actin cytoskeleton organization and biogenesis /// negative regulation of cell migration /// receptor activity
Immune-Response and General Interest		
Ier3	immediate early response 3	membrane /// integral to membrane /// integral to membrane
Ier5l	immediate early response 5-like	///
Irf2bp1	interferon regulatory factor 2 binding protein 1	negative regulation of transcription from RNA polymerase II promoter
Ppp1r13b	protein phosphatase 1, regulatory (inhibitor) subunit 13B	induction of apoptosis /// defense response /// negative regulation of progression through cell cycle
Apaf1	apoptotic peptidase activating factor 1	neural tube closure /// proteolysis /// apoptosis /// caspase activation /// defense response /// multicellular organismal development /// regulation of apoptosis
Bcl3	B-cell leukemia/lymphoma 3	protein import into nucleus, translocation /// follicular dendritic cell differentiation /// marginal zone B cell differentiation /// humoral immune response mediated by circulating immunoglobulin /// transcription /// antimicrobial humoral response /// positive regulation of interferon-gamma production /// T-helper 1 type immune response /// negative regulation of tumor necrosis factor biosynthetic process /// defense response to bacterium /// regulation of apoptosis /// T-helper 2 cell differentiation /// positive regulation of interleukin-10 biosynthetic process ///
Banp	Btg3 associated nuclear protein	protein binding
Ercc4	excision repair cross-complementing rodent repair deficiency, complementation group 4	DNA metabolic process /// DNA repair /// nucleotide-excision repair /// endonuclease activity /// endodeoxyribonuclease activity /// hydrolase activity
Gbp6	guanylate binding protein 6	immune response /// nucleotide binding /// GTPase activity
Hsp110	heat shock protein 110	response to heat /// chaperone cofactor-dependent protein folding /// nucleotide binding /// ATP binding
Hspa1a	heat shock protein 1A	telomere maintenance /// DNA repair /// protein folding /// response to heat /// ATP binding
Hspa1b	heat shock protein 1B	telomere maintenance /// DNA repair /// protein folding /// anti-apoptosis /// response to heat /// negative regulation of caspase activity /// ATP binding

Table 4.15 Gene list derived from ASCA analysis of genes down-regulated during infection

ASCA analysis highlighted 270 genes negatively regulated during *S. Typhimurium* infection. Potentially genes are organized into categories.

Gene Symbol	Gene Title	Biological and molecular functions
Cyclins		
Ccnt1	cyclin T1	regulation of progression through cell cycle /// regulation of cyclin-dependent protein kinase activity /// transcription /// protein amino acid phosphorylation /// cell cycle
Ccnu	cyclin U	regulation of progression through cell cycle /// DNA repair /// response to DNA damage stimulus /// metabolic process
Cdkn1a	cyclin-dependent kinase inhibitor 1A (P21)	regulation of progression through cell cycle /// response to DNA damage stimulus /// negative regulation of cell proliferation /// positive regulation of B cell proliferation /// negative regulation of apoptosis /// positive regulation of non-apoptotic programmed cell death
Hmox1	heme oxygenase (decycling) 1	heme oxidation /// response to stimulus /// iron ion binding /// ER /// integral membrane
Ubiquitin		
Cbx4	chromobox homolog 4 (Drosophila Pc class)	chromatin assembly or disassembly /// transcription /// ubiquitin cycle /// chromatin modification
Nfkbia	nuclear factor of kappa light chain gene enhancer in B-cells inhibitor, alpha	protein import into nucleus, translocation /// lipopolysaccharide-mediated signaling pathway /// response to lipopolysaccharide /// regulation of cell proliferation /// response to exogenous dsRNA /// negative regulation of myeloid cell differentiation /// negative regulation of Notch signaling pathway /// NF-kappaB binding
Ranbp2	RAN binding protein 2	protein folding /// ubiquitin cycle /// intracellular transport /// protein binding /// metal ion binding
Rnf103	ring finger protein 103	ubiquitin cycle /// nucleic acid binding /// protein binding /// metal ion binding
Rnf12	ring finger protein 12	transcription /// ubiquitin cycle /// metal ion binding
Rnf128	ring finger protein 128	proteolysis /// ubiquitin cycle /// negative regulation of cytokine biosynthetic process /// metal ion binding
Tbl1xr1	transducin (beta)-like 1X-linked receptor 1	transcription /// ubiquitin cycle /// signal transduction /// chromatin modification /// GTPase activity
Tceb1	transcription elongation factor B (SIII), polypeptide 1	transcription /// ubiquitin cycle /// protein binding
Trim63	tripartite motif-containing 63	ubiquitin cycle /// muscle contraction /// proteasomal ubiquitin-dependent protein catabolic process /// metal ion binding
Ube2e3	ubiquitin-conjugating enzyme E2E 3, UBC4/5 homolog (yeast)	regulation of cell growth /// protein modification process /// ubiquitin-dependent protein catabolic process /// ubiquitin cycle
Mitochondrion, ER, Golgi		
Trp53	transformation related protein 53	protein import into nucleus, translocation /// regulation of progression through cell cycle /// transcription /// induction of apoptosis /// response to DNA damage stimulus /// ER overload response /// cell cycle /// caspase activation via cytochrome c /// positive regulation of transcription from RNA polymerase II promoter /// negative regulation of fibroblast proliferation
Abcb7	ATP-binding cassette, sub-family B (MDR/TAP), member 7	transport /// ATPase activity /// ATP binding /// nucleotide binding /// mitochondrial inner membrane
Bbc3	Bcl-2 binding component 3	release of cytochrome c from mitochondria /// induction of apoptosis /// caspase activation /// negative regulation of cell growth /// DNA damage response, signal transduction by p53 class mediator resulting in induction of apoptosis /// mitochondrial envelope
Gad1	glutamic acid decarboxylase 1	synaptic transmission /// carboxylic acid metabolic process /// neurotransmitter biosynthetic process /// mitochondrion
Agpat2	1-acylglycerol-3-phosphate O-acyltransferase 2 (lysophosphatidic acid acyltransferase, beta)	metabolic process /// phospholipid biosynthetic process /// 1-acylglycerol-3-phosphate O-acyltransferase activity /// ER /// integral to membrane
Asah3l	N-acylsphingosine amidohydrolase 3-like	lipid metabolic process /// ceramide metabolic process /// Golgi membrane /// ER membrane
Cds1	CDP-diacylglycerol synthase 1	phospholipid biosynthetic process /// CDP-diacylglycerol biosynthetic process /// phosphatidate cytidyltransferase activity /// magnesium binding /// ER membrane

Cyp1a1	cytochrome P450, family 1, subfamily a, polypeptide 1	electron transport /// monooxygenase activity /// iron ion binding /// extracellular space /// ER /// microsome
Cyp1b1	cytochrome P450, family 1, subfamily b, polypeptide 1	electron transport /// monooxygenase activity /// iron ion binding /// extracellular space /// ER /// microsome
Cyp2s1	cytochrome P450, family 2, subfamily s, polypeptide 1	electron transport /// monooxygenase activity /// iron ion binding /// extracellular space /// ER /// microsome
Fvt1	follicular lymphoma variant translocation 1	metabolic process /// oxidoreductase activity /// ER /// integral to membrane
Lrpap1	low density lipoprotein receptor-related protein associated protein 1	receptor activity /// heparin binding /// low-density lipoprotein receptor binding /// ER /// plasma membrane
Tmc6	transmembrane channel-like gene family 6	transpor /// transporter activity /// ER /// integral to membrane
Gnpnat1	glucosamine-phosphate N-acetyltransferase 1	UDP-N-acetylglucosamine biosynthetic process /// glucosamine 6-phosphate N-acetyltransferase activity /// N-acetyltransferase activity /// late endosome /// ER-Golgi intermediate compartment
Optn	optineurin	protein targeting to Golgi /// Golgi organization and biogenesis /// biological_process /// Golgi to plasma membrane protein transport /// Golgi apparatus
Sgms2	sphingomyelin synthase 2	lipid metabolic process /// sphingolipid metabolic process /// sphingomyelin biosynthetic process /// kinase activity /// transferase activity /// Golgi apparatus
St6gal1	beta galactoside alpha 2,6 sialyltransferase 1	protein amino acid glycosylation /// transferase activity /// integral to Golgi membrane
St8sia1	ST8 alpha-N-acetyl-neuraminide alpha-2,8-sialyltransferase 1	protein amino acid glycosylation /// positive regulation of cell proliferation /// transferase activity /// integral to Golgi membrane
Chic2	cysteine-rich hydrophobic domain 2	Golgi to plasma membrane transport /// Golgi-associated vesicles /// Golgi apparatus
Cytokine & Chemokine		
Klf6	Kruppel-like factor 6	transcription /// cytokine and chemokine mediated signaling pathway /// metal ion binding /// nucleus
Ltb	lymphotoxin B	immune response /// lymph node development /// cytokine activity /// tumor necrosis factor receptor binding /// plasma membrane
Nodal	nodal	in utero embryonic development /// transforming growth factor beta receptor signaling pathway /// multicellular organismal development /// positive regulation of cell proliferation /// cell migration /// stem cell maintenance /// cytokines activity /// extracellular scape
Socs2	suppressor of cytokine signaling 2	regulation of cell growth /// intracellular signaling cascade /// negative regulation of signal transduction /// growth hormone receptor binding /// insuline-like growth factor receptor binding
Socs3	suppressor of cytokine signaling 3	regulation of cell growth /// regulation of protein amino acid phosphorylation /// intracellular signaling cascade /// negative regulation of signal transduction /// negative regulation of insulin receptor signaling pathway
Zc3h15	Zinc finger CCCH-type containing 15	cytokine and chemokine mediated signaling pathway
Bmp4	bone morphogenetic protein 4	skeletal development /// positive regulation of protein amino acid phosphorylation /// multicellular organismal development /// BMP signaling pathway /// positive regulation of cell differentiation /// cytokine activity /// growth factor activity /// heparin binding
Ccl25	chemokine (C-C motif) ligand 25	chemotaxis /// chemotaxis /// inflammatory response /// immune response /// signal transduction /// leukocyte migration /// cytokine and chemokine activity
Cxcl16	chemokine (C-X-C motif) ligand 16	chemotaxis /// immune response /// low-density lipoprotein receptor activity /// scavenger receptor activity /// cytokine activity /// chemokine activity
Cytoskeleton		
Cdc42ep3	CDC42 effector protein (Rho GTPase binding) 3	regulation of cell shape /// actin cytoskeleton
Ctnna1	catenin (cadherin associated protein), alpha 1	cell adhesion /// establishment and/or maintenance of cell polarity /// negative regulation of apoptosis /// positive regulation of smoothed signaling pathway /// cadherin binding /// actin filament binding /// adherens junction /// lamellipodium /// zonula lamellipodium
Dsg2	desmoglein 2	cell adhesion /// homophilic cell adhesion /// calcium ion binding /// integral of membrane /// desmosome
Epb4.9	erythrocyte protein band 4.9	cytoskeleton organization and biogenesis /// barbed-end actin filament capping /// actin binding

Flnb	filamin, beta	striated muscle development /// actin binding /// stress fiber cytoplasm /// focal adhesion /// cytoskeleton
Frmd4a	FERM domain containing 4A	binding /// cytoskeleton
Gphn	gephyrin	protein targeting /// Mo-molybdopterin cofactor biosynthetic process /// establishment of synaptic specificity at neuromuscular junction /// catalytic activity /// cytoskeletal protein binding
Kras	v-Ki-ras2 Kirsten rat sarcoma viral oncogene homolog	regulation of progression through cell cycle /// small GTPase mediated signal transduction /// Ras protein signal transduction /// positive regulation of cell proliferation /// actin cytoskeleton organization and biogenesis /// regulation of synaptic transmission, GABAergic /// positive regulation of Rac protein signal transduction ///
Mtss1	metastasis suppressor 1	cell motility /// actin filament organization /// cell adhesion /// signal transduction /// transmembrane receptor protein tyrosine kinase signaling pathway /// actin filament polymerization /// filopodium formation /// actin binding /// ruffle /// endocytic vesicle
Synpo2l	synaptopodin 2-like	actin binding /// protein binding /// cytoskeleton
Ttl	tubulin tyrosine ligase	microtubule cytoskeleton organization and biogenesis /// protein modification process /// regulation of axon extension /// tubulin-tyrosin ligase activity /// magnesium-potassium ion binding /// microtubule
Arhgap8	Rho GTPase activating protein 8	actin cytoskeleton organization and biogenesis /// positive regulation of cell migration /// GTPase activator activity
Immune-Response and General Interest		
Relb	avian reticuloendotheliosis viral (v-rel) oncogene related B	regulation of progression through cell cycle /// transcription /// cellular process /// antigen processing and presentation /// T-helper 1 type immune response /// myeloid dendritic cell differentiation /// T-helper 1 cell differentiation /// regulation of transcription
Arl6ip2	ADP-ribosylation factor-like 6 interacting protein 2	immune response /// nucleotide response /// GTPase activity
Cd55	CD55 antigen	immune response /// complement activation, classical pathway /// innate immune response /// GPI anchor binding
Eif2ak2	eukaryotic translation initiation factor 2-alpha kinase 2	translation /// protein amino acid phosphorylation /// immune response /// response to virus /// unfolded protein response /// protein amino acid autophosphorylation /// RNA binding /// transferase binding /// protein kinase activity /// protein serine/threonine kinase activity
Centd3	centaurin, delta 3	signal transduction /// regulation of cell shape /// negative regulation of cell migration /// negative regulation of Rac protein signal transduction /// negative regulation of Rho protein signal transduction /// regulation of GTPase activity /// ruffle /// lamellipodium /// Rho GTPase activator activity
Gpr160	G protein-coupled receptor 160	signal transduction /// G-protein coupled receptor protein signaling pathway /// rhodopsin-like receptor activity
Gpr83	G protein-coupled receptor 83	signal transduction /// G-protein coupled receptor protein signaling pathway /// rhodopsin-like receptor activity
Mcf2l	mcf.2 transforming sequence-like	intracellular signaling cascade /// Rho protein signal transduction /// regulation of Rho protein signal transduction /// lamellipodia
Tbc1d24	TBC1 domain family, member 24	regulation of Rab GTPase activity
Tbc1d9	TBC1 domain family, member 9	regulation of Rab GTPase activity /// GTPase activator activity
Kbtbd8	Kelch repeat and BTB (POZ) domain containing 8	intracellular protein transport /// exocytosis /// biological process /// regulation of calcium ion-dependent exocytosis /// glucose homeostasis /// negative regulation of G-protein coupled receptor protein signaling pathway /// Rab GTOase binding
Rab11fp2	RAB11 family interacting protein 2 (class I)	///
Rims2	regulating synaptic membrane exocytosis 2	transport /// intracellular protein transport /// exocytosis /// intracellular signaling cascade /// calcium ion-dependent exocytosis /// cAMP-mediated signaling /// insulin secretion /// Rab GTPase binding

4.3.4.3.2 Functional category analysis using FatiGO on ASCA results

One of the problems related to functional genomics is the description of biological properties, functions and interactions shared by a set of genes. An answer to this problem is Gene Ontology that extracts information from scientific journals and provides a structured description of biological functions dividing them into molecular functions, biological processes and cellular components (Ashburner *et al.*, 2000). FatiGO is a web-based application [<http://fatiGO.bioinfo.cnio.es>] able to extract relevant GO terms for a group of genes with respect to a set of reference genes. FatiGO is used here to investigate which functional categories are over- or under-represented in the two groups of genes up-regulated and down-regulated obtained from ASCA analysis compared to the entire list of genes on the microarray chip. FatiGO extracts the function category from GO once the level at which the statistical contrast is going to be performed is indicated. Usually level 3 is used but lower terms in GO hierarchy are more precise. Also FatiGO returns adjusted p-values based on three different ways of accounting for multiple testing (Al-Shahrour *et al.*, 2004). The analysis was performed to determine the functional categories of cellular-component, molecular-function, biological process and pathway reported in KEGG (Kyoto Encyclopedia of Genes and Genomes), and the results are reported in Tables 4.16 and 4.17 for up- and down-regulated genes, respectively.

Table 4.16 FatiGO analysis of up-regulated genes from ASCA analysis

The list of up-regulated genes was analyzed for Functional Category enrichment with FatiGO and the results are reported here. Among the genes up-regulated, enrichment of four categories was identified but no pathway was statistically significant.

ASCA analysis up-regulated genes				
Biological process	Level	n of genes	Unadj. p-value	Adj. p-value
response to unfolded protein	5	5	0.000006	0.017700
macromolecule metabolic process	3	37	0.000010	0.020200
primary metabolic process	3	39	0.000037	0.047000
Cellular component	Level	n of genes	Unadj. p-value	Adj. p-value
Nucleus	8	31	0.000013	0.020600

Table 4.17 FatiGO analysis of down-regulated genes from ASCA analysis

The list of down-regulated genes was analyzed for Functional Category enrichment with FatiGO and the results are reported here. Among the genes down-regulated, enrichments can be observed in the TGF- β signaling pathway, and predominantly in transcription or DNA binding proteins.

ASCA down-regulated genes analyzed with FatiGO				
KEGG	Genes list	Number of Genes	Unadj. p-value	Adj. p-value
TGF-beta signaling pathway	Id3, Fst, Nodal, Id2, Bmp4, Id1	6	0	0.0096

Cellular components	Level	Number of Genes	Unadj. p-value	Adj. p-value
nucleus	8	34	0.0004	0.0825

Biological process	Level	number of genes	Unadj. p-value	Adj. p-value
multicellular organismal development	3	25	0	0.0115
anatomical structure development	3	22	0.0001	0.0462
negative regulation of transcription	8	9	0	0.0221
regulation of transcription, DNA-dependent	8	26	0.0001	0.0434
negative regulation of transcription factor activity	9	3	0	0.0115

Cellular functions	Level	Number of Genes	Unadj. p-value	Adj. p-value
nucleic acid binding	3	29	0.0002	0.0541
transcriptional repressor activity	3	6	0.0002	0.0602
nucleotide binding	3	1	0.0003	0.0688
DNA binding	4	23	0	0.0096
unspecific monooxygenase activity	6	3	0.0003	0.0688

4.3.4.3.3 Real Time RT-PCR relative quantification on genes derived from ASCA analysis

ASCA analysis does not provide the fold change in expression so it is difficult to confirm this data by real time RT-PCR. However RT-PCR can give a confirmation of the expression trend of a gene during infection. For this reason, total RNA extracted at 2 and 4 hours post-infection were employed in this experiment as well as appropriate control RNA populations. The genes were chosen for their potential relevance to host-pathogen interaction studies. In addition, a few genes that were identified in previous analyses described in this thesis were included. These were Lamp2 and Socs3, already shown to be down- and up-regulated during ES cell infection. Other genes included examples involved in the regulation of apoptosis, cytoskeleton rearrangement and a TGF- β binding protein. For a more detailed description of each gene please refer to Table 4.14 and 4.15. The data are reported here as $\ln 2^{-\Delta\Delta Ct}$ that represents the ratio between the expression level of the target gene and the control gene (β -actin) expressed in ln scale (Figure 4.11).

Gene selected by the ASCA analysis to be up- or down- regulated during AB2.2 ES cells infection with *S. Typhimurium*

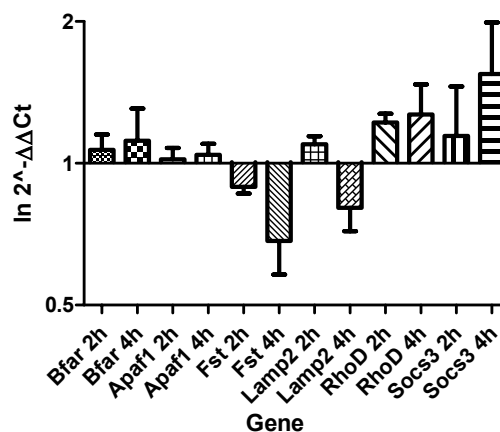


Figure 4.11 Real time RT-PCR relative quantification on ASCA analysis

A few genes selected by ASCA analysis to be positively or negatively regulated in murine ES cells AB2.2 during *S. Typhimurium* infection were chosen to perform relative quantification by real time RT-PCR. In this analysis the Ct values of target genes were compared to the Ct value of an internal control β -actin and the ratios were calculated and plotted as $\ln 2^{-\Delta\Delta Ct}$. The reactions were carried out in triplicate for each biological replicate at 0h, 2h and 4h infection and the mean values are reported here. The error bars represent the standard error for each replicate.

RT-PCR was performed in order to confirm the results obtained by bioinformatics analysis of up- or down-regulated genes. In this case the genes to be confirmed by RT-PCR were chosen as they seemed relevant to this study. The RT-PCR results partially confirmed that those genes reported to be up- or down-regulated by bioinformatics analysis were in fact up- or down-regulated. The Socs3 gene, however, was reported to be down-regulated by ASCA analysis, whereas it was up-regulated in the other analysis as also confirmed by RT-PCR. Refer to Appendix A for a short description of the genes used in this experiment.

4.3.4.3.4 Statistical analysis of RT-PCR data on genes identified by ASCA

Statistical analysis was performed on the real time RT-PCR Ct values obtained on a few genes identified by ASCA analysis. The analysis was performed comparing the expression levels at 4 hours post-infection to the uninfected cells since there were larger expression difference between these samples. The statistical analysis was conducted using REST© 2005. The results from this analysis are shown in Figure 4.12 as a graph plotting the expression range for each gene. This analysis reported no significant difference in the expression levels of the genes taken into consideration here.

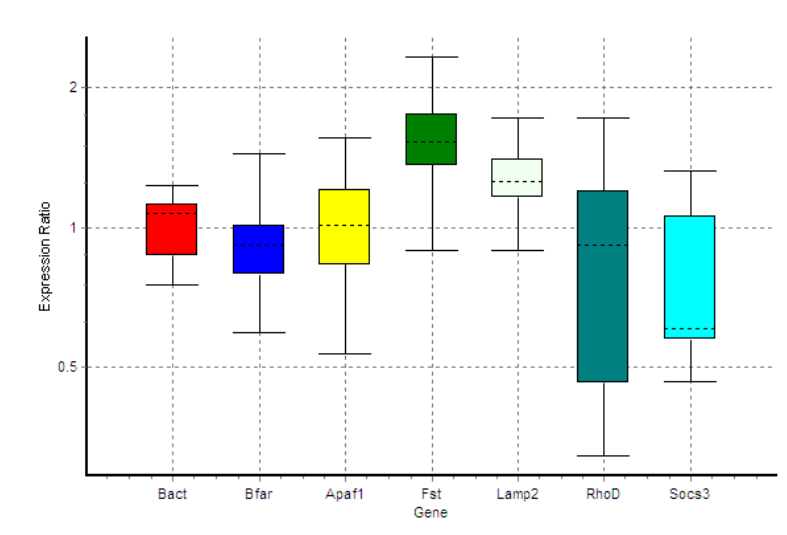


Figure 4.12 Whisker box of the RT-PCR analysis on genes identified by ASCA

The statistical analysis of the Ct values determined from the RT-PCR analysis is here represented as whisker boxes representing the mean value of three independent reactions for each gene. The statistical analysis did not identify any statistically significant difference between the mean Ct values of the target genes compared to the mean Ct value of the control gene β -actin.

4.4 Discussion

This chapter reports the results from the transcription profile of AB2.2 murine ES cells during infection with *S. Typhimurium* SL1344. The concept behind these experiments was to investigate whether ES cells could be developed as a novel *in vitro* model by which to study the response of eukaryotic cells to bacterial infection. It is now well established that microarrays can be used to monitor how immunological cells subjected to bacterial invasion respond in terms of gene expression patterns (Detweiler *et al.*, 2001; Rosenberger *et al.*, 2000). Further work has also been reported on infected epithelial cells that can respond by producing cytokines and other immune factors (Eckmann *et al.*, 2000). Two factors should be kept in mind in the interpretation of the data presented here. Firstly, at least 30% of the cells were infected at 2 hours and 4 hours post-infection. The percentage of cells infected will inevitably have effects on the resulting p-values and fold expression. However it has not been common practise in published papers reporting transcription profile during bacterial infection, to include data on percentage of infected cells. The second factor to consider is that, as noted in previous publications, the response of differentiated cells to pathogen invasion overwhelmingly involves genes linked to the immune response. Interestingly, in the ES cell model used here, this response was not observed and it is possible that by using murine ES cells, that lack a strong immune signature, to highlight other components involved in alternative cellular reaction to pathogen invasion.

Pathogens are able to manipulate host components to their advantage. For example, it has previously been described how *Salmonella* secretes SPI-1 TIISS effector proteins inside non-phagocytic cells directing its own phagocytosis. The TIISS are specialized protein structure with the ability to deliver a specific set of bacterial proteins into the host cells to modulate or interfere with cellular functions; this mechanism is essential for the virulence of many important bacteria such as *Salmonella*, *Shigella* and *Yersinia pestis* (Kubori & Galan, 2003). Also a second *Salmonella* TIISS, harboured on the SPI-2 loci, injects proteins inside the host from the SCV. Examples of SPI-2 effectors include SifA which is involved in the maintenance and survival of the bacteria inside the host cells (Brumell *et al.*, 2002).

In the analysis reported here at least four important groups of genes can be distinguished that are apparently differentially regulated during bacterial infection. These include a limited number of immunological genes, genes involved in cell cycle regulation, many genes involved in stress response, associated with ER and protein folding, and components of the mitochondrion. Finally the expression of several transcription factors is affected. Hereafter, I will talk briefly about some genes that are included in these categories.

Among the genes involved in the cell cycle regulation one that comes up as strongly up-regulated in all the analyses is *Banp*, Btg3 associated nuclear protein. This is part of the BTG family of proteins, of which several members play a role in the negative control of the cell cycle. It was reported that BTG3 is induced by redox changes, with RNA levels peaking at the end of G1 phase of the cell cycle (Biro *et al.*, 2000). In other studies investigating host-pathogen response BTG1 was reported to be up-regulated in swine lymph nodes after infection with *S. Choleraesuis* (Uthe *et al.*, 2007) and in human epithelial cells infected with *S. Dublin* (Eckmann *et al.*, 2000).

Genes involved in ubiquitination were also identified as differentially expressed in this experiment. Ubiquitination can have an important role in bacterial infection, for example *Pseudomonas aeruginosa* (Balachandran *et al.*, 2007). In this study, the ‘ubiquitin mediated proteolysis’ pathway was determined to be differentially up-regulated by InnateDB analysis (Table 4.6). In the ASCA time course analysis seven genes involved in the ubiquitin cycle were also identified as up-regulated (Table 4.14) and ten were apparently attenuated during infection (Table 4.15). Ubiquitination is the main protein degradation pathway that governs a variety of cellular processes including cell cycle, vesicle trafficking and signal transduction. Bonifacino and Weissman (1998) report an exhaustive review on ubiquitins and their role in the immune system (Bonifacino & Weissman, 1998). During *Salmonella* invasion at least one protein secreted inside host cells by SPI-1, SopE, is an object of ubiquitination and rapid degradation soon after injection (Kubori & Galan, 2003). SopA can also serve as a substrate for HsRMA1-mediated ubiquitination. In this case though, it was speculated that mono- or poly-ubiquitination can modulate the protein activity and *Salmonella* SCV escape inside the host cells (Zhang *et al.*, 2005). However, the first *Salmonella* protein to be described to be ubiquitinated, once inside the host cell, was a SIP-1

secreted protein, SopB. Although the authors did not observe a rapid degradation by the proteasome thereafter, they hypothesized that the ubiquitination would regulate SopB activity and attenuate cyto-toxicity (Marcus *et al.*, 2002). In fact it was reported that ubiquitination not only has a role in protein metabolism but in particular mono-ubiquitination is a regulator of the location and activity of diverse cellular proteins (Hicke, 2001). The gene involved in ubiquitination with the highest differential expression during infection of murine ES cells was *Herpud1*. The homocystein-inducible, endoplasmic reticulum stress-inducible, ubiquitin-like domain member 1 (Herpud1), was reported to be involved in the ER-stress response where it is a resident-chaperone protein. Herpud1 was originally described as the first integral membrane protein regulated by the ER stress response pathway and was suggested to play an unknown role in the cellular survival response to stress in the unfolded protein response (UPR) (Kokame *et al.*, 2000).

The ER stress response can also activate another cellular signalling pathway named EOR (ER overloaded response); this is activated by the accumulation of membrane proteins in the ER and is distinct from the signalling induced by UPR. The EOR signalling pathway activates nuclear factor (NF)- κ B which then induces the transcription of pro-inflammatory and immune response genes. GeneSpring analysis revealed the up-regulation of *NF κ biz* (nuclear factor kappa light chain polypeptide gene enhancer in B-cell, inhibitor zeta) (Table 4.10) and ASCA analysis reported the down-regulation of *NF κ bia* (nuclear factor kappa light chain polypeptide gene enhancer in B-cell, inhibitor alpha) (Table 4.15). *NF κ biz* gene is a member of the ankyrin-repeat family with high sequence similarity to the C-terminal of I κ B proteins. Bioconductor analysis also revealed mRNA encoding for the ankyrin-repeat member 37 to be up-regulated (Table 4.3, Table 4.4), reported also in GeneSpring analysis (Table 4.12). The transcription factor NF- κ B plays a crucial role in a wide variety of cellular functions and its activity is strictly regulated by cytosolic inhibitors known as I κ Bs. I κ B is induced by lipopolysaccharide (LPS) or IL-1 β and is localized in the nucleus where it is thought to bind NF- κ B thus preventing an excessive inflammatory response. Also, *NF κ biz* supports the regulation of a subset of inflammatory genes represented by IL-6, it inhibits the expression of TNF- α and is reported to promote TNF- α -induced apoptosis (Yamazaki *et al.*, 2001). *NF κ bia* is reported to play a role in viral infection (Hiscott *et*

al., 1997). The regulation of NF κ B is complex and this transcription factor itself regulates the expression of many cellular biological functions including inflammation, stress and immune responses, embryonic development and apoptosis (Liu-Mares *et al.*, 2007).

Microarray analysis also identified a few transcription factors as being differentially expressed during *Salmonella* infection. Two transcription factors whose expression was significantly induced during bacterial infection were *eIf2ak2* and 3 (eukaryotic initiation factor 2 alpha, kinase 2 and 3). They were identified during both GeneSpring and ASCA analysis (Tables 4.11 and 4.14). The phosphorylation of this class of proteins immediately inhibits additional translational initiation events (Kaufman, 1999). The time course analysis revealed that *eIf2ak2*, also described as IFN-type I-induced and ds-RNA activated kinase, was down regulated during infection (Table 4.15).

Another transcription factor displaying a strong signal of differential expression in this study is XBP-1 (X-box binding protein-1). This transcription factor is essential for the differentiation of plasma cells and the UPR activation. This gene was also reported to be positively expressed in another publication detailing human macrophage-pathogen interactions (Nau *et al.*, 2002). In 2003 Iwakoshi *et al.* concluded that XBP-1 is absolutely required for plasma cell differentiation (Iwakoshi *et al.*, 2003). The same authors in 2007 reported that XBP-1 is necessary for maintaining ER homeostasis and preventing activation of cell death pathways caused by sustained ER stress. Also they reported that *XBP-1* expression is essential for dendritic cell development and survival, which confirms its importance in the differentiation of highly secretory cells like embryonic hepatocytes, exocrine pancreatic acinar cells and plasma cells (Iwakoshi *et al.*, 2007).

Among the genes involved in the mitochondrion homeostasis, monooxygenase genes such as cytochrome P450a and b were strongly down-regulated at 4 hours post-infection with *S. Typhimurium* (Table 4.3, 4.4, 4.11, 4.12, 4.15) although they were first up-regulated at 2 hours post-infection (Table 4.2 and 4.10). The alteration of the expression of the oxidoreductase genes was reported in other studies investigating the host response to pathogens (Handley & Miller, 2007; Rosenberger *et al.*, 2001). The smooth ER expands as the enzymes that oxidize and detoxify are induced to meet their demand

and the overproduction of recombinant *Candida maltosa* P450Alk1 in *S. cerevisiae* activates the UPR to proliferate the ER extensively (Kaufman, 1999). It was proposed that the P-450 down-regulation is a pathophysiological effect of the inflammation progression, a scheme of which is reported in Figure 4.13 (Morgan, 2001).

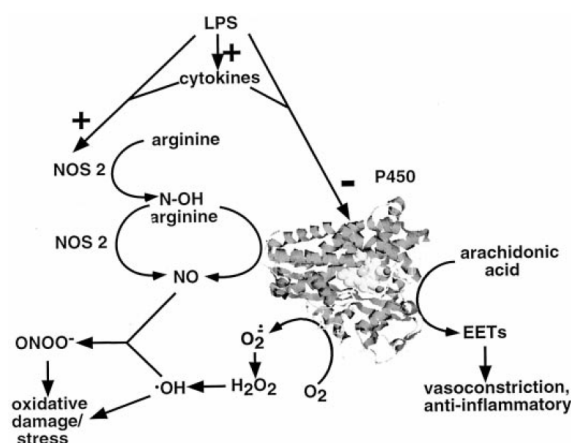


Figure 4.13 Supposed regulation of P450 cytochrome during cellular response to inflammation (Morgan, 2001)

Pathway analysis conducted with InnateDB did not reveal any significantly (for adjusted p-value) up-regulated (Table 4.5, 4.6, 4.8) or down-regulated pathways (Table 4.7, 4.9). However among the potentially up-regulated pathways identified, a few were quite interesting and they highlight how *Salmonella* invasion may interfere with lipid synthesis, ER trafficking and cell motility signalling pathways (Table 4.6).

Among these, the ERAD pathway or ER-associated degradation pathway is involved in the cytosolic degradation of misfolded proteins present in the ER. Once in the cytosol the proteins are deglycosylated, ubiquitinated and directed to proteasome degradation (Tsai *et al.*, 2002). It has been observed that ERAD can be subverted by viral infection to trigger MHC class I breakdown (Tortorella *et al.*, 2000). It is also possible that bacterial invasion triggers the ER stress response similar to that for viral infection, depicted in Figure 4.14 (Medigeschi *et al.*, 2007). This response may also be a defense mechanism since, under conditions of severe ER stress, eukaryotic cells generate a signal that induces programmed cell death known as apoptosis. However, the molecular signalling mechanisms that link ER stress to downstream caspase activation resulting in cell death remain largely unknown (Kaufman, 1999).

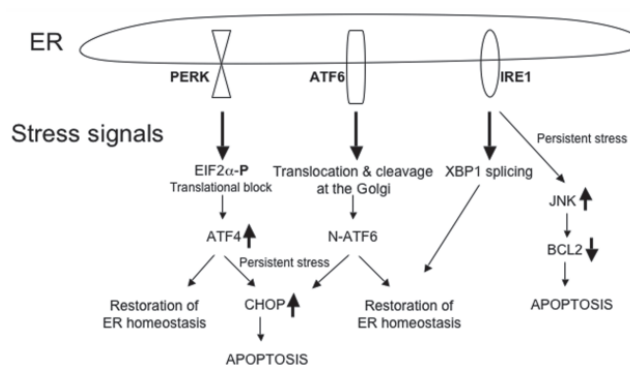


Figure 4.14 ER stress response to viral infection (Medigeshi et al., 2007)

The stringency of statistical analysis often does not accommodate the flexibility and variability of biological systems very well. In this study the data analysis using GeneSpring software revealed more interesting and previously reported genes implicated in host-bacteria interactions. For example among the positively regulated genes can be recognized *Socs* (suppressor of cytokine signalling) (Dalpke *et al.*, 2008), *Stat2* (involved in the transduction and transcription of type I interferon signalling), *Lyst*, (lysosomal trafficking regulator) and *clk2* (CDC-like kinase 2) all of which were previously described to be somehow involved with the pathogen interaction.

This study reported that several genes of murine ES cells were significantly differentially expressed during *S. Typhimurium* invasion, however a few of these are known to be involved in immunological responses. Most of the genes reported are principally involved in the cellular reaction to bacterial invasion. Few of them have been documented in previous host-pathogen transcription profile studies but perhaps they were not discussed because they were not thought relevant to the immune response. Sometimes the interpretation of microarray data can be distorted by the expectations and previous observations of the system studied.

The use of whole genome arrays gives the researcher new insight into host-pathogen interactions that can potentially lead to the discovery of new pathways likely to be promising as new drug targets. However, only their combined use with sequence information, computational tools and the traditional approaches of biology, biochemistry, chemistry, physics, mathematics and genetics can increase the hope of

understanding the function and the regulation of all genes and proteins (Lockhart & Winzeler, 2000).

4 Transcription profiling of murine ES cells infected by *S. Typhimurium* SL1344

4.1 Introduction

4.1.1 Microarrays in host-pathogen interactions studies

Microarray analysis was introduced in the mid-1990s and since then this approach has been the method of choice for large-scale gene expression studies. Microarrays provide an efficient and rapid method to investigate the entire transcriptome of a cell or cell population. Perhaps no research field has benefited more from microarray technology than the study of the interplay between pathogens and their hosts (McGuire & Glass, 2005). Figure 4.1 summarize examples of the applications that microarrays can have in infectious diseases and host-pathogen interactions studies (Bryant *et al.*, 2004). The expansion of this technology takes advantage of the recent escalation in DNA sequence resources. In fact the complete genome of a large number of pathogens has now been fully sequenced in addition to the human and mouse genomes, permitting an exhaustive investigation of host-pathogen interactions.

Host-pathogen interactions can be investigated from either the perspective of the host or from that of the pathogen. Microarrays have been designed for a large range of pathogens including *Escherichia coli*, *Leishmania* species, *Bordetella pertussis*, *Yersinia pestis* and *S. Typhimurium* (McGuire & Glass, 2005). Even without the whole genome level of sequence knowledge, shotgun microarrays can be constructed from genomic DNA libraries (Hayward *et al.*, 2000b). One intriguing feature of pathogen microarray studies is the differential expression patterns observed in a large number of genes with no known function. This is the case even in the extensively genetically mapped bacteria *S. Typhimurium* where the function of many genes has been determined. *S. Typhimurium* has been the subject of expression profile studies looking at the bacterial SCV transcriptome profile during infection of macrophages (Clements *et al.*, 2002; Eriksson *et al.*, 2003).

Microarray studies performed on host RNA responses have exploited a variety of *in vivo* and *in vitro* models of human, mouse and other species. These studies can now exploit commercial species-specific arrays such as the Affymetrix porcine GeneChip, specific for pig. A few groups have conducted investigations on the host response to *Salmonella*, both on *ex-vivo* tissues or on *in vitro* models. One of the first reports to be published was in 2000 by Rosenberger *et al.*, who reported changes in gene expression in mouse macrophages during *S. Typhimurium* infection and the effects of LPS as a bacterial virulence factor (Rosenberger *et al.*, 2000). In this study Atlas mouse cDNA expression arrays were employed. These arrays contained duplicate spots of 588 mouse partial cDNAs. Murine macrophages RAW 264.7 were infected with *S. Typhimurium* SL1344 or stimulated with 100ng/ml of LPS, and at 4 hours post infection (pi) total RNA was isolated. At 4 hours post-infection the expression levels of 77 out of 588 genes represented on the array were detectably altered by two-fold or more in the RAW 264.7 macrophages. Among the up-regulated genes were LIF, CD40, IL-1 β , ICAM-1, TGF β 2, MIP-1(α , β and 2 α) and iNOS, and among the down-regulated genes were the IL-6 receptor and a few cyclins. Many of these genes are involved in the immune response. Also a number of transcription factors were regulated by *S. Typhimurium* infection; Egr-1, NF-E2, IRF-1 and c-rel were induced whereas Ski, B-myb, Fli-1 and c-Fes were suppressed. This study highlighted a remarkable overlap of genes induced by *S. Typhimurium* and purified *S. Typhimurium* LPS suggesting a ‘redundancy’ in host response to bacteria and some of their products (Rosenberger *et al.*, 2000).

In a second study on the *in vitro* host response to *S. Typhimurium*, Detweiler *et al.* investigated the response of U-937 human macrophages to wild-type SL1344 and a *phoP* mutant using an in-house human spotted array with 22,571 cDNA. This study reported 68 genes with a two-fold or greater difference in expression level between uninfected and infected macrophages. Among the genes reported to be induced were IL-8, MIP-1 α and β , IL1 β , IL-23p19, NF- κ B and a several transcription factors. However they did not present any data on genes that were down regulated, although genes that were unregulated in the cells infected with the wild-type compared to the *phoP* mutant bacteria were included. Among these genes were CD9, cathepsin D, SSI-3 and contactin 1. The *phoP::Tn10* mutant strain elicited many of the same mRNA transcripts as the wild-type bacteria and overall the inflammatory response in U-937 macrophages to

wild-type *Salmonella* and the *phoP::Tn10* mutant strain were similar. Nevertheless, this report identified 34 mRNAs with expression levels 1.9 times lower in *phoP::Tn10* infected macrophages than in wild-type infected macrophages. Of these about a third of the twenty-one with known function were involved in cell death. In this study, microarray analysis provided a tool to identify host molecular pathways influenced by a virulence determinant (Detweiler *et al.*, 2001). In fact as a long-term survival strategy, pathogens can alter host gene transcription to maintain a hospitable niche and prevent detection and clearance by the immune system (Rosenberger *et al.*, 2001).

In another study conducted in 2002, Nau *et al.* investigated the macrophage response to different bacterial pathogens in the hope of improving our understanding of host defenses and discovering the theme that defines the innate immune responses of the macrophage to bacteria (Nau *et al.*, 2002). With this purpose in mind they infected human monocytes with *Staphylococcus aureus* strain ISP794, *Listeria monocytogenes* strain EGD, *Mycobacterium tuberculosis* Erdam strain, *M. bovis* BCG, *S. Typhi* Quail strain, *S. Typhimurium* (ATCC no. 14028), *E. coli* strain sd-4, and enterohaemorrhagic *E. coli* O157:H7. Human macrophages derived from primary monocytes were exposed to bacteria and bacterial components and the resulting expression levels of 6,800 genes were monitored over 24 hours. The researchers were able to highlight a common core of genes differentially expressed during the infection of all the bacteria: 132 genes were induced and 59 genes were suppressed. The up-regulated genes were listed in the following categories: cytokines, chemokine, proliferation, tissue remodelling, adhesion, receptors, transcription, transporters, enzymes, pro-inflammatory, anti-apoptotic, stress response and signaling; the down-regulated genes were organized in the categories: anti-inflammatory, pro-inflammatory, adhesion, receptors, signaling, transcription, transporters, tissue remodelling, and enzymes (Nau *et al.*, 2002).

These studies were conducted on macrophages but *Salmonella* is also able to invade epithelial cells and in 2000, Eckmann *et al.* reported the response of human HT-29 colorectal epithelial cells and T84 human colon epithelial cells to *S. dublin*. In their studies they utilised two different cDNA arrays: GF211 Human “Named genes” GeneFiltered Release I from Research Genetics Inc. (Huntsville, AL) and the Atlas Cytokine/Receptor cDNA Expression Array from CLONTECH Laboratories (Palo Alto, CA) (Eckmann *et al.*, 2000). In the first experiments they employed the GF211 array

(which incorporated 4000 human cDNAs). They analysed mRNA extracted from epithelial cells at 3, 8 and 20 hours, post-infection and reported that the vast majority of the genes (~95%) showed relatively little change. They postulated that the up-regulated genes may be more important than those down-regulated so they concentrated their attention on the former. Among the genes differentially expressed at 3 hours infection were IL-12p40, IL-8 and MHC Class I heavy chain, LI-cadherin and ubiquitin-conjugating enzyme E2. Subsequently, they investigated the RNA expression profile of similar epithelial cells during *S. dublin* infection using the Atlas Human Cytokines/Receptor array (CLONTECH) (with 277 cDNAs from cytokines and receptors). They reported the top 25 differentially expressed genes, which included ubiquitin, LIF, insulin receptor along with IL-8, IL-17 and G-CSF (Eckmann *et al.*, 2000).

It is somewhat surprising that cyclins were not differentially expressed in this study because others have reported differences in similar assays (Nau *et al.*, 2002). Possibly, these researchers were very much interested in looking at the immune response and not at the events at the cellular level in reaction to the pathogen. It can be concluded from these studies that many variables are potentially present in this type of research (cell type, pathogen type, time of infection, type of array platform and data analysis methods) and they can influence the outcome of the analysis and the subsequent conclusions. These studies also reveal the complexity of the models employed. Perhaps it might be useful to interpret host-pathogen interactions on three levels: immunological response, usually predominant; the pathogen orchestration of the host genome, that is not very easy to discern; and the cellular reaction to invasion.

The experimental results reported in Chapter 3 suggested that mouse ES cells could be a promising model to study host-pathogen interactions and to further confirm this hypothesis experiments were performed to explore ES cell mRNA expression profiles during bacterial infection by microarray analysis. These data could advance the understanding of mouse ES cell gene regulation and other characteristics in addition to providing insight into host-pathogen interactions. The results from microarray expression profiling of AB2.2 murine embryonic stem (ES) cells infected with *S. Typhimurium* SL1344 at 2 and 4 hours are reported in this chapter. The rationale for these studies was to provide insight into the response of ES cells to pathogen invasion,

helping us to understand how this new *in vitro* model compares to those previously characterized. This is part of the planned investigation of the feasibility of using murine ES cells to study infectious diseases. It is hoped that the results obtained here will help to direct future investigations involving genetically mutated ES cells or differentiated cells.

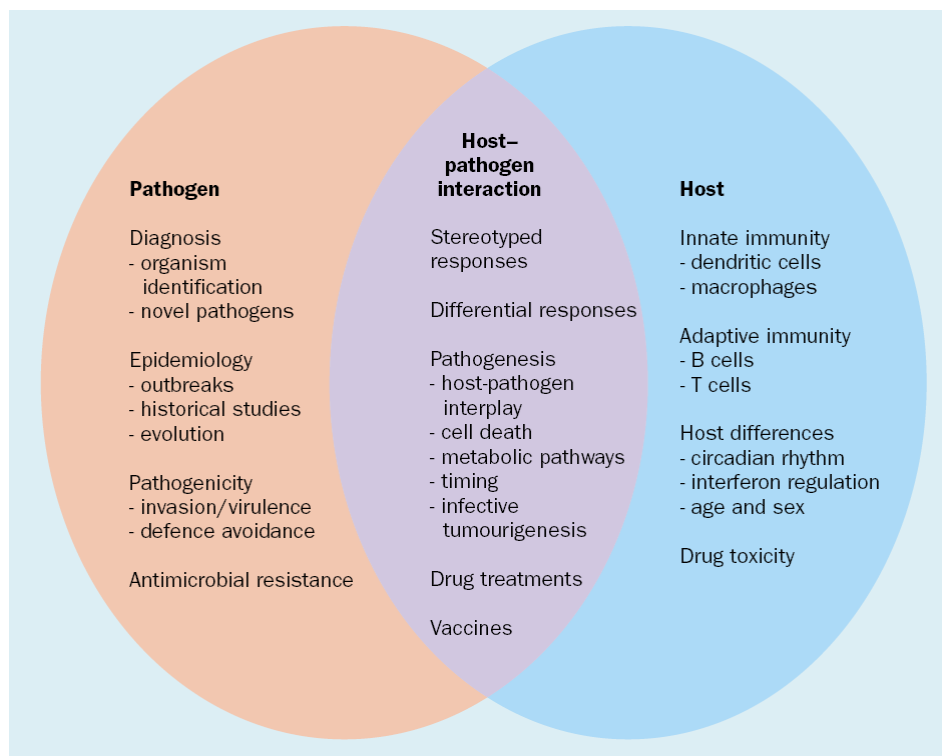


Figure 4.1 Host-pathogen interactions that can be exploited using microarray technology

Microarray technology has a great potential in infectious disease research, helping to explore the complex interactions between host and pathogen and reveal new routes for treatments (Bryant et al., 2004).

4.2 Experimental design

Three independent biological replicates of AB2.2 murine ES cells were infected for 2 hours and 4 hours with *S. Typhimurium* SL1344. Each biological replicate was treated in the same way and total RNA was extracted at time zero from uninfected cells and at 2 hours and 4 hours infection after 30 minutes incubation with the bacterial suspension. Samples of the cells infected at each time point were analyzed by FACS in order to establish the percentage of infected cells. For this reason *S. Typhimurium* SL1344 (p1C/1) expressing GFP was used in these experiments. Three time points (0h, 2h, 4h) were chosen for each of the three biological replicates, giving a total of nine RNA samples for analysis. Also, for each time point three technical replicates were performed for a total of 27 arrays. For each technical replicate an independent cDNA synthesis and cRNA labelling was performed and analyzed by Agilent Bioanalyzer before being hybridized on Affymetrix GenChip[®] Mouse 430.20 arrays (Affymetrix, 2004). The expression data were then analyzed using three different packages: Bioconductor and GeneSpring were used to compare the gene expression profile at 2h and 4h infection to the uninfected cells' mRNA profile and between each other; and ANOVA Simultaneous Component Analysis (ASCA) platform was used to carry out a time course analysis where the time was counted as a variable.

4.3 Results

4.3.1 Murine ES cell infection with *S. Typhimurium* and total RNA extraction

AB2.2 mouse ES cells were maintained undifferentiated in culture media with 1000U/ml of LIF, at 37°C and 5% CO₂. The cells were seeded at 2.5x10⁵ cells per well in 6-well plates and grown for 2 days until 90% confluent. *S. Typhimurium*(p1C/1) expressing GFP was used in these experiments in order to perform parallel flow cytometric examination of the percent of infected cells. *Salmonella* was grown as described in M&M and was seeded into cell culture at MOI ~ 100. After 30 minutes incubation at 37°C the cells were washed with warm Dulbecco's PBS Ca²⁺Mg²⁺ and incubated for 2 hours or 4 hours with complete DMEM medium containing 50µg/ml of gentamicin antibiotic. The cells were then washed and the cells from three wells were trypsinized and analyzed by FACS, whereas the cells in the other three wells were scraped and frozen at -80°C.

Only those cells in which the infection rate was above 30%, as determined by cytometric analysis, were further used for total RNA extraction with the QIAGEN RNeasy Midi kit. The first biological replicate of AB2.2 murine ES cells (passage 33) was infected with *S. Typhimurium* and it was established by flow cytometric analysis that at 2 hours and 4 hours, 30% and 32% of the cells were infected respectively. In the second biological replicate AB2.2 murine ES cells were infected at passage 27 and flow cytometric analysis established that at 2 hours and 4 hours, 42% and 36% of the cells were infected respectively. The third replicate AB2.2 murine ES cells were infected at passage 26 and at 2 hours and 4 hours, 34% and 30% of the cells were infected respectively. An example of the FACS analysis of these cells can be found in Figure 4.2.

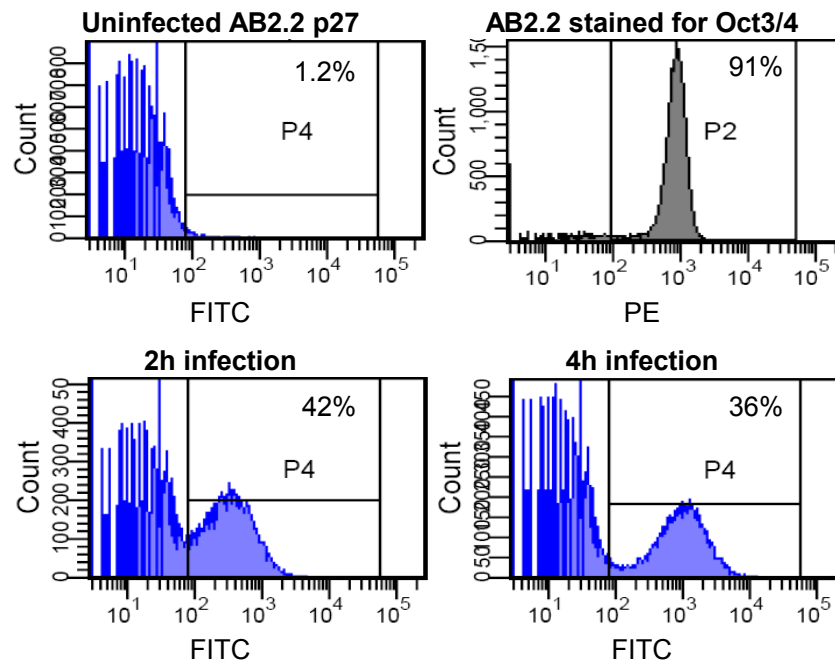


Figure 4.2 Flow cytometric analysis of murine ES cells infected with *S. Typhimurium* SL1344. The AB2.2 murine ES cells were analyzed in parallel by FACS in order to investigate the percentage of infected cells prior to RNA extraction. For this reason *S. Typhimurium*(pC1/1) expressing GFP protein was used for these experiments. In addition Oct3/4 analysis was performed on uninfected cells in order to confirm their pluripotency characteristic.

4.3.2 Murine ES cell total RNA extraction and analysis

The total RNA was extracted using the QIAGEN RNeasy Midi Kit following the manufacturer's instructions. The concentration of total RNA extracted was measured using the NanoDrop1000 (Thermo) spectrophotometer. NanoDrop1000 is a full-spectrum UV/Visible (220-750nm) spectrophotometer used to quantify nucleic acids in a small volume as little as 1 μ l. The technology used exploits surface tension of small volumes [www.nanodrop.com]. The final concentrations obtained for each sample are reported in Table 4.1.

Table 4.1 Total RNA concentration of murine ES cells infected by *S. Typhimurium*(p1C/1) measured with NanoDrop1000 technology

Sample ID	Description	ng/ μ l	260/280 Ratio
1	AB2.2 First Biological Replicate	718	2.12
2	AB2.2 First Biological Replicate Infected with SL1344/p1C/1 2h	642	2.12
3	AB2.2 First Biological Replicate Infected with SL1344/p1C/1 4h	830	2.12
4	AB2.2 Second Biological Replicate	914	2.12
5	AB2.2 Second Biological Replicate Infected with SL1344/p1C/1 2h	792	2.12
6	AB2.2 Second Biological Replicate Infected with SL1344/p1C/1 4h	855	2.13
7	AB2.2 Third Biological Replicate	909	2.12
8	AB2.2 Third Biological Replicate Infected with SL1344/p1C/1 2h	707	2.04
9	AB2.2 Third Biological Replicate Infected with SL1344/p1C/1 4h	892	2.12

To test the RNA quality, the samples were analyzed using the Agilent 2100 Bioanalyzer (Agilent Technologies, Palo Alto, CA, USA). The Bioanalyzer is an automated bio-analytical device using microfluidics technology that provides electrophoretic separation in an automated and reproducible manner (Schroeder *et al.*, 2006). Bioanalyzer was used in this study to evaluate the quality of the total RNA extracted from mouse ES cells uninfected and infected by *S. Typhimurium*. Figure 4.3 reports an example of the quality of the total RNA obtained from AB2.2 murine ES cells uninfected and infected at 2 hours and 4 hours with *S. Typhimurium* SL1344(p1C/1).

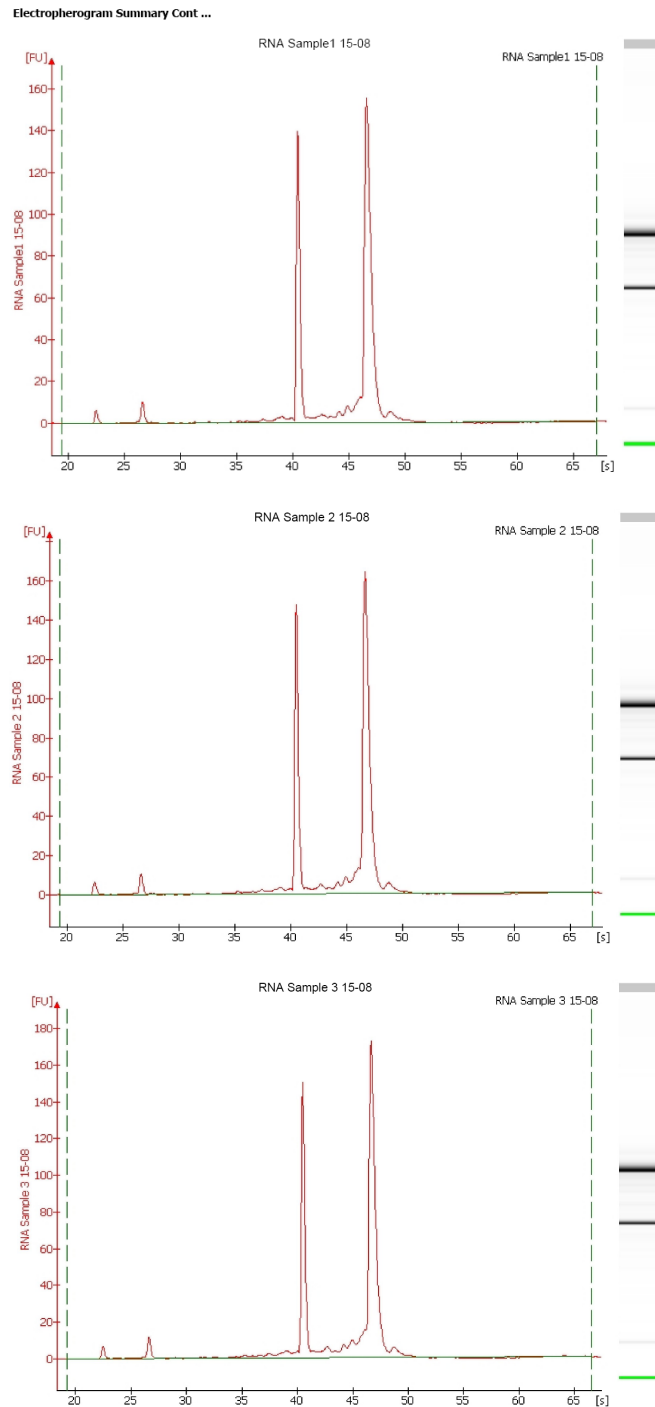


Figure 4.3 Bioanalyzer analysis of total RNA from infected and uninfected ES cells

The quality of the total RNA extracted from each sample was analyzed by Bioanalyzer before microarray analysis.. Representative histograms of the RNA quality from AB2.2 murine ES cells uninfected (top) or infected with *S. Typhimurium* SL1344(p1C/1) at the 2h (middle) and 4h invasion (bottom histogram) with the respective virtual gel, are represented. The histograms reveal two peaks representing the ribosomal RNA 18S and the 28S, from the left. The intensity of the gel band of 28S ribosomal RNA should be about twice that of the 18S ribosomal band.

4.3.3 cRNA synthesis, labelling and microarray hybridization

In order to analyze the expression profile of murine ES cells, the total RNA extracted was hybridized on the Affymetrix GeneChip[®] Mouse 430 2.0 Array following the manufacturer's instructions. Briefly, the 5 μ g of total RNA was used to synthesize double stranded cDNA using the One-Cycle cDNA Synthesis Kit which use poly-T primers. This was 'cleaned' from traces of RNA and used as template for the synthesis of Biotin-Labeled cRNA with the One-cycle Target Labelling Assay kit, following the manufacturer's directions. Then cRNA was cleaned and quantified and its quality was analyzed by Bioanalyzer before hybridization (Figure 4.4). An independent cDNA synthesis and cRNA labelling reaction was carried out for each technical replicate. The cRNA was first fragmented before hybridization and 15 μ g of cRNA per chip was used for hybridization at 45°C in constant rotation (60 rpm) overnight. The chips were washed and scanned at the Fluidics Station 450 operated using GCOS/Microarray Suite software.

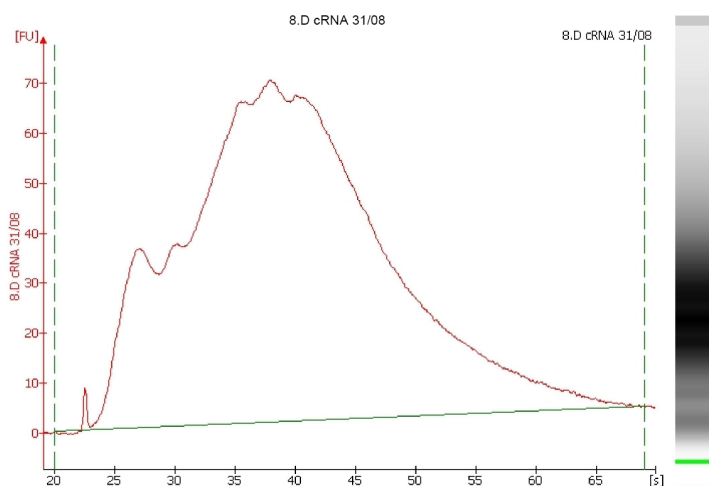


Figure 4.4 Bioanalyzer analysis of the biotin-labelled cRNA

As the Affymetrix manual reports, the cRNA quality needs to be confirmed by Bioanalyzer to prove that the cRNA amplification reaction worked. The optimum is to obtain cRNA fragments between 500-1500 nucleotides, which corresponds to 35 and 40 seconds, respectively. This picture reports an example of the cRNA obtained in this study.

The Affymetrix GeneChip[®] Mouse Genome 430 2.0 Array used harbours 45,000 probes representing transcripts and variants from over 34,000 well characterized mouse genes (Affymetrix, 2004). The Affymetrix expression array uses a set of features (spots), each designed to recognize a molecule of interest. Each feature consists of millions of identical single-stranded 25-mer nucleotide probes designed to hybridize to a specific transcript. The probes are defined Perfect-Match (PM) features and each is accompanied by an adjacent Mis-Match (MM) feature in which the middle residue is changed. Hybridization conditions are designed to maximize binding to the PM feature while minimizing binding to the MM ones. The MM signal can be used to provide a measure of probe specific background for its PM partner. Multiple PM/MM pairs are used for each transcript (Okoniewski & Miller, 2008).

4.3.4 Microarray data analysis

4.3.4.1 Bioconductor analysis

4.3.4.1.1 Results from Bioconductor pair-comparison analysis

Microarray expression profile analysis was initially conducted using Bioconductor [Bioconductor: <http://www.bioconductor.org>] (Gentleman *et al.*, 2004). Bioconductor is a collection of open source software packages designed to support the analysis of biological data. Bioconductor is written using the programming language R, which itself provides access to a wide range of tools for statistical analysis, data presentation, and visualization (Okoniewski & Miller, 2008). In this analysis the mouse ES cell microarray profiles at 2 hours and 4 hours post-infection were compared with the profile of uninfected cells (0h). The arrays were first subjected to quality control and the report can be seen in Appendix A. Normalization using GCRMA (Wu *et al.*, 2004) was then performed and this includes background adjustment, quantile normalization, and median-polish summarization at the probe level. The data were then further analyzed using the Limma package and applying a linear model to estimate the effect of each factor on the variance of the data [limma : <http://bioinf.wehi.edu.au/limma/>]. The results from this analysis are reported in Tables 4.2, 4.3 and 4.4

Table 4.2 Bioconductor analysis of RNA expression profile of murine ES cells at 2h infection

The mRNA expression profile of uninfected AB2.2 murine ES cells and that obtained following 2h infection with *S. Typhimurium* were compared and analyzed using the Bioconductor package; significantly differentially expressed genes are reported (p-value <0.05 and fold change +/- 1.5).

Fold Change	Adj.p-value	Gene Symbol	Gene Title	Process and Functions
10.63	0.0007	Cyp1b1	cytochrome P450, family 1, subfamily b, polypeptide 1	oxidation reduction// monoxygenase activity// iron ion binding// electron carrier activity// ER membrane
4.38	0.0147	Cyp1a1	cytochrome P450, family 1, subfamily a, polypeptide 1	dibenzo-p-dioxin metabolic process // oxidation reduction// monoxygenase activity// iron ion binding// ER membrane

Table 4.3 Bioconductor analysis of RNA expression profile of murine ES cells at 4h infection

Genes determined to be differentially expressed following Bioconductor analysis of arrays hybridized with mRNA from uninfected AB2.2 ES cells and infected with *S. Typhimurium* for 4h. The 30 genes reported are significantly differentially expressed at 4h infection compared to uninfected cells (0h) (p value < 0.05 and fold change +/- 1.5; * = gene reported twice; ** = gene reported three times)

Fold Change	Adj. p value	Gene symbol	Gene Name	Process and Functions
2.32	0.0327	Banp	Btg3 associated nuclear protein	Transcription/ cell cycle/ DNA binding
2.25	0.0002	Hspa1b**	Heat shock protein1B	DNA repair//anti-apoptotic//response to stress
2.01	0.0053	Pdxp	Pyridoxal (vitB6) phosphatase	Magnesium ion binding//catalytic activity
2	0.0065	Zbtb40	Zinc finger and BTB domain containing 40	Nucleic acid binding//zinc binding// prot. binding
1.88	0.0464	Ccng2	Cyclin G2	Cyclin-dependent protein kinase regulator activity
1.84	0.002	Herpud1	Homocystein-inducible, ER stress-inducible, ubiquitin-like domain member 1	Response to stress// response to unfolded protein
1.64	0.0011	Tbl2	Transducin(beta)-like 2	//
1.62	0.0211	Ankrd37	Ankyrin repeat domain 37	//
1.6	0.0336	Aof1	Amine oxidase, flavin containing 1	Zinc binding // electron carrier activity
1.55	0.0016	Clk2	CDC-like kinase 2	Nucleotide binding// protein kinase activity// ATP binding
1.55	0.017	Pex11a	Peroxisomal biogenesis factor 11a	Peroxisome organization and biogenesis
1.54	0.0125	Ccdc117	Coiled-coil domain containing 117	//
1.53	0.0049	Luc7l	Luc7 homolog (<i>S. cerevisiae</i>)-like	Zinc ion binding// metal ion binding
1.53	0.017	Xbp1	X-box binding protein 1	Transcription factor activity
1.51	0.0334	C430002E04Rik	RIKEN cDNA C430002E04 gene	//
-1.51	0	Sfrs5	Splicing factor arginine/serine-rich 5 (SRp40, HRS)	Nucleic acid binding
-1.52	0.0336	LOC100044766	Similar tow domain-containing adapter protein with coiled-coil	Protein binding
-1.55	0.0334	Msc	Musculin	Transcription regulator activity
-1.55	0.0052	Chic2	Cysteine-rich hydrophobic domain 2	Golgi to plasma membrane transport
-1.57	0.0129	1810013L24Rik	RIKEN cDNA 1819913L24gene	//
-1.65	0.0039	Lrpap1*	Low density lipoprotein receptor-related protein associated protein 1	Receptor activity// low-density lipoprotein receptor binding
-1.65	0.0084	Slc7a1	Soluble carrier family 7 member 1	Receptor activity// amino acid transmembrane transporter activity
-1.78	0.0001	LOC100046855	Similar to BKLF	Nucleic acid binding// zinc ion binding
-1.86	0.0003	Foxp1	Forkhead box P1	Nucleic acid binding// transcription factor activity// zinc ion binding
-1.98	0.0341	Luc7l2	LUC7-like 2 (<i>S. cerevisiae</i>)	Protein binding// zinc ion binding
-2.41	0.0403	LOC100045546	Similar to Id4	//
-3	0.0336	Cyp1b1	Cytochrome P450, family 1 subfamily b, polypeptide 1	Monooxygenase activity// iron ion binding// electron carrier activity

Table 4.4 Bioconductor analysis of RNA expression profile of murine ES cells at 4h infection compared to 2h

Gene list resulting from the Bioconductor analysis comparing the expression profiles of murine ES cells at 2h and 4h infection. This analysis identified 39 differentially expressed genes, of which 33 have been annotated and therefore reported here. (* = gene reported twice; ** = gene reported three times)

Fold Change	Adj. p value	Gene Symbol	Gene Name	Process and Functions
2.11	0.00	Hspa1b**	heat shock protein 1B	DNA repair /// anti-apoptosis /// response to stress /// response to heat /// negative regulation of caspase activity
1.98	0.02	Ccng2	cyclin G2	cell cycle /// mitosis /// cell division /// regulation of cell cycle
1.97	0.01	LOC638050 /// Zbtb40	zinc finger and BTB domain containing 40 /// similar to zinc finger and BTB domain containing 40	nucleic acid binding /// protein binding /// zinc ion binding /// metal ion binding
1.78	0.00	Herpud1*	homocysteine-inducible, endoplasmic reticulum stress-inducible, ubiquitin-like domain member 1	protein modification process /// response to stress /// response to unfolded protein /// response to unfolded protein
1.75	0.00	Ankrd37	ankyrin repeat domain 37	---
1.69	0.00	Xbp1**	X-box binding protein 1	transcription /// regulation of transcription, DNA-dependent
1.55	0.02	C430002E04 Rik	RIKEN cDNA C430002E04 gene	---
1.50	0.05	Gdap10	ganglioside-induced differentiation-associated-protein 10	---
-1.52	0.04	Klf10	Kruppel-like factor 10	regulation of transcription, DNA-dependent /// positive regulation of osteoclast differentiation /// zinc-metal ion binding
-1.52	0.01	Zbtb7a	zinc finger and BTB domain containing 7a	negative regulation of transcription from RNA polymerase II promoter /// negative regulation of transcription, DNA-dependent /// zinc ion binding
-1.52	0.04	Gm505	Gene model 505, (NCBI)	---
-1.54	0.04	Lrpap1*	low density lipoprotein receptor-related protein associated protein 1	receptor activity /// heparin binding /// low-density lipoprotein receptor binding /// membrane protein
-1.56	0.01	1810013L24 Rik	RIKEN cDNA 1810013L24 gene	---
-1.56	0.00	Nodal	nodal	negative regulation of transcription from RNA polymerase II promoter // positive regulation of cell proliferation // anterior/posterior pattern formation // stem cell maintenance // negative regulation of cell differentiation /// cytokine activity // growth factor activity
-1.58	0.00	Snai1	snail homolog 1 (Drosophila)	multicellular organismal development // nucleic acid binding // zinc ion binding
-1.58	0.04	Sesn2	sestrin 2	cell cycle arrest

-1.59	0.02	Elf3	E74-like factor 3	regulation of transcription, DNA-dependent /// inflammatory response /// embryonic development /// cell differentiation /// epithelial cell differentiation /// transcription factor activity/// protein binding
-1.61	0.02	Pcmt1	protein-L-isoaspartate (D-aspartate) O-methyltransferase domain containing 1	protein modification process /// methyltransferase activity
-1.68	0.00	Slc7a1	solute carrier family 7 (cationic amino acid transporter, y+ system), member 1	receptor activity /// amino acid transmembrane transporter activity /// arginine transmembrane transporter activity
-1.70	0.00	Foxp1	forkhead box P1	negative regulation of transcription from RNA polymerase II promoter /// pre-B cell differentiation /// positive regulation of immunoglobulin production /// regulation of transcription, DNA-dependent ///embryonic development /// immunoglobulin V(D)J recombination /// positive regulation of epithelial cell proliferation
-1.71	0.03	Rnase4	ribonuclease, RNase A family 4	positive regulation of endothelial cell proliferation /// activation of phospholipase C activity /// multicellular organismal development actin filament polymerization /// activation of phospholipase A2 /// positive regulation of protein secretion/// nucleic acid binding/// receptor binding/// basal lamina
-1.78	0.04	Arl4a	ADP-ribosylation factor-like 4A	small GTPase mediated signal transduction/// GTPase activity
-1.80	0.00	Aff1	AF4/FMR2 family, member 1	transcription /// positive regulation of transcription, DNA-dependent
-1.97	0.02	Ndr1	N-myc downstream regulated gene 1	mast cell activation
-2.06	0.00	Cdkn1a	cyclin-dependent kinase inhibitor 1A (P21)	G1/S and G2/M transition of mitotic cell cycle /// response to DNA damage stimulus /// cell cycle arrest /// positive regulation of B cell proliferation /// cellular response to extracellular stimulus /// negative regulation of apoptosis /// positive regulation of fibroblast proliferation /// protein kinase inhibitor activity
-2.10	0.00	Zfp296	zinc finger protein 296	nucleic acid binding /// zinc ion binding
-2.35	0.00	Klf3 /// LOC100046855	Kruppel-like factor 3 (basic) /// similar to BKLF	transcription /// regulation of transcription, DNA-dependent
-2.49	0.00	LOC100046855	similar to BKLF	nucleic acid binding /// zinc ion binding
-2.60	0.02	LOC100045546	similar to Id4	---
-13.13	0.00	Cyp1b1*	cytochrome P450, family 1, subfamily b, polypeptide 1	monooxygenase activity/// iron ion binding /// oxidoreductase activity aromatic compound metabolic process /// metal ion binding
-22.66	0.00	Cyp1a1	cytochrome P450, family 1, subfamily a, polypeptide 1	oxidation reduction /// monooxidoreductase activity/// electron carrier activity /// metal ion binding

4.3.4.1.2 InnateDB pathways analysis

InnateDB has been developed to facilitate systems-level investigations of the innate immune response in human and mice. Its goal is to provide a manually-curated database of the genes, proteins and, particularly, the interactions and signaling responses involved in the mammalian innate immune response. InnateDB is freely available to the public as a tool for innate immunity research where users can search for particular genes or proteins of interest and their relative interactions and pathways [InnateDB: <http://innatedb.ca/index.jsp>] (Lynn *et al.*, 2008). For this analysis the corresponding human ortholog genes were used since more than 3 quarters of the interactions reported in InnateDB are for *Homo sapiens*. The list of all probes with their respective p-value and the expression fold change determined by pair-comparison of mouse ES cell mRNA expressed at 4h post-infection with *S. Typhimurium* versus uninfected cells, were uploaded and analyzed using InnateDB. The gene expression values obtained at 2 hours infection and those obtained comparing 4 hours to 2 hours were also analyzed with InnateDB. The pathways obtained were further ‘enriched’ using the ‘over-representation’ analysis which uses the genes’ fold expression (± 1.5) and p-value (<0.1) in order to evaluate the proportion of differentially expressed genes for each pathway (using the default settings for the analysis algorithm: Hypergeometric and the correction method: Benjamini Hochberg).

Table 4.5 InnateDB analysis of genes expressed by murine ES cells at 2h infection with *S. Typhimurium*

The analysis reported only up-regulated pathways at 2h infection of AB2.2 murine ES cells with *S. Typhimurium* SL1344, although they are not statistically significant (corrected p-value).

Name of Pathway up-regulated at 2h infection of AB2.2	Source Name	Pathway uploaded gene count	Pathway up-regulated genes count	Pathway up-regulated p-value	Pathway up-regulated p-value (corrected)
P450 Epoxidations	REACTOME	3	1	0.000602	0.790329
Metabolism of xenobiotics by cytochrome P450	KEGG	28	1	0.005618	1.000000
Tryptophan metabolism	KEGG	52	1	0.010433	1.000000

Table 4.6 InnateDB pathway analysis of murine ES cells expression profile at 4h infection: up-regulated pathways

The whole gene list derived from Bioconductor analysis of the expression data at 4h infection with *S. Typhimurium* SL1344 versus uninfected AB2.2 murine ES cells (0h) was used for this analysis. The analysis did not reveal significantly up-regulated pathways according to adjusted p-values.

Name of pathway up-regulated at 4h infection of AB2.2	Source Name	Pathway uploaded gene count	Pathway up-regulated genes count	Pathway up-regulated p-value	Pathway up-regulated p-value (corrected)
Lipoic acid metabolism	KEGG	3	1	0.006008	1
Ubiquitin mediated proteolysis	KEGG	127	2	0.025359	1
Circadian rhythm	KEGG	13	1	0.025802	1
Sprouty regulation of tyrosine kinase signals	PID BIOCARTA	17	1	0.033620	1
Er associated degradation (erad) pathway	PID BIOCARTA	18	1	0.035566	1
Pkc-catalyzed phosphorylation of inhibitory phosphoprotein of myosin phosphatase	PID BIOCARTA	20	1	0.039446	1
EGFR downregulation	REACTOME	22	1	0.043313	1
Maturity onset diabetes of the young	KEGG	23	1	0.045241	1
Rho cell motility signaling pathway	PID BIOCARTA	31	1	0.060540	1
Rac1 cell motility signaling pathway	PID BIOCARTA	35	1	0.068106	1
N-Glycan biosynthesis	KEGG	38	1	0.073745	1

Table 4.7 InnateDB pathway analysis of murine ES cells expression profile at 4h infection: down-regulated pathways

The genes resulting from the analysis of gene expression at 4h infection compared to uninfected AB2.2 murine ES cells were analyzed with InnateDB. The pathway analysis did not reveal any statistically significantly for down regulated pathway after p-value adjustment.

Name of Pathway down-regulated at 4h infection of AB2.2	Source Name	GO term uploaded gene count	GO term down-regulated genes count	GO term down-regulated p-value	GO term down-regulated p-value (corrected)
P450 Epoxidations	REACTOME	3	1	0.003007	1
Gene expression of IL2 by AP-1	INOH	5	1	0.005008	1
TGF-beta Receptor Signaling Pathway	NETPATH	130	2	0.006412	1
Pertussis toxin-insensitive ccr5 signaling in macrophage	PID BIOCARTA	7	1	0.007006	1
Tsp-1 induced apoptosis in microvascular endothelial cell	PID BIOCARTA	7	1	0.007006	1
Il 3 signaling pathway	PID BIOCARTA	8	1	0.008003	1
JNK cascade	INOH	10	1	0.009996	1

Table 4.8 InnateDB analysis of genes expressed by murine ES cells at 4h infection with *S. Typhimurium* compared to 2h: up-regulated pathways

The analysis reported one up-regulated pathway at 4h versus 2h infection of AB2.2 murine ES cells with *S. Typhimurium* SL1344, although the corrected p-value is not statistically significant.

Name of Pathway up-regulated at 4h vs.2h	Source Name	Pathway uploaded gene count	Pathway up-regulated genes count	Pathway up-regulated p-value	Pathway up-regulated p-value (corrected)
Lipoic acid metabolism	KEGG	3	1	0.000602	0.790329

Table 4.9 InnateDB analysis of genes expressed by murine ES cells at 4h infection with *S. Typhimurium* compared to 2h: down-regulated pathways

The analysis reported a few down-regulated pathways at 4h versus 2h infection of AB2.2 murine ES cells with *S. Typhimurium* SL1344, although the corrected p-value is not statistically significant.

Name of Pathway down-regulated at 4h vs. 2h	Source Name	Pathway uploaded gene count	Pathway up-regulated genes count	Pathway down-regulated p-value	Pathway down-regulated p-value (corrected)
P450 Epoxidations	REACTOME	3	1	0.002406	1
Downregulated of mta-3 in er-negative breast tumors	PID BIOCARTA	15	1	0.011988	1
Metabolism of xenobiotics by cytochrome P450	KEGG	28	1	0.022290	1
Tryptophan metabolism	KEGG	52	1	0.041097	1
Viral Messenger RNA Synthesis	REACTOME	59	1	0.046531	1
Adherens junction	KEGG	70	1	0.055023	1
TGF-beta signaling pathway	KEGG	76	1	0.059632	1

4.3.4.1.3 Real time RT-PCR to confirm Bioconductor analysis

Real time Reverse Transcription (RT) followed by polymerase chain reaction (PCR) is a powerful tool for the detection and quantification of mRNA. It is important to confirm bioinformatics analysis with an alternative method although this has been the centre of debate in the scientific community (Allison *et al.*, 2006; Rajeevan *et al.*, 2001). The total RNA extracted from the *S. Typhimurium* infected cells and uninfected controls was subjected to RT-PCR analysis in order to confirm the data obtained from the microarray study and subsequent Bioconductor analysis. The total RNA was reverse transcribed using QuantiTect (QIAGEN). A SYBR Green-based detection reaction was used and the data were analysed using the $\Delta\Delta C_t$ value method developed by Perkin Elmer (Applied Biosystems) to measure the relative quantification of a target gene in comparison to a reference gene. This method is an approximation of the RNA quantity assuming that RT-PCR reaction efficiencies are all equal to 2 (i.e. that each cycle of PCR results in two-fold increase in the number of RNA species). The fold change of the target genes were then calculated in relation to the expression of the internal control gene chosen, β -actin in this study, using the equation “ratio= $2^{\Delta\Delta C_t}$ ” where C_t is the thermo cycle at which the green fluorescence dye is first detectable and 2 represents the reaction efficiency. A few genes determined to be significantly up- or down-regulated by microarray analysis were chosen to be confirmed by semi-quantitative RT-PCR. The genes were selected in order to cover a representative set of genes or pathways exhibiting differential expression. These genes were involved in cholesterol metabolism, cell-cycle regulation, stress responses, apoptosis regulation and transcription factors. For a more detailed description of each gene please refer to Table 4.3.

RT-PCR confirming Bioconductor analysis
of expression data from murine ES infected with *S. Typhimurium* at 4h

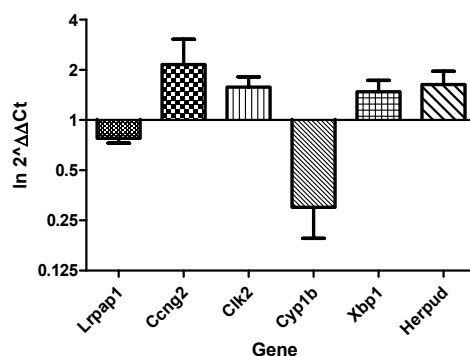


Figure 4.5 RT-PCR results conducted on representative genes identified by the Bioconductor analysis of genes differentially expressed at 4h infection vs. uninfected cells

A few genes with high fold change and significantly differentially expressed during infection, revealed through Bioconductor analysis, were chosen for relative quantification using RT-PCR. In this analysis the Ct values of the target genes were compared to the Ct value of an internal control gene, β -actin, and the ratios calculated and plotted as $\ln 2^{-\Delta\Delta Ct}$. The reactions were carried out in triplicate for each biological replicate at 0h and 4h infection and are reported here as the mean values. The error bars represent the standard error for each replicate. The initial amount of template cDNA is inversely proportional to the parameter measured for each reaction, which is the threshold cycle (Ct).

4.3.4.1.4 Statistical analysis of RT-PCR data on genes identified by Bioconductor

Statistical analysis of the RT-PCR results was carried out using the online Relative expression software tool (REST[©]), and the results can be found in Figure 4.6. This mathematical model compares two groups with up to 16 data points in a sample and 16 in a control group, and is based on the PCR efficiencies and the mean Ct deviation between the sample and the control group (Herrmann & Pfaffl, 2005). Subsequently, the expression ratio results of the investigated transcripts are tested for significance using a randomization test. Permutation or randomization tests are a useful alternative to more standard parametric tests for analysing experimental data. They have the advantage of making no distributional assumptions about the data, while remaining as powerful as parametric tests (Pfaffl *et al.*, 2002).

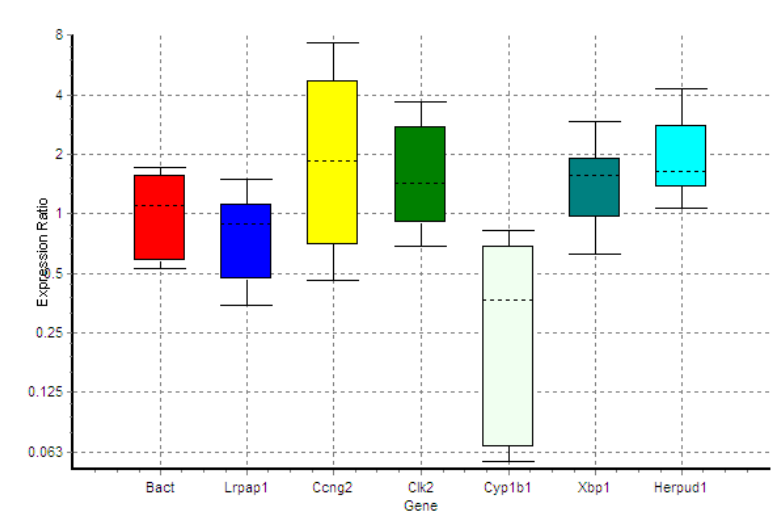


Figure 4.6 Whisker box plot of the RT-PCR results for the Bioconductor-generated differentially expressed genes

The Ct values obtained from RT-PCR for a few of the genes that were identified Bioconductor analysis as differentially expressed in AB2.2 mouse ES cells at 4h invasion with *S. Typhimurium* were statistically investigated by REST©. The random statistical analysis was performed using the triplicate mean values from three different biological replicates; however none of the genes' expression was significantly different in comparison to the internal control gene β -actin.

RT-PCR meant to confirm the results obtained by bioinformatics analysis of up- or down-regulated genes. In this case the genes chosen to be confirmed showed the higher difference in fold expression at 4h infection. However, statistical analysis didn't highlight a significant difference between the level of expression of the genes at 0h and at 4h.

4.3.4.2 GeneSpring analysis

4.3.4.2.1 Results from GeneSpring pair-comparison analysis

In our laboratory microarray data were historically analyzed by GeneSpring. The Agilent GeneSpring version 7.3.1 platform is an expression analysis tool. Here it was used to analyse the Affymetrix Mouse GeneChip[®] 430 2.0 Array used to investigate the murine AB2.2 ES cell RNA expression profile during *S. Typhimurium* infection at 2h and 4h post-infection.

The array QC is shown in Appendix A. The data were first normalized using GCRMA (Wu *et al.*, 2004), which takes into consideration GC content, and then the data was then filtered using the Benjamini-Hochberg false discovery rate (FDH) method, which assumes independent p-values across genes; the genes were filtered for confidence p-value < 0.05. This procedure provides a good balance between discovery of significant genes and protection against false positives, since the occurrence of the latter is confined to a small proportion of the list, and it is the best choice of multiple-testing correction for most analyses (GeneSpring Manual).

Table 4.10 GeneSpring analysis of the mRNA expression profile of AB2.2 murine ES cells at 2h infection

This comparative analysis revealed 26 genes significantly differentially regulated for p-value < 0.05 and fold expression change of +/- 1.5. 19 annotated genes are reported here. (* = reported twice; ** = reported three times)

Genes selected from condition Time 2.0 that have Normalised Data values that are greater or less than those in condition(s) Time 0.0 by a factor of 1.5 fold. Starting gene list: Filter for confidence t-test p-value 0 - 0.05, Benj and Hoch FDR, 1 cond of 3.			
Fold Change	Common	Description	Biological Process and or Molecular Function
8.91	Cyp1a1	cytochrome P450, family 1, subfamily a, polypeptide 1	electron transport// monoxygenase activity; oxidoreductase activity// ER
3.52	Cyp1b1*	cytochrome P450, family 1, subfamily b, polypeptide 1	oxidation reduction /// electron carrier /// ER
1.97	Nfkbiz	nuclear factor of kappa light polypeptide gene enhancer in B-cells inhibitor, zeta	inflammatory response // regulation of transcription // DNA binding
1.66	Clstn3	calsyntenin 3	cell adhesion // ER // Golgi apparatus // calcium ion binding // protein binding
1.65	Anpep	alanyl (membrane) aminopeptidase	proteolysis and peptidolysis // zinc ion binding
1.65	Map3k3	mitogen-activated protein kinase kinase kinase 3	protein amino acid autophosphorylation // ATP binding // kinase activity
1.64	Mark2	MAP/microtubule affinity-regulating kinase 2	cell differentiation // ATP binding // kinase activity
1.59	Slc6a6	solute carrier family 6 (neurotransmitter transporter, taurine), member 6	beta-alanine transport // integral to plasma membrane
1.59	Lpp	LIM domain containing preferred translocation partner in lipoma	cell adhesion // cell junction // metal ion binding // protein binding
1.56	Klf3*	Kruppel-like factor 3 (basic)	regulation of transcription // zinc ion binding
1.55	Zfp296	zinc finger protein 296	//
1.55	Snai1	snail homolog 1 (Drosophila)	development // DNA binding // zinc ion binding
1.54	Inf2	inverted formin, FH2 and WH2 domain containing	actin cytoskeleton organization and biogenesis // actin binding // Rho GTPase binding
1.53	Pdpk1	3-phosphoinositide dependent protein kinase-1	ATP binding // protein serine/threonine kinase activity // signal transduction // cytoplasmic vesicle //
1.52	Synj1	Synaptojanin 1	endocytosis // clathrin coat // cytoplasm // hydrolase activity // inositol or phosphatidylinositol phosphatase activity
1.51	Mint	Msx2 interacting nuclear target protein	regulation of transcription from Pol II promoter // binds G/T-rich dsDNA and ssDNA // mitochondrial inner membrane // nucleus
-1.59	Xist	inactive X specific transcripts	dosage compensation by inactivation of X chromosome
-1.62	Tpd52l2	tumor protein D52-like 2	//

Table 4.11 GeneSpring analysis of the mRNA expression profile of AB2.2 murine ES cells at 4h infection

A total of 89 genes were revealed to be differentially expressed by murine AB2.2 ES cells at 4h infection with *S. Typhimurium* SL1344. 56 annotated genes are reported here. The genes were filtered for p-value < 0.05 and fold change +/- 1.5. A few genes are repeated, as indicated by asterisks, and this is a sign that a gene is particularly relevant (* = reported twice; ** = reported three times).

Genes selected from condition Time 4.0 that have Normalised Data values that are greater or less than those in condition(s) Time 0.0 by a factor of 1.5 fold. Starting gene list: Filter for confidence t-test p-value 0 - 0.05, Benj and Hoch FDR, 1 cond of 3.

Fold Change	Common	Description	Biological Process and or Molecular Function
2.43	Banp	Btg3 associated nuclear protein	protein binding
2.17	Hspa1b**	heat shock protein 1A	anti-apoptosis; inhibition of caspase activation; ATP binding
2.03	Ccng2*	cyclin G2	cell cycle regulation
1.83	Pdpx	pyridoxal (pyridoxine, vitamin B6) phosphatase	catalytic activity // metabolic process
1.82	Stat2	signal transducer and activator of transcription 2	involved in signal transduction and transcription for type I interferon signaling
1.73	AA408868	expressed sequence AA408868	inflammatory response; regulation of transcription, DNA-dependent
1.71	Ier3	immediate early response 3	integral membrane
1.69	Herpud1*	homocysteine-inducible, endoplasmic reticulum stress-inducible, ubiquitin-like domain member 1	response to stress // response to unfolded protein // ER membrane
1.66	Mrpl29/1200010C09Rik	mitochondrial ribosomal protein L49	translation /// structural component of ribosome
1.59	Cnm3*	cyclin M3	ion transport // integral to membrane
1.57	Sel1h	Sel1 (suppressor of lin-12) 1 homolog (<i>C. elegans</i>)	Notch signaling pathway // endoplasmic reticulum // extracellular space
1.56	Socs3	suppressor of cytokine signaling 3	intracellular signaling cascade; regulation of cell growth; signal transduction
1.56	Meg3	maternally expressed 3	
1.54	Lyst	lysosomal trafficking regulator	cellular defense response // response to bacterium // cytoplasm
1.54	1200010C09Rik	RIKEN cDNA 1200010C09 gene	response to unfolded protein// ubiquitin-protein ligase activity
1.54	BC018601	cDNA sequence BC018601	
1.54	Aof1	amine oxidase, flavin containing 1	oxidation reduction // electron carrier // metal ion binding
1.53	Xbp1	X-box binding protein 1	regulation of transcription DNA-dependent
1.52	Eif2ak3	eukaryotic translation initiation factor 2 alpha kinase 3	eIF2a kinase // electron transport// kinase activity // ATP binding
1.52	Cebpd	CCAAT/enhancer binding protein (C/EBP), delta	transcription regulation // DNA binding
1.52	Tbl2	transducin (beta)-like 2	extracellular space
1.52	Zc3h10	zinc finger CCCH type containing 10	metal ion binding // nucleic acid binding
1.51	Mkx	mohawk homeobox	multicellular organismal development // DNA binding
1.51	Irf2bp1	interferon regulatory factor 2 binding protein 1	negative regulation of transcription from Pol II promoter
1.5	Clk2	CDC-like kinase 2	autophosphorylation; protein amino acid phosphorylation// ATP binding; kinase activity
1.5	Hspa1a	heat shock protein 1A	DNA repair // response to heat // ATP binding

-1.5	Spic	Spi-C transcription factor (Spi-1/PU.1 related)	DNA binding; transcription factor activity
-1.5	Sfrs5	splicing factor, arginine/serine-rich 5 (SRp40, HRS)	splicesome // mRNA splice site selection // nucleic acid binding
-1.51	Cphx	cytoplasmic polyadenylated homeobox	transcription regulation // DNA binding
-1.52	Chic2	platelet derived growth factor receptor, alpha polypeptide	Golgi to plasma membrane transport // Golgi-associated vesicle
-1.52	Plaur	urokinase plasminogen activator receptor	binding of urokinase// cell surface receptor// kinase activity
-1.52	Plxdc1	plexin domain containing 1	receptor activity // integral to membrane
-1.54	Foxd3	forkhead box D3	DNA binding // transcription factor activity
-1.54	Mllt6	myeloid/lymphoid or mixed lineage-leukemia translocation to 6 homolog (Drosophila)	transcription regulation // DNA binding // metal ion binding
-1.54	Txnip	thioredoxin interacting protein	response to oxidative stress// anzyme inhibitor activity
-1.56	Cirbp	cold inducible RNA binding protein	RNA binding // nucleic acid binding
-1.56	Lrpap1*	low density lipoprotein receptor-related protein associated protein 1	heparin binding // low-density lipoprotein receptor binding // cytoplasm // ER// contain alpha-2-macroglobulin RAP domain
-1.57	Idb2	inhibitor of DNA binding 2	protein binding // transcription regulation
-1.58	Luc7l2	LUC7-like 2 (S. cerevisiae)	
-1.58	Rpl27a	ribosomal protein L27a	translaction // cytosolic ribosome
-1.59	Arl4a	ADP-ribosylation factor-like 4	small-GTPase mediate signal transduction // GTP binding
-1.64	Rnpc2	RNA-binding region (RNP1, RRM) containing 2	mRNA processing // nuclear mRNA splicing via spliceosome // regulation of transcription
-1.64	Idb3	inhibitor of DNA binding 3	negative regulation of transcription from Pol II promoter
-1.67	Ndrp1*	N-myc downstream regulated 1	mast cell activation // cytoplasm-nucleus
-1.7	Wac	WW domain containing adaptor with coiled-coil	spliceosome // protein binding
-1.76	Foxp1	forkhead box P1	cell differentiation // DNA binding // metal ion binding
-1.76	Klf3	Kruppel-like factor 3 (basic)	transcription regulation // DNA binding // metal ion binding
-1.81	Nab2	Ngfi-A binding protein 2	negative regulation of transcription // regulation of transcription DNA-dependent
-1.82	Slc30a1	solute carrier family 30 (zinc transporter), member 1	cation transport; zinc ion transport
-1.9	Tiparp	TCDD-inducible poly(ADP-ribose) polymerase	NAD + ADP ribosiltransferase activity // metal ion binding // nucleus
-1.94	Luc7l2	LUC7-like 2 (S. cerevisiae)	metal ion binding // protein binding
-2	Cyp1a1	cytochrome P450, family 1, subfamily a, polypeptide 1	electron transport// monooxygenase activity; oxidoreductase activity// ER
-2.18	Idb4**	inhibitor of DNA binding 4	cell proliferation // protein binding // transcription regulation
-2.29	Slc30a1	solute carrier family 30 (zinc transporter), member 1	cation transport // cellular zinc ion homeostasis // integral to membrane
-2.32	Pou4f2	POU domain, class 4, transcription factor 2	axon extension involved in development // chromatin binding
-2.82	Cyp1b1*	cytochrome P450, family 1, subfamily b, polypeptide 1	oxidation reduction // electron carrier // ER

Table 4.12 GeneSpring analysis of the mRNA expression profile of AB2.2 murine ES cells at 4h vs. 2h infection

GeneSpring analysis results of murine ES cell genes differentially expressed at 4h infection vs. 2h infection with *S. Typhimurium*. The genes were filtered for p-value < 0.05 and fold change +/- 1.5. Genes reported more than once are indicated by asterisks (* = reported twice; ** = reported three times).

Genes selected from condition Time 4.0 that have Normalised Data values that are greater or less than those in condition(s) Time 2.0 by a factor of 1.5 fold. Starting gene list: Filter for confidence t-test p-value 0 - 0.05, Benj and Hoch FDR, 1 cond of 3. In total 87 genes were differentially expressed of which 63 were previously annotated

Fold Change	Common	Description	Biological Process and or Molecular Function
2.02	Hspa1b**	heat shock protein 1A	anti-apoptosis // inhibition of caspase activation // response to heat // ATP binding // chaperon activity
1.85	Banp	Btg3 associated nuclear protein	protein binding
1.78	Ccng2	cyclin G2	cell cycle regulation // cyclin-dependent protein kinase regulator activity
1.72	Ier3	immediate early response 3	integral to membrane
1.7	Zbtb40	zinc finger and BTB domain containing 40	nucleus// metal ion binding // zinc ion binding
1.69	Cebpd	CCAAT/enhancer binding protein (C/EBP), delta	regulation of transcription// DNA binding // protein dimerization activity // nucleus
1.68	Gadd45g	growth arrest and DNA-damage-inducible 45 gamma	T-helper 1 cell differentiation // activation of MAPKK // apoptosis // interferon-gamma biosynthesis // negative regulation of protein kinase activity // protein biosynthesis // regulation of cell cycle // nucleus // structural constituent of ribosome
1.65	Ankrd37	ankirin repeat domain 37	cytoplasm // nucleus
1.64	Herpud1*	homocysteine-inducible, endoplasmic reticulum stress-inducible, ubiquitin-like domain member 1	protein modification // response to stress // ER membrane
1.64	Mkx	mohawk homeobox	multicellular organismal development // DNA binding
1.64	Xbp1**	X-box binding protein 1	regulation of transcription DNA-dependent
1.59	Tnfsf11	tumor necrosis factor (ligand) superfamily, member 11	regulates osteoclast differentiation and activation // immune response // cytokine activity // protein binding // tumor necrosis factor receptor binding // integral to membrane
1.58	Pdpx	pyridoxal (pyridoxine, vitamin B6) phosphatase	catalytic activity // metabolic process
1.52	Purg	purine-rich element binding protein G	nucleus // DNA binding
1.52	L3mbtl3	l(3)mbt-like 3 (Drosophila)	regulation of transcription // nucleus
1.5	Ccng2	cyclin G2	cell cycle regulation
-1.5	Lamp2	lysosomal membrane glycoprotein 2	tRNA aminoacylation for protein translation // integral to membrane; lysosome // ATP binding; tRNA ligase activity
-1.5	Syt11	synaptotagmin 11	transport // cell junction //cytoplasmic vesicle // calcium ion binding
-1.5	Sesn2	sestrin 2	cell cycle arrest // nucleus
-1.51	Spic	Spi-C transcription factor (Spi-1/PU.1 related)	regulation of transcription// transcription factor complex // DNA binding // nucleus
-1.51	Tieg1	TGFB inducible early growth response 1	transcription factor
-1.52	Hist1h1c	histone 1, H1c	chromosome organization and biogenesis // nucleosome // DNA binding // protein binding
-1.52	Frm4a	FERM domain containing 4A	cytoplasm // cytoskeleton // binding
-1.52	Idb4	inhibitor of DNA binding 4	cell proliferation // protein binding // transcription regulation
-1.52	Gpr160	G protein-coupled receptor 160	G-protein coupled receptor protein signaling pathway // signaling transduction // integral to

			membrane // receptor activity
-1.53	Luc7l2	LUC7-like 2 (S. cerevisiae)	metal ion binding // protein binding
-1.53	Bcor	Bcl6 interacting corepressor	chromatin modification // regulation of transcription // DNA binding
-1.55	Daf1	decay accelerating factor 1	complement activation, classical pathway // integral to membrane
-1.56	Flnb	filamin beta	skeletal muscle development // cytoplasm// cytoskeleton // actin binding // protein binding
-1.56	Pwwp2b	PWWP domain containing 2B	//
-1.57	Slc7a1	solute carrier family 7 (cationic amino acid transporter, y + system), number 1	amino acid transport// arginine transport // integral to membrane
-1.57	Trak1	trafficking protein, kinesin binding 1	GABA receptor binding
-1.57	Mapk4	mitogen-activated protein kinase 4	cell cycle // protein amino acid phosphorylation // ATP binding // kinase activity
-1.57	Nodal*	nodal	cytokine activity // growth factor activity // determination of left/right symmetry // development
-1.58	Zbtb7*	zinc finger and BTB domain containing 7	cartilage development // negative regulation of transcription from RNA polymerase II promoter // DNA binding // histone acetyltransferase binding
-1.59	Idb1	inhibitor of DNA binding 1	development // negative regulation of transcription from Pol II promoter // regulation of angiogenesis // nucleus
-1.6	Zmat4	zinc finger, matrin type 4	intracellular // nucleus // DNA binding// metal ion binding
-1.61	Spry4	sprouty homolog 4 (Drosophila)	multicellular organismal development // negative regulation of MAP kinase activity // cytoplasm // membrane // protein binding
-1.63	Foxp1	forkhead box P1	cell differentiation // DNA binding // metal ion binding
-1.63	Socs2	suppressor of cytokine signaling 2	intracellular signaling cascade // negative regulation of multicellular organism growth // growth hormone receptor binding // protein binding
-1.67	Rnase4	ribonuclease, Rnase A family 4	endonuclease activity; hydrolase activity; nucleic acid binding; pancreatic ribonuclease activity
-1.68	Plxdc1	plexin domain containing 1	receptor activity // integral to membrane
-1.69	Nab2	Ngfi-A binding protein 2	transcriptional repressor activity //
-1.69	Cyp2s1	cytochrome P450, family 2, subfamily s, polypeptide 1	monooxygenase activity; oxidoreductase activity // integral to membrane
-1.72	Arl4	ADP-ribosylation factor-like 4	small GTPase mediated signal transduction // intracellular // GTP binding // GTPase activity
-1.73	Mllt2h	homolog of human MLLT2 unidentified gene	transcription factor activity // cell growth and/or maintenance
-1.74	Snai1	snail homolog 1 (Drosophila)	DNA binding; nucleic acid binding; zinc ion binding
-1.76	Mllt6	myeloid/lymphoid or mixed lineage-leukemia translocation to 6 homolog (Drosophila)	regulation of transcription // metal ion binding // DNA binding
-1.8	Pqlc1	PQ loop repeat containing 1	integral to membrane
-1.8	Nr4a1	nuclear receptor subfamily 4, group A, member 1	inhibition of caspase activation // regulation of transcription // steroid hormone receptor activity // nucleus
-1.81	Ccno	cyclin O	DNA repair // hydrolase activity // nucleus
-1.89	Slc30a1	solute carrier family 30 (zinc transporter), member 1	cation transporter activity; zinc ion transporter activity // integral to membrane
-1.95	Ndr1***	N-myc downstream regulated 1	mast cell activation // cytoplasm // nucleus
-1.96	Cdkn1a	cyclin-dependent kinase inhibitor 1A (P21)	cell cycle arrest // negative regulation of apoptosis // positive regulation of B-cell proliferation // positive regulation of non-apoptotic programmed cell death // response to DNA damage stimulus
-2.06	Zfp296	zinc finger protein 296	//
-2.33	Idb4*	inhibitor of DNA binding 4	//
-2.38	Pou4f2	POU domain, class 4, transcription factor 2	axon extension involved in development // chromatin binding

-2.44	Slc30a1	solute carrier family 30 (zinc transporter), member 1	cation transporter activity // zinc ion transporter activity // integral to membrane
-2.48	Klf3***	Kruppel-like factor 3 (basic)	transcription regulation // DNA binding // metal ion binding
-9.9	Cyp1b1*	cytochrome P450, family 1, subfamily b, polypeptide 1	oxidation reduction // electron carrier // ER
-17.79	Cyp1a1	cytochrome P450, family 1, subfamily a, polypeptide 1	electron transport// monooxygenase activity; oxidoreductase activity // ER

4.3.4.2.2

4.3.4.2.3 Gene Ontology analysis of the genes differentially expressed at 4h

The Gene Ontology (GO) Consortium [<http://geneontology.org>], maintains a database of controlled vocabularies for the description of molecular functions, biological processes and cellular components of gene products. A gene product can have one or more molecular functions, be used in one or more biological processes, and may be associated with one or more cellular components. The results from GO analysis can provide insights into the biology of the systems being studied.

GO analysis for molecular functions is performed on the genes significantly differentially expressed at 4h infection as determined by GeneSpring analysis. The genes are filtered for p-value < 0.05 and expression fold change greater than +/- 1.5. The GO results appear as a spreadsheet in Table 4.15 that reports the number and the percentage of genes annotated in each category, the number of analyzed genes and a p-value also known as ‘enrichment score’ per category. The p-value reported indicates the relative importance or significance of the GO term among the entities in the selection compared to the entities in the whole dataset (Ashburner *et al.*, 2000).

The lists of GO analysis for biological processes and cellular components are available in Appendix A.

Table 4.13 Gene Ontology results in the molecular-function category for GeneSpring analysis

The 58 annotated genes, out of 89 total, differentially expressed following 4h of *S. Typhimurium* infection (p-value < 0.05, fold change +/- 1.5) are analyzed.

Filter on 1.5 fold change 4-0h (89 genes, 58 annotated) selected with GO:3674:molecular_function					
GO Category	Genes in Category	% of Genes in Category	Genes in List in Category	% of Genes in List in Category	p-Value
GO:4497: monooxygenase activity	152	0.666	3	5.172	0.00683
GO:16712: oxidoreductase activity	18	0.0789	1	1.724	0.0448
GO:30377: U-plasminogen activator receptor activity	1	0.00438	1	1.724	0.00254
GO:15082: di-, tri-valent inorganic cation transporter activity	44	0.193	2	3.448	0.0056
GO:5385: zinc ion transporter activity	10	0.0438	2	3.448	0.000282
GO:46873: metal ion transporter activity	77	0.337	2	3.448	0.0164
GO:46915: transition metal ion transporter activity	39	0.171	2	3.448	0.00443
GO:1871: pattern binding	125	0.548	2	3.448	0.0403
GO:30247: polysaccharide binding	121	0.53	2	3.448	0.038
GO:5539: glycosaminoglycan binding	119	0.521	2	3.448	0.0369
GO:8201: heparin binding	86	0.377	2	3.448	0.0202
GO:3676: nucleic acid binding	4624	20.26	18	31.03	0.0346
GO:3743: translation initiation factor activity	135	0.591	2	3.448	0.0463
GO:19207: kinase regulator activity	82	0.359	2	3.448	0.0185
GO:19887: protein kinase regulator activity	80	0.35	2	3.448	0.0177
GO:16538: cyclin-dependent protein kinase regulator activity	24	0.105	2	3.448	0.00169
GO:30528: transcription regulator activity	1800	7.885	10	17.24	0.0145
GO:16564: transcriptional repressor activity	164	0.718	3	5.172	0.00841

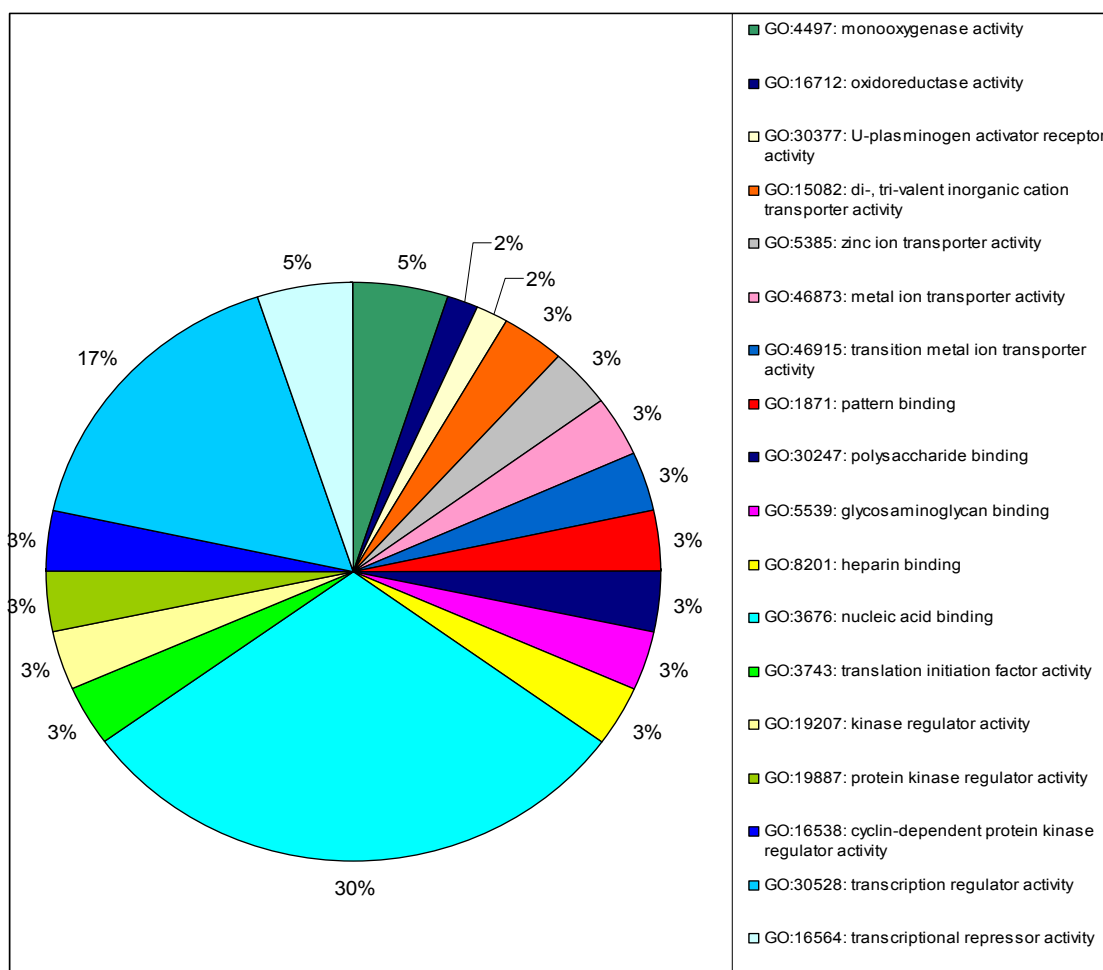


Figure 4.7 Graphical representation of the Gene Ontology analysis for molecular function of genes differentially expressed at 4h

The 89 genes determined to be significantly differentially expressed by GeneSpring analysis of murine AB2.2 ES cells at 4h infection with *S. Typhimurium*, (compared to uninfected controls) were further examined for Gene Ontology annotation describing the molecular function. This analysis highlighted that about a third of the listed genes have ‘nucleic acid binding’ ability and about a quarter have ‘transcription regulator activity’.

4.3.4.2.4 Real time RT-PCR to confirm GeneSpring analysis

The conditions used are the same as previously described for RT-PCR. Briefly, cDNAs were amplified using the QuantiTect QIAGEN kit and the real time RT-PCRs were carried out using the Quantum SYBR Green kit on a Stratagene real time machine. . It is important to validate the results of the bioinformatic analysis and a few genes reported to be significantly up- or down-regulated were selected to be confirmed using the relative quantification method, $\Delta\Delta C_t$. Gene selection was based on their potential relevance to *Salmonella*-host interaction studies suggested by close reading of the literature. These genes were distinct from those identified by Bioconductor analysis. Genes involved in early response, cellular trafficking regulation, cytokine signaling and anti-inflammatory response were included. For a more detailed description of each gene please refer to Table 4.11. The resulting fold changes are reported in Figure 4.8.

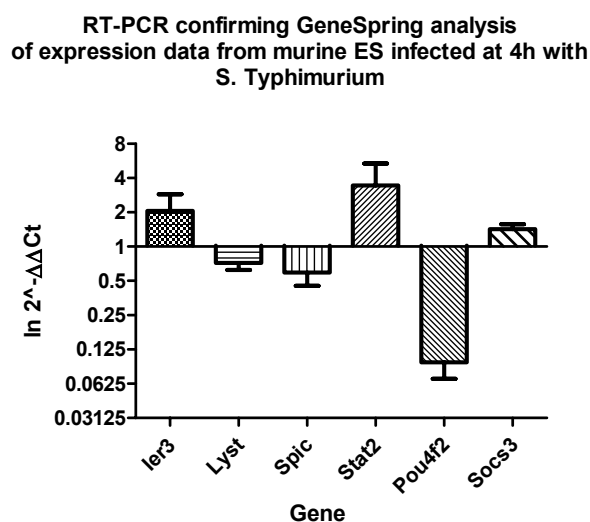


Figure 4.8 RT-PCR results conducted on a few genes identified by GeneSpring analysis

Some of the genes determined by GeneSpring analysis to be up- or down- regulated and with a significant p-value during infection were tested for relative quantification by RT-PCR. In this analysis the Ct values of target genes were compared to the Ct value of an internal control β -actin and the ratios were calculated and plotted as $\ln 2^{-\Delta\Delta C_t}$. The reactions were carried out in triplicate for each biological replicate at 0h and at 4h infection and reported here are the mean values. The error bars represent the standard error for each replicate. The initial amount of template cDNA is inversely proportional to the parameter measured for each reaction, the Ct.

Semi-quantitative RT-PCR confirms the results obtained by bioinformatics analysis of up- or down-regulated genes. In this case the genes chosen to be confirmed were identified by Gene Spring analysis as differentially expressed at 4h infection. The RT-PCR results confirmed that those genes reported to be up- or down-regulated by bioinformatics analysis were really up- or down-regulated.

4.3.4.2.5 Statistical analysis of RT-PCR data on genes identified by GeneSpring

Statistical analysis was conducted on the Ct values obtained from the real time RT-PCR conducted on a few genes identified by GeneSpring analysis. The REST[©] statistical program was used as described before. This analysis indicated that the Ct values of target genes were not significantly (p -value < 0.05) different to the Ct value of the target gene β actin (Figure 4.9). Nevertheless one gene, Pou4f2 reported a p -value < 0.1 . This gene contributes to the maintenance of the stemness characteristic. This result suggests that ES cells may be initiating a differentiation process during infection or that bacterial infection induce cell differentiation. However, further supporting evidence would be required to confirm this possibility.

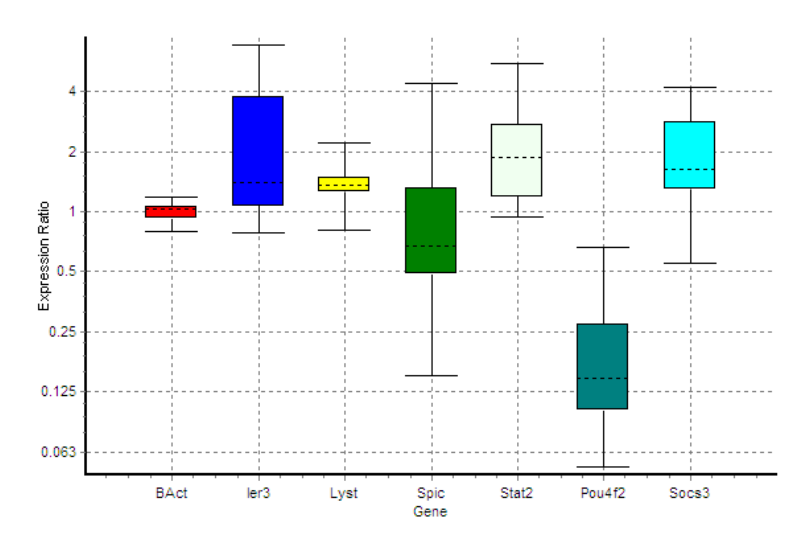


Figure 4.9 Whisker box plot of RT-PCR reaction conducted on genes identified by GeneSpring

This figure represents the Ct mean of three replicate reactions conducted on each gene. The genes were identified by GeneSpring analysis and the expression level of each one was compared to the expression level of an internal control gene: β -actin. In this experiment total RNA extracted from AB2.2 mouse ES cells uninfected and infected at 4h with *S. Typhimurium* SL1344 were used.

4.3.4.3 GEPAS: ASCA analysis

4.3.4.3.1 Time course analysis using ASCA

The mRNA profile of murine ES cells infected with *S. Typhimurium* SL1344 was further examined in a time course analysis. The analysis using time as a variable was carried out in order to highlight interesting expression patterns in gene expression during infection. A similar expression pattern might indicate co-regulation by a common transcription factor. For this purpose the Gene Expression Profile Analysis Suite (GEPAS) [<http://www.gepas.org>], which has been designed to provide an intuitive web-based interface (Montaner *et al.*, 2006), was employed. The ANOVA-simultaneous component analysis (ASCA) was proposed in order to analyze metabolomics data, and in this study was used in order to take into consideration the ‘time’ as a variable over the experiment (Smilde *et al.*, 2005). Basically ASCA fits an ANOVA model for each gene. In this case the ANOVA model has two factors, one is the time, which will give the temporal gene expression change related upon treatment, and the other is the individual. This method looks for different expression profile models that a gene can follow during treatment, and can detect if a gene follows the trend very well, but does not necessarily reach a sufficient significance in the traditional way. For a gene to be selected by ASCA, it must follow the trend of the majority of the changing genes (of the 2-3 major patterns). (Dr. Conesa personal communication)

ASCA analysis reported 943 genes, which were grouped into nine arbitrary clusters according to how their expression changed over time during the infection. The trend in each group is reported in Figure 4.10. Each graph reports the expression of the genes contained in each group represented as the mean log₂ for each gene’s expression divided by its expression at time zero. The three lines represent the three biological replicates. A value of 1 on the y axis represents two-fold up-regulation and a value of -1 represents two-fold down-regulation.

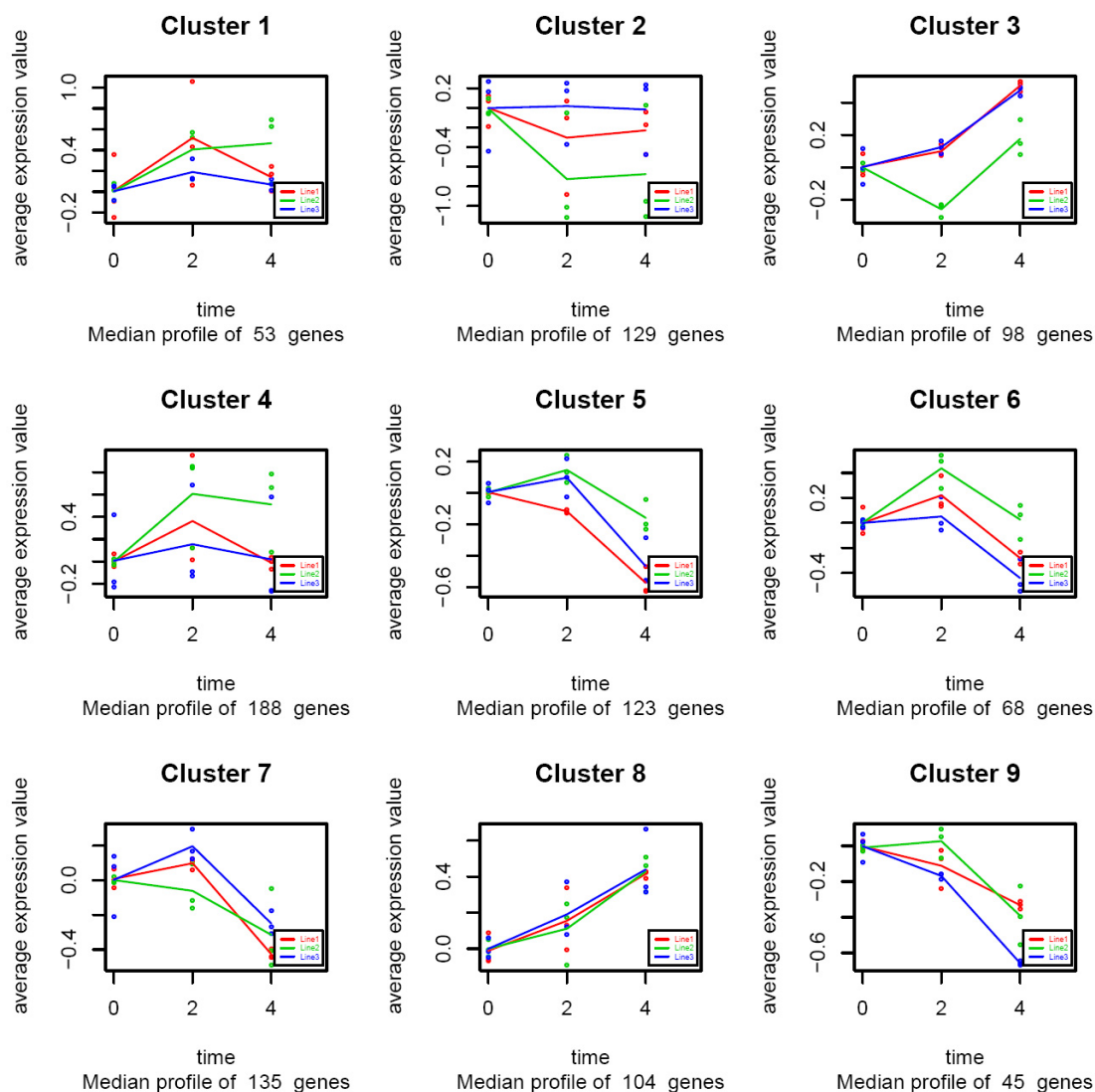


Figure 4.10 Gene clusters derived from ASCA analysis

ASCA analysis was used to investigate the data using time as a variable, and the genes whose expression profile changed during infection are reported. The 953 genes initially listed were then divided into nine arbitrary clusters and only those that best fit each trend were further analyzed.

This study included groups 3 and 8 for up-regulated genes and groups 5, 6, 7 and 9 for down-regulated genes. This analysis revealed 152 genes positively expressed during infection and 271 genes negatively expressed during infection. Tables 4.14 and 4.15 report some of the positively and the negatively regulated genes derived from this analysis, divided in categories that I think are relevant to this study based on current literature. For this reason the genes were organized into six groups: Cyclins, Ubiquitins, Mitochondrion, ER and Golgi apparatus, Cytokines and Chemokines, Cytoskeleton, Immune response and General interest.

Table 4.14 Gene list derived from ASCA analysis of the genes up-regulated during infection

Of the 153 genes found to be up-regulated during infection by ASCA analysis 45 are reported here. The genes are divided in categories that I think are interesting and relevant to this study based on close reading of the literature.

Gene Symbol	Gene Title	Biological and molecular functions
Cyclins		
Ccng2	cyclin G2	regulation of progression through cell cycle /// cell cycle /// mitosis /// cell division/// kinase regularoty activity
Ccnj1	cyclin J-like	regulation of progression through cell cycle
Cnm3	cyclin M3	biological_process
Ubiquitin		
Herpud1	homocysteine-inducible, endoplasmic reticulum stress-inducible, ubiquitin-like domain member 1	response to stress /// response to unfolded protein /// ER membrane // circadian regulation
Shprh	SNF2 histone linker PHD RING helicase	DNA repair /// nucleosome assembly /// transcription /// ubiquitin cycle /// ATP-binding /// zinc ion binding
Syv1	synovial apoptosis inhibitor 1, synoviolin	in utero embryonic development /// ubiquitin cycle /// anti-apoptosis /// response to unfolded protein /// multicellular organismal development /// integral to membrane /// ER membrane
Trim32	tripartite motif protein 32	ubiquitin cycle /// nucleic acid binding /// zinc ion binding
Usp26	ubiquitin specific peptidase 26	ubiquitin-dependent protein catabolic process /// ubiquitin cycle
Vps37a	vacuolar protein sorting 37A (yeast)	protein modification process /// ubiquitin cycle /// transport /// protein transport
Armet	arginine-rich, mutated in early stage tumors	ubiquitin cycle /// biological_process
Mitochondrion, ER, Golgi		
Gls	glutaminase	glutamine metabolic process/// mitochondrial inner membrane
Mtus1	mitochondrial tumor suppressor 1	ATP synthesis coupled proton transport /// receptor activity /// proton-transporting two-sector ATPase complex
Bfar	bifunctional apoptosis regulator	anti-apoptosis /// protein binding /// ER
Dhcr7	7-dehydrocholesterol reductase	blood vessel development /// steroid biosynthetic process /// cholesterol biosynthetic process /// lipid biosynthetic process /// regulation of cell proliferation /// nuclear outer membrane and ER
Eif2ak3	eukaryotic translation initiation factor 2 alpha kinase 3	skeletal development /// electron transport /// translation /// protein amino acid phosphorylation /// caspase activation /// virus-infected cell apoptosis /// ER overload response /// response to unfolded protein /// calcium-mediated signaling /// insulin secretion /// protein kinase activity
Ero1b	ERO1-like beta (S. cerevisiae)	electron transport /// oxidoreductase activity// ER
Gcs1	glucosidase 1	metabolic process /// oligosaccharide metabolic process /// ER /// integral to membrane
Hspa5	heat shock 70kD protein 5 (glucose-regulated protein)	anti-apoptosis /// ER overload response /// negative regulation of caspase activity /// ATP binding /// ribosome binding
Pigc	phosphatidylinositol glycan anchor biosynthesis, class C	GPI anchor biosynthetic process /// transferase activity /// ER membrane
Gopc	golgi associated PDZ and coiled-coil motif containing	transport /// autophagy /// protein transport /// protein homooligomerization /// small GTPase regulator activity /// membrane fraction/// trans-Golgi network transport vescicle
Slc35a5	solute carrier family 35, member A5	carbohydrate transport /// nucleotide-sugar transport /// Golgi membrane
Kif1b	kinesin family member 1B	microtubule-based process /// microtubule-based movement /// nerve-nerve synaptic transmission /// anterograde axon cargo transport /// embryonic development /// cytoskeleton-dependent intracellular transport /// mitochondrion transport along microtubule /// microtubule associated complex/// ATPase activity
Acbd3	acyl-Coenzyme A binding domain containing 3	steroid biosynthetic process /// transport /// acyl-CoA binding /// mitochondrion
EG623661	predicted gene, EG623661	protein modification process /// catalytic activity /// mitochondrion

Cytokine & Chemokine		
Nfat5	nuclear factor of activated T-cells 5	cytokine production /// transcription /// positive regulation of transcription from RNA polymerase II promoter /// protein binding
Tnfsf11	tumor necrosis factor (ligand) superfamily, member 11	immune response /// multicellular organismal development /// lymph node development /// protein homooligomerization /// receptor activity /// cytokine activity /// tumor necrosis factor binding
Cytoskeleton		
Taok2	TAO kinase 2	activation of MAPKK activity /// protein amino acid phosphorylation /// response to stress /// regulation of cell shape /// actin cytoskeleton organization and biogenesis /// positive regulation of JNK cascade /// focal adhesion formation
Actr1b	ARP1 actin-related protein 1 homolog B (yeast)	nucleotide binding /// structural constituent of cytoskeleton /// microtubule associated complex /// actin filament
Elmo2	engulfment and cell motility 2, ced-12 homolog (C. elegans)	phagocytosis /// apoptosis /// cytoskeleton
Enc1	ectodermal-neural cortex 1	proteolysis /// multicellular organismal development /// actin binding /// cysteine-type endopeptidase activity /// cytoskeleton
Hook1	hook homolog 1 (Drosophila)	microtubule cytoskeleton organization and biogenesis /// multicellular organismal development /// actin binding /// microtubule binding /// cytoskeleton
Lyst	lysosomal trafficking regulator	transport /// cellular defense response /// signal transduction /// endosome to lysosome transport /// protein transport /// endosome-microtubule-cytoskeleton
Nisch	nischarin	cell communication /// Rac protein signal transduction /// actin cytoskeleton organization and biogenesis /// negative regulation of cell migration /// receptor activity
Immune-Response and General Interest		
Ier3	immediate early response 3	membrane /// integral to membrane /// integral to membrane
Ier5l	immediate early response 5-like	///
Irf2bp1	interferon regulatory factor 2 binding protein 1	negative regulation of transcription from RNA polymerase II promoter
Ppp1r13b	protein phosphatase 1, regulatory (inhibitor) subunit 13B	induction of apoptosis /// defense response /// negative regulation of progression through cell cycle
Apaf1	apoptotic peptidase activating factor 1	neural tube closure /// proteolysis /// apoptosis /// caspase activation /// defense response /// multicellular organismal development /// regulation of apoptosis
Bcl3	B-cell leukemia/lymphoma 3	protein import into nucleus, translocation /// follicular dendritic cell differentiation /// marginal zone B cell differentiation /// humoral immune response mediated by circulating immunoglobulin /// transcription /// antimicrobial humoral response /// positive regulation of interferon-gamma production /// T-helper 1 type immune response /// negative regulation of tumor necrosis factor biosynthetic process /// defense response to bacterium /// regulation of apoptosis /// T-helper 2 cell differentiation /// positive regulation of interleukin-10 biosynthetic process ///
Banp	Btg3 associated nuclear protein	protein binding
Ercc4	excision repair cross-complementing rodent repair deficiency, complementation group 4	DNA metabolic process /// DNA repair /// nucleotide-excision repair /// endonuclease activity /// endodeoxyribonuclease activity /// hydrolase activity
Gbp6	guanylate binding protein 6	immune response /// nucleotide binding /// GTPase activity
Hsp110	heat shock protein 110	response to heat /// chaperone cofactor-dependent protein folding /// nucleotide binding /// ATP binding
Hspa1a	heat shock protein 1A	telomere maintenance /// DNA repair /// protein folding /// response to heat /// ATP binding
Hspa1b	heat shock protein 1B	telomere maintenance /// DNA repair /// protein folding /// anti-apoptosis /// response to heat /// negative regulation of caspase activity /// ATP binding

Table 4.15 Gene list derived from ASCA analysis of genes down-regulated during infection

ASCA analysis highlighted 270 genes negatively regulated during *S. Typhimurium* infection. Potentially genes are organized into categories.

Gene Symbol	Gene Title	Biological and molecular functions
Cyclins		
Ccnt1	cyclin T1	regulation of progression through cell cycle /// regulation of cyclin-dependent protein kinase activity /// transcription /// protein amino acid phosphorylation /// cell cycle
Ccnu	cyclin U	regulation of progression through cell cycle /// DNA repair /// response to DNA damage stimulus /// metabolic process
Cdkn1a	cyclin-dependent kinase inhibitor 1A (P21)	regulation of progression through cell cycle /// response to DNA damage stimulus /// negative regulation of cell proliferation /// positive regulation of B cell proliferation /// negative regulation of apoptosis /// positive regulation of non-apoptotic programmed cell death
Hmox1	heme oxygenase (decycling) 1	heme oxidation /// response to stimulus /// iron ion binding /// ER /// integral membrane
Ubiquitin		
Cbx4	chromobox homolog 4 (Drosophila Pc class)	chromatin assembly or disassembly /// transcription /// ubiquitin cycle /// chromatin modification
Nfkbia	nuclear factor of kappa light chain gene enhancer in B-cells inhibitor, alpha	protein import into nucleus, translocation /// lipopolysaccharide-mediated signaling pathway /// response to lipopolysaccharide /// regulation of cell proliferation /// response to exogenous dsRNA /// negative regulation of myeloid cell differentiation /// negative regulation of Notch signaling pathway /// NF-kappaB binding
Ranbp2	RAN binding protein 2	protein folding /// ubiquitin cycle /// intracellular transport /// protein binding /// metal ion binding
Rnf103	ring finger protein 103	ubiquitin cycle /// nucleic acid binding /// protein binding /// metal ion binding
Rnf12	ring finger protein 12	transcription /// ubiquitin cycle /// metal ion binding
Rnf128	ring finger protein 128	proteolysis /// ubiquitin cycle /// negative regulation of cytokine biosynthetic process /// metal ion binding
Tbl1xr1	transducin (beta)-like 1X-linked receptor 1	transcription /// ubiquitin cycle /// signal transduction /// chromatin modification /// GTPase activity
Tceb1	transcription elongation factor B (SIII), polypeptide 1	transcription /// ubiquitin cycle /// protein binding
Trim63	tripartite motif-containing 63	ubiquitin cycle /// muscle contraction /// proteasomal ubiquitin-dependent protein catabolic process /// metal ion binding
Ube2e3	ubiquitin-conjugating enzyme E2E 3, UBC4/5 homolog (yeast)	regulation of cell growth /// protein modification process /// ubiquitin-dependent protein catabolic process /// ubiquitin cycle
Mitochondrion, ER, Golgi		
Trp53	transformation related protein 53	protein import into nucleus, translocation /// regulation of progression through cell cycle /// transcription /// induction of apoptosis /// response to DNA damage stimulus /// ER overload response /// cell cycle /// caspase activation via cytochrome c /// positive regulation of transcription from RNA polymerase II promoter /// negative regulation of fibroblast proliferation
Abcb7	ATP-binding cassette, sub-family B (MDR/TAP), member 7	transport /// ATPase activity /// ATP binding /// nucleotide binding /// mitochondrial inner membrane
Bbc3	Bcl-2 binding component 3	release of cytochrome c from mitochondria /// induction of apoptosis /// caspase activation /// negative regulation of cell growth /// DNA damage response, signal transduction by p53 class mediator resulting in induction of apoptosis /// mitochondrial envelope
Gad1	glutamic acid decarboxylase 1	synaptic transmission /// carboxylic acid metabolic process /// neurotransmitter biosynthetic process /// mitochondrion
Agpat2	1-acylglycerol-3-phosphate O-acyltransferase 2 (lysophosphatidic acid acyltransferase, beta)	metabolic process /// phospholipid biosynthetic process /// 1-acylglycerol-3-phosphate O-acyltransferase activity /// ER /// integral to membrane
Asah3l	N-acylsphingosine amidohydrolase 3-like	lipid metabolic process /// ceramide metabolic process /// Golgi membrane /// ER membrane
Cds1	CDP-diacylglycerol synthase 1	phospholipid biosynthetic process /// CDP-diacylglycerol biosynthetic process /// phosphatidate cytidyltransferase activity /// magnesium binding /// ER membrane

Cyp1a1	cytochrome P450, family 1, subfamily a, polypeptide 1	electron transport /// monooxygenase activity /// iron ion binding /// extracellular space /// ER /// microsome
Cyp1b1	cytochrome P450, family 1, subfamily b, polypeptide 1	electron transport /// monooxygenase activity /// iron ion binding /// extracellular space /// ER /// microsome
Cyp2s1	cytochrome P450, family 2, subfamily s, polypeptide 1	electron transport /// monooxygenase activity /// iron ion binding /// extracellular space /// ER /// microsome
Fvt1	follicular lymphoma variant translocation 1	metabolic process /// oxidoreductase activity /// ER /// integral to membrane
Lrpap1	low density lipoprotein receptor-related protein associated protein 1	receptor activity /// heparin binding /// low-density lipoprotein receptor binding /// ER /// plasma membrane
Tmc6	transmembrane channel-like gene family 6	transpor /// transporter activity /// ER /// integral to membrane
Gnpnat1	glucosamine-phosphate N-acetyltransferase 1	UDP-N-acetylglucosamine biosynthetic process /// glucosamine 6-phosphate N-acetyltransferase activity /// N-acetyltransferase activity /// late endosome /// ER-Golgi intermediate compartment
Optn	optineurin	protein targeting to Golgi /// Golgi organization and biogenesis /// biological_process /// Golgi to plasma membrane protein transport /// Golgi apparatus
Sgms2	sphingomyelin synthase 2	lipid metabolic process /// sphingolipid metabolic process /// sphingomyelin biosynthetic process /// kinase activity /// transferase activity /// Golgi apparatus
St6gal1	beta galactoside alpha 2,6 sialyltransferase 1	protein amino acid glycosylation /// transferase activity /// integral to Golgi membrane
St8sia1	ST8 alpha-N-acetyl-neuraminide alpha-2,8-sialyltransferase 1	protein amino acid glycosylation /// positive regulation of cell proliferation /// transferase activity /// integral to Golgi membrane
Chic2	cysteine-rich hydrophobic domain 2	Golgi to plasma membrane transport /// Golgi-associated vesicles /// Golgi apparatus
Cytokine & Chemokine		
Klf6	Kruppel-like factor 6	transcription /// cytokine and chemokine mediated signaling pathway /// metal ion binding /// nucleus
Ltb	lymphotoxin B	immune response /// lymph node development /// cytokine activity /// tumor necrosis factor receptor binding /// plasma membrane
Nodal	nodal	in utero embryonic development /// transforming growth factor beta receptor signaling pathway /// multicellular organismal development /// positive regulation of cell proliferation /// cell migration /// stem cell maintenance /// cytokines activity /// extracellular scape
Socs2	suppressor of cytokine signaling 2	regulation of cell growth /// intracellular signaling cascade /// negative regulation of signal transduction /// growth hormone receptor binding /// insuline-like growth factor receptor binding
Socs3	suppressor of cytokine signaling 3	regulation of cell growth /// regulation of protein amino acid phosphorylation /// intracellular signaling cascade /// negative regulation of signal transduction /// negative regulation of insulin receptor signaling pathway
Zc3h15	Zinc finger CCCH-type containing 15	cytokine and chemokine mediated signaling pathway
Bmp4	bone morphogenetic protein 4	skeletal development /// positive regulation of protein amino acid phosphorylation /// multicellular organismal development /// BMP signaling pathway /// positive regulation of cell differentiation /// cytokine activity /// growth factor activity /// heparin binding
Ccl25	chemokine (C-C motif) ligand 25	chemotaxis /// chemotaxis /// inflammatory response /// immune response /// signal transduction /// leukocyte migration /// cytokine and chemokine activity
Cxcl16	chemokine (C-X-C motif) ligand 16	chemotaxis /// immune response /// low-density lipoprotein receptor activity /// scavenger receptor activity /// cytokine activity /// chemokine activity
Cytoskeleton		
Cdc42ep3	CDC42 effector protein (Rho GTPase binding) 3	regulation of cell shape /// actin cytoskeleton
Ctnna1	catenin (cadherin associated protein), alpha 1	cell adhesion /// establishment and/or maintenance of cell polarity /// negative regulation of apoptosis /// positive regulation of smoothed signaling pathway /// cadherin binding /// actin filament binding /// adherens junction /// lamellipodium /// zonula lamellipodium
Dsg2	desmoglein 2	cell adhesion /// homophilic cell adhesion /// calcium ion binding /// integral of membrane /// desmosome
Epb4.9	erythrocyte protein band 4.9	cytoskeleton organization and biogenesis /// barbed-end actin filament capping /// actin binding

Flnb	filamin, beta	striated muscle development /// actin binding /// stress fiber cytoplasm /// focal adhesion /// cytoskeleton
Frmd4a	FERM domain containing 4A	binding /// cytoskeleton
Gphn	gephyrin	protein targeting /// Mo-molybdopterin cofactor biosynthetic process /// establishment of synaptic specificity at neuromuscular junction /// catalytic activity /// cytoskeletal protein binding
Kras	v-Ki-ras2 Kirsten rat sarcoma viral oncogene homolog	regulation of progression through cell cycle /// small GTPase mediated signal transduction /// Ras protein signal transduction /// positive regulation of cell proliferation /// actin cytoskeleton organization and biogenesis /// regulation of synaptic transmission, GABAergic /// positive regulation of Rac protein signal transduction ///
Mtss1	metastasis suppressor 1	cell motility /// actin filament organization /// cell adhesion /// signal transduction /// transmembrane receptor protein tyrosine kinase signaling pathway /// actin filament polymerization /// filopodium formation /// actin binding /// ruffle /// endocytic vesicle
Synpo2l	synaptopodin 2-like	actin binding /// protein binding /// cytoskeleton
Ttl	tubulin tyrosine ligase	microtubule cytoskeleton organization and biogenesis /// protein modification process /// regulation of axon extension /// tubulin-tyrosin ligase activity /// magnesium-potassium ion binding /// microtubule
Arhgap8	Rho GTPase activating protein 8	actin cytoskeleton organization and biogenesis /// positive regulation of cell migration /// GTPase activator activity
Immune-Response and General Interest		
Relb	avian reticuloendotheliosis viral (v-rel) oncogene related B	regulation of progression through cell cycle /// transcription /// cellular process /// antigen processing and presentation /// T-helper 1 type immune response /// myeloid dendritic cell differentiation /// T-helper 1 cell differentiation /// regulation of transcription
Arl6ip2	ADP-ribosylation factor-like 6 interacting protein 2	immune response /// nucleotide response /// GTPase activity
Cd55	CD55 antigen	immune response /// complement activation, classical pathway /// innate immune response /// GPI anchor binding
Eif2ak2	eukaryotic translation initiation factor 2-alpha kinase 2	translation /// protein amino acid phosphorylation /// immune response /// response to virus /// unfolded protein response /// protein amino acid autophosphorylation /// RNA binding /// transferase binding /// protein kinase activity /// protein serine/threonine kinase activity
Centd3	centaurin, delta 3	signal transduction /// regulation of cell shape /// negative regulation of cell migration /// negative regulation of Rac protein signal transduction /// negative regulation of Rho protein signal transduction /// regulation of GTPase activity /// ruffle /// lamellipodium /// Rho GTPase activator activity
Gpr160	G protein-coupled receptor 160	signal transduction /// G-protein coupled receptor protein signaling pathway /// rhodopsin-like receptor activity
Gpr83	G protein-coupled receptor 83	signal transduction /// G-protein coupled receptor protein signaling pathway /// rhodopsin-like receptor activity
Mcf2l	mcf.2 transforming sequence-like	intracellular signaling cascade /// Rho protein signal transduction /// regulation of Rho protein signal transduction /// lamellipodia
Tbc1d24	TBC1 domain family, member 24	regulation of Rab GTPase activity
Tbc1d9	TBC1 domain family, member 9	regulation of Rab GTPase activity /// GTPase activator activity
Kbtbd8	Kelch repeat and BTB (POZ) domain containing 8	intracellular protein transport /// exocytosis /// biological process /// regulation of calcium ion-dependent exocytosis /// glucose homeostasis /// negative regulation of G-protein coupled receptor protein signaling pathway /// Rab GTOase binding
Rab11fp2	RAB11 family interacting protein 2 (class I)	///
Rims2	regulating synaptic membrane exocytosis 2	transport /// intracellular protein transport /// exocytosis /// intracellular signaling cascade /// calcium ion-dependent exocytosis /// cAMP-mediated signaling /// insulin secretion /// Rab GTPase binding

4.3.4.3.2 Functional category analysis using FatiGO on ASCA results

One of the problems related to functional genomics is the description of biological properties, functions and interactions shared by a set of genes. An answer to this problem is Gene Ontology that extracts information from scientific journals and provides a structured description of biological functions dividing them into molecular functions, biological processes and cellular components (Ashburner *et al.*, 2000). FatiGO is a web-based application [<http://fatiGO.bioinfo.cnio.es>] able to extract relevant GO terms for a group of genes with respect to a set of reference genes. FatiGO is used here to investigate which functional categories are over- or under-represented in the two groups of genes up-regulated and down-regulated obtained from ASCA analysis compared to the entire list of genes on the microarray chip. FatiGO extracts the function category from GO once the level at which the statistical contrast is going to be performed is indicated. Usually level 3 is used but lower terms in GO hierarchy are more precise. Also FatiGO returns adjusted p-values based on three different ways of accounting for multiple testing (Al-Shahrour *et al.*, 2004). The analysis was performed to determine the functional categories of cellular-component, molecular-function, biological process and pathway reported in KEGG (Kyoto Encyclopedia of Genes and Genomes), and the results are reported in Tables 4.16 and 4.17 for up- and down-regulated genes, respectively.

Table 4.16 FatiGO analysis of up-regulated genes from ASCA analysis

The list of up-regulated genes was analyzed for Functional Category enrichment with FatiGO and the results are reported here. Among the genes up-regulated, enrichment of four categories was identified but no pathway was statistically significant.

ASCA analysis up-regulated genes				
Biological process	Level	n of genes	Unadj. p-value	Adj. p-value
response to unfolded protein	5	5	0.000006	0.017700
macromolecule metabolic process	3	37	0.000010	0.020200
primary metabolic process	3	39	0.000037	0.047000
Cellular component	Level	n of genes	Unadj. p-value	Adj. p-value
Nucleus	8	31	0.000013	0.020600

Table 4.17 FatiGO analysis of down-regulated genes from ASCA analysis

The list of down-regulated genes was analyzed for Functional Category enrichment with FatiGO and the results are reported here. Among the genes down-regulated, enrichments can be observed in the TGF- β signaling pathway, and predominantly in transcription or DNA binding proteins.

ASCA down-regulated genes analyzed with FatiGO				
KEGG	Genes list	Number of Genes	Unadj. p-value	Adj. p-value
TGF-beta signaling pathway	Id3, Fst, Nodal, Id2, Bmp4, Id1	6	0	0.0096

Cellular components	Level	Number of Genes	Unadj. p-value	Adj. p-value
nucleus	8	34	0.0004	0.0825

Biological process	Level	number of genes	Unadj. p-value	Adj. p-value
multicellular organismal development	3	25	0	0.0115
anatomical structure development	3	22	0.0001	0.0462
negative regulation of transcription	8	9	0	0.0221
regulation of transcription, DNA-dependent	8	26	0.0001	0.0434
negative regulation of transcription factor activity	9	3	0	0.0115

Cellular functions	Level	Number of Genes	Unadj. p-value	Adj. p-value
nucleic acid binding	3	29	0.0002	0.0541
transcriptional repressor activity	3	6	0.0002	0.0602
nucleotide binding	3	1	0.0003	0.0688
DNA binding	4	23	0	0.0096
unspecific monooxygenase activity	6	3	0.0003	0.0688

4.3.4.3.3 Real Time RT-PCR relative quantification on genes derived from ASCA analysis

ASCA analysis does not provide the fold change in expression so it is difficult to confirm this data by real time RT-PCR. However RT-PCR can give a confirmation of the expression trend of a gene during infection. For this reason, total RNA extracted at 2 and 4 hours post-infection were employed in this experiment as well as appropriate control RNA populations. The genes were chosen for their potential relevance to host-pathogen interaction studies. In addition, a few genes that were identified in previous analyses described in this thesis were included. These were Lamp2 and Socs3, already shown to be down- and up-regulated during ES cell infection. Other genes included examples involved in the regulation of apoptosis, cytoskeleton rearrangement and a TGF- β binding protein. For a more detailed description of each gene please refer to Table 4.14 and 4.15. The data are reported here as $\ln 2^{-\Delta\Delta Ct}$ that represents the ratio between the expression level of the target gene and the control gene (β -actin) expressed in ln scale (Figure 4.11).

Gene selected by the ASCA analysis to be up- or down- regulated during AB2.2 ES cells infection with *S. Typhimurium*

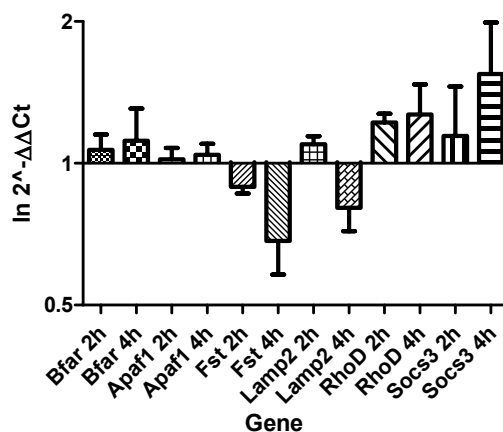


Figure 4.11 Real time RT-PCR relative quantification on ASCA analysis

A few genes selected by ASCA analysis to be positively or negatively regulated in murine ES cells AB2.2 during *S. Typhimurium* infection were chosen to perform relative quantification by real time RT-PCR. In this analysis the Ct values of target genes were compared to the Ct value of an internal control β -actin and the ratios were calculated and plotted as $\ln 2^{-\Delta\Delta Ct}$. The reactions were carried out in triplicate for each biological replicate at 0h, 2h and 4h infection and the mean values are reported here. The error bars represent the standard error for each replicate.

RT-PCR was performed in order to confirm the results obtained by bioinformatics analysis of up- or down-regulated genes. In this case the genes to be confirmed by RT-PCR were chosen as they seemed relevant to this study. The RT-PCR results partially confirmed that those genes reported to be up- or down-regulated by bioinformatics analysis were in fact up- or down-regulated. The Socs3 gene, however, was reported to be down-regulated by ASCA analysis, whereas it was up-regulated in the other analysis as also confirmed by RT-PCR. Refer to Appendix A for a short description of the genes used in this experiment.

4.3.4.3.4 Statistical analysis of RT-PCR data on genes identified by ASCA

Statistical analysis was performed on the real time RT-PCR Ct values obtained on a few genes identified by ASCA analysis. The analysis was performed comparing the expression levels at 4 hours post-infection to the uninfected cells since there were larger expression difference between these samples. The statistical analysis was conducted using REST© 2005. The results from this analysis are shown in Figure 4.12 as a graph plotting the expression range for each gene. This analysis reported no significant difference in the expression levels of the genes taken into consideration here.

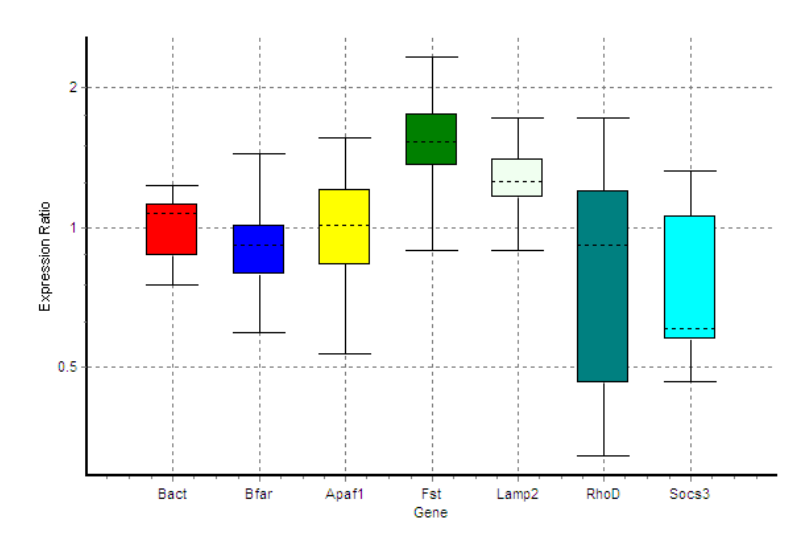


Figure 4.12 Whisker box of the RT-PCR analysis on genes identified by ASCA

The statistical analysis of the Ct values determined from the RT-PCR analysis is here represented as whisker boxes representing the mean value of three independent reactions for each gene. The statistical analysis did not identify any statistically significant difference between the mean Ct values of the target genes compared to the mean Ct value of the control gene β -actin.

4.4 Discussion

This chapter reports the results from the transcription profile of AB2.2 murine ES cells during infection with *S. Typhimurium* SL1344. The concept behind these experiments was to investigate whether ES cells could be developed as a novel *in vitro* model by which to study the response of eukaryotic cells to bacterial infection. It is now well established that microarrays can be used to monitor how immunological cells subjected to bacterial invasion respond in terms of gene expression patterns (Detweiler *et al.*, 2001; Rosenberger *et al.*, 2000). Further work has also been reported on infected epithelial cells that can respond by producing cytokines and other immune factors (Eckmann *et al.*, 2000). Two factors should be kept in mind in the interpretation of the data presented here. Firstly, at least 30% of the cells were infected at 2 hours and 4 hours post-infection. The percentage of cells infected will inevitably have effects on the resulting p-values and fold expression. However it has not been common practise in published papers reporting transcription profile during bacterial infection, to include data on percentage of infected cells. The second factor to consider is that, as noted in previous publications, the response of differentiated cells to pathogen invasion overwhelmingly involves genes linked to the immune response. Interestingly, in the ES cell model used here, this response was not observed and it is possible that by using murine ES cells, that lack a strong immune signature, to highlight other components involved in alternative cellular reaction to pathogen invasion.

Pathogens are able to manipulate host components to their advantage. For example, it has previously been described how *Salmonella* secretes SPI-1 TIISS effector proteins inside non-phagocytic cells directing its own phagocytosis. The TIISS are specialized protein structure with the ability to deliver a specific set of bacterial proteins into the host cells to modulate or interfere with cellular functions; this mechanism is essential for the virulence of many important bacteria such as *Salmonella*, *Shigella* and *Yersinia pestis* (Kubori & Galan, 2003). Also a second *Salmonella* TIISS, harboured on the SPI-2 loci, injects proteins inside the host from the SCV. Examples of SPI-2 effectors include SifA which is involved in the maintenance and survival of the bacteria inside the host cells (Brumell *et al.*, 2002).

In the analysis reported here at least four important groups of genes can be distinguished that are apparently differentially regulated during bacterial infection. These include a limited number of immunological genes, genes involved in cell cycle regulation, many genes involved in stress response, associated with ER and protein folding, and components of the mitochondrion. Finally the expression of several transcription factors is affected. Hereafter, I will talk briefly about some genes that are included in these categories.

Among the genes involved in the cell cycle regulation one that comes up as strongly up-regulated in all the analyses is *Banp*, Btg3 associated nuclear protein. This is part of the BTG family of proteins, of which several members play a role in the negative control of the cell cycle. It was reported that BTG3 is induced by redox changes, with RNA levels peaking at the end of G1 phase of the cell cycle (Biro *et al.*, 2000). In other studies investigating host-pathogen response BTG1 was reported to be up-regulated in swine lymph nodes after infection with *S. Choleraesuis* (Uthe *et al.*, 2007) and in human epithelial cells infected with *S. Dublin* (Eckmann *et al.*, 2000).

Genes involved in ubiquitination were also identified as differentially expressed in this experiment. Ubiquitination can have an important role in bacterial infection, for example *Pseudomonas aeruginosa* (Balachandran *et al.*, 2007). In this study, the ‘ubiquitin mediated proteolysis’ pathway was determined to be differentially up-regulated by InnateDB analysis (Table 4.6). In the ASCA time course analysis seven genes involved in the ubiquitin cycle were also identified as up-regulated (Table 4.14) and ten were apparently attenuated during infection (Table 4.15). Ubiquitination is the main protein degradation pathway that governs a variety of cellular processes including cell cycle, vesicle trafficking and signal transduction. Bonifacino and Weissman (1998) report an exhaustive review on ubiquitins and their role in the immune system (Bonifacino & Weissman, 1998). During *Salmonella* invasion at least one protein secreted inside host cells by SPI-1, SopE, is an object of ubiquitination and rapid degradation soon after injection (Kubori & Galan, 2003). SopA can also serve as a substrate for HsRMA1-mediated ubiquitination. In this case though, it was speculated that mono- or poly-ubiquitination can modulate the protein activity and *Salmonella* SCV escape inside the host cells (Zhang *et al.*, 2005). However, the first *Salmonella* protein to be described to be ubiquitinated, once inside the host cell, was a SIP-1

secreted protein, SopB. Although the authors did not observe a rapid degradation by the proteasome thereafter, they hypothesized that the ubiquitination would regulate SopB activity and attenuate cyto-toxicity (Marcus *et al.*, 2002). In fact it was reported that ubiquitination not only has a role in protein metabolism but in particular mono-ubiquitination is a regulator of the location and activity of diverse cellular proteins (Hicke, 2001). The gene involved in ubiquitination with the highest differential expression during infection of murine ES cells was *Herpud1*. The homocystein-inducible, endoplasmic reticulum stress-inducible, ubiquitin-like domain member 1 (Herpud1), was reported to be involved in the ER-stress response where it is a resident-chaperone protein. Herpud1 was originally described as the first integral membrane protein regulated by the ER stress response pathway and was suggested to play an unknown role in the cellular survival response to stress in the unfolded protein response (UPR) (Kokame *et al.*, 2000).

The ER stress response can also activate another cellular signalling pathway named EOR (ER overloaded response); this is activated by the accumulation of membrane proteins in the ER and is distinct from the signalling induced by UPR. The EOR signalling pathway activates nuclear factor (NF)- κ B which then induces the transcription of pro-inflammatory and immune response genes. GeneSpring analysis revealed the up-regulation of *NF κ biz* (nuclear factor kappa light chain polypeptide gene enhancer in B-cell, inhibitor zeta) (Table 4.10) and ASCA analysis reported the down-regulation of *NF κ bia* (nuclear factor kappa light chain polypeptide gene enhancer in B-cell, inhibitor alpha) (Table 4.15). *NF κ biz* gene is a member of the ankyrin-repeat family with high sequence similarity to the C-terminal of I κ B proteins. Bioconductor analysis also revealed mRNA encoding for the ankyrin-repeat member 37 to be up-regulated (Table 4.3, Table 4.4), reported also in GeneSpring analysis (Table 4.12). The transcription factor NF- κ B plays a crucial role in a wide variety of cellular functions and its activity is strictly regulated by cytosolic inhibitors known as I κ Bs. I κ B is induced by lipopolysaccharide (LPS) or IL-1 β and is localized in the nucleus where it is thought to bind NF- κ B thus preventing an excessive inflammatory response. Also, *NF κ biz* supports the regulation of a subset of inflammatory genes represented by IL-6, it inhibits the expression of TNF- α and is reported to promote TNF- α -induced apoptosis (Yamazaki *et al.*, 2001). *NF κ bia* is reported to play a role in viral infection (Hiscott *et*

al., 1997). The regulation of NF κ B is complex and this transcription factor itself regulates the expression of many cellular biological functions including inflammation, stress and immune responses, embryonic development and apoptosis (Liu-Mares *et al.*, 2007).

Microarray analysis also identified a few transcription factors as being differentially expressed during *Salmonella* infection. Two transcription factors whose expression was significantly induced during bacterial infection were *eIf2ak2* and 3 (eukaryotic initiation factor 2 alpha, kinase 2 and 3). They were identified during both GeneSpring and ASCA analysis (Tables 4.11 and 4.14). The phosphorylation of this class of proteins immediately inhibits additional translational initiation events (Kaufman, 1999). The time course analysis revealed that *eIf2ak2*, also described as IFN-type I-induced and ds-RNA activated kinase, was down regulated during infection (Table 4.15).

Another transcription factor displaying a strong signal of differential expression in this study is XBP-1 (X-box binding protein-1). This transcription factor is essential for the differentiation of plasma cells and the UPR activation. This gene was also reported to be positively expressed in another publication detailing human macrophage-pathogen interactions (Nau *et al.*, 2002). In 2003 Iwakoshi *et al.* concluded that XBP-1 is absolutely required for plasma cell differentiation (Iwakoshi *et al.*, 2003). The same authors in 2007 reported that XBP-1 is necessary for maintaining ER homeostasis and preventing activation of cell death pathways caused by sustained ER stress. Also they reported that *XBP-1* expression is essential for dendritic cell development and survival, which confirms its importance in the differentiation of highly secretory cells like embryonic hepatocytes, exocrine pancreatic acinar cells and plasma cells (Iwakoshi *et al.*, 2007).

Among the genes involved in the mitochondrion homeostasis, monooxygenase genes such as cytochrome P450a and b were strongly down-regulated at 4 hours post-infection with *S. Typhimurium* (Table 4.3, 4.4, 4.11, 4.12, 4.15) although they were first up-regulated at 2 hours post-infection (Table 4.2 and 4.10). The alteration of the expression of the oxidoreductase genes was reported in other studies investigating the host response to pathogens (Handley & Miller, 2007; Rosenberger *et al.*, 2001). The smooth ER expands as the enzymes that oxidize and detoxify are induced to meet their demand

and the overproduction of recombinant *Candida maltosa* P450Alk1 in *S. cerevisiae* activates the UPR to proliferate the ER extensively (Kaufman, 1999). It was proposed that the P-450 down-regulation is a pathophysiological effect of the inflammation progression, a scheme of which is reported in Figure 4.13 (Morgan, 2001).

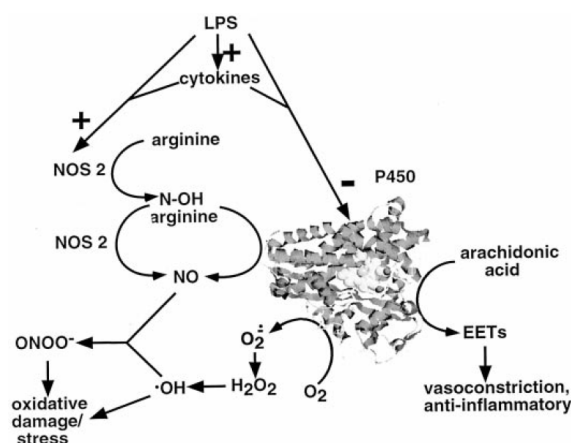


Figure 4.13 Supposed regulation of P450 cytochrome during cellular response to inflammation (Morgan, 2001)

Pathway analysis conducted with InnateDB did not reveal any significantly (for adjusted p-value) up-regulated (Table 4.5, 4.6, 4.8) or down-regulated pathways (Table 4.7, 4.9). However among the potentially up-regulated pathways identified, a few were quite interesting and they highlight how *Salmonella* invasion may interfere with lipid synthesis, ER trafficking and cell motility signalling pathways (Table 4.6).

Among these, the ERAD pathway or ER-associated degradation pathway is involved in the cytosolic degradation of misfolded proteins present in the ER. Once in the cytosol the proteins are deglycosylated, ubiquitinated and directed to proteasome degradation (Tsai *et al.*, 2002). It has been observed that ERAD can be subverted by viral infection to trigger MHC class I breakdown (Tortorella *et al.*, 2000). It is also possible that bacterial invasion triggers the ER stress response similar to that for viral infection, depicted in Figure 4.14 (Medigeschi *et al.*, 2007). This response may also be a defense mechanism since, under conditions of severe ER stress, eukaryotic cells generate a signal that induces programmed cell death known as apoptosis. However, the molecular signalling mechanisms that link ER stress to downstream caspase activation resulting in cell death remain largely unknown (Kaufman, 1999).

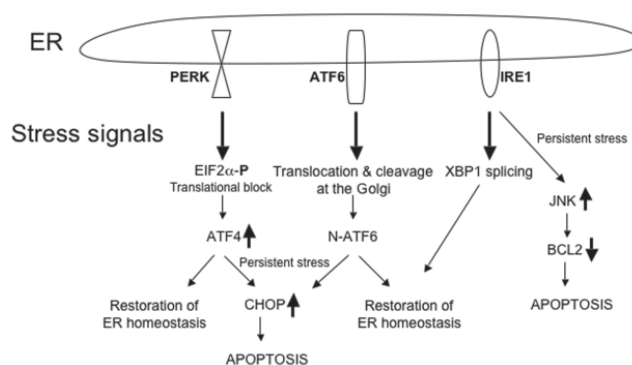


Figure 4.14 ER stress response to viral infection (Medigeshi et al., 2007)

The stringency of statistical analysis often does not accommodate the flexibility and variability of biological systems very well. In this study the data analysis using GeneSpring software revealed more interesting and previously reported genes implicated in host-bacteria interactions. For example among the positively regulated genes can be recognized *Socs* (suppressor of cytokine signalling) (Dalpke *et al.*, 2008), *Stat2* (involved in the transduction and transcription of type I interferon signalling), *Lyst*, (lysosomal trafficking regulator) and *clk2* (CDC-like kinase 2) all of which were previously described to be somehow involved with the pathogen interaction.

This study reported that several genes of murine ES cells were significantly differentially expressed during *S. Typhimurium* invasion, however a few of these are known to be involved in immunological responses. Most of the genes reported are principally involved in the cellular reaction to bacterial invasion. Few of them have been documented in previous host-pathogen transcription profile studies but perhaps they were not discussed because they were not thought relevant to the immune response. Sometimes the interpretation of microarray data can be distorted by the expectations and previous observations of the system studied.

The use of whole genome arrays gives the researcher new insight into host-pathogen interactions that can potentially lead to the discovery of new pathways likely to be promising as new drug targets. However, only their combined use with sequence information, computational tools and the traditional approaches of biology, biochemistry, chemistry, physics, mathematics and genetics can increase the hope of

understanding the function and the regulation of all genes and proteins (Lockhart & Winzeler, 2000).

5 Procedures for differentiating mouse Embryonic Stem cells into dendritic cell

5.1 Introduction

5.1.1 Stem cells and *in vitro* differentiation

A hallmark and defining property of stem cells is their capacity for self-renewal and differentiation. The science of stem cell biology is still young and the properties of these cells have not been fully explored and there is more to be discovered in terms of research and their potential therapeutic applications. Few stem cells types have been characterised and described since their discovery in the early 1980s. Denham and co-workers distinguished five types of stem cells: unipotent stem cells, which are a type of cell that undergoes self-renewal and gives rise to only one mature cell type; multipotent stem cells that are characterized by the ability to undergo self-renewal and have the capacity to yield at least two differential foetal or adult cell types; pluripotent stem cells, which are capable of self-renewal and give rise to a vast array of mature cell types; totipotent stem cells, which replicate and generate all adult and extraembryonic tissues of their species but undergo limited self-renewal. The final type of stem cells are cancer stem cells, which replicate and undergo self-renewal but their compromised self-renewal pathway results in neoplasia (Denham *et al.*, 2005).

Pluripotent stem cells are heavily utilized in research and these cells are currently favoured for the exploitation of their therapeutic potential. *In vitro*-generated embryonic germ (EG) cells, embryonal carcinoma (EC) cells and embryonic stem (ES) cells can be generated from this type of stem cell. ES cells originate from the inner cell mass of an embryo at the blastocyst developmental stage, and thus they theoretically possess the capacity to give rise to every cell type of the adult organism. This quality of pluripotent stem cells has already been largely demonstrated. ES cells have the ability to provide replacement tissue or they can be used as a means to understand disease mechanisms. Before these goals can be routinely and rationally achieved, the precise methods of how to differentiate stem cells into exactly the right lineage, in a homogenous or near-

homogenous form needs to be addressed. Also other areas where progress still has to be made include the ethics of their use, the suppression of immune rejection and the accessibility of sites within the patient (Denham *et al.*, 2005).

Mouse ES cells are nowadays the best characterized stem cells lines and they have already been driven to differentiate *in vitro* into diverse cell lineages such as cardiac muscle, neural crest, neural stem and haematopoietic lineages, just to mention a few. It is believed, or hoped, that human ES cells may eventually be driven *in vitro* to differentiate into any desired cell of the body for potential use therapeutically (Denham *et al.*, 2005). The first reports of the *in vitro* differentiation of ES cells into haematopoietic lineages came in 1991 using direct differentiation from *in vitro* grown ES cells. Wiles and colleagues (1991) reported the differentiation of four haematopoietic lineages from embryoid bodies: erythroid cells, macrophages, neutrophils and mast cells. In their publication, Wiles and colleagues commented with enthusiasm and a little surprise about the consistency and the large number of cells produced by their method (Wiles & Keller, 1991). Moreover the practical exploitation of differentiated antigen presenting cells (APC) deriving from ES cells was reported by Moore *et al.* in 1998. Here *in vitro* ES cells differentiated into macrophages were used in a study on atherosclerosis. In addition, these authors reported the use of transfected ES cells (Moore *et al.*, 1998). They recognized the advantage of using ES cells differentiated into APC resides in the fact that genetic manipulations can be performed on primary stem cells prior to differentiation. Schmitt *et al.* (2004) reported the possibility of differentiating ES cells into mature and functioning T cells. They successfully reconstituted the T cell compartment of immunodeficient mice using differentiated stem cells, enabling an effective response to a viral infection (Schmitt *et al.*, 2004).

The potential of murine ES cells to be differentiated into dendritic cells (DCs) with the ability to present antigen to naïve T cells was explored in order to further investigate the potential application of stem cells to infectious diseases studies.

5.1.2 Dendritic cells and their *ex-vivo* extraction and research application

Dendritic cells are highly specialized APCs that perform a very important role in the immune system, which is to link innate and adaptive immune responses mediating T cell activation and antigen-specific responses. DCs together with macrophages are considered a primary target for initiating immune responses to infection and they play a central role in the body's fight against pathogens. DCs are sentinel cells that continuously sense the environment and coordinate defenses for the protection of mucosal tissues. Mucosal surfaces represent the main site of interaction with microorganisms and antigens from the external environment. Immature DCs are essential cells with phagocytic potential, resident in the sub-epithelial and intra-epithelial compartments of the mucosa. Here, DCs play an active role in bacterial uptake by sampling the lumen content. This is possible because DCs are able to open the tight junctions connecting epithelia cells (Rimoldi *et al.*, 2004). Upon maturation, normally induced by either pathogen-associated molecular patterns or microorganisms, DCs function as APCs and commonly migrate into mucosal-associated lymph nodes to initiate adaptive immunity (Niedergang *et al.*, 2004). Some researchers believe that a major "bottleneck" in mucosal DC research is the difficulty to isolate DCs without altering their phenotype. This is one of the reasons that the application of ES in the *in vitro* differentiation of DCs could have a great impact in mucosal and pathogen-host interaction research. Usually DCs are isolated from *ex-vivo* tissue like spleen and blood in a post-mitotic form by flow cytometry or magnetic bead sorting, which can be rather inefficient and expensive when a small number of target cells are present in the sample. For example, myeloid DCs make up less than 1% of the mononuclear cells present in the peripheral blood (van Helden *et al.*, 2008). In addition the life span of such culture is limited since DCs obtained in this way are terminally differentiated and cannot divide. The source of the sample can also have an impact on the quality and the quantity of cells you can obtain from an *ex-vivo* model. Larger numbers of DCs can be obtained from bone marrow stem cells, peripheral blood mononuclear cells or monocytes (Inaba *et al.*, 1992). However, it is not possible to avoid variability in the source cell population and the consequent variability in the resulting DCs. The common downside in research on this type of cell is that transfection and electroporation with recombinant DNA or short hairpin RNAs is generally very ineffective and associated with significant cell death (van Helden *et al.*, 2008).

The results of attempts to *in vitro* differentiate AB2.2 murine ES cells into dendritic cells are reported in this chapter. A protocol published by Dr. Fairchild was employed (Fairchild *et al.*, 2000) for the first time in the laboratory of Professor Gordon Dougan and in other labs at the Sanger Institute. The ES cell derived dendritic cells (esDC) were characterized for surface marker expression by flow cytometric analysis and these were compared to bone marrow derived DCs (BMDC). Primary DCs were obtained as control from the bone marrow of 129/Sv mice. Here, the monocytes present in bone marrow were incubated *in vitro* with IL-4 and GM-CSF cytokines. The subsequent esDCs were further characterized by confocal and electron microscopy. Cytokine secretion was measured and antigen presentation assays were carried out to demonstrate the ability of esDCs to process and expose antigens to naïve T cells. These were successfully accomplished using ovalbumin (OVA) protein presented to T cells responding to species-specific OVA peptide.

5.2 Results

5.2.1 Formation of embryoid bodies and differentiation into dendritic cells

In order to differentiate murine ES cells into DCs, murine ES cells at a very low passage (nine passages) were employed. Early passage cells should guarantee the integrity of their karyotype and retain their full pluripotent ability to generate any kind of somatic cells. ES cells were donated by Professor Allan Bradley's laboratory, which also kindly supplied the irradiated feeder cells to maintain the primary ES cells in an undifferentiated state. Prior to differentiation ES cells were grown in feeder cell-free culture for 2 passages using gelatin treated culture flasks and the medium was enriched with 1000 U/ml of LIF to maintain the undifferentiated state. This procedure eliminated feeder cells that could interfere with the differentiation process and I was thus able to obtain a pure ES cell culture. The ES cells produced through this approach were then trypsinized and 4×10^5 cells per Petri dish were grown in suspension in 20ml of LIF-free medium for 14 days. The cells were not able to adhere to the bacteriological plastic, which had not been treated with extracellular matrix proteins, and the absence of LIF allowed the single cells to replicate and form embryoid bodies (EBs). EBs are three dimensional structures in which the growing cells are differentiating spontaneously into many cell types including myeloid cells. EBs become macroscopic structures in 4-5 days and they can appear as a simple cluster of cells with no polarity or can become cystic, forming a large fluid-filled blister-like structure. Cells within either of those structures should maintain the ability to differentiate into DCs. Figure 5.1 shows an image of a cystic EB.



Figure 5.1 Image of a cystic EB

EBs were obtained from single ES cells growing in suspension in medium free of LIF. These culture conditions potentially permit the growth from a single cell to form a cluster of cells differentiating into any type of precursor cells. EBs can then be used to obtain differentiated cells via specific cytokines that drive the multipotent cells into a specific differentiation pathway.

Fourteen day old EBs were seeded into tissue culture dishes with selective medium containing 25ng/ml of mouse recombinant granulocyte-macrophage colony stimulating factor (GM-CSF) and 200 WHOSU/ml of recombinant IL-3. It is important that the EBs have enough space to adhere, grow and expand to produce DCs. For this reason about 10-15 EBs were seeded per 10cm tissue culture dish. After 48 hours of incubation the majority of EBs adhered to the culture plastic. At this stage many morphologically distinct cell types may be observed. For example, cardiomyocytes are normally easily distinguished. Cardiomyocytes develop spontaneously without the addition of external factors and their appearance is an indication of the ‘good health’ of the culture and their presence indicates that the EBs are following a normal differentiation program. Each culture can have a slightly different differentiation time, but it was possible to observe the first esDCs as early as 5 days after incubation with GM-CSF and IL-3. In these culture conditions differentiated cells with the features expected for DCs could be observed at the edge of an EB (Figure 5.2 panels 1 and 2). After a few more days of growth some esDCs were observed to relocate, forming little clusters of cells that subsequently became foci of replication for esDCs (Figure 5.2 panels 3 and 4). All these data correspond to and confirm the data published by Fairchild (Fairchild *et al.*, 2003), Figure 5.3 represents a schematic diagram of the process.

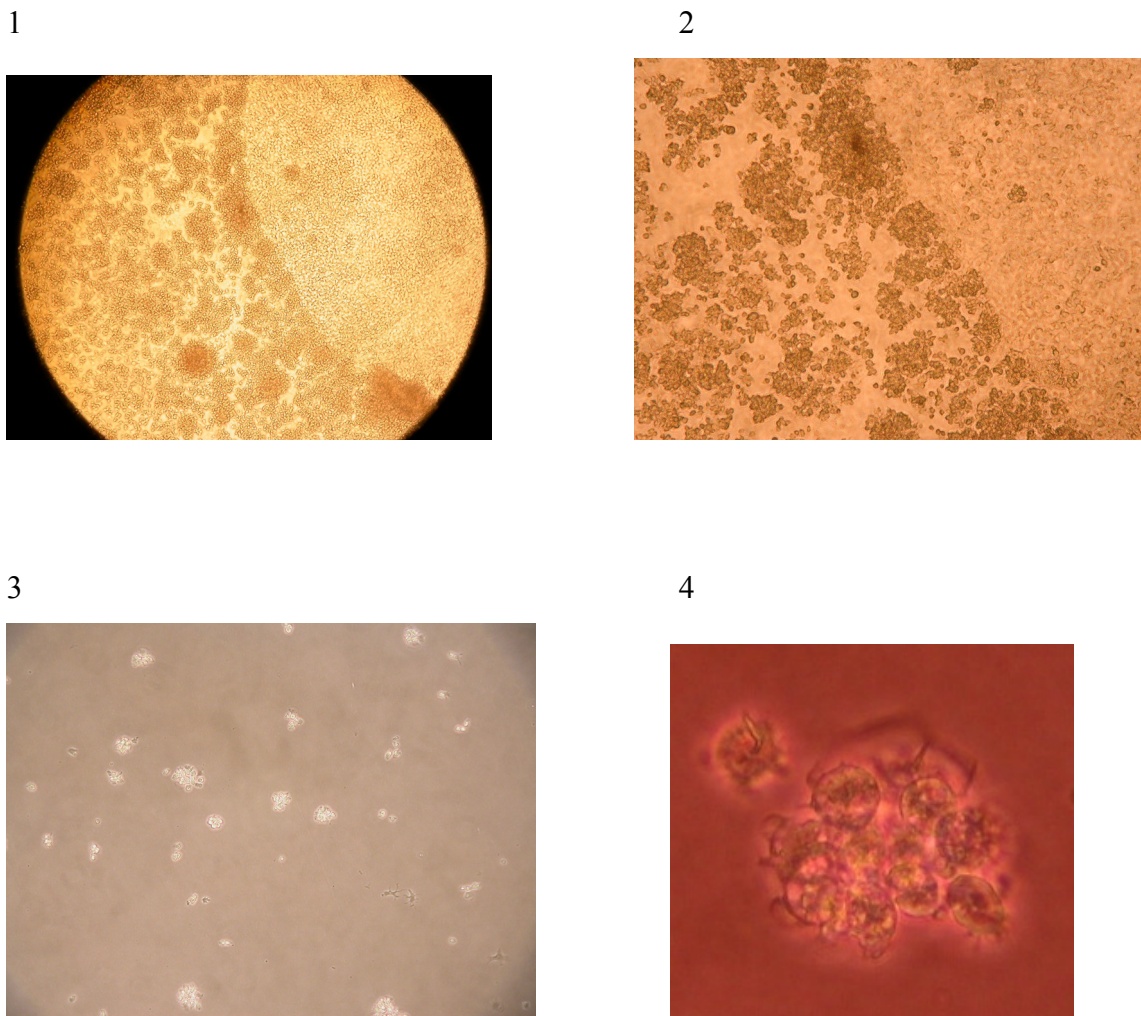


Figure 5.2 Images of esDCs emerging during differentiation from EBs

These optical microscopic images illustrate esDCs differentiating from EBs deriving from AB2.2 murine ES cells. Panel 1 shows the edge of an EB starting to ‘produce’ differentiated esDCs from the periphery. Clear morphological differences can be observed between the two types of cells. Particular features can be observed on panel 2. Panel 3 illustrates clusters of esDCs that are relocated outside the EB site and these will subsequently grow in proliferating foci of esDC. In panel 4 one can observe a cluster with cells bearing little protrusions. These are young esDCs.

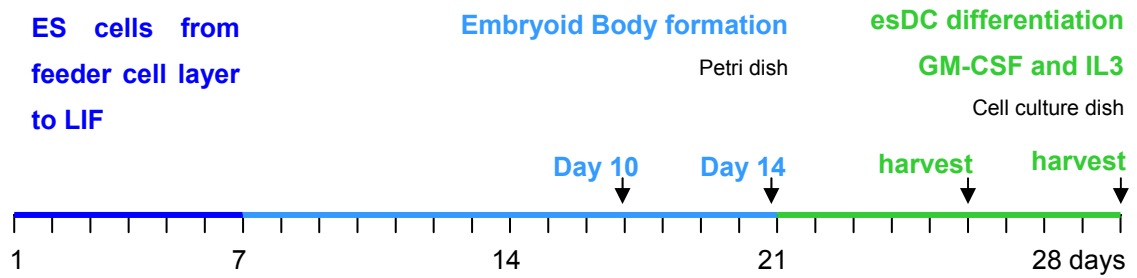


Figure 5.3 Scheme of the differentiation protocol for transforming murine ES cells into esDCs

The process was normally initiated using a new vial of cells each time but in a laboratory where the culturing of ES cells is routine and ongoing the first 7/10 days can be shortened. At the beginning of the project the ability to produce esDCs from EBs at different growth times (10 and 14 days) was investigated. Subsequently, the 14 day time point was favored. The esDCs can be harvested a few times from the same tissue culture dish, but a limiting factor is the culture surface and the ability to detach esDCs without dislocating EBs.

5.2.2 EsDC characterization by flow cytometric analysis

Murine esDCs were monitored for the expression of a number of surface markers characteristic of myeloid cells by flow cytometric analysis. Initially, surface markers similar to those used by Fairchild during the original characterisation of murine esDCs were employed (Fairchild *et al.*, 2003). Coloured beads were used to calculate the compensation parameters for overlapping fluorochrome, and unstained immature or mature cells were employed as negative controls as appropriate. The BMDCs, obtained from the same mouse allotype 129/Sv, were also employed as controls. The initial surface markers investigated included CD11b ($\alpha_M\beta_2$ integrin), also known as complement receptor 3 or CR3, which mediates adhesion to C3bi and ICAM-1 (CD54). CD11b is expressed at different levels on granulocytes, NK cells, macrophages, DCs and B-1 cells. CD11c expression was tested. CD11c it interacts with the integrin α -chain of gp150, which is expressed on DCs and at low levels on macrophages. To detect the expression of MHC class I and class II, anti-mouse H-2K^b and anti-mouse I-A/I-E antibodies were employed respectively. Other markers tested were CD40, normally expressed on APC; CD44, widely expressed on haematopoietic cells and non-haematopoietic cells; CD45, reacting with the leukocyte common antigens (LCA) found on haematopoietic cells; CD54, also known as ICAM-1 a 95-kDa member of the Ig superfamily found on lymphocytes, macrophages and DC; CD80 (B7-1) also a member of the Ig superfamily that along with CD86 participates in the costimulation of T cells, CD80 constitutively expressed on DC, monocytes and peritoneal macrophages; CD86 (B7-2), a costimulatory molecule expressed on a broad spectrum of leukocytes with levels enhanced after antigen co-incubation; F4/80, a marker expressed on a wide range of mature macrophages and on a subpopulation of DC; CD205, also known as the dendritic and epithelial cell 205kDa antigen, which acts as an endocytic receptor expressed at high level on mouse DCs; Ly-6C or Gr-1, a characteristic marker of haematopoietic progenitors and granulocyte differentiation and maturation; DC-SIGN differentially expressed by sub-populations of DC and an antigen that may play a role in T cell-DC interaction. Additionally, TLR4, TLR2, TLR9 and TLR5 receptors were analyzed. This information was derived from the data sheet provided with each antibody.

Initially, the immature DCs were compared with mature DCs that were activated using the non-protein antigen *Salmonella* LPS at 10µg/ml a protein antigen ovalbumin (OVA) at 10µg/ml and TNFα at 5000WHOSU/ml, which are known to be able to activate DCs. LPS is a bacterial product reacting with TLR4 and has been described to activate DCs (Poltorak *et al.*, 1998). OVA is a non-TLR dependent antigen and needs to be actively phagocytosed by the cell and processed through the phagosome vesicle traffic system and then presented on the cell surface on MHC class I and II (Tangri *et al.*, 1998). TNFα is an inflammatory cytokine that strongly promotes the activation and maturation of DCs (Kikuchi *et al.*, 2003). However, TNFα was described to be able to semi-activate DC (Menges *et al.*, 2002). The activation and maturation of DCs is regulated by a variety of extracellular stimuli including cytokines, co-stimulatory molecules and bacterial products. These events induce profound alteration of the morphological, phenotypical and functional properties of DCs. The results from flow cytometric analysis are summarized in Table 5.1. The histograms resulting from these analyses and subsequently used to produce the table are reported in Appendix B.

Table 5.1 Flow cytometric analysis of surface markers of AB2.2 murine ES cells, esDC and BMDC, immature and matured with LPS, OVA and TNF α

This table summarizes the flow cytometric data obtained for surface markers detected on AB2.2 murine ES cells, esDCs and BMDCs either immature or incubated with LPS, OVA or TNF α . +/- indicates ~ 20% of the cells were positive, + indicates that at least 30% of the cells were positive, ++ indicates ~ 60% of the cells were positive, +++ indicates that ~ 90% of the cells were positive for the marker tested. All the cells were detached from the culture plastic using Cell Dissotiation buffer. N/A = not available.

* – indicates no difference with the isotype antibody control; + indicates a shift to the right of the peak specific for the target marker. ** CD44 antibody proved later to have a high background.

Marker	AB2.2*	esDC	esDC LPS 24h	esDC TNF α 24h	esDC OVA 24h	BMDC	BMDC LPS 24h	BMDC TNF α 48h	BMDC OVA 24h
CD11b	-	++	+++	+++	++	++	++	+	++
CD11c	-	++	+++	+++	++	++	++	+	++
CD205	-	+	+	+	-	+	+	+	+/-
CD4	-	+	++	+	N/A	N/A	N/A	N/A	N/A
CD40	+	++	+++	++	+	++	++	+	+
CD44**	-	+++	+++	+++	+++	+++	+++	+++	+++
CD45	-	+++	+++	+++	+++	++	++	++	+++
CD54	+	++	+++	++	++	+	+	++	++
CD8	-	-	-/+	-	N/A	N/A	N/A	N/A	N/A
CD80	-	++	++	++	+++	-/+	+	+	++
CD86	-	-	-/+	-	-	-/+	+	-/+	+
DC-SIGN	+	+	++	+	N/A	+/-	-/+	-/+	-
F4/80	+	+++	+++	+++	+++	+++	+++	++	++
H-2K	-	+	++	+	+/-	++	+	+	+
IA/IE	-	-	-/+	-/+	-/+	+	++	+	++
TLR2	-	++	++	++	N/A	+	+	+	+
TLR4	-	+	++	+	++	+	-/+	+	+/-
TLR5	-	+	+	-/+	+	-/+	-	+/-	-
TLR9	-	+/-	+	-	N/A	N/A	N/A	N/A	N/A
Ly6C	N/A	-	+	N/A	N/A	-	-	-	-

5.2.3 Confocal characterization esDCs

The morphology and appearance of esDCs, immature and mature, was routinely investigated by light microscopy and typical images of these cells are shown in Figure 5.4 and 5.5. EsDCs showed long cellular protrusion, lamellipodia and filopodia as observed before in BMDCs. These cell populations were then further characterized for MHC II expression by fluorescent antibody coupled with confocal microscopy. Such cells were grown on coverslips pre-treated with poly-L-lysine and seeded at 2×10^5 cells per well in 24 well plates. After 24 hours culture they were fixed with 1% paraformaldehyde and stained with rat anti-mouse MHC II antibody and finally mounted on a cover slip holder. Immature esDCs were permeabilised by exposure to saponin buffer in order to stain internal MHC class II (Figure 5.4). Mature esDCs were treated overnight with TNF α or LPS and were stained for surface expression of MHC class II using non-permeabilised cells (Figure 5.5). Mature esDCs clearly change morphology and strongly adhere to plastic. This experiment indicates that these cells may exist as immature and mature forms.

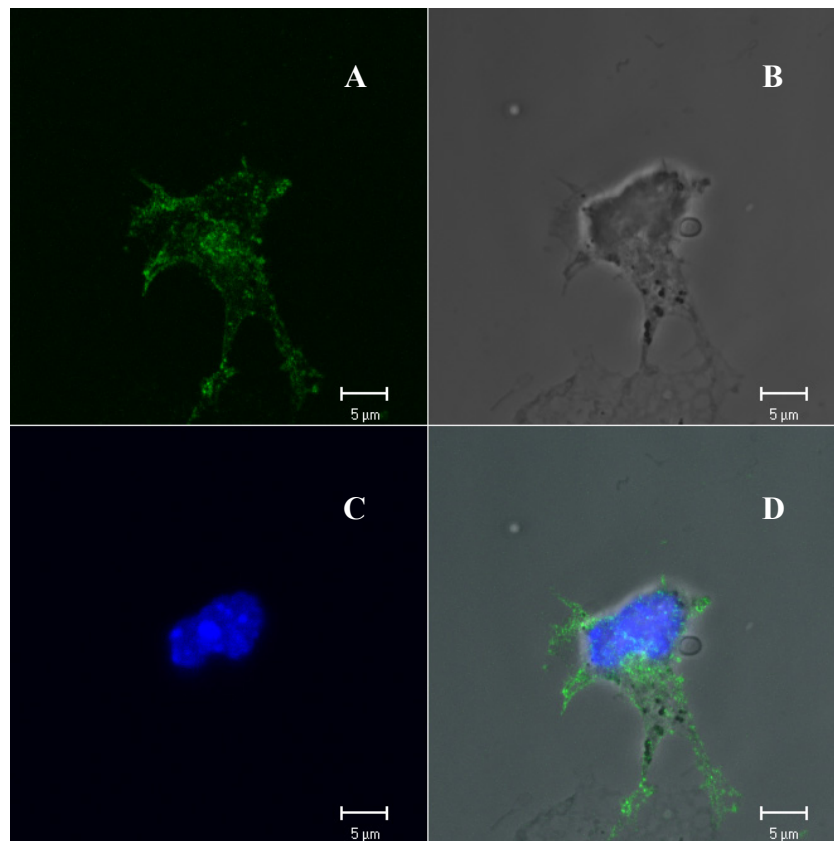


Figure 5.4 Images of immature esDC stained for the expression of MHC class II

EsDCs were seeded on to glass coverslips pre-treated with poly-L-lysine and incubated overnight before being washed, fixed with 1% paraformaldehyde, and permeabilised with saponin buffer and stained with IA-IE (MHC II) FITC conjugated antibody. In this picture we can notice that the cell is semi-adherent to the plastic. Indeed DCs usually strongly adhere to the culture dish once in the mature state. The coverslip was then mounted on a glass slide using ProLong Gold containing DAPI. Panel A shows MHC class II marker (green), panel B reports the phase contrast image of the cells. Panel C reports in blue the DNA stained by DAPI, Panel D shows the combination of the previous panels.

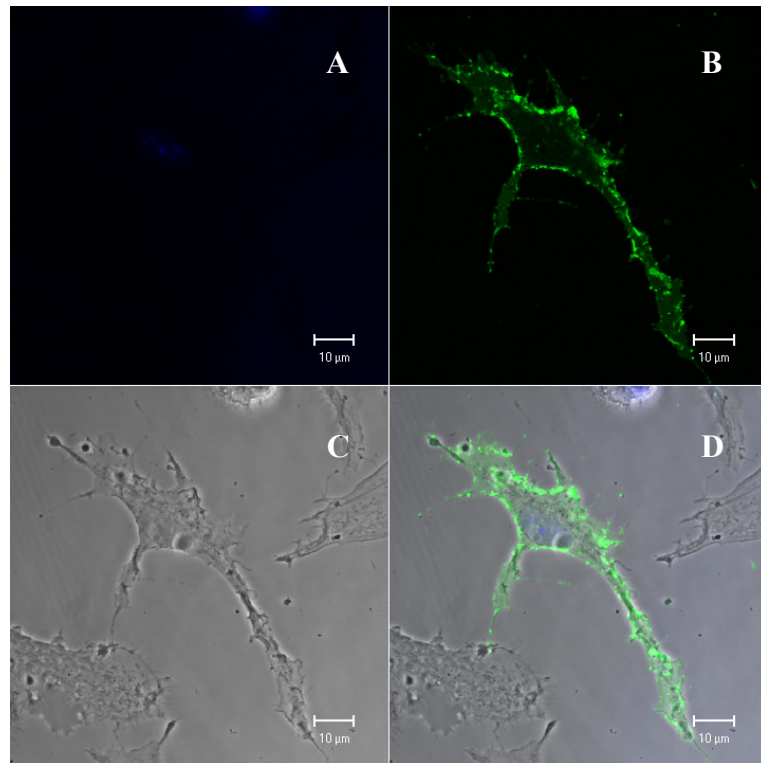


Figure 5.5 Confocal image of murine esDC after over night activation with $\text{TNF}\alpha$ and stained for MHC II

Mouse esDCs were seeded onto a 24 well plate containing a glass cover slip treated with poly-L-lysine and incubated overnight with GM-CFS and IL-3 free medium that contained $\text{TNF}\alpha$. The cells were then fixed and stained for IA-IE (MHC II) marker (green). The cover-slip was then mounted on a glass slide using ProLong Gold containing DAPI (blue) which binds to DNA (panel A). Panel B reports the MHC class II marker (green), panel C reports the phase contrast image of the cells and panel D reports the combination of the previous panels. This is only one example of the images taken of esDC activated either with $\text{TNF}\alpha$ or LPS.

In order to verify if the candidate esDCs possessed the ability to degrade antigens, DQ-OVA was applied. DQ-OVA is a self-quenched conjugated protein that displays green fluorescence upon photolytic degradation. Antigen processing involves protein internalization, denaturation, proteolysis and the resulting peptides are associated with MHC class II to be presented on the cellular surface. Digested fragments of DQ-OVA accumulate in organelles at high enough concentration to be visualized by confocal microscopy (French *et al.*, 1997). This experiment proved that esDCs are able to process OVA, as a control protein antigen. In this experiment esDCs were seeded onto a cover-slip pre-treated with poly-L-Lysine, after overnight incubation, these were incubated for 2 hours with the labelled protein probe and then washed and incubated for 4 hours (after being treated with mitomycin C, which stops cell proliferation) to enable observation of the same cell over a long period of time. The cells were then mounted on a glass slide using ProLong Gold with DAPI to label DNA. Confocal images were taken and examples of these images can be found in Figure 5.6.

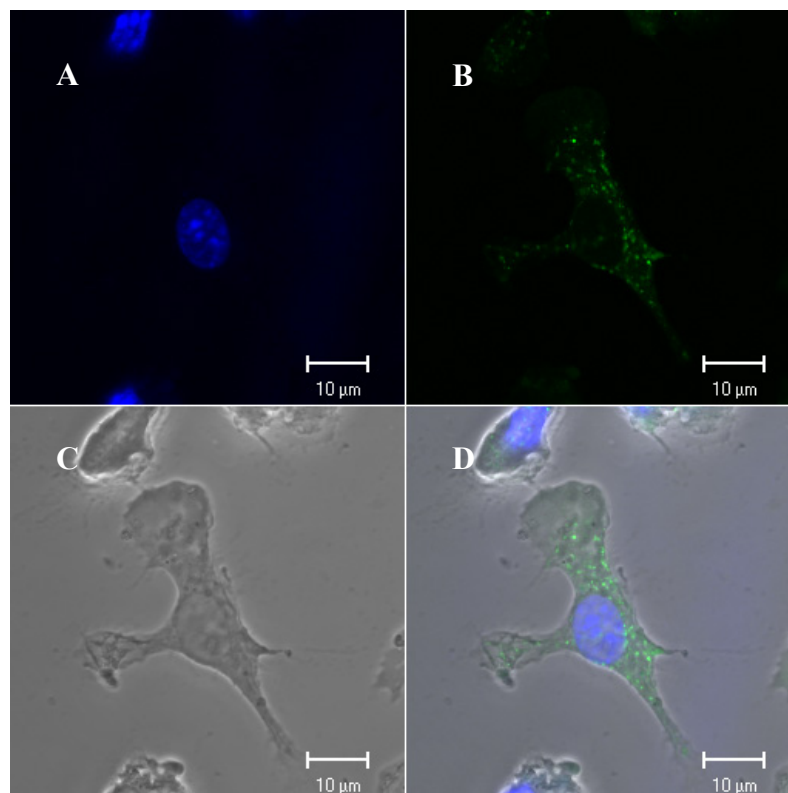


Figure 5.6 Confocal images of esDC incubated with DQ OVA

Confocal images of esDCs processing DQ-OVA. Panel A shows DAPI labeled nuclei; panel B shows processed DQ-OVA (green); panel C shows phase contrast image of the cell. Panel D shows the overlap of all these channels. The processed DQ-OVA can be noticed in green. Note also a large lamellipodium projecting from the cell.

5.2.4 Confocal investigation of esDCs infected with *S. Typhimurium* SL1344

Once a procedure for generating candidate esDCs had been developed the ability of these cells to interact with *S. Typhimurium* SL1344 was investigated. The interaction between esDCs and *S. Typhimurium* SL1344 was initially tracked using confocal imaging, following the initial bacterial contact and aspects of the subsequent internal vesicle trafficking. To this end murine esDCs were grown overnight on glass coverslips pre-treated with poly-L-lysine in medium free of GM-CSF and IL-3 and these were subsequently infected with *S. Typhimurium* SL1344(p1C/1), which expresses GFP. At 30 minutes post infection the esDCs were stained with an EEA-1 marker typically associated with the early endosome. At 3h similar esDCs exposed to *S. Typhimurium* SL1344 (p1C/1) were stained for the late lysosomal membrane glycoproteins (LMG) LAMP-1 and LAMP-2. These experiments were designed to investigate esDC-*Salmonella* interaction, potentially identifying the intracellular compartment occupied by *Salmonella*. Images representing this work can be found in Figure 5.7, 5.8 and 5.9.

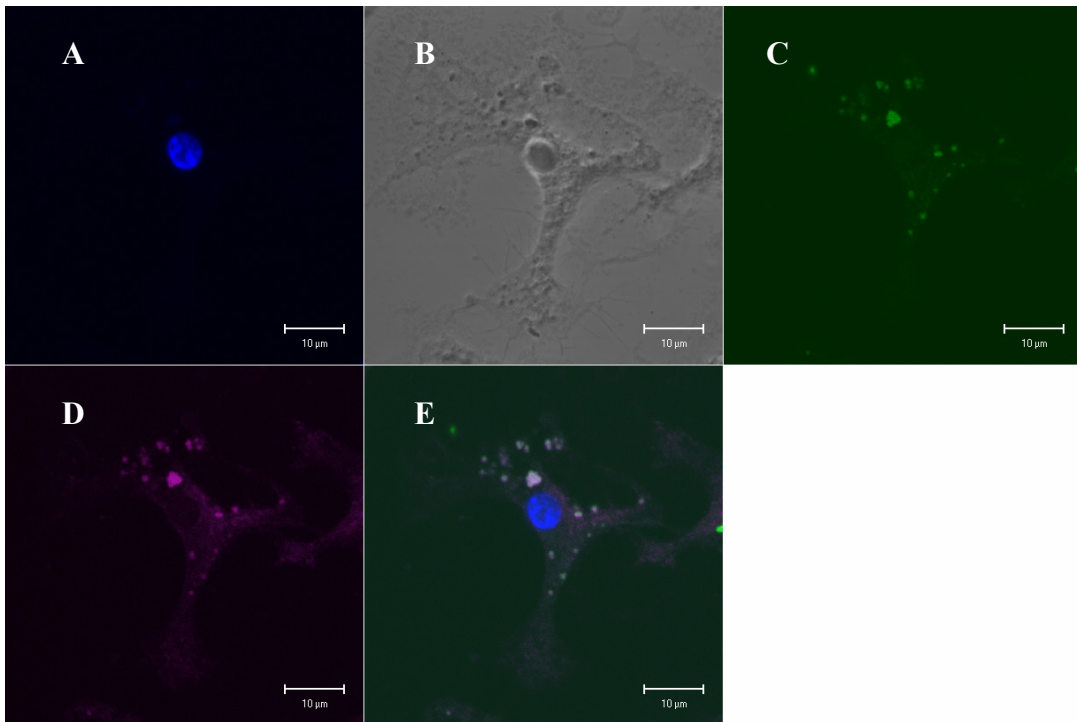


Figure 5.7 Confocal image of esDC infected with *S. Typhimurium* SL1344 (p1C/1)

Images of esDCs infected with *S. Typhimurium* SL1344(p1C/1) expressing GFP at 30 min post infection and stained with an antibody against EEA-1, a specific marker for early endosome revealed with a secondary antibody conjugated to APC Cy-7 fluorochrome. Panel A shows cell nuclei stained with DAPI (blue), panel B shows phase-contrast channel, panel C shows internalized bacteria (green), panel D shows EEA-1 marker (purple), panel E reports the alignment of the previous panels minus the light-contrast channel in order to improve the visualization of the colocalization. The images provide evidence for clear colocalization between the bacteria and the endosomal marker.

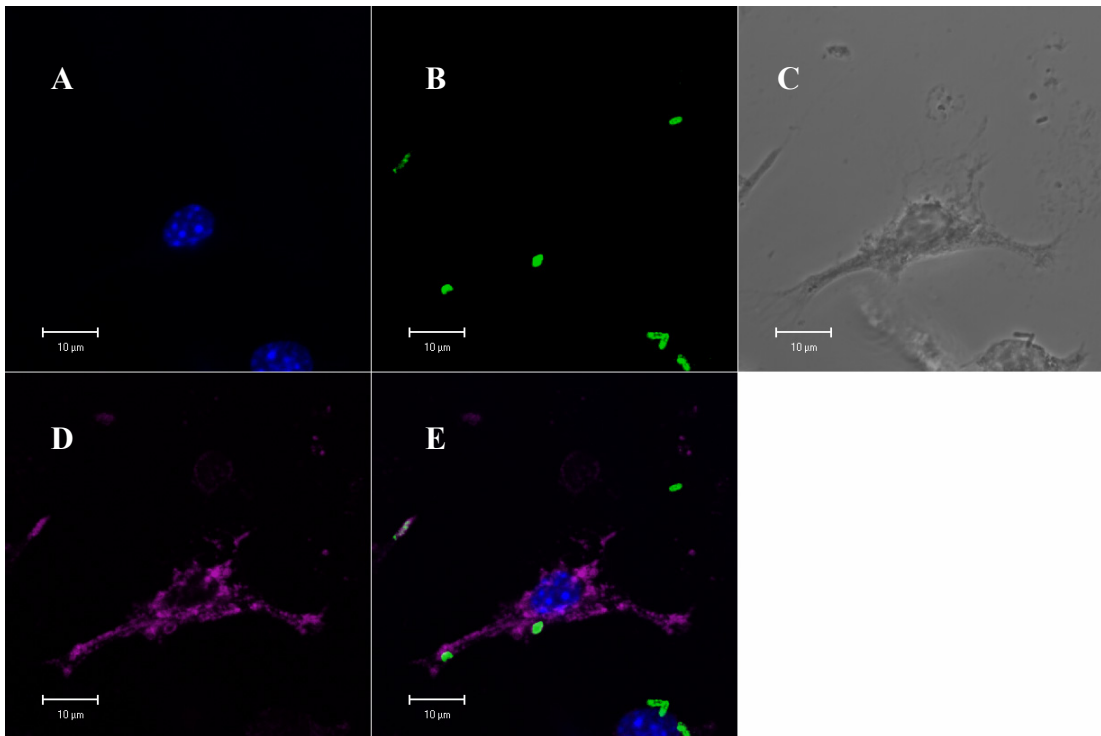
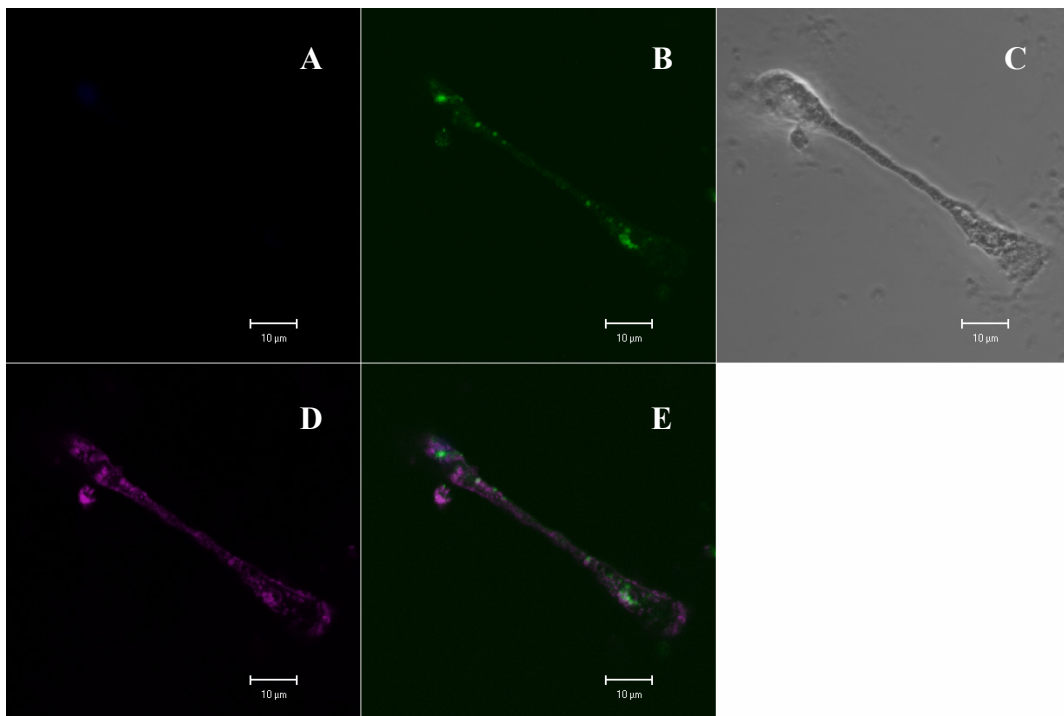


Figure 5.8 Confocal image of esDC incubated for 3h with *S. Typhimurium* SL1344 (p1C/1)

The images show in blue the nuclei stained by DAPI (panel A), green GFP-expressing *S. Typhimurium* SL1344(p1C/1) (panel B) and in purple LAMP-1 (panel D) is highlighted by a secondary antibody conjugated to APC-Cy7. Panel C reports the phase-contrast channel and panel E reports the combination of all the panels minus the light-contrast channel. This images indicates colocalization of the green bacteria and the LGP LAMP-1 at 3h infection time.

Murine esDCs were then examined by confocal microscopy for colocalization of *S. Typhimurium* with lysosome marker LAMP-2 at 3 hours post exposure. The esDCs were infected as described in M&M and fixed with 1% paraformaldehyde on ice for 20 min permeabilised with saponin buffer and stained with the appropriate primary and secondary antibodies. The result can be seen in Figure 5.9.

1



2

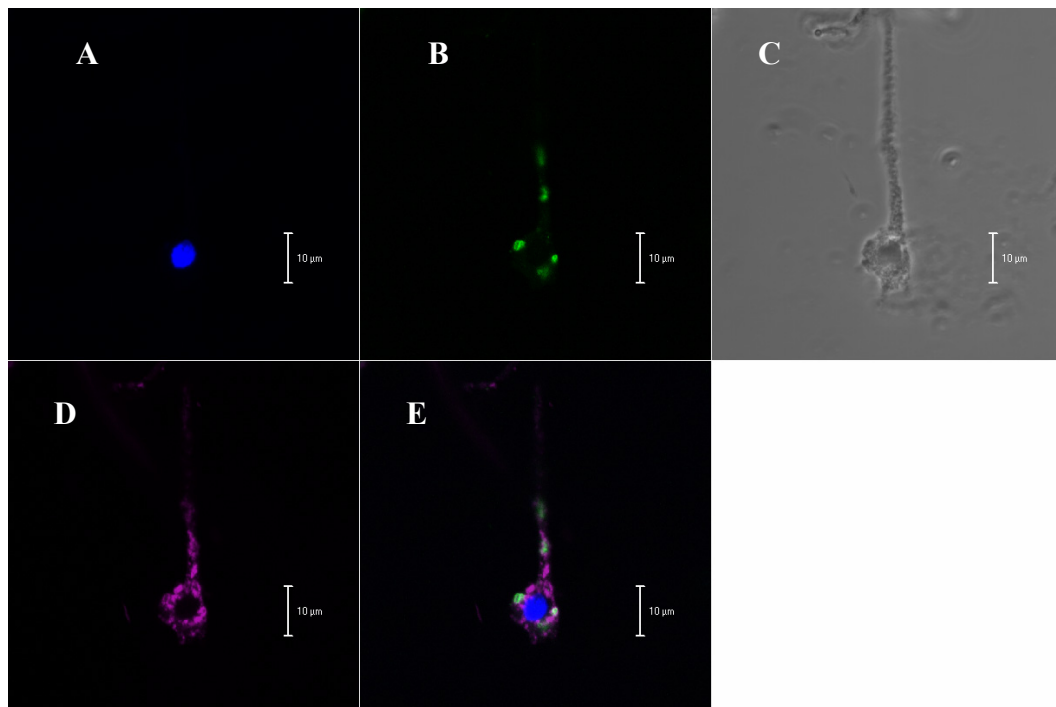


Figure 5.9 Confocal image of esDCs infected with *S. Typhimurium* SL1344 (p1C/1)

These images show esDCs infected with *S. Typhimurium* SL1344 (p1C/1) expressing GFP (green) panel B, at 3h post infection stained with an antibody against the LAMP-2 marker specific for late lysosomes and revealed by a secondary antibody conjugated with APC-Cy7 (purple), panel D. In blue are reported the nuclei labeled with DAPI, panel A. The phase-contrast channel images are reported in panel C. Panel E report the overlapping of all the channels for each image minus the light-contrast to simplify the

observation of colocalization. Here there is evidence for both colocalization and non-colocalization suggesting not all endosomes are fused to lysosomes. These observations agree with the contemporary literature on the interaction of terminally differentiated DCs with *S. Typhimurium*, where researchers have conflicting opinions. See Discussion.

5.2.5 Electron microscopy characterization of esDCs

Murine esDCs were investigated for morphology changes and general integrity using electron microscopy. These images were taken using AB2.2 ES cells and derived esDCs with the help of Dave Goulding, the electron microscope officer at the WTSI (Figure 5.10). The EM observations highlighted the differences in morphology between the original murine ES cells and the derived esDC, in particular the presence of membrane protrusion, ER expansion and the higher number of mitochondria in esDC. These traits are characteristic of antigen presenting cells, whereas ES cells are characterized by a large nuclei and small cytosol content (Figure 5.10, image 1). Murine AB2.2 ES and esDCs were observed using transmission electron microscopy at 1 hour post exposure to *S. Typhimurium* SL1344. In both cell types the *Salmonella* associated vacuole can be seen in some cases adjacent to or fused with lysosomal vacuoles (Figure 5.10, black arrows).

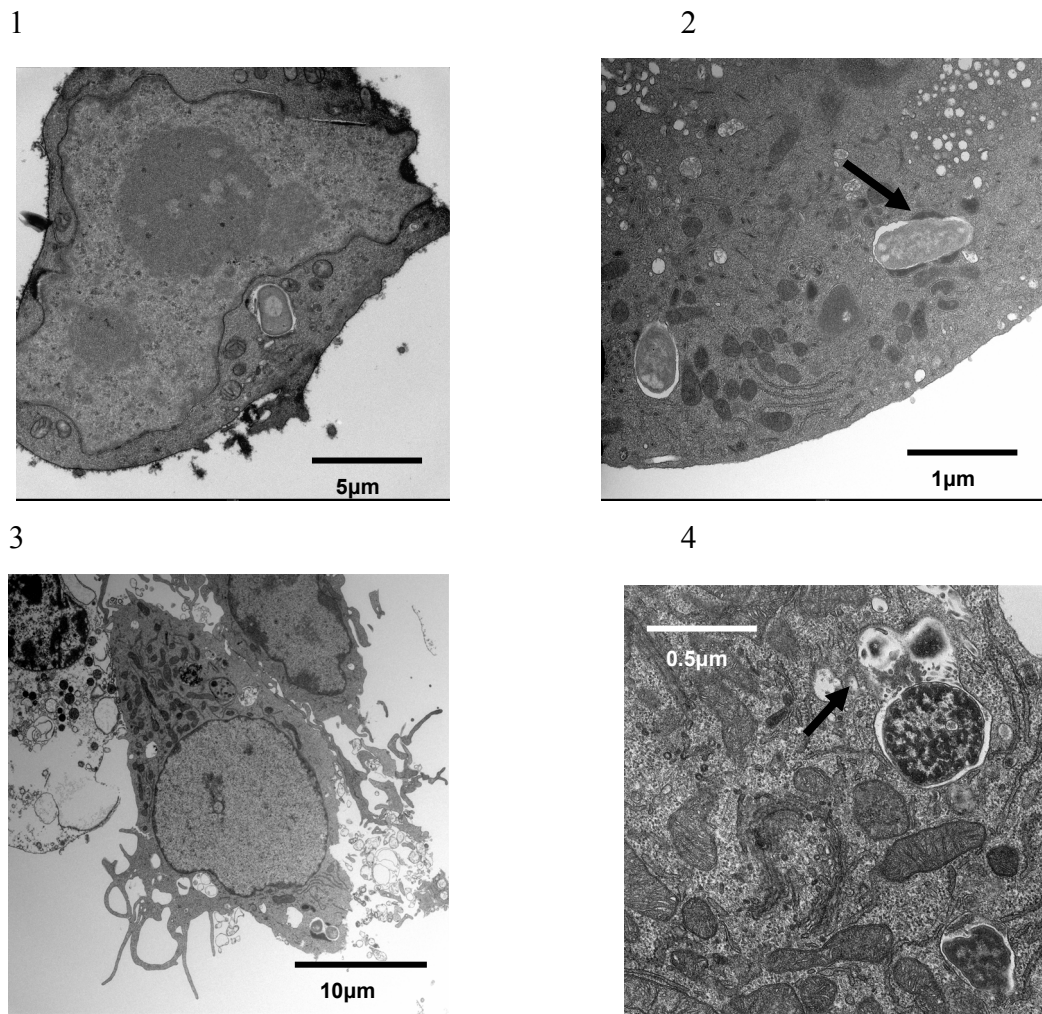


Figure 5.10 Transmission electron microscopic images of undifferentiated murine ES cells AB2.2 and derived esDC during infection with *S. Typhimurium* SL1344

Panel 1 shows a whole AB2.2 murine ES cells infected by *S. Typhimurium* SL1344. Panel 2 *S. Typhimurium* SL1344 bacteria can be seen inside the SCV apparently under attack by lysosomes. Panels 3 and 4 show the morphology of a whole esDC and a *S. Typhimurium* bacterium inside the cell. The black arrows indicate potential lysosomal vacuole fusion with the SCV.

5.2.6 Functional assays on esDCs

5.2.6.1 Cytokine production by esDCs

In order to investigate the functional activity of esDCs, the expression of cytokines was measured using a Cytometric Bead Array (CBA) assay from Becton Dickinson Biosciences as described in M&M. A standard kit, normally used for mouse inflammation analysis monitored the production of Interferon γ (IFN γ), Interleukin-10 (IL-10), Interleukin-12p70 (IL-12p70), Interleukin-6 (IL-6), Monocyte Chemo-attractant Protein-1 (MCP-1) and TNF. Experiments monitored potential cytokine expression during *S. Typhimurium* SL1344 invasion of murine AB2.2 ES cells and derived esDCs. The results are shown in Table 5.2. Cytokine production after incubation of esDCs with LPS, OVA or TNF α was also assessed (Table 5.3).

Table 5.2 The levels in pg/ml of cytokines produced by AB2.2 murine ES cells and esDCs infected and uninfected with *S. Typhimurium* SL1344.

The amount of cytokine produced by AB2.2 murine ES cells and esDC alone or during infection with *S. Typhimurium* are reported in pg/ml. Each value represents the mean of at least two measurements \pm 1 SD. The detection limits of the assay are 2.5pg/ml for IFN γ , 17.5pg/ml for IL-10, 10.7 pg/ml for IL-12p70, 5pg/ml for IL-6, 52.5pg/ml for MCP-1 and 7.3pg/ml for TNF. ND = Not determined (below the detection limit).

Cytokines pg/ml	AB2.2 no bacteria	AB2.2 with SL1344 30minutes	AB2.2 with SL1344 2hours	AB2.2 with SL1344 4hours	esDC no bacteria	esDC with SL1344 30minutes	esDC with SL1344 2hours	esDC with SL1344 4hours
IFN γ	ND	ND	ND	ND	ND	ND	ND	ND
IL-10	ND	ND	ND	ND	ND	ND	33 \pm 21	56 \pm 35
IL-12p70	ND	ND	ND	ND	ND	ND	ND	ND
IL-6	ND	ND	ND	ND	ND	5.5 \pm 1.4	30.5 \pm 0.7	400.5 \pm 108
MCP	ND	ND	ND	ND	108 \pm 117	138 \pm 80	181 \pm 54	339 \pm 0
TNF	ND	ND	ND	ND	26 \pm 24	134.5 \pm 67	1673 \pm 287	3538 \pm 1254

Table 5.3 Cytokine production by esDCs and BMDCs activated with *S. Typhimurium* LPS 10µg/ml, OVA protein 10µg/ml or TNFα 5000 WHOSU/ml

The DCs were seeded in 96 well plates at 1×10^5 cells per well and incubated overnight with LPS, OVA or TNFα. The supernatants were collected and frozen at -20°C until analyzed by CBA. EsDC and BMDC were each maintained in their own medium. Results obtained with TNFα are not reported in this table. (See below). The detection limits of the assay are 5pg/ml for IL-6, 17.5pg/ml for IL-10, 52.5pg/ml for MCP-1, 2.5pg/ml for IFNγ, 7.3pg/ml for TNFα and 10.7 pg/ml for IL-12p70. ND = Not determined (below the detection limit).

Cytokine pg/ml	esDCs alone	esDC with OVA 24h	esDC with LPS 24h	BMDC alone	BMDC with OVA 24h	BMDC with LPS 24h
IFNγ	ND	ND	ND	ND	ND	35
IL-10	ND	ND	575	ND	ND	ND
IL-12p70	ND	ND	ND	ND	ND	215
IL-6	15	643	13262	ND	166	10541
MCP	3607	6205	9709	102	175	1162
TNF	545	1356	6005	53	212	7068

Table 5.4 Cytokine production by esDCs and BMDCs during antigen presentation assay

The same supernatants derived from the antigen presentation assay tested for IL-2 concentration (Table 5.5) were also tested for cytokine production. The detection limits of the assay are 5pg/ml for IL-6, 17.5pg/ml for IL-10, 52.5pg/ml for MCP-1, 2.5pg/ml for IFNγ, 7.3pg/ml for TNFα and 10.7 pg/ml for IL-12p70. ND = Not determined (below the detection limit).

Cytokine pg/ml	BMDC	BMDC with T cells	BMDC with T cells and OVA 24h	BMDC with T cells and OVA 48h	BMDC with T cells and TNFα 24h	BMDC with T cells and TNFα 48h	T cells with ConA
IFNγ	ND	ND	ND	ND	ND	ND	ND
IL-10	ND	ND	ND	ND	20	23	97
IL-12p70	ND	ND	ND	ND	ND	ND	ND
IL-6	98	42	1243	1927	206	167	ND
MCP	1558	1745	2176	2490	2525	1909	ND
TNF	1973	892	3794	3875	9839	8805	145
Cytokine pg/ml	esDC	esDC with T cells	esDC with T cells and OVA 24h	esDC with T cells and OVA 48h	esDC with T cells and TNFα 24h	esDC with T cells and TNFα 48h	T cells with ConA
IFNγ	ND	ND	ND	ND	ND	ND	ND
IL-10	ND	21	ND	ND	ND	ND	62
IL-12p70	ND	ND	ND	ND	ND	ND	ND
IL-6	17	9	218	156	29	18	ND
MCP	1339	1638	4009	1834	1825	862	ND
TNF	1264	348	1099	776	6621	5220	147

5.2.6.2 Antigen presentation assay

In order to test the ability of esDC to process and present antigens to the allogenic T cell line MF2.2d9, antigen presentation assays were performed and IL-2 production measured with a CBA kit as described in M&M. The same supernatants were also used in standard CBA assays to measure IFN γ , IL-10, IL-12p70, IL-6, MCP and TNF concentrations (Table 5.4). The IL-2 concentrations reported here is an example from a typical assay. The two types of dendritic cells were treated on the same day and the same T cell stock was applied. The data can be found in Table 5.5

Table 5.5 IL-2 production by T cells activated during antigen presentation assays involving BMDCs and esDCs

The MF2.2d9 T cells were incubated for 24 and 48h with 12 day old BMDCs and 14 day old esDCs at a 1:5 ratio with OVA 10 μ g/ml. TNF α 5000 WHOSU/ml was also included in this assay as negative control. The culture supernatant was collected and the concentration of IL-2 was tested using a CBA Flex Set from BD Biosciences. ND = Not determined (below the detection limit of 2pg/ml).

Sample	BMDC	BMDC with T cells	BMDC with T cells and OVA 24h	BMDC with T cells and OVA 48h	BMDC with T cells and TNF 24h	BMDC with T cells and TNF 48h	T cells with ConA in IMDM
IL-2 pg/ml	ND	11	77	85	3	5	147
Sample	esDC	esDC with T cells	esDC with T cells and OVA 24h	esDC with T cells and OVA 48h	esDC with T cells and TNF α 24h	esDC with T cells and TNF α 48h	T cells with ConA in DMEM
IL-2 pg/ml	ND	3	43	47	5	8	101

5.3 Discussion

This chapter reports a summary of the results of investigations on the properties of murine AB2.2 ES cells differentiated *in vitro* into APCs which resemble DCs (esDCs). To this end a version of the protocol published by Dr. Fairchild from the Sir William Dunn School of Pathology, Oxford (Fairchild *et al.*, 2000; Fairchild *et al.*, 2003) was exploited. In 2003 a second group reported the differentiation of DCs from mouse ES cells using embryoid body formation and co-culture with an OP9 feeder cell layer (Senju *et al.*, 2003). The authors of these papers recognized the potential importance of these *in vitro* methods combined with the ability of ES cells to be genetically engineered. Indeed, an ever increasing number of different gene-trap ES libraries are already available [www.genetrap.org].

DCs are the most potent APCs present in the body and they are considered to be the connection between the innate and the adaptive immune responses. In fact DCs are the cells responsible for the priming of naïve T cells in an antigen-specific manner. Immature DCs exhibit endocytic activity that occurs via several pathways: fluid phase pinocytosis, including macropinocytosis; receptor-mediated uptake via Fc receptors and the action of lectin receptors, such as the macrophage mannose receptor (MMR). In addition DCs are able to phagocytose microbes and dying cells. The capacity of DCs to process dying cells has drawn enormous attention since it may lie at the heart of many challenging problems in medicine including transplant rejection, self-tolerance, immunity to viral and bacteria-infected cells and tumor immunity. This highlights the importance of these cells in the body homeostasis.

Flow cytometry results

EsDC were initially characterized for their surface marker expression by flow cytometric assays. They were compared to undifferentiated ES cells and BMDCs. Undifferentiated ES cells do not express markers normally distinctly described as specific immune cell markers but they do express significant levels of cytokines (Guo *et al.*, 2006). Examples of markers specific for leukocyte cells and a few specific for DCs include CD11b, CD11c, H-2K, I-A/I-E, CD40, CD44, CD45, CD54, CD80, CD86, DC-SIGN, Ly-6C and CD-205. The expression of these markers by murine AB2.2 ES cells,

BMDCs and esDCs in the immature state and in the mature state obtained following treatment with LPS, OVA protein or TNF α was assessed. As expected the murine AB2.2 ES cells did not express the majority of these markers. However, after growth under the conditions reported here they expressed detectable levels of CD40, CD54, and F4/80 markers in addition to DC-SIGN (Table 5.1). These results do not match with previously published information on ES cells. However, it is known that ES cells do not produce detectable amounts of MHC class II and only a small amount of MHC class I (Magliocca *et al.*, 2006; Menendez *et al.*, 2005); consistent with the results reported. Reports indicate that ES cells should not normally produce CD40, B7-1 and B7-2 (Tartour & Kadereit, 2006). However some of these markers have been reported on myeloid progenitor cells (Odegaard *et al.*, 2007). Also, this may mean that the Sv/129 ES cells described here have the right qualities to differentiate into leukocytes. Murine AB2.2 ES cells were first maintained on a feeder cells layer before being cultured for two passages on medium containing LIF in order to obtain a pure culture. Subsequently, the cells were cultured in suspension on a bacteriological Petri dish with medium free of LIF in order to produce EBs. Fourteen day old EBs were then seeded onto a culture dish with medium containing GM-CSF and IL-3 and esDCs were harvested in the following 7 to 30 days. The esDC so obtained were theoretically in the immature state..

During maturation experiments esDCs were exposed overnight to *S. Typhimurium* LPS at 10 μ g/ml and an increase in the expression of CD11b, CD11c, CD4, CD40, CD54, CD8, CD80 and 86, DC-SIGN, H-2K, TLR2 and TLR4 was detected by flow cytometric analysis (Table 5.1). After overnight incubation with TNF α esDCs displayed enhanced the expression of CD11b, CD11c and IA-IE, whereas after incubation with OVA protein, esDCs showed an increased expression of the markers CD80 and TLR4. All together a stronger enhanced expression of activated markers was observed after overnight incubation with *S. Typhimurium* LPS. However BMDCs showed even stronger expression of activation markers. All the DC lines were positive for a DC selectively expressed lectin called DC-specific intercellular adhesion molecule 3-grabbing non-integrin (DC-SIGN), which binds to the intracellular adhesion molecule (ICAM)-3 on resting T cells and enhances the DC-T cell interaction. This indicated that esDCs could harbour the potential to initiate specific immune responses from resting T cells (Soilleux, 2003).

Microscopic observations

The expression of MHC class II was not clearly demonstrated by flow cytometric analysis. It is possible that the FITC fluorochrome chosen to reveal this marker was too weak to assess its expression. Consequently, confocal examination of the expression of MHC class II molecules by esDCs was carried out. Observations at the confocal microscope reported in Figures 5.4 and 5.5 confirm that some candidate esDCs expressed detectable MHC class II markers but other cells did not, so a non-uniformity in the maturation of esDC can be seen although all the cells show the characteristic morphology of DCs. The ability of esDCs to process DQ-OVA was also investigated by confocal microscopy (Figure 5.6). It was possible to observe that all the cells contained green-OVA at 4 hours incubation. Unfortunately, a clear observation of the antigen presentation on the cell surface at 24 hours post incubation was not possible since it was impossible to distinguish between the internal OVA and the surface OVA. It is also likely that only an accumulation of DQ-OVA can be detected, like in lysosome compartments, but the surface exposure of processed peptides cannot.

A number of reports have indicated that *S. Typhimurium* is unable to replicate efficiently inside DCs (Jones & Falkow, 1996; Niedergang *et al.*, 2000). This may be a deliberate act by the bacteria that is possibly connected to the ability of *S. Typhimurium* to avoid the MHC class I and II compartments in order to survive inside the host cell. Indeed it is recognized that the TIISS harbored by SPI-2 alters lysosome trafficking in order to avoid phagosome-lysosome fusion (Abrahams & Hensel, 2006; Uchiya *et al.*, 1999).

Interestingly, there is an on going debate in the scientific community regarding whether *S. Typhimurium* colocalizes inside DCs with LAMP-1 and LAMP-2 lysosomes markers. Garcia-Del Portillo and coworkers reported only 5% of the internalized bacteria were colocalized with the lysosomal membrane glycoprotein (LPGs) LAMP-1, and no colocalization was detected with other LGP markers such as LAMP-2 during infection of murine splenic DC line CB1 (Garcia-Del Portillo *et al.*, 2000). However other researchers reported strong evidence of the colocalization of wild type *S. Typhimurium* with the LAMP-1 marker 90 min after infection and clear colocalization with MHC class II (Jantsch *et al.*, 2003; Petrovska *et al.*, 2004). In this study, colocalization was detected between *S. Typhimurium* and the early endosome marker

EEA-1 and with LAMP-1 in esDCs (Figure 5.7 and 5.8). However, confocal observation detected both colocalization and non-colocalization with LAMP-2 marker in this study, suggesting there may be a mixed pattern within cells (Figure 5.9.). This confirms the need to further investigate the vesicular pathway used by *S. Typhimurium* inside DCs.

In this chapter electron microscopic investigations were also described to confirm the difference in morphology between the original murine AB2.2 ES cells and the derived esDCs. Expanded ER and Golgi apparatus and increased number of mitochondria were consistently observed in esDCs. Also numerous lysosomes vacuoles were detected. Moreover, the multi-laminar structures, typical of 'empty' MHC class II compartment, or *Salmonella* containing vacuoles were also identified lately. The latter structures, SCV with multilaminar membrane, were previously observed in only 5% of the SCV containing wild-type *Salmonella*, after 20h of infection (Garcia-Del Portillo *et al.*, 2000).

Functional assay results

Finally, esDCs were further analyzed using functional immune assays. The ability of esDCs to produce cytokines during *S. Typhimurium* infection was measured by CBA assays and their level of secretion was compared to the production of cytokine by the original murine AB2.2 ES cells. The production of cytokine by murine ES cells is not surprising and in fact it had been described previously that ES cells are regulated by cytokines (Kristensen *et al.*, 2005). Murine ES cells were described to produce, in the presence of LIF, cytokine including IL-10, MCP-1 and TNF α (Guo *et al.*, 2006) but in the present study they were all below detection limits. Immature DCs usually do not produce high levels of cytokine (Lutz & Schuler, 2002). In this study esDC supernatant was tested after 24 hours incubation for cytokine content and revealed the production of IL-6 and MCP-1. The other cytokine levels were below detection limits (Table 5.2).

Maturation of DCs is a process that involves the down-regulation of the antigen capturing capacity and up-regulation of MHC molecule synthesis and enhancement of the intracellular trafficking (Wick, 2002). In order to prove that esDCs are real functioning APCs, their ability to process protein antigen and activate T cells was tested together with cytokine production. The cytokines TNF, IL-12p70 and IFN γ were

measured since they play an important role in the survival of the host during *Salmonella* infection (Mittrucker & Kaufmann, 2000), and the ability of DCs to produce these cytokines upon encountering this bacteria has been demonstrated. Most reports describe the production of IL12-p40 and little production of the bioactive form IL12-p70 (Svensson *et al.*, 2000; Yrlid & Wick, 2002). One hypothesis to justify this observation could be the lack of accessory signals or cytokines from the surroundings to sustain and enhance the DC response (Niedergang *et al.*, 2000; Schulz *et al.*, 2000). Also, IFN γ secretion by infected and mature DCs was investigated. IFN γ is a cytokine important in controlling many bacterial infections. The capacity of DCs to produce IFN γ is controlled and dependent on IL-12 production (Fukao *et al.*, 2000; Hochrein *et al.*, 2001; Stober *et al.*, 2001). In this study, the production of IL-12p70 by esDCs was not observed during bacterial infection or after overnight incubation with LPS, OVA or TNF α . However, a substantial production of IL-12p70 was observed for BMDCs coincubated with *S. Typhimurium* LPS. The same sample contained a significant concentration of IFN γ , confirming the literature cited (Table 5.3).

The level of IL-10 production was also investigated. IL-10 is an anti-inflammatory cytokine involved in the immune response to bacteria, down regulating the inflammation stimulus that can damage the tissues and help infection spread. Although previous studies reported that DCs can prime T cells to produce IL-10, the production of IL-10 by DCs infected by *S. Typhimurium* is not always detected (Marriott *et al.*, 1999). EsDCs produced detectable amounts of IL-10 during infection with *S. Typhimurium* at 2 hours and 4 hours (Table 5.2) incubation time and after overnight incubation with LPS (Table 5.3), whereas it was not possible to detect significant amount of IL-10 produced by BMDCs (Table 5.3). It should be noted that the production of even low amounts of IL-10 can reduce remarkably the release of IL-12p40 (Siegemund *et al.*, 2007), which could explain the lack of IL-12 production in the experiments here reported.

Additionally in this study the pro-inflammatory cytokines IL-6 and TNF were investigated. The data here reported revealed that esDCs and BMDCs produce IL-6 in the presence of *S. Typhimurium*, after activation with *Salmonella* LPS and OVA (probably due to LPS contamination) (Table 5.3) and after incubation with TNF α (Table 5.4). The production of IL-6 during the *in vitro* infection of DCs was previously observed (Marriott *et al.*, 1999). Also the production of TNF α was detected during

esDCs and BMDCs infection with *S. Typhimurium* (Table 5.2) and during activation with LPS or OVA (Table 5.3). The production of TNF α by DCs during infection with *Salmonella* and incubation with LPS was described previously (Siegemund *et al.*, 2007). These cytokines have been reported to be important for DC maturation (Park *et al.*, 2004; Sundquist & Wick, 2005).

DCs can produce MCP-1 of which secretion is TLR mediated. This cytokine was produced by esDCs infected with *S. Typhimurium* SL1344 (Table 5.2) and BMDCs incubated with *Salmonella* LPS (Table 5.3). The production of MCP-1 probably is related to the binding of TLR ligands, one of which is LPS, and this is a MyD88 dependent process. Also the contribution of MAPK and NF- κ B signaling to TLR-mediated MCP-1 secretion was reported previously. Moreover, using IFN $\alpha\beta$ R $^{-/-}$ knock-out mice it was observed that MCP-1 expression by TLR is dependent on the production of type-I interferon, in our assay we tested for type-II IFN, γ (Vivekanandhana & Klinmana, 2007). This may be the reason why IFN γ wasn't detected in the experiments here reported. Moreover the production of MCP-1 by esDCs thought to be in the immature state may be a sign that these DCs are really in the mature state (Table 5.2).

Perhaps the critical data presented here is that esDCs were able to process the protein antigen OVA, express the peptide antigen on their surface and activate T cells CD4 $^{+}$ to produce IL-2 (Table 5.5). This activation also absolutely requires the co-expression of co-stimulatory signals like CD80 and CD86 by the same APC (Greenwald *et al.*, 2005). This is the best proof that esDCs are real APC.

In conclusion, this chapter described the differentiation and characterization of APC deriving from *in vitro* differentiation of murine ES cells. In the next chapter these cells will be investigated during *S. Typhimurium* infection, applying microarray technology to investigate their biological response to bacterial infection. This technique might help also to clarify the doubts about the real nature of esDCs.

6 Messenger RNA expression profile analysis of *S. Typhimurium* infected esDCs

6.1 Introduction

6.1.1 *Salmonella*-DC interactions

S. Typhimurium is a food-borne pathogen that causes gastroenteritis in humans. After the bacteria have survived the acidic milieu of the stomach, they compete with the intestinal flora, cross the intestinal mucus layer and contact the gut epithelium cells, eventually penetrating the intestinal mucosa (Giannella *et al.*, 1972). It is believed that *Salmonella* preferentially invade the gut epithelium through M cells, which are specialized cells that lack the overlying mucus glycocalyx, making them more readily accessible to penetration by intestinal microbes (Gebert, 1997; Jepson & Clark, 2001; Neutra *et al.*, 2001). The underlying lamina propria is rich in DCs and macrophages poised to initiate and activate the immune response to pathogens. In this location, DCs can also inadvertently play an active role in facilitating the penetration of pathogenic bacteria through the gut epithelium barrier (Chieppa *et al.*, 2006; Rescigno *et al.*, 2001; Vallon-Eberhard *et al.*, 2006). DCs can extend cellular protrusion between epithelium cells and sample the lumen content, a process known as diapodosis. DCs express tight junction proteins that are able to open the tight junctions present between epithelial cells and sample the gut lumen while still preserving the integrity of the epithelial barrier. The DCs' ability to take up antigens, process and present them to naïve T cells on MHC molecules makes them indispensable for raising a specific and efficient immune response to invading pathogens.

DCs are key immune cells that are able to move around within the body and locate themselves in strategic sites anywhere pathogens are likely to attack the body, such as in the intestine. In the gut, DCs can be found in the lamina propria, in Peyer's patches, in the subepithelial dome, and beneath the follicle epithelium. *Salmonella* can be internalized by DCs resident in the subepithelial dome of Peyer's patches (Hopkins *et al.*, 2000) and infected DCs can serve as an alternative invasion route contributing to the

spread of bacteria inside the host (Cheminay *et al.*, 2002). Invading *Salmonella* are able to survive inside DCs without replicating, suggesting that this persistence is potentially the foundation of the development of the adaptative immune response to live *Salmonella*. This process could partially explain the systemic proliferation of bacteria even after a long period after infection and might be a requirement for the development of the carrier state. The persistence of *Salmonella* inside DCs appears to be associated with the ability of the bacteria to interfere with the MHC class II dependent antigen presentation through the activity of the SPI-2 system (Cheminay *et al.*, 2002; Jantsch *et al.*, 2003). The TIISS encoded on SPI-2 can interfere with lysosomal fusion with the SCV (Uchiya *et al.*, 1999) and can promote the formation of the F-actin filament network around the SCV which is necessary for bacterial survival inside the vacuole (Meresse *et al.*, 2001).

The interaction between *S. Typhimurium* and DC has been the subject of a good deal of research since the first DCs were discovered in 1973. The importance of understanding the *Salmonella* interactions with the host may help to develop new more effective vaccines. Due to the emergence of multi-drug resistant strains (Cooke & Wain, 2006; Mirza *et al.*, 1996), *Salmonella* infections are occurring more frequently and are more difficult to cure.

6.1.2 Microarray analysis on DCs

Dendritic cells are versatile cells involved in the initiation of both innate and adaptive immunity. They are involved in the differentiation of regulatory T reg cells required for the preservation of self-tolerance. The plasticity of these cells has fascinated researchers for years and now it is possible to investigate aspects of the complete genetic reprogramming that these cells undergo in response to external stimuli using a microarray platform (Foti *et al.*, 2007). DCs can be stimulated to different degrees by various impulses and consequently it is possible to distinguish semi-mature DCs and fully-mature DCs. The semi-mature state is induced by two cytokines, TNF α and IL-4 (Granucci *et al.*, 2001; Menges *et al.*, 2002; Terme *et al.*, 2004). Full DC maturation is induced by microbial products, pathogen associated molecular patterns (PAMP) that bind to TLRs or toxins, and prostaglandins (Ausiello *et al.*, 2002; Hayashi *et al.*, 2001;

Poltorak *et al.*, 1998). However, our understanding of the biology of DCs is still advancing and we still have much to learn about mature and immature states.

In the last few years there has been an increased use of microarray analysis to investigate the nature of human and mouse DCs in order to unravel the mechanisms by which this complicated cell is regulated during infection (de Jong *et al.*, 2002; Jayakumar *et al.*, 2008; Konopka *et al.*, 2007; Lupo *et al.*, 2008; Yam *et al.*, 2008). Similar studies have also been directed at understanding the maturation process (de Jong *et al.*, 2002; de Jong *et al.*, 2005; Granucci *et al.*, 2001; Shin *et al.*, 2008). Microarray technology has proven to be a powerful tool to apply in this analysis.

The activation of the splenic DC line D1 by LPS and TNF α was investigated by microarray analysis by Granucci (2001) using GeneChip oligonucleotide probe arrays representing approximately 6,500 distinct mouse genes and ESTs (expressed sequence tags). They reported in total 59 'interesting' genes, among which cyclins and anti-proliferative genes were up-regulated during LPS treatment suggesting a definitive growth arrest and full cell maturation. Growth arrest is important to permit mature DCs to migrate into lymph nodes and prime CD8 $^{+}$ and CD4 $^{+}$ T cells. DCs activated with LPS also up-regulated IL-12p40, IL-1 β and IL-6 in addition to the down-regulation of MHC class II, a further sign of cell maturation (Granucci *et al.*, 2001). This type of research can potentially lead to the identification of weaknesses in the host response and strategies employed by 'smart' pathogens. In this sense, very interesting work was carried out on *M. tuberculosis*, monitoring the interaction of this pathogen with macrophages and dendritic cells. In this study the researchers highlight some of the key pathways potentially involved in host-pathogen 'cross talk' (Tailleux *et al.*, 2008).

In addition to improving the understanding of natural events that occur in cell systems, microarrays can be used in applied research. Transcription profiling can assist in understanding how viral vaccine vectors trigger immune responses to chronic infections by studying the interaction between myeloid cells and vaccine vectors (Harenberg *et al.*, 2008). This research may reveal new mechanisms that lead to the activation of specific immune responses to target pathogens or cancer cells, information that may translate into effective vaccines or other immune therapies.

This chapter describes the results of transcriptome and FACS analysis looking at the esDC reaction to infection with *S. Typhimurium*.

6.2 Experimental design

Murine AB2.2 ES cells were driven to differentiation into esDCs in three independent experiments. After characterization by FACS the esDCs were infected with *S. Typhimurium*(p1C/1) expressing the GFP protein with the aim of FACS sorting infected from uninfected cells. Total RNA was extracted from nine samples: three samples were from sorted uninfected esDCs, three samples were from sorted infected esDC at 2 hours post-infection and three samples were from sorted infected esDCs at 4 hours post-infection. Relative amounts of cRNAs were hybridized onto whole genome Illumina MouseWG v1.1 arrays. The expression data were analyzed initially using the Bioconductor package and subsequently the InnateDB (Lynn *et al.*, 2008) platform was used to investigate cellular pathways that were significantly affected during infection.

6.3 Results

6.3.1 Infection of esDCs by *S. Typhimurium* SL1344

EsDCs infected with *S. Typhimurium* SL1344(p1C/1) expressing GFP were investigated by FACS analysis. EsDCs were collected and seeded at 2×10^5 cells per well in 24 well plates and incubated overnight in medium without GM-CSF or IL-3. The cells were then infected at a MOI of 100. After 30 min incubation they were washed with warm PBS Ca²⁺Mg²⁺ and incubated for 2, 4 and 6 hours with complete media containing 50 µg/ml of gentamicin. Then they were washed and treated with a non-enzymatic cell dissociation buffer. Before FACS analysis the cells were fixed with 1% paraformaldehyde. The results of a typical infection are presented in Figure 6.1.

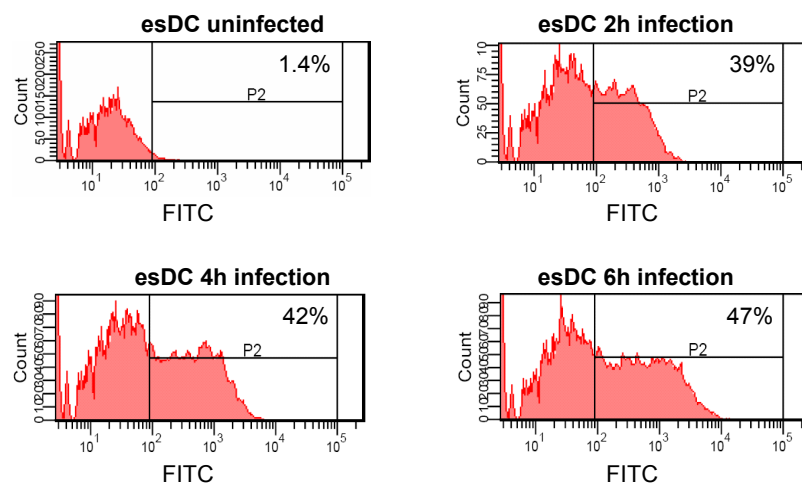


Figure 6.1 FACS analysis of esDCs infected with *S. Typhimurium* SL1344(p1C/1)

The esDCs were infected with *S. Typhimurium*(p1C/1) expressing GFP at MOI 100. The green bacteria were revealed by FACS and recorded in the FITC channel. Here, the results are reported from three time points of infection.

6.3.2 FACS sorting of esDCs infected with *S. Typhimurium*(p1C/1)

Three independent differentiation runs, performed on three independent AB2.2 murine ES cell cultures obtained from three different frozen stocks were infected with *S. Typhimurium* SL1344(p1C/1). The esDCs were sorted in order to collect the infected cells and extract total RNA to perform transcription analysis.

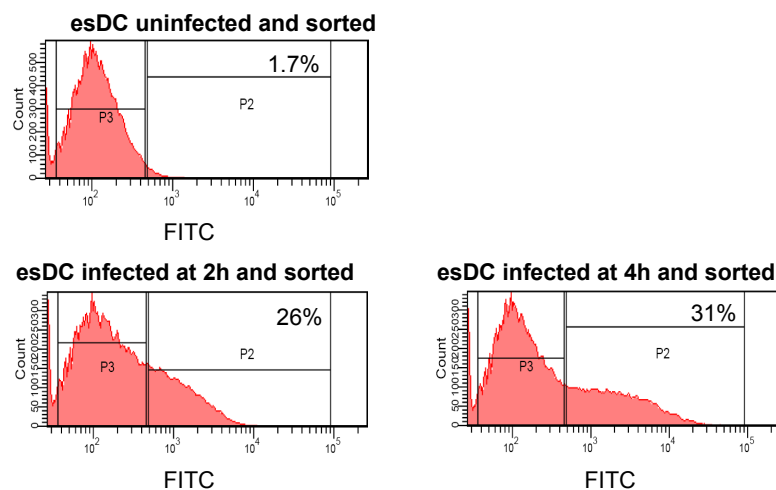


Figure 6.2 EsDCs were infected with *S. Typhimurium* SL1344(p1C/1) and FACS sorted for transcriptome analysis

This figure shows the second biological replicate of infected esDCs sorted in order to perform transcription profiling during *S. Typhimurium* infection. After excluding the debris, the cells were divided into two populations P3 (uninfected), and P2 (infected, positive for FITC) and these were sorted into two 15ml Falcon tubes containing 2ml of RNA ladder buffer. The sorting was carried out using a FACS Aria Cell-Sorting System with sorting mask 16-16-0 which defines the yield, the purity and the phase mask respectively. This sorting mask is suggested by the manufacture as optimal for two-way sorting.

6.3.3 Total RNA extraction, quantification and quality assessment

EsDCs were fully characterized for surface marker expression two days before infection. Total RNA from infected esDCs was extracted immediately after sorting. RNA quantification and quality analysis were carried out prior to storage at -80°C. The total RNA was extracted using QIAGEN Mini Kit and after quantification using NanoDrop 1000 (Thermo) (Table 6.1), the RNA quality was tested by Bioanalyzer analysis (Figure 6.3).

Table 6.1 Total RNA concentration from esDC uninfected and infected with *S. Typhimurium* SL1344(p1C/1)

This table shows the efficiency of the sorting process and the amount of RNA extracted from each sorted population of cells used for microarray hybridization. N/A = not available.

ID	esDC	Status	Number of cells sorted	RNA quantity ng/ μ l	260/280
1B	1st biol rep	uninfected	1,874,218	222.98	2.02
2B	1st biol rep	infected 2h	753,621	59.85	2.06
4B	1st biol rep	infected 4 h	978,863	93.84	2.04
1E	2nd biol rep	uninfected	2,007,081	164.45	2.06
2E	2nd biol rep	infected 2h	754,809	55.45	1.97
4E	2nd biol rep	infected 4 h	1,054,440	59.94	1.95
1G	3rd biol rep	uninfected	N/A	82.67	2.08
2G	3rd biol rep	infected 2h	655,284	36.13	2.00
4G	3rd biol rep	infected 4 h	714,970	41.74	2.00

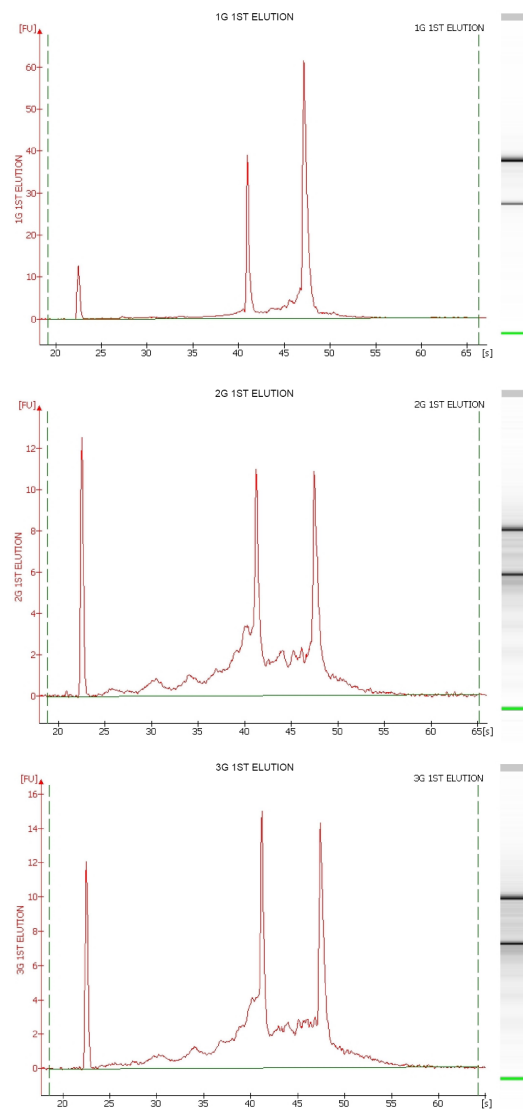


Figure 6.3 Bioanalyzer profile of the total RNA quality extracted from esDCs uninfected and infected with *S. Typhimurium* SL1344(p1C/1) at 2h and 4h

Three electropherograms from Bioanalyzer analysis of total RNA extracted from esDCs uninfected and sorted (top histogram) and infected with *S. Typhimurium* at 2h (middle histogram) and at 4h (bottom histogram). The cells were sorted at the FACSaria Cell-Sorter System in 2ml of RNA ladder solution that preserves the RNA. Some degradation in the total RNA can be seen especially in the sample extracted from infected esDCs. However the two peaks corresponding to ribosome RNA 18S and 28S it can be still observed and their ratio is about 1:2.

6.3.4 cRNA synthesis, labeling and hybridization on Illumina arrays

The cRNA synthesis was performed by Peter Ellis working at the microarray facility at the WTSI following the manufacturer's instruction. Briefly 300ng of total RNA were employed to synthesize double stranded cDNA which was used to produce biotinylated antisense RNA (cRNA) using the Illumina TotalPrep-96 RNA Amplification Kit. The labelled cRNA was hybridized onto the MouseWG-6 v1.1 BeadChips at 58°C overnight. Probe summaries were calculated prior to normalisation and analysis using BeadStudio.

6.3.5 Bioconductor analysis and pathway analysis with InnateDB

Bioconductor analysis was performed with Dr. Robert Andrew from the Microarray Facility at the Wellcome Trust Sanger Institute. Bioconductor was used to complete pair comparison analyses of genes differentially expressed at 2 hours and 4 hours infection versus uninfected esDC. At 2 hours infection 3615 genes were differentially expressed with p-value <0.01, of these 1465 genes had p-value <0.001, of which 376 genes had p-value <0.0001. Of the latter class, 325 had a > 2 fold difference in expression, 101 had > 4 fold fold change (of which only one gene was down-regulated), and 8 genes showed and increase in expression higher than 5 and they all were positively activated. Tables of these gene lists can be found in the attached CD. Since there was a high number of gene reported by Bioconductor analysis a further analysis was performed using Innate DB for immune pathway representation. All the corresponding human orthologs were uploaded with the respective p-value and fold change and the results for enrichment in pathway over-representation through InnateDB is reported in Table 6.2 and 6.3.

Table 6.2 InnateDB analysis of genes differentially expressed by esDCs at 2h infection with *S. Typhimurium* SL1344(p1C/1); pathways up-regulated

All the mouse genes with an Ensemble number were further analyzed with InnateDB for pathways. The corresponding human orthologs were determined and the results were enriched using the ‘over-representation analysis’ option which allows selection of genes on the basis of their fold change (+/- 1.5) and p-value (0.05). The default settings for the analysis algorithm (Hypergeometric) and the multiple testing correction method (The Benjamin & Hochberg correction for the FDR) were used. Only pathways that are significantly up-regulated with p-value < 0.1 are reported here.

Pathway Name of up-regulated pathways at 2h infection	Source Name	Pathway uploaded gene count	Pathway up-regulated genes count	Pathway up-regulated p-value (corrected)
Cytokine-cytokine receptor interaction	KEGG	104	25	0.000930
MAPK signaling pathway	KEGG	171	29	0.059145
Jak-STAT signaling pathway	KEGG	80	17	0.062079
IL12-mediated signaling events	PID NCI	36	11	0.068245
Hematopoietic cell lineage	KEGG	33	10	0.076410

Table 6.3 InnateDB analysis of genes differentially expressed by esDCs at 2h infection with *S. Typhimurium* SL1344(p1C/1); pathways down-regulated

This table reports the pathways down-regulated in esDCs at 2h infection. No down-regulated pathway reported ‘corrected p-value’ lower than 0.1. For this reason only the top 5 down-regulated pathways with their respective ‘non-corrected’ p-values are reported here.

Pathway Name of down-regulated pathways at 2h infection	Source Name	Pathway uploaded gene count	Pathway down-regulated genes count	Pathway down-regulated p-value
Valine, leucine and isoleucine degradation	KEGG	28	10	0.000441
Rho GTPase cycle	REACTOME	72	17	0.001369
Vitamin B5 (pantothenate) metabolism	REACTOME	6	4	0.001725
Beta-Alanine metabolism	KEGG	10	5	0.002342
Propanoate metabolism	KEGG	20	7	0.003731

The analysis of genes differentially expressed at 4 hours infection in comparison to uninfected esDC reported 4040 genes with p-value <0.01, of which 1881 had p-value <0.001 including 619 with p-value <0.0001. Of these genes 525 had a fold change in expression > 2, 175 had a fold change in expression > 4 and 117 had a fold change in expression > 5. Due to the large number of genes identified, pathway analysis was used to evaluate the data. Pathways analysis was carried out using InnateDB [www.innatedb.ca] (Lynn *et al.*, 2008) using all the genes resulting from the Bioconductor analysis with the respective p-value and fold change. In this analysis human orthologs were used since InnateDB report a high number of curated interactions in *homo sapiens*. The analysis reported several pathways that were significantly up or down-regulated. The results of this analysis are reported in Tables 6.4 and 6.5.

Table 6.4 InnateDB analysis of genes differentially expressed by esDCs at 4h infection with *S. Typhimurium* SL1344(p1C/1); pathways up-regulated

The expression data obtained from Bioconductor analysis were further analyzed here pathway enrichment using InnateDB. The human orthologs of all genes were uploaded into the browser with the corresponding fold change and p-value. A first pathway analysis was carried out and then an ‘over-representation analysis’ was conducted using a fold change cut-off of 1.5 and expression p-value 0.05 using the default settings for the analysis algorithm (Hypergeometric) and the multiple testing correction method (The Benjamin & Hochberg correction for the FDR). Only those pathways with adjusted p-values lower than 0.05 are reported here.

GO term Name of pathways up-regulated at 4 hours infection	Source Name	GO term uploaded gene count	GO term up-regulated genes count	GO term up-regulated p-value (corrected)
Cytokine-cytokine receptor interaction	KEGG	104	26	0.000495
IL4-mediated signaling events	PID NCI	33	12	0.004275
IL23-mediated signaling events	PID NCI	24	10	0.004445
Jak-STAT signaling pathway	KEGG	80	20	0.005834
CDK-mediated phosphorylation and removal of Cdc6	REACTOME	36	11	0.019010
IL12-mediated signaling events	PID NCI	36	11	0.019010
Ubiquitin-dependent degradation of Cyclin D1	REACTOME	36	11	0.019010
Ubiquitin Mediated Degradation of Phosphorylated Cdc25A	REACTOME	35	11	0.020413
Vif-mediated degradation of APOBEC3G	REACTOME	35	11	0.020413
Vpu mediated degradation of CD4	REACTOME	34	11	0.021213
Gene expression of SOCS by STAT dimer	INOH	12	6	0.028337
Beta-catenin phosphorylation cascade	REACTOME	39	11	0.032173
Degradation of beta-catenin by the destruction complex	REACTOME	39	11	0.032173
CDT1 association with the CDC6:ORC:origin complex	REACTOME	41	11	0.039599
DNA Replication	REACTOME	41	11	0.039599
Synthesis of DNA	REACTOME	41	11	0.039599
EPO signaling pathway(JAK2 STAT1 STAT3 STAT5)	INOH	9	5	0.041590
Association of licensing factors with the pre-replicative complex	REACTOME	42	11	0.046824

Table 6.5 InnateDB pathway analysis of genes differentially expressed by esDCs at 4h infection with *S. Typhimurium* SL1344(p1C/1); pathways down-regulated

The same gene list analyzed for up-regulated pathways also reported significantly down-regulated pathways. The same parameters were used. This table shows those down-regulated pathways with corrected p-values < 0.05.

GO term Name of pathways down-regulated at 4 hours infection	Source Name	GO term uploaded gene count	GO term down-regulated genes count	GO term down-regulated p-value (corrected)
Citric acid cycle (TCA cycle)	REACTOME	103	26	0.008018
Cori Cycle (interconversion of glucose and lactate)	REACTOME	101	26	0.008018
Glucose metabolism	REACTOME	28	26	0.008018
Oxidative decarboxylation of alpha-ketoglutarate to succinyl CoA by alpha-ketoglutarate dehydrogenase	REACTOME	100	26	0.008018
Pyruvate metabolism and TCA cycle	REACTOME	96	26	0.008018
ChREBP activates metabolic gene expression	REACTOME	101	29	0.008137
Integration of energy metabolism	REACTOME	97	29	0.008137
PP2A-mediated dephosphorylation of key metabolic factors	REACTOME	103	29	0.008137
Electron Transport Chain	REACTOME	94	27	0.008420
Lysine catabolism	REACTOME	95	27	0.008420
Oxidative decarboxylation of pyruvate to acetyl CoA by pyruvate dehydrogenase	REACTOME	95	27	0.008420
Propionyl-CoA catabolism	REACTOME	95	27	0.008420
Regulation of pyruvate dehydrogenase complex (PDC)	REACTOME	95	27	0.008420
Insulin effects increased synthesis of Xylulose-5-Phosphate	REACTOME	95	29	0.008645
Oxidative decarboxylation of alpha-keto-beta-methylvalerate to alpha-methylbutyryl-CoA by branched-chain alpha-ketoacid dehydrogenase	REACTOME	106	29	0.008740
Gamma-Hexachlorocyclohexane degradation	KEGG	106	7	0.008914
Phosphoenolpyruvate and ADP react to form pyruvate and ATP	REACTOME	106	28	0.009170
Oxidative decarboxylation of alpha-ketoisovalerate to isobutyryl-CoA by branched-chain alpha-ketoacid dehydrogenase	REACTOME	92	30	0.009263
Isoleucine catabolism	REACTOME	92	29	0.009771
Mitochondrial fatty acid beta-oxidation of unsaturated fatty acids	REACTOME	92	31	0.009828
Beta oxidation of decanoyl-CoA to octanoyl-CoA-CoA	REACTOME	92	23	0.010158
Beta oxidation of octanoyl-CoA to hexanoyl-CoA	REACTOME	92	23	0.010158
Transcriptional activation of glucose metabolism genes by ChREBP:MLX	REACTOME	108	28	0.010431
Valine, leucine and isoleucine degradation	KEGG	11	13	0.010588
Valine catabolism	REACTOME	79	29	0.010676
Oxidative decarboxylation of alpha-ketoadipate to glutaryl CoA by alpha-ketoglutarate dehydrogenase	REACTOME	79	27	0.010708
Beta oxidation of lauroyl-CoA to decanoyl-CoA-CoA	REACTOME	80	23	0.011196
Beta oxidation of myristoyl-CoA to lauroyl-CoA	REACTOME	80	23	0.011196
Beta oxidation of palmitoyl-CoA to myristoyl-CoA	REACTOME	80	23	0.011196
Beta oxidation of butanoyl-CoA to acetyl-CoA	REACTOME	87	22	0.015703
Oxidative phosphorylation	KEGG	77	24	0.015859
Beta oxidation of hexanoyl-CoA to butanoyl-CoA	REACTOME	78	22	0.018565
Mets affect on macrophage differentiation	PID BIOCARTA	13	7	0.025547

Limonene and pinene degradation	KEGG	13	7	0.025547
Fructose catabolism	REACTOME	7	33	0.027501
Bisphenol A degradation	KEGG	140	5	0.027860
Alanine metabolism	REACTOME	135	32	0.028981
Pentose phosphate pathway (hexose monophosphate shunt)	REACTOME	137	32	0.036902
Dihydroxyacetone phosphate is isomerized to form glyceraldehyde-3-phosphate	REACTOME	139	32	0.045444
Glycolysis	REACTOME	139	32	0.045444

The analysis for pair comparison of esDC expression profile at 4 hours versus 2 hours infection using Bioconductor revealed a few genes differentially expressed. This analysis reported 88 genes differentially expressed with p-value <0.01, and no genes with p-value < 0.001. Pathway analysis was conducted on this gene set using InnateDB as previously described. The ‘over-represented analysis’ identified one pathway significantly down-regulated at 4 hours compared to 2 hours post-infection, and no up-regulated pathways (Table 6.6).

Table 6.6 InnateDB analysis of genes differentially expressed by esDCs at 4h versus 2h infection with *S. Typhimurium* SL1344(p1C/1); pathway down-regulated

The genes differentially expressed at 4h infection versus 2h infection with *S. Typhimurium* SL1344(p1C/1) were analyzed by InnateDB software to identify pathways significantly up- or down-regulated. The analysis was conducted using human orthologs and the ‘over-representation analysis’ was conducted using fold change +/- 1.5, p-value <0.1, default settings for the analysis algorithm (Hypergeometric) and the multiple testing correction method (The Benjamin & Hochberg correction for the FDR). No up-regulated pathways were reported and only one down-regulated pathway was revealed as statistically significant.

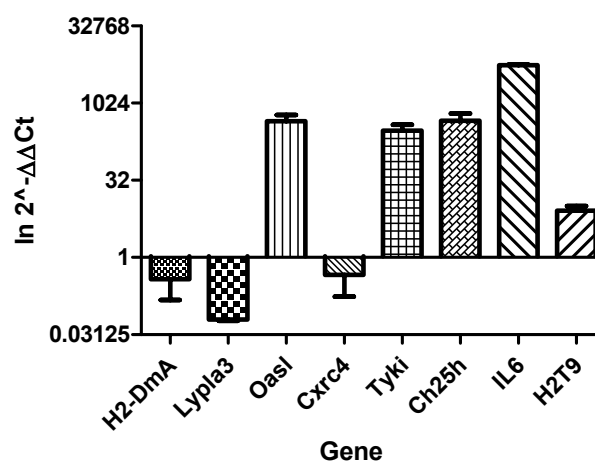
Name of Pathway down-regulated at 4 hours vs. 2h infection	Source Name	Pathway uploaded gene count	Pathway down-regulated genes count	Pathway down-regulated p-value (corrected)
Arachidonic acid metabolism	KEGG	22	6	0.006221

6.3.6 Real time RT-PCR data on genes differentially expressed by esDCs during infection

Some of the more interesting highly up- or down-regulated genes were chosen for confirmation of the expression results obtained from Bioconductor analysis. For this experiment were selected genes that are involved in ubiquitinylation, Osl1, genes involved in lipid methabolism, Ch25h and Lypla3, components of MHC class I and II, H2-T9 and H2Dma, secreted C-X-C chemokine and interleukine and LPS-inducible kinase localized in the mitochondria. All these genes express proteins probably involved in the immune response and cellular response to the pathogen invasion also a list of functions in which each gene is involved can be found in Table 6.7. The cDNA synthesis was conducted using QIAGEN QuantiTect Reverse Transcription kits. Quantitative RT-PCR was conducted on a STRATAGENE Mx3000P machine using SensiMix Plus SYBR Kit (Quantace) and S18 was employed as an internal control gene. The primers were tested for dissociation products and for efficiency slope before being utilized. The data obtained were analysed using the $\Delta\Delta CT$ method (Livak & Schmittgen, 2001) and the graphical representation of the RT-PCR results is reported in Figure 6.4.

Table 6.7 List of genes chosen to be tested at the RT-PCR to confirm microarray data expression analysis are reported in this table

GeneSymbol	Name	FC	adj.P.Val	GO description
Oasl1	2'-5' oligoadenylate synthetase-like 1	64.00	0.000002	transferase activity // nucleotidyltransferase activity
Tyki	thymidylate kinase family LPS-inducible member	56.49	0.000002	thymidylate kinase activity // ATP binding // dTDP biosynthesis // dTTP biosynthesis
Ch25h	Cholesterol 25-hydroxylase	24.93	0.000021	cellular_component unknown // integral to membrane // steroid hydroxylase activity // oxidoreductase activity // cholesterol metabolism // metabolism
Il6	interleukin 6	8.34	0.000090	extracellular // extracellular space // growth factor activity // cytokine activity // interleukin-6 receptor binding // immune response // acute-phase response
H2-T9	histocompatibility 2, T region locus 9	5.90	0.000062	integral to membrane // defense response
Cxcr4	chemokine (C-X-C motif) receptor 4	-2.83	0.004630	integral to membrane // G-protein coupled receptor activity // chemokine receptor activity // rhodopsin-like receptor activity // C-X-C chemokine receptor activity // T-cell proliferation // defense response // brain development // chemotaxis // regulation of cell migration
H2-Dma	histocompatibility 2, class II, locus Mb1	-3.89	0.001420	integral to membrane // extracellular space // MHC class II receptor activity // defense response //immune response // antigen processing, exogenous antigen via MHC class II
Lypla3	lysophospholipase 3	-11.08	0.000019	soluble fraction // lysophospholipase activity // calcium-independent cytosolic phospholipase A2 activity // calcium-independent phospholipase A2 activity // ceramide metabolism

Genes differentially expressed genes by esDCs at 4h infection with *S. Typhimurium***Figure 6.4** Graphical representation of qRT-PCR results

The Ct values obtained from three technical replicates for each biological replicate were analyzed using the delta-delta method and reported as the $\ln 2^{-\Delta\Delta C_t}$ values. These data confirm the Bioconductor analysis of up- or down-regulated genes.

6.3.7 Statistical analysis of the RT-PCR data on genes differentially expressed by esDCs during infection

The RT-PCR data were statistically analyzed using REST© software, designed to analyse relative quantitation in qRT-PCR to determine whether there is a significant difference between samples and control, while taking into account reaction efficiency and reference gene normalization. It applies a simple statistical randomization test (Herrmann & Pfaffl, 2005). The results of this analysis are reported in Figure 6.5 and in Table 6.8.

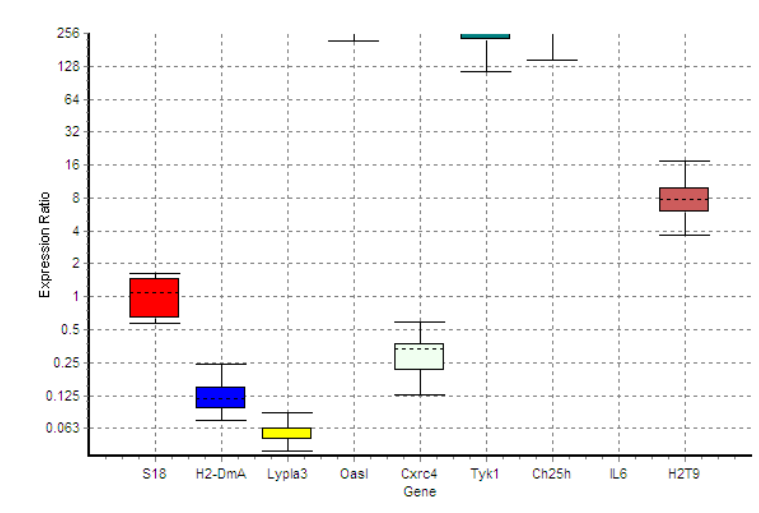


Figure 6.5 Whisker-Box plots for RT-PCR results statistical analysis

The RT-PCR Ct values obtained from three technical replicates for each biological replicate, to test the expression of eight genes, were statistically analysed with REST-2005. This graph reports the skew of distribution of the values reporting the sample median (dotted line), box represents 50% of all observations, and the whiskers represent outer 50% of all observations.

Table 6.8 Summary of the statistical analysis on Ct values obtained from qRT-PCR analysed with REST-2005

Gene	Type	Reaction Efficiency	Expression	Std. Error	P(H1)	Result
H2-DmA	TRG	1	0.041	0.029 - 0.056	0.031	DOWN
Lypla3	TRG	1	0.019	0.016 - 0.026	0.032	DOWN
Oasl	TRG	1	127.803	78.835 - 185.476	0	UP
Cxrc4	TRG	1	0.095	0.052 - 0.155	0.016	DOWN
Tyk1	TRG	1	96.838	56.722 - 193.327	0	UP
Ch25h	TRG	1	128.494	69.293 - 222.202	0	UP
IL6	TRG	1	1,574.37	1,136.096 - 2,555.907	0	UP
H2T9	TRG	1	2.569	1.671 - 4.027	0.068	

The target genes' Ct values were analyzed for statistical significant difference compared to the internal control gene S18's Ct value. All the genes were confined to be significantly differentially expressed with p-value < 0.07. These results confirmed the Bioconductor analysis performed on esDC expression during *S. Typhimurium* infection.

6.4 Discussion

The ability of microarray analysis to detect expression patterns across the entire genome permits an investigation of a large number of genes in a few experiments. Since tens of thousands of genes are investigated the number of genes differentially expressed and transcripts involved in the same biological function can be identified. However, the data interpretation of the data can be challenging. In this study thousands of genes were revealed as up- or down-regulated in esDCs during infection with *S. Typhimurium* SL1344(p1C/1), and although it was possible to recognize some genes with known involvement in host-pathogen interactions, pathway analysis was used to provide a further insights into host-pathogen interaction. For this reason transcription results obtained in this study on esDCs infected with *S. Typhimurium* were analyzed to identify pathways that were up- or down-regulated during infection. Below is a discussion of some of the pathways revealed in this study and their possible role in *Salmonella* invasion.

The pathways significantly up- or down-regulated at 2 hours and at 4 hours post-infection are reported in Table 6.2, 6.3 6.4 and 6.5. After 2 hours infection five pathways were significantly up-regulated: ‘cytokine-cytokine receptor interaction’, ‘Jak-STAT signaling pathway’ and ‘IL-12 mediated signaling events’ (these were also up-regulated at 4 hours), and the ‘hematopoietic cell lineage’ and ‘MAPK signaling pathway’ (which were up-regulated only at 2 hours).

It is important to note that the ‘IL-12 mediated signaling events’ was up-regulated both at 2 hours and at 4 hours infection. The production of IL-12 is a specific signature of APCs and although IL-12 subunits themselves weren’t identified as up-regulated in the Bioconductor analysis, the pathway analysis reveals that probably at the 4 hours post-infection, time of analysis, this pathway was not expressed completely as can be seen in Figure 6.6 where the final products of the pathway are not reported. Previous studies highlighted a predominant expression of IL-12p40 during *Salmonella* infection (Johansson & Wick, 2004). However other studies demonstrated that *Salmonella* infection of BMDC induce stronger production of p40, IL-12, IL-23 and IL-27p28 than bone marrow-derived macrophages (Siegemund *et al.*, 2007). IL-12, a heterodimeric

cytokine composed by two subunits p35 and p40 covalently linked, is part of a family of cytokine comprising IL-12, IL-23, IL27 and IL12p40. The subunit p35 is produced in small amounts whereas the subunit p40 is produced in surplus. Homodimeric p40 can act as an IL-12 antagonist for its receptor and can bind to another protein p19, related to p35, and form another cytokine IL-23. Interestingly, the 'IL-23-mediated signaling events' pathway was also up-regulated at 4 hours post-infection, Table 6.4. IL-12 is involved in the induction of cell-mediated immunity to intracellular pathogens by promoting the differentiation of the Th1 cellular response via IFN γ production from T cells and NK cells. IL-12 is essential for the ability of the host to fight against intracellular bacteria and its lack results in immunodeficiency and induce susceptibility to infections (de Jong *et al.*, 1998; Magram *et al.*, 1996a; Magram *et al.*, 1996b; Mattner *et al.*, 1996). The activities of IL-12 are mediated by a high affinity receptor formed by two subunits β 1 and β 2, which are members of the class I cytokine receptor family and are most closely related to glycoprotein gp130. Binding to the receptor subunit β 1 induce a chain reaction involving the binding of STAT4 (signal transducer and activator of transcription 4) supporting the data that STAT pathways were also up-regulated. Bioconductor analysis revealed the expression of two IL-12 receptors in esDCs at 4 hours infection with *S. Typhimurium*, IL-12R was down regulated slightly (-1.1 fold) with a p-value of 0.0793 and IL-12R β 2 was not significantly up- or down-regulated (1 fold with a p-value 0.785). Figure 6.6 shows the IL-12 mediated pathway.

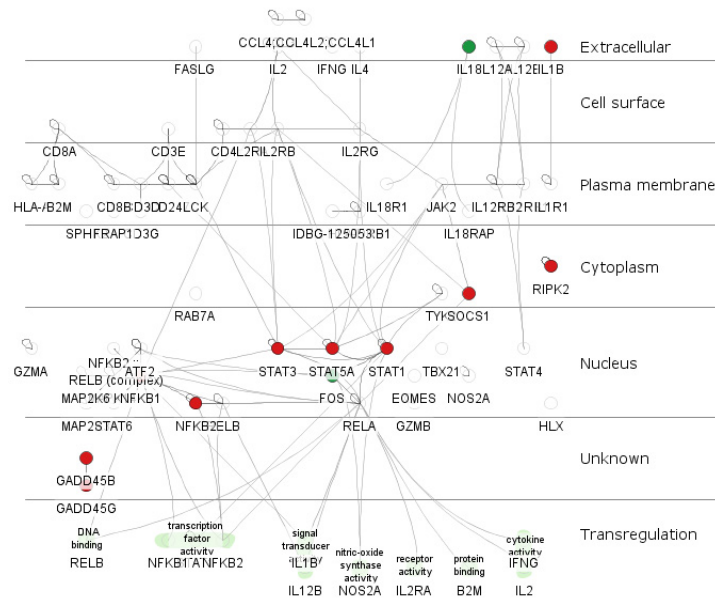


Figure 6.6 This Cytoscape picture represents the IL-12-mediated pathway at 4h

In red are the genes up-regulated and in green the genes down-regulated as result of the Bioconductor analysis.

One other interesting pathway up-regulated by esDCs during infection with *S. Typhimurium* is the ‘IL-4-mediated signaling events’. IL-4, together with IL-10, forms part of an anti-inflammatory pathway. IL-4 is an important cytokine since it is involved in the maturation of naïve T cells into Th2 cells. Interestingly, it is still not clear which type of cell produces this cytokine *in vivo*. A recent study has shown how basophils have the ability to produce IL-4 cytokine in response to a model protease allergen, papain, following recruitment into the lymph node (Sokol *et al.*, 2008). However, production of IL-4 from DCs during *C. albicans* hyphae infection but not during the yeast phagocytosis has also been described. The researchers advanced the hypothesis that DCs are capable of discriminating between the two forms of the fungus (d'Ostiani *et al.*, 2000). In the Bioconductor pair comparison analysis IL-4 was found to be up-regulated 2.6 fold (p-value 0.0743) in esDCs at 4 hours after infection with *S. Typhimurium* SL1344.

Furthermore, the data indicated that suppressor cytokine signaling (SOCS) genes 1 and 3 were up-regulated and that SOCS2 was down-regulated. This pathway is probably connected to the ‘Cytokine-cytokine receptor interaction’, the ‘Jak-STAT signaling pathway’ and the ‘EPO signaling pathway’. SOCS genes encode a family of 7 proteins

which act as negative regulators of the JAK/STAT signaling pathway usually activated in response to cytokine and hormones. The phosphorylation of STAT by JAK is necessary for dimerization, nuclear transportation, DNA binding and gene transcription (Yasukawa *et al.*, 2000). Alteration in the expression of these genes during *Salmonella* infection has been described previously. Uchiya and Nikai (2005) reported that SOCS 1 and 3 expression is regulated by SPI-2 products. In addition, it was previously reported that SpiC protein, expressed from SPI-2, is able to inhibit the lysosomal fusion with the SCV (Uchiya *et al.*, 1999). Other published work has shown that this protein is translocated in the host cell cytoplasm through the TIISS encoded on SPI-2 and that it is able to interact with the host proteins TassC (Lee *et al.*, 2002) and Hook3 (Shotland *et al.*, 2003), involved in cellular trafficking. SpiC appears to play a central role in the pathogen intracellular survival (Freeman *et al.*, 2002; Yu *et al.*, 2004). The enhanced expression of SOCS3 in macrophages during *Salmonella* infection is driven by the SpiC protein. Finally, SOCS3 inhibits cytokine signaling by blocking the phosphorylation of STAT-1 or STAT-3, inducing respectively the inhibition of IL-6 and IFN γ secretion (Uchiya & Nikai, 2005). Figure 6.8 shows the SOCS pathway with up- and down-regulated genes identified by Bioconductor analysis.

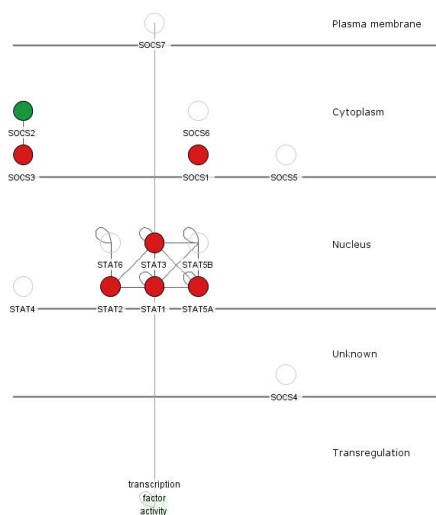


Figure 6.7 Cytoscape representation of the SOCS pathway in esDCs at 4h infection

The red genes were up-regulated and the green genes were down-regulated in the pair comparison analysis at 4h infection performed with Bioconductor.

Among the down-regulated pathways, there are many oxidative pathways involving acetyl-CoA and most of the down-regulated pathways take place in the mitochondrion. Unfortunately these pathways are not as well annotated as are the up-regulated pathways. It can be quite challenging in this situation to advance a hypothesis and speculate on what really happens during infection. However a comparison with the literature can help; for example it was reported early in 2008 that *S. Typhimurium* SR-11 carrying mutations in the tricarboxylic acid (TCA) cycle and unable to convert succinate to fumarate, are attenuated, whereas mutants that were not able to run a reductive branch of the TCA were fully virulent (Mercado-Lubo *et al.*, 2008). It can be speculated that these mutant bacteria use the host cells apparatus, and in this situation the host cell attempts to down-regulate its own TCA in order make components less available to the bacteria.

On the other hand, the mitochondria are important organelles involved in the regulation of many different pathways including the KREB cycle, heme synthesis, ATP and NADPH synthesis. The general down-regulation of the oxidative pathways could affect heme synthesis. Although the heme synthesis pathway was not differentially expressed in the analysis reported here. Heme synthesis relies on the mitochondrion and the cytosol and involves succinyl-CoA and glycine. Heme is synthesized in all human nucleated cells at different rates. Accumulation of intracellular or extracellular heme can be harmful to cells and free heme mediates oxidative stress and inflammation. Heme can affect a wide range of regulatory factors and can influence gene expression at almost every level regulating transcription (Zhang & Guarente, 1995), mRNA stability (Maniatis *et al.*, 1976), protein synthesis (via eIF-2 α kinase, that was up-regulated during murine ES cells infection) (Chen *et al.*, 1994), splicing (Ponka, 1999), and post-translational modifications (Swenson *et al.*, 1991). Heme also induces nitric oxide synthesis and regulated Cytochrome P450 expression (Wagener *et al.*, 2003). A strong down-regulation of P450 was observed during ES cells infection. It is possible that the infected cells try to starve the pathogen for iron supply. In fact it has been shown previously that bacteria require iron to survive inside the host cell and for this reason they have evolved mechanisms that permit them to acquire iron from mammalian iron carriers: transferrin and heme, in addition to the production of low-molecular weight molecules with high affinity for Fe³⁺ denominated siderophores (Milne *et al.*, 2007).

In conclusion, in this chapter are reported the results of a transcriptome analysis of esDCs during *S. Typhimurium* infection. As in all of this type of work, the whole microarray analysis cannot possibly give any kind of specific answer but gives ideas and direction for future research and this report is a good example of its type.

7 Final remarks and future work

The main aim of this study was to assess the potential of murine ES cells as tools for probing interactions between pathogens and mammalian cells. ES cells could potentially form the foundation of novel cell-based assays employing either normal or mutant ES cell lines. The study demonstrates for the first time that murine ES cells can be infected independently by the two pathogenic bacteria, *Shigella flexneri* and *Salmonella* Typhimurium. Using Gentamicin assays, similar invasion rates were observed in ES-cell based *in vitro* models and in previously characterized terminally differentiated cell lines for both the bacteria *S. flexneri* and *S. Typhimurium*. This report showed that both pathogens were able to invade ES cells in a manner that was dependent on the expression of bacterial pathogenicity genes that contribute to active cellular invasion. From the observations, the patterns of invasion and intracellular trafficking seemed quite similar in ES cells compared to terminally differentiated cells, although more detailed investigations are required to confirm this observation. Confocal observation revealed that *Shigella* entered murine ES cells via the induction of cytoskeleton rearrangements as previously reported (Adam *et al.*, 1995) and no co-localization was observed with either EEA-1 or LAMP-1 markers suggesting that the bacteria live free inside the cellular cytosol. Observations at 2 hours infection also revealed that *Shigella* produced actin tails once inside ES cells. *Salmonella*-ES cell interaction however was less easy to decipher due to the lack of co-localization with the EEA-1 marker of early endosomes. Nevertheless, it was possible to observe a co-localization of SCV with LAMP-1 and LAMP-2 markers characteristic of lysosomes. A limited number of intracellular markers was used in this study to probe the intracellular location of these pathogens but in the future it would be interesting to investigate the involvement of both the Rho protein family and Rab proteins in the invasion of ES cells as has been suggested for other cell types (Patel & Galan, 2006; Smith *et al.*, 2007). The identification and comparison of the pathogenic mechanisms used during ES cell invasion was useful as so little is known about their interactions and will help in future research to highlight differences in mutated ES cells.

After exploring the basic cellular interactions between murine ES cells and pathogenic bacteria, the transcriptomic profiles of ES cells were determined during *Salmonella*

infection. Perhaps the most striking feature of these profiles was an almost total absence of an immunological response in murine ES cells during bacterial invasion. This is perhaps not surprising since the cell model investigated does not represent an immunological cell line. However, these results may have been a little unexpected since ES cells do produce some cytokines even in an uninfected state (Guo *et al.*, 2006) and a stronger immune reaction after invasion was a possibility. Nevertheless, some interesting genes were revealed by the different type of analyses, especially GeneSpring and the time course analyses highlighted a few interesting genes. For example STAT2 was up-regulated at 4 hours post-infection. STAT2 is involved in the IFN type I and II signal transduction of innate immunity against microorganisms (Decker *et al.*, 2002). Up-regulation of SOCS3 was also detected, this gene is involved in *Salmonella* responses induced by SPiC, a SPI-2 secreted protein. SOCS3 is also involved in the inhibition of cytokine signaling via the JAK/STAT activation pathway (Crocker *et al.*, 2008). All of the different analyses identified the up-regulation of cytochrome P450 at 2 hours, followed by a strong down-regulation at 4 hours post-infection, which is intriguing. This could be linked to a stress response in the cells or to a mechanism of auto-defense. The identification of transcription factor XBP1 also reported in other studies is interesting as this factor is known to be involved in the differentiation of myeloid cells (Iwakoshi *et al.*, 2003). This study was restricted to a limited number of post-infection time-points due to the rapid onset of cell detachment. One possible reason for the low immunological signature may be that being undifferentiated, ES cells might not have immunological defense machinery capable of a rapid response which could have an effect on the 'reaction time' of the cell. In a previous study conducted on haematopoietic stem cells, it was observed that bacterial infection can induce differentiation and expression of components of immune response (Kolb-Maurer *et al.*, 2004). However, in those experiments there was no observable difference in surface marker expression at 4 hours post-infection. Consequently, the haematopoietic stem cells were incubated with bacteria for longer periods of three and six days in order to detect the expression of immunological genes. In the present study ES cells were treated in a similar manner to epithelial cells and they were incubated with *Salmonella* for shorter times of 2 and 4 hours. However, this approach could be reconsidered and other treatments such as longer incubation times or employing different attenuated bacteria could provide additional insights. Unfortunately several of the mutated bacterial strains

used in this study were restricted in their ability to enter or replicate in the ES cells. This is one of the challenges presented by the use of a new model.

In order to further explore if ES cells can be realistically applied to studies of infectious disease, they were differentiated into dendritic cells, a cell type relevant to the host's fight against infection. The approach also provides a means to possibly generate large quantities of DCs to further advance research on antigenic presentation and immunization. Overall, DCs are perhaps less well studied compared to macrophages since they are less easily produced or differentiated *ex-vivo*, because they can be involuntarily activated during manipulation. The majority of DCs employed in research are obtained from bone marrow, derived from the femurs of mice. These cells have a limited life span and the outcome of experiments can vary depending on the age of the mice, the mouse strain and the differentiation protocol used. The interactions between *Salmonella* and bone marrow derived DCs have been the object of previous studies. However, there is still some controversy on how *Salmonella* and DCs interact due to the contradictory results obtained by different laboratories focusing on the localization of lysosomal markers and the SCV. In this study *Salmonella* intracellular localization within esDCs coincided with both the early endosome marker EEA-1 and the lysosomal markers LAMP-1 and 2. Also, the contribution that DCs bring to the host fight against this intracellular pathogen is not completely defined. It is speculated that DC's cross-epithelial protrusions and by sampling the lumen content might inadvertently help spread the pathogen. The protocol used in this study offers an efficient method to produce DCs *in vitro* thus providing an opportunity to further study DC-*Salmonella* interactions. In addition, the protocol to differentiate ES cells into esDCs has the potential to be further optimized in order to obtain different subpopulations of DCs. This will require further investigation into the dynamics of different DC subpopulation differentiation *in vivo* and *in vitro*.

In this report a transcriptomic analysis of esDCs during infection with *Salmonella* Typhimurium highlighted several distinct pathways that were differentially expressed. Some of these observations confirmed interactions previously described between *Salmonella* and DCs. For example, up-regulation of the IL-12 and IL-4 pathways and the activation of SOCS proteins and Cyclin D1 was reported here and in other similar studies. However, one of the most interesting aspects of this data was the relatively high

number of down-regulated pathways revealed by the analysis. This was a little unexpected since the statistical method used to analyze the data has a very low rate of false discovery for negatively-regulated genes. However, using my data the number of pathways down-regulated was still higher than those up-regulated. Many of these down-regulated pathways are involved in oxidative processes. Perhaps there is more to explore in terms of the pathways down-regulated during infection than in those up-regulated. Obviously, computational analysis plays a pivotal role in functional genomic research. To advance in this field new powerful analytical tools need to take into consideration complex cell signaling-dynamics in time and space allowing for special relocations, organization of different proteins complexes, kinetic data and post-translational modifications (Kholodenko, 2006). In the mean time it is important to integrate gene transcription observations with other techniques such as proteomic analysis.

Taken together the results obtained in this work provide encouragement for the applicability of ES cell models to infectious disease research for several reasons. Firstly, ES cells present a normal karyotype and they can replicate *in vitro* for a potentially infinite number of passages whilst still maintaining ‘normal’ characteristics. Secondly, ES cells can be genetically manipulated and therefore new genes important in host-pathogen interactions can be highlighted. In addition, it has been proposed that ES cells represent the best type of cell to use for this purpose because, by mutating one cell type, the effect of the same mutation can be investigated in either *in vitro* differentiated cells or *in vivo* produced chimeric mice. Following in this direction, conditional mutations will have an important role to play with the formation of a public mutagenesis library opening the possibility of applying these mutants to any kind of research (Sparwasser & Eberl, 2007). The usefulness of mutant knockout mice in host-pathogen interaction analysis has already been proven by the discovery of the NRAMP gene (Lara-Tejero *et al.*, 2006).

In today’s medical and therapeutic scene, DCs are assuming a growing importance as ‘targeting’ vaccines allowing the medical research community to forge immunotherapeutic strategies around applications that directly regulate immunity (Plotkin, 2005). For this reason the elucidation of pathways induced by specific molecules that stimulate DC maturation is becoming more important and these advances have the potential for use in

genetically engineered vaccines. In the future, vaccines based on the targeting and manipulation of DCs will find application in infectious diseases as well as in the fight against autoimmune disorders and cancer (Pal *et al.*, 2007). Microarray technology will have an important role to play in this research.

Future directions that this research can take are numerous, including ES cell differentiation, mutation and the development of new cellular techniques. The ability of ES cells to differentiate into any somatic cell lineage opens up many options. For example, the differentiation of gut-like structures from *in vitro* EBs has already been described (Torihashi, 2006). This technique could be applied to study host-pathogen interactions by rebuilding, *in vitro*, the structures found *in vivo*. Also, from a mutational point of view, it will be very interesting to see if the ‘genetics-squared’ (Persson & Vance, 2007) approach that combines host and pathogen genetic manipulation will prove to be a key player in the study of host-pathogen interactions. Finally, one of the next goals in this field is to knockout not just a single gene but a whole pathway to investigate its relationship to pathogenicity. It is possible to imagine the induction of pathways normally down-regulated during infection in order to investigate their contra-effects on the progression of the disease. For this purpose conditional genetic manipulation will be a key factor in understanding the mechanisms that regulate genomic expression.

Lastly, the growing interest in immunomics reflects the urgency of researchers and society to see research move forward in this field (Braga-Neto & Marques, 2006). The application of DNA microarrays, used to identify genomic regulatory networks gives remarkable insight into the host systems. However this represents only one aspect of immunomics which makes use of antibody, peptide, peptide-MHC and cell microarrays. For further advancements in the battle against pathogens a deeper understanding of host-pathogen interactions is needed and future research will benefit from the introduction of new techniques and technologies. In relation to the study reported here it positively paves the way for future applications of ES cells in the field of infectious diseases and host-pathogen interactions.

References

- Abbasi, K. (2001).** Progress is slow in narrowing the health research divide. *BMJ (Clinical research ed)* **323**, 886.
- Abe, K., Niwa, H., Iwase, K., Takiguchi, M., Mori, M., Abe, S. I., Abe, K. & Yamamura, K. I. (1996).** Endoderm-specific gene expression in embryonic stem cells differentiated to embryoid bodies. *Experimental cell research* **229**, 27-34.
- Abrahams, G. L. & Hensel, M. (2006).** Manipulating cellular transport and immune responses: dynamic interactions between intracellular *Salmonella enterica* and its host cells. *Cellular microbiology* **8**, 728-737.
- Ackerman, A. L., Giodini, A. & Cresswell, P. (2006).** A role for the endoplasmic reticulum protein retrotranslocation machinery during crosspresentation by dendritic cells. *Immunity* **25**, 607-617.
- Adam, T., Arpin, M., Prevost, M. C., Gounon, P. & Sansonetti, P. J. (1995).** Cytoskeletal rearrangements and the functional role of T-plastin during entry of *Shigella flexneri* into HeLa cells. *The Journal of cell biology* **129**, 367-381.
- Adams, D. J., Quail, M. A., Cox, T. & other authors (2005).** A genome-wide, end-sequenced 129Sv BAC library resource for targeting vector construction. *Genomics* **86**, 753-758.
- Affymetrix (2004).** GeneChip Mouse Genome Arrays. *Part No 701525 Rev 4*.
- Akira, S., Uematsu, S. & Takeuchi, O. (2006).** Pathogen recognition and innate immunity. *Cell* **124**, 783-801.
- Al-Shahrour, F., Diaz-Uriarte, R. & Dopazo, J. (2004).** FatiGO: a web tool for finding significant associations of Gene Ontology terms with groups of genes. *Bioinformatics (Oxford, England)* **20**, 578-580.
- Albert, M. L., Pearce, S. F., Francisco, L. M., Sauter, B., Roy, P., Silverstein, R. L. & Bhardwaj, N. (1998a).** Immature dendritic cells phagocytose apoptotic cells via α 5 β 1 and CD36, and cross-present antigens to cytotoxic T lymphocytes. *The Journal of experimental medicine* **188**, 1359-1368.
- Albert, M. L., Sauter, B. & Bhardwaj, N. (1998b).** Dendritic cells acquire antigen from apoptotic cells and induce class I-restricted CTLs. *Nature* **392**, 86-89.
- Albertini, S., Suter-Dick, L., Boess, F. & Weiser, T. (2006).** How Predictive is In Vitro Toxicogenomics for In Vivo Toxicity? *INVITOX 2006 Session 3 - New in vitro models and strategies Abstract I3.1*.

- Allan, R. S., Waithman, J., Bedoui, S. & other authors (2006).** Migratory dendritic cells transfer antigen to a lymph node-resident dendritic cell population for efficient CTL priming. *Immunity* **25**, 153-162.
- Allaoui, A., Mounier, J., Prevost, M. C., Sansonetti, P. J. & Parsot, C. (1992).** icsB: a *Shigella flexneri* virulence gene necessary for the lysis of protrusions during intercellular spread. *Molecular microbiology* **6**, 1605-1616.
- Allaoui, A., Sansonetti, P. J. & Parsot, C. (1993).** MxiD, an outer membrane protein necessary for the secretion of the *Shigella flexneri* Ipa invasins. *Molecular microbiology* **7**, 59-68.
- Allison, D. B., Cui, X., Page, G. P. & Sabripour, M. (2006).** Microarray data analysis: from disarray to consolidation and consensus. *Nature reviews* **7**, 55-65.
- Altwegg, M. & Bockemuhl, J. (1998).** Escherichia and Shigella. In *Microbiology and Microbial Infections* pp. 935-967: Hodder Arnold.
- Ardavin, C. (2007).** Subpopulation and differentiation of mouse dendritic cells. In *Dendritic Cells interactions with bacteria*, pp. 3-26. Edited by M. Rescigno: Cambridge University Press.
- Ashburner, M., Ball, C. A., Blake, J. A. & other authors (2000).** Gene ontology: tool for the unification of biology. The Gene Ontology Consortium. *Nature genetics* **25**, 25-29.
- Ausiello, C. M., Fedele, G., Urbani, F., Lande, R., Di Carlo, B. & Cassone, A. (2002).** Native and genetically inactivated pertussis toxins induce human dendritic cell maturation and synergize with lipopolysaccharide in promoting T helper type 1 responses. *The Journal of infectious diseases* **186**, 351-360.
- Austin, C. P., Battey, J. F., Bradley, A. & other authors (2004).** The knockout mouse project. *Nature genetics* **36**, 921-924.
- Auwerx, J., Avner, P., Baldock, R. & other authors (2004).** The European dimension for the mouse genome mutagenesis program. *Nature genetics* **36**, 925-927.
- Bahrani, F. K., Sansonetti, P. J. & Parsot, C. (1997).** Secretion of Ipa proteins by *Shigella flexneri*: inducer molecules and kinetics of activation. *Infection and immunity* **65**, 4005-4010.
- Balachandran, P., Dragone, L., Garrity-Ryan, L., Lemus, A., Weiss, A. & Engel, J. (2007).** The ubiquitin ligase Cbl-b limits *Pseudomonas aeruginosa* exotoxin T-mediated virulence. *The Journal of clinical investigation* **117**, 419-427.
- Bennett, C. L. & Clausen, B. E. (2007).** DC ablation in mice: promises, pitfalls, and challenges. *Trends in immunology* **28**, 525-531.
- Bernardini, M. L., Mounier, J., d'Hauteville, H., Coquis-Rondon, M. & Sansonetti, P. J. (1989).** Identification of icsA, a plasmid locus of *Shigella flexneri* that governs

bacterial intra- and intercellular spread through interaction with F-actin. *Proceedings of the National Academy of Sciences of the United States of America* **86**, 3867-3871.

Beuzon, C. R., Meresse, S., Unsworth, K. E., Ruiz-Albert, J., Garvis, S., Waterman, S. R., Ryder, T. A., Boucrot, E. & Holden, D. W. (2000). Salmonella maintains the integrity of its intracellular vacuole through the action of SifA. *The EMBO journal* **19**, 3235-3249.

Birot, A., Duret, L., Bartholin, L., Santalucia, B., Tigaud, I., Magaud, J. & Rouault, J. (2000). Identification and molecular analysis of BANP. *Gene* **253**, 189-196.

Blocker, A., Gounon, P., Larquet, E., Niebuhr, K., Cabiliaux, V., Parsot, C. & Sansonetti, P. (1999). The tripartite type III secretin of *Shigella flexneri* inserts IpaB and IpaC into host membranes. *The Journal of cell biology* **147**, 683-693.

Blocker, A., Jouihri, N., Larquet, E., Gounon, P., Ebel, F., Parsot, C., Sansonetti, P. & Allaoui, A. (2001). Structure and composition of the *Shigella flexneri* "needle complex", a part of its type III secretin. *Molecular microbiology* **39**, 652-663.

Bonifacino, J. S. & Weissman, A. M. (1998). Ubiquitin and the control of protein fate in the secretory and endocytic pathways. *Annual review of cell and developmental biology* **14**, 19-57.

Bourdet-Sicard, R., Rudiger, M., Jockusch, B. M., Gounon, P., Sansonetti, P. J. & Nhieu, G. T. (1999). Binding of the *Shigella* protein IpaA to vinculin induces F-actin depolymerization. *The EMBO journal* **18**, 5853-5862.

Bowie, A. G. & Fitzgerald, K. A. (2007). RIG-I: tri-ling to discriminate between self and non-self RNA. *Trends in immunology* **28**, 147-150.

Bradley, A., Evans, M., Kaufman, M. H. & Robertson, E. (1984). Formation of germ-line chimaeras from embryo-derived teratocarcinoma cell lines. *Nature* **309**, 255-256.

Braga-Neto, U. M. & Marques, E. T., Jr. (2006). From functional genomics to functional immunomics: new challenges, old problems, big rewards. *PLoS computational biology* **2**, e81.

Brault, V., Pereira, P., Duchon, A. & Herault, Y. (2006). Modeling chromosomes in mouse to explore the function of genes, genomic disorders, and chromosomal organization. *PLoS genetics* **2**, e86.

Brinkmann, V., Reichard, U., Goosmann, C., Fauler, B., Uhlemann, Y., Weiss, D. S., Weinrauch, Y. & Zychlinsky, A. (2004). Neutrophil extracellular traps kill bacteria. *Science (New York, NY)* **303**, 1532-1535.

Brumell, J. H., Perrin, A. J., Goosney, D. L. & Finlay, B. B. (2002). Microbial pathogenesis: new niches for salmonella. *Curr Biol* **12**, R15-17.

- Bryant, P. A., Venter, D., Robins-Browne, R. & Curtis, N. (2004).** Chips with everything: DNA microarrays in infectious diseases. *The Lancet infectious diseases* **4**, 100-111.
- Buchrieser, C., Glaser, P., Rusniok, C., Nedjari, H., D'Hauteville, H., Kunst, F., Sansonetti, P. & Parsot, C. (2000).** The virulence plasmid pWR100 and the repertoire of proteins secreted by the type III secretion apparatus of *Shigella flexneri*. *Molecular microbiology* **38**, 760-771.
- Buehring, G. C. (1996).** Contributions of cell culture to the investigation and control of infectious diseases. *Methods in Cell Science* **18**, 195-200.
- Capecchi, M. R. (2005).** Gene targeting in mice: functional analysis of the mammalian genome for the twenty-first century. *Nature reviews* **6**, 507-512.
- Chakravortty, D., Rohde, M., Jager, L., Deiwick, J. & Hensel, M. (2005).** Formation of a novel surface structure encoded by *Salmonella* Pathogenicity Island 2. *The EMBO journal* **24**, 2043-2052.
- Chambers, I. & Smith, A. (2004).** Self-renewal of teratocarcinoma and embryonic stem cells. *Oncogene* **23**, 7150-7160.
- Chaudry, A. (2004).** Cell culture. *The Science Creative Quaterly August 2004*.
- Cheminay, C., Schoen, M., Hensel, M., Wandersee-Steinhauser, A., Ritter, U., Korner, H., Rollinghoff, M. & Hein, J. (2002).** Migration of *Salmonella typhimurium* --harboring bone marrow--derived dendritic cells towards the chemokines CCL19 and CCL21. *Microbial pathogenesis* **32**, 207-218.
- Cheminay, C., Mohlenbrink, A. & Hensel, M. (2005).** Intracellular *Salmonella* inhibit antigen presentation by dendritic cells. *J Immunol* **174**, 2892-2899.
- Chen, H. & Li, J. (2007).** Nanotechnology: moving from microarrays toward nanoarrays. *Methods in molecular biology (Clifton, NJ)* **381**, 411-436.
- Chen, J. J., Crosby, J. S. & London, I. M. (1994).** Regulation of heme-regulated eIF-2 alpha kinase and its expression in erythroid cells. *Biochimie* **76**, 761-769.
- Chieppa, M., Rescigno, M., Huang, A. Y. & Germain, R. N. (2006).** Dynamic imaging of dendritic cell extension into the small bowel lumen in response to epithelial cell TLR engagement. *The Journal of experimental medicine* **203**, 2841-2852.
- Clark, A. T., Bodnar, M. S., Fox, M., Rodriguez, R. T., Abeyta, M. J., Firpo, M. T. & Pera, R. A. (2004).** Spontaneous differentiation of germ cells from human embryonic stem cells in vitro. *Hum Mol Genet* **13**, 727-739.
- Clements, M. O., Eriksson, S., Thompson, A., Lucchini, S., Hinton, J. C., Normark, S. & Rhen, M. (2002).** Polynucleotide phosphorylase is a global regulator of virulence and persistency in *Salmonella enterica*. *Proceedings of the National Academy of Sciences of the United States of America* **99**, 8784-8789.

- Coloma, J. & Harris, E. (2008).** Sustainable transfer of biotechnology to developing countries: fighting poverty by bringing scientific tools to developing-country partners. *Annals of the New York Academy of Sciences* **1136**, 358-368.
- Cooke, F. J. & Wain, J. (2006).** Antibiotic resistance in Salmonella infections. In *Salmonella Infections: Clinical, Immunological and Molecular Aspects*, pp. 25-56. Edited by P. Mastroeni & D. Maskell: Cambridge University Press.
- Cooper, H. M., Tamura, R. N. & Quaranta, V. (1991).** The major laminin receptor of mouse embryonic stem cells is a novel isoform of the alpha 6 beta 1 integrin. *The Journal of cell biology* **115**, 843-850.
- Crocker, B. A., Kiu, H. & Nicholson, S. E. (2008).** SOCS regulation of the JAK/STAT signalling pathway. *Seminars in cell & developmental biology*.
- d'Ostiani, C. F., Del Sero, G., Bacci, A., Montagnoli, C., Spreca, A., Mencacci, A., Ricciardi-Castagnoli, P. & Romani, L. (2000).** Dendritic cells discriminate between yeasts and hyphae of the fungus *Candida albicans*. Implications for initiation of T helper cell immunity in vitro and in vivo. *The Journal of experimental medicine* **191**, 1661-1674.
- Dalpke, A., Heeg, K., Bartz, H. & Baetz, A. (2008).** Regulation of innate immunity by suppressor of cytokine signaling (SOCS) proteins. *Immunobiology* **213**, 225-235.
- de Jong, E. C., Vieira, P. L., Kalinski, P., Schuitemaker, J. H., Tanaka, Y., Wierenga, E. A., Yazdanbakhsh, M. & Kapsenberg, M. L. (2002).** Microbial compounds selectively induce Th1 cell-promoting or Th2 cell-promoting dendritic cells in vitro with diverse th cell-polarizing signals. *J Immunol* **168**, 1704-1709.
- de Jong, E. C., Smits, H. H. & Kapsenberg, M. L. (2005).** Dendritic cell-mediated T cell polarization. *Springer seminars in immunopathology* **26**, 289-307.
- de Jong, R., Altare, F., Haagen, I. A. & other authors (1998).** Severe mycobacterial and Salmonella infections in interleukin-12 receptor-deficient patients. *Science (New York, NY)* **280**, 1435-1438.
- Decker, T., Stockinger, S., Karaghiosoff, M., Muller, M. & Kovarik, P. (2002).** IFNs and STATs in innate immunity to microorganisms. *The Journal of clinical investigation* **109**, 1271-1277.
- Denham, M., Conley, B., Olsson, F., Cole, T. J. & Mollard, R. (2005).** Stem cells: an overview. *Current protocols in cell biology / editorial board, Juan S Bonifacino [et al]* **Chapter 23**, Unit 23 21.
- Detweiler, C. S., Cunanan, D. B. & Falkow, S. (2001).** Host microarray analysis reveals a role for the Salmonella response regulator phoP in human macrophage cell death. *Proceedings of the National Academy of Sciences of the United States of America* **98**, 5850-5855.

- Doetschman, T. C., Eistetter, H., Katz, M., Schmidt, W. & Kemler, R. (1985).** The in vitro development of blastocyst-derived embryonic stem cell lines: formation of visceral yolk sac, blood islands and myocardium. *Journal of embryology and experimental morphology* **87**, 27-45.
- Domenech, J., Lubroth, J., Eddi, C., Martin, V. & Roger, F. (2006).** Regional and international approaches on prevention and control of animal transboundary and emerging diseases. *Annals of the New York Academy of Sciences* **1081**, 90-107.
- Ducibella, T., Albertini, D. F., Anderson, E. & Biggers, J. D. (1975).** The preimplantation mammalian embryo: characterization of intercellular junctions and their appearance during development. *Dev Biol* **45**, 231-250.
- Ducibella, T. & Anderson, E. (1975).** Cell shape and membrane changes in the eight-cell mouse embryo: prerequisites for morphogenesis of the blastocyst. *Dev Biol* **47**, 45-58.
- Eckmann, L., Smith, J. R., Housley, M. P., Dwinell, M. B. & Kagnoff, M. F. (2000).** Analysis by high density cDNA arrays of altered gene expression in human intestinal epithelial cells in response to infection with the invasive enteric bacteria Salmonella. *The Journal of biological chemistry* **275**, 14084-14094.
- Editorial (2008).** The value of vaccines. *Nature Review Microbiology* **6**.
- Egile, C., d'Hauteville, H., Parsot, C. & Sansonetti, P. J. (1997).** SopA, the outer membrane protease responsible for polar localization of IcsA in *Shigella flexneri*. *Molecular microbiology* **23**, 1063-1073.
- Eriksson, S., Lucchini, S., Thompson, A., Rhen, M. & Hinton, J. C. (2003).** Unravelling the biology of macrophage infection by gene expression profiling of intracellular *Salmonella enterica*. *Molecular microbiology* **47**, 103-118.
- Evans, M. J. & Kaufman, M. H. (1981).** Establishment in culture of pluripotential cells from mouse embryos. *Nature* **292**, 154-156.
- Ewis, A. A., Zhelev, Z., Bakalova, R., Fukuoka, S., Shinohara, Y., Ishikawa, M. & Baba, Y. (2005).** A history of microarrays in biomedicine. *Expert review of molecular diagnostics* **5**, 315-328.
- Fairchild, P. J., Brook, F. A., Gardner, R. L., Graca, L., Strong, V., Tone, Y., Tone, M., Nolan, K. F. & Waldmann, H. (2000).** Directed differentiation of dendritic cells from mouse embryonic stem cells. *Curr Biol* **10**, 1515-1518.
- Fairchild, P. J., Nolan, K. F. & Waldmann, H. (2003).** Probing dendritic cell function by guiding the differentiation of embryonic stem cells. *Methods in enzymology* **365**, 169-186.
- Fairchild, P. J., Nolan, K. F. & Waldmann, H. (2007).** Genetic modification of dendritic cells through the directed differentiation of embryonic stem cells. In *Methods in molecular biology (Clifton, NJ)*, pp. 59-72.

- Falkow, S. (1988).** Molecular Koch's postulates applied to microbial pathogenicity. *Reviews of infectious diseases* **10 Suppl 2**, S274-276.
- Finlay, B. B. & Falkow, S. (1988).** Comparison of the invasion strategies used by *Salmonella cholerae-suis*, *Shigella flexneri* and *Yersinia enterocolitica* to enter cultured animal cells: endosome acidification is not required for bacterial invasion or intracellular replication. *Biochimie* **70**, 1089-1099.
- Forsyth, J. R. L. (1998).** Typhoid and paratyphoid. In *Microbiology and microbial infections V 3 Bacterial infections*. Edited by W. J. J. Hausler & M. Sussman: Hodder Arnold.
- Foti, M., Ricciardi-Castagnoli, P. & Granucci, F. (2007).** Gene expression profiling of dendritic cells by microarray. *Methods in molecular biology (Clifton, NJ)* **380**, 215-224.
- Franchi, L., Amer, A., Body-Malapel, M. & other authors (2006).** Cytosolic flagellin requires Ipaf for activation of caspase-1 and interleukin 1beta in salmonella-infected macrophages. *Nature immunology* **7**, 576-582.
- Franchi, L., Park, J. H., Shaw, M. H., Marina-Garcia, N., Chen, G., Kim, Y. G. & Nunez, G. (2008).** Intracellular NOD-like receptors in innate immunity, infection and disease. *Cellular microbiology* **10**, 1-8.
- Freeman, J. A., Rappl, C., Kuhle, V., Hensel, M. & Miller, S. I. (2002).** SpiC is required for translocation of *Salmonella* pathogenicity island 2 effectors and secretion of translocon proteins SseB and SseC. *Journal of bacteriology* **184**, 4971-4980.
- French, T., So, P. T., Weaver, D. J., Jr., Coelho-Sampaio, T., Gratton, E., Voss, E. W., Jr. & Carrero, J. (1997).** Two-photon fluorescence lifetime imaging microscopy of macrophage-mediated antigen processing. *Journal of microscopy* **185**, 339-353.
- Frey, R. J. (2002).** Gale Encyclopedia of Medicine.
- Fukao, T., Matsuda, S. & Koyasu, S. (2000).** Synergistic effects of IL-4 and IL-18 on IL-12-dependent IFN-gamma production by dendritic cells. *J Immunol* **164**, 64-71.
- Garcia-del Portillo, F., Pucciarelli, M. G., Jefferies, W. A. & Finlay, B. B. (1994).** *Salmonella typhimurium* induces selective aggregation and internalization of host cell surface proteins during invasion of epithelial cells. *Journal of cell science* **107 (Pt 7)**, 2005-2020.
- Garcia-Del Portillo, F., Jungnitz, H., Rohde, M. & Guzman, C. A. (2000).** Interaction of *Salmonella enterica* Serotype Typhimurium with Dendritic Cells Is Defined by Targeting to Compartments Lacking Lysosomal Membrane Glycoproteins. *Infect Immun* **68**, 2985-2991.
- Gebert, A. (1997).** The role of M cells in the protection of mucosal membranes. *Histochemistry and cell biology* **108**, 455-470.

- Gentleman, R. C., Carey, V. J., Bates, D. M. & other authors (2004).** Bioconductor: open software development for computational biology and bioinformatics. *Genome biology* **5**, R80.
- Gershon, A. A. (2000).** Infectious diseases have shaped our world. In *38th Annual Meeting of the Infectious Diseases Society of America*. New Orleans.
- Giannella, R. A., Broitman, S. A. & Zamcheck, N. (1972).** Gastric acid barrier to ingested microorganisms in man: studies in vivo and in vitro. *Gut* **13**, 251-256.
- Ginocchio, C. C. & Galan, J. E. (1995).** Functional conservation among members of the Salmonella typhimurium InvA family of proteins. *Infection and immunity* **63**, 729-732.
- Gorba, T. & Allsopp, T. E. (2003).** Pharmacological potential of embryonic stem cells. *Pharmacol Res* **47**, 269-278.
- Graham, S. M., Molyneux, E. M., Walsh, A. L., Cheesbrough, J. S., Molyneux, M. E. & Hart, C. A. (2000).** Nontyphoidal Salmonella infections of children in tropical Africa. *The Pediatric infectious disease journal* **19**, 1189-1196.
- Granucci, F., Vizzardelli, C., Virzi, E., Rescigno, M. & Ricciardi-Castagnoli, P. (2001).** Transcriptional reprogramming of dendritic cells by differentiation stimuli. *European journal of immunology* **31**, 2539-2546.
- Green, J. M. (2000).** The B7/CD28/CTLA4 T-cell activation pathway. Implications for inflammatory lung disease. *American journal of respiratory cell and molecular biology* **22**, 261-264.
- Greenwald, R. J., Freeman, G. J. & Sharpe, A. H. (2005).** The B7 family revisited. *Annual review of immunology* **23**, 515-548.
- Guo, Y., Graham-Evans, B. & Broxmeyer, H. E. (2006).** Murine embryonic stem cells secrete cytokines/growth modulators that enhance cell survival/anti-apoptosis and stimulate colony formation of murine hematopoietic progenitor cells. *Stem cells (Dayton, Ohio)* **24**, 850-856.
- Handley, S. A. & Miller, V. L. (2007).** General and specific host responses to bacterial infection in Peyer's patches: a role for stromelysin-1 (matrix metalloproteinase-3) during Salmonella enterica infection. *Molecular microbiology* **64**, 94-110.
- Harenberg, A., Guillaume, F., Ryan, E. J., Burdin, N. & Spada, F. (2008).** Gene profiling analysis of ALVAC infected human monocyte derived dendritic cells. *Vaccine* doi:10.1016/j.vaccine.2008.07.050.
- Hawiger, D., Inaba, K., Dorsett, Y., Guo, M., Mahnke, K., Rivera, M., Ravetch, J. V., Steinman, R. M. & Nussenzweig, M. C. (2001).** Dendritic cells induce peripheral T cell unresponsiveness under steady state conditions in vivo. *The Journal of experimental medicine* **194**, 769-779.

- Hayashi, F., Smith, K. D., Ozinsky, A. & other authors (2001).** The innate immune response to bacterial flagellin is mediated by Toll-like receptor 5. *Nature* **410**, 1099-1103.
- Hayward, R. D., McGhie, E. J. & Koronakis, V. (2000a).** Membrane fusion activity of purified SipB, a Salmonella surface protein essential for mammalian cell invasion. *Molecular microbiology* **37**, 727-739.
- Hayward, R. E., Derisi, J. L., Alfarhli, S., Kaslow, D. C., Brown, P. O. & Rathod, P. K. (2000b).** Shotgun DNA microarrays and stage-specific gene expression in Plasmodium falciparum malaria. *Molecular microbiology* **35**, 6-14.
- Hensel, M. (2006).** Pathogenicity island and virulence of Salmonella enterica. In *Salmonella infections*. Edited by P. Mastroeni & D. Maskell: Cambridge University Press.
- Hermant, D., Menard, R., Arricau, N., Parsot, C. & Popoff, M. Y. (1995).** Functional conservation of the Salmonella and Shigella effectors of entry into epithelial cells. *Molecular microbiology* **17**, 781-789.
- Herrmann, M. & Pfaffl, M. W. (2005).** REST 2005 Greater certainty in expression studies. *Corbbet Research Pty Ltd*.
- Hicke, L. (2001).** Protein regulation by monoubiquitin. *Nat Rev Mol Cell Biol* **2**, 195-201.
- High, N., Mounier, J., Prevost, M. C. & Sansonetti, P. J. (1992).** IpaB of Shigella flexneri causes entry into epithelial cells and escape from the phagocytic vacuole. *The EMBO journal* **11**, 1991-1999.
- Hilbi, H., Moss, J. E., Hersh, D. & other authors (1998).** Shigella-induced apoptosis is dependent on caspase-1 which binds to IpaB. *The Journal of biological chemistry* **273**, 32895-32900.
- Hiscott, J., Beauparlant, P., Crepieux, P., DeLuca, C., Kwon, H., Lin, R. & Petropoulos, L. (1997).** Cellular and viral protein interactions regulating I kappa B alpha activity during human retrovirus infection. *Journal of leukocyte biology* **62**, 82-92.
- Hochrein, H., Shortman, K., Vremec, D., Scott, B., Hertzog, P. & O'Keeffe, M. (2001).** Differential production of IL-12, IFN-alpha, and IFN-gamma by mouse dendritic cell subsets. *J Immunol* **166**, 5448-5455.
- Hopkins, S. A., Niedergang, F., Cortesy-Theulaz, I. E. & Kraehenbuhl, J. P. (2000).** A recombinant Salmonella typhimurium vaccine strain is taken up and survives within murine Peyer's patch dendritic cells. *Cellular microbiology* **2**, 59-68.

- Inaba, K., Metlay, J. P., Crowley, M. T. & Steinman, R. M. (1990).** Dendritic cells pulsed with protein antigens in vitro can prime antigen-specific, MHC-restricted T cells in situ. *The Journal of experimental medicine* **172**, 631-640.
- Inaba, K., Inaba, M., Romani, N., Aya, H., Deguchi, M., Ikehara, S., Muramatsu, S. & Steinman, R. M. (1992).** Generation of large numbers of dendritic cells from mouse bone marrow cultures supplemented with granulocyte/macrophage colony-stimulating factor. *The Journal of experimental medicine* **176**, 1693-1702.
- Ivanova, N. B., Dimos, J. T., Schaniel, C., Hackney, J. A., Moore, K. A. & Lemischka, I. R. (2002).** A stem cell molecular signature. *Science* **298**, 601-604.
- Iwakoshi, N. N., Lee, A. H., Vallabhajosyula, P., Otipoby, K. L., Rajewsky, K. & Glimcher, L. H. (2003).** Plasma cell differentiation and the unfolded protein response intersect at the transcription factor XBP-1. *Nature immunology* **4**, 321-329.
- Iwakoshi, N. N., Pypaert, M. & Glimcher, L. H. (2007).** The transcription factor XBP-1 is essential for the development and survival of dendritic cells. *The Journal of experimental medicine* **204**, 2267-2275.
- Jantsch, J., Cheminay, C., Chakravorty, D., Lindig, T., Hein, J. & Hensel, M. (2003).** Intracellular activities of *Salmonella enterica* in murine dendritic cells. *Cellular microbiology* **5**, 933-945.
- Jarvelainen, H. A., Galmiche, A. & Zychlinsky, A. (2003).** Caspase-1 activation by *Salmonella*. *Trends in cell biology* **13**, 204-209.
- Jayakumar, A., Donovan, M. J., Tripathi, V., Ramalho-Ortigao, M. & McDowell, M. A. (2008).** *Leishmania major* infection activates NF-kappaB and interferon regulatory factors 1 and 8 in human dendritic cells. *Infection and immunity* **76**, 2138-2148.
- Jensen, P. E. (2007).** Recent advances in antigen processing and presentation. *Nature immunology* **8**, 1041-1048.
- Jepson, M. A. & Clark, M. A. (2001).** The role of M cells in *Salmonella* infection. *Microbes and infection / Institut Pasteur* **3**, 1183-1190.
- Johansson, C. & Wick, M. J. (2004).** Liver dendritic cells present bacterial antigens and produce cytokines upon *Salmonella* encounter. *J Immunol* **172**, 2496-2503.
- Jones, B. D. & Falkow, S. (1996).** Salmonellosis: host immune responses and bacterial virulence determinants. *Annual review of immunology* **14**, 533-561.
- Kafatos, F. C., Jones, C. W. & Efstratiadis, A. (1979).** Determination of nucleic acid sequence homologies and relative concentrations by a dot hybridization procedure. *Nucleic acids research* **7**, 1541-1552.

- Kaler, S. G. (2008).** Diseases of poverty with high mortality in infants and children: malaria, measles, lower respiratory infections, and diarrheal illnesses. *Annals of the New York Academy of Sciences* **1136**, 28-31.
- Kaufman, R. J. (1999).** Stress signaling from the lumen of the endoplasmic reticulum: coordination of gene transcriptional and translational controls. *Genes & development* **13**, 1211-1233.
- Keller, G. (2005).** Embryonic stem cell differentiation: emergence of a new era in biology and medicine. *Genes & development* **19**, 1129-1155.
- Keller, G. M. (1995).** In vitro differentiation of embryonic stem cells. *Current opinion in cell biology* **7**, 862-869.
- Kholodenko, B. N. (2006).** Cell-signalling dynamics in time and space. *Nat Rev Mol Cell Biol* **7**, 165-176.
- Kikuchi, K., Yanagawa, Y., Aranami, T., Iwabuchi, C., Iwabuchi, K. & Onoe, K. (2003).** Tumour necrosis factor-alpha but not lipopolysaccharide enhances preference of murine dendritic cells for Th2 differentiation. *Immunology* **108**, 42-49.
- Kokame, K., Agarwala, K. L., Kato, H. & Miyata, T. (2000).** Herp, a new ubiquitin-like membrane protein induced by endoplasmic reticulum stress. *The Journal of biological chemistry* **275**, 32846-32853.
- Kolb-Maurer, A., Weissinger, F., Kurzai, O., Maurer, M., Wilhelm, M. & Goebel, W. (2004).** Bacterial infection of human hematopoietic stem cells induces monocytic differentiation. *FEMS immunology and medical microbiology* **40**, 147-153.
- Konopka, J. L., Penalva, L. O., Thompson, J. M., White, L. J., Beard, C. W., Keene, J. D. & Johnston, R. E. (2007).** A two-phase innate host response to alphavirus infection identified by mRNP-tagging in vivo. *PLoS pathogens* **3**, e199.
- Kopper, O. & Benvenisty, N. (2005).** Manipulation of the human genome in human embryonic stem cells. *Stem cell reviews* **1**, 145-150.
- Korecka, J. A., Verhaagen, J. & Hol, E. M. (2007).** Cell-replacement and gene-therapy strategies for Parkinson's and Alzheimer's disease. *Regenerative medicine* **2**, 425-446.
- Kristensen, D. M., Kalisz, M. & Nielsen, J. H. (2005).** Cytokine signalling in embryonic stem cells. *Apmis* **113**, 756-772.
- Kubori, T., Matsushima, Y., Nakamura, D., Uralil, J., Lara-Tejero, M., Sukhan, A., Galan, J. E. & Aizawa, S. I. (1998).** Supramolecular structure of the Salmonella typhimurium type III protein secretion system. *Science (New York, NY)* **280**, 602-605.
- Kubori, T. & Galan, J. E. (2003).** Temporal regulation of salmonella virulence effector function by proteasome-dependent protein degradation. *Cell* **115**, 333-342.

- Kuhle, V. & Hensel, M. (2002).** SseF and SseG are translocated effectors of the type III secretion system of Salmonella pathogenicity island 2 that modulate aggregation of endosomal compartments. *Cellular microbiology* **4**, 813-824.
- Kuhle, V., Abrahams, G. L. & Hensel, M. (2006).** Intracellular Salmonella enterica redirect exocytic transport processes in a Salmonella pathogenicity island 2-dependent manner. *Traffic (Copenhagen, Denmark)* **7**, 716-730.
- Kweon, M. N. (2008).** Shigellosis: the current status of vaccine development. *Current opinion in infectious diseases* **21**, 313-318.
- Lara-Tejero, M., Sutterwala, F. S., Ogura, Y., Grant, E. P., Bertin, J., Coyle, A. J., Flavell, R. A. & Galan, J. E. (2006).** Role of the caspase-1 inflammasome in Salmonella typhimurium pathogenesis. *The Journal of experimental medicine* **203**, 1407-1412.
- Lee, A. H., Zareei, M. P. & Daefler, S. (2002).** Identification of a NIPSNAP homologue as host cell target for Salmonella virulence protein SpiC. *Cellular microbiology* **4**, 739-750.
- Lengeling, A., Pfeffer, K. & Balling, R. (2001).** The battle of two genomes: genetics of bacterial host/pathogen interactions in mice. *Mamm Genome* **12**, 261-271.
- Lindvall, O. (2003).** Stem cells for cell therapy in Parkinson's disease. *Pharmacol Res* **47**, 279-287.
- Lisowski, L. & Sadelain, M. (2008).** Current status of globin gene therapy for the treatment of beta-thalassaemia. *British journal of haematology* **141**, 335-345.
- Liu-Mares, W., Sun, Z., Bamlet, W. R., Atkinson, E. J., Fridley, B. L., Slager, S. L., de Andrade, M. & Goode, E. L. (2007).** Analysis of variation in NF-kappaB genes and expression levels of NF-kappaB-regulated molecules. *BMC proceedings* **1 Suppl 1**, S126.
- Liu, Y. J. (2005).** IPC: professional type 1 interferon-producing cells and plasmacytoid dendritic cell precursors. *Annual review of immunology* **23**, 275-306.
- Livak, K. J. & Schmittgen, T. D. (2001).** Analysis of relative gene expression data using real-time quantitative PCR and the 2(-Delta Delta C(T)) Method. *Methods (San Diego, Calif)* **25**, 402-408.
- Lockhart, D. J. & Winzeler, E. A. (2000).** Genomics, gene expression and DNA arrays. *Nature* **405**, 827-836.
- Loh, Y. H., Wu, Q., Chew, J. L. & other authors (2006).** The Oct4 and Nanog transcription network regulates pluripotency in mouse embryonic stem cells. *Nature genetics* **38**, 431-440.
- Lopez, S. M. C. d. S. & Mummery, C. L. (2004).** Differentiation in Early Development. *Handbook of Stem Cells* **1**, 143-156.

- Luo, X., Tarbell, K. V., Yang, H., Pothoven, K., Bailey, S. L., Ding, R., Steinman, R. M. & Suthanthiran, M. (2007).** Dendritic cells with TGF-beta1 differentiate naive CD4+CD25- T cells into islet-protective Foxp3+ regulatory T cells. *Proceedings of the National Academy of Sciences of the United States of America* **104**, 2821-2826.
- Lupo, P., Chang, Y. C., Kelsall, B. L., Farber, J. M., Pietrella, D., Vecchiarelli, A., Leon, F. & Kwon-Chung, K. J. (2008).** The presence of capsule in *Cryptococcus neoformans* influences the gene expression profile in dendritic cells during interaction with the fungus. *Infection and immunity* **76**, 1581-1589.
- Lutz, M. B. & Schuler, G. (2002).** Immature, semi-mature and fully mature dendritic cells: which signals induce tolerance or immunity? *Trends in immunology* **23**, 445-449.
- Lynn, D. J., Winsor, G. L., Chan, C. & other authors (2008).** InnateDB: facilitating systems-level analyses of the mammalian innate immune response. *Molecular systems biology* **4**, 218.
- Magliocca, J. F., Held, I. K. & Odorico, J. S. (2006).** Undifferentiated murine embryonic stem cells cannot induce portal tolerance but may possess immune privilege secondary to reduced major histocompatibility complex antigen expression. *Stem cells and development* **15**, 707-717.
- Magnuson, T., Demsey, A. & Stackpole, C. W. (1977).** Characterization of intercellular junctions in the preimplantation mouse embryo by freeze-fracture and thin-section electron microscopy. *Dev Biol* **61**, 252-261.
- Magram, J., Connaughton, S. E., Warrior, R. R. & other authors (1996a).** IL-12-deficient mice are defective in IFN gamma production and type 1 cytokine responses. *Immunity* **4**, 471-481.
- Magram, J., Sfarra, J., Connaughton, S. & other authors (1996b).** IL-12-deficient mice are defective but not devoid of type 1 cytokine responses. *Annals of the New York Academy of Sciences* **795**, 60-70.
- Maniatis, G. M., Ramirez, F., Cann, A., Marks, P. A. & Bank, A. (1976).** Translation and stability of human globin mRNA in *Xenopus* oocytes. *The Journal of clinical investigation* **58**, 1419-1427.
- Marcus, S. L., Knodler, L. A. & Finlay, B. B. (2002).** *Salmonella enterica* serovar Typhimurium effector SigD/SopB is membrane-associated and ubiquitinated inside host cells. *Cellular microbiology* **4**, 435-446.
- Margulies, M., Egholm, M., Altman, W. E. & other authors (2005).** Genome sequencing in microfabricated high-density picolitre reactors. *Nature* **437**, 376-380.
- Marriott, I., Hammond, T. G., Thomas, E. K. & Bost, K. L. (1999).** *Salmonella* efficiently enter and survive within cultured CD11c+ dendritic cells initiating cytokine expression. *European journal of immunology* **29**, 1107-1115.

- Martin, G. R. (1981).** Isolation of a pluripotent cell line from early mouse embryos cultured in medium conditioned by teratocarcinoma stem cells. *Proceedings of the National Academy of Sciences of the United States of America* **78**, 7634-7638.
- Mathers, C. D. & Loncar, D. (2006).** Projections of global mortality and burden of disease from 2002 to 2030. *PLoS medicine* **3**, e442.
- Mattner, F., Magram, J., Ferrante, J., Launois, P., Di Padova, K., Behin, R., Gately, M. K., Louis, J. A. & Alber, G. (1996).** Genetically resistant mice lacking interleukin-12 are susceptible to infection with *Leishmania major* and mount a polarized Th2 cell response. *European journal of immunology* **26**, 1553-1559.
- McGuire, K. & Glass, E. J. (2005).** The expanding role of microarrays in the investigation of macrophage responses to pathogens. *Veterinary immunology and immunopathology* **105**, 259-275.
- McKelvie, N. D., Stratford, R., Wu, T. & other authors (2004).** Expression of heterologous antigens in *Salmonella Typhimurium* vaccine vectors using the in vivo-inducible, SPI-2 promoter, *ssaG*. *Vaccine* **22**, 3243-3255.
- Medigeshi, G. R., Lancaster, A. M., Hirsch, A. J. & other authors (2007).** West Nile virus infection activates the unfolded protein response, leading to CHOP induction and apoptosis. *Journal of virology* **81**, 10849-10860.
- Medzhitov, R. (2001).** Toll-like receptors and innate immunity. *Nat Rev Immunol* **1**, 135-145.
- Melton, D. A. & Cowan, C. (2004).** "Stemness": Definitions, Criteria, and Standards. *Handbook of Stem Cells* **1**, XXV-XXXi.
- Menard, R., Sansonetti, P. & Parsot, C. (1994).** The secretion of the *Shigella flexneri* Ipa invasins is activated by epithelial cells and controlled by IpaB and IpaD. *The EMBO journal* **13**, 5293-5302.
- Menendez, P., Bueno, C., Wang, L. & Bhatia, M. (2005).** Human embryonic stem cells: potential tool for achieving immunotolerance? *Stem cell reviews* **1**, 151-158.
- Menges, M., Rossner, S., Voigtlander, C., Schindler, H., Kukutsch, N. A., Bogdan, C., Erb, K., Schuler, G. & Lutz, M. B. (2002).** Repetitive injections of dendritic cells matured with tumor necrosis factor alpha induce antigen-specific protection of mice from autoimmunity. *The Journal of experimental medicine* **195**, 15-21.
- Mercado-Lubo, R., Gauger, E. J., Leatham, M. P., Conway, T. & Cohen, P. S. (2008).** A *Salmonella enterica* serovar typhimurium succinate dehydrogenase/fumarate reductase double mutant is avirulent and immunogenic in BALB/c mice. *Infection and immunity* **76**, 1128-1134.
- Meresse, S., Unsworth, K. E., Habermann, A., Griffiths, G., Fang, F., Martinez-Lorenzo, M. J., Waterman, S. R., Gorvel, J. P. & Holden, D. W. (2001).**

- Remodelling of the actin cytoskeleton is essential for replication of intravacuolar Salmonella. *Cellular microbiology* **3**, 567-577.
- Meslin, F. X., Heymann, D. L. & Witt, C. (1998).** Monitoring infectious diseases. *Annals of the New York Academy of Sciences* **862**, 205-210.
- Miao, E. A., Alpuche-Aranda, C. M., Dors, M., Clark, A. E., Bader, M. W., Miller, S. I. & Aderem, A. (2006).** Cytoplasmic flagellin activates caspase-1 and secretion of interleukin 1beta via Ipaf. *Nature immunology* **7**, 569-575.
- Milne, T. S., Michell, S. L., Diaper, H., Wikstrom, P., Svensson, K., Oyston, P. C. & Titball, R. W. (2007).** A 55 kDa hypothetical membrane protein is an iron-regulated virulence factor of Francisella tularensis subsp. novicida U112. *Journal of medical microbiology* **56**, 1268-1276.
- Miold, S., Ehrbar, K., Weissmuller, A., Prager, R., Tschape, H., Russmann, H. & Hardt, W. D. (2001).** Salmonella host cell invasion emerged by acquisition of a mosaic of separate genetic elements, including Salmonella pathogenicity island 1 (SPI1), SPI5, and sopE2. *Journal of bacteriology* **183**, 2348-2358.
- Mirza, S. H., Beeching, N. J. & Hart, C. A. (1996).** Multi-drug resistant typhoid: a global problem. *Journal of medical microbiology* **44**, 317-319.
- Mitchell, E. K., Mastroeni, P., Kelly, A. P. & Trowsdale, J. (2004).** Inhibition of cell surface MHC class II expression by Salmonella. *European journal of immunology* **34**, 2559-2567.
- Mittrucker, H. W. & Kaufmann, S. H. (2000).** Immune response to infection with Salmonella typhimurium in mice. *Journal of leukocyte biology* **67**, 457-463.
- Monack, D. M., Hersh, D., Ghori, N., Bouley, D., Zychlinsky, A. & Falkow, S. (2000).** Salmonella exploits caspase-1 to colonize Peyer's patches in a murine typhoid model. *The Journal of experimental medicine* **192**, 249-258.
- Montaner, D., Tarraga, J., Huerta-Cepas, J. & other authors (2006).** Next station in microarray data analysis: GEPAS. *Nucleic acids research* **34**, W486-491.
- Moore, K. J., Fabunmi, R. P., Andersson, L. P. & Freeman, M. W. (1998).** In vitro-differentiated embryonic stem cell macrophages: a model system for studying atherosclerosis-associated macrophage functions. *Arteriosclerosis, thrombosis, and vascular biology* **18**, 1647-1654.
- Morgan, E. T. (2001).** Regulation of cytochrome p450 by inflammatory mediators: why and how? *Drug metabolism and disposition: the biological fate of chemicals* **29**, 207-212.
- Nakano, T., Kodama, H. & Honjo, T. (1994).** Generation of lymphohematopoietic cells from embryonic stem cells in culture. *Science (New York, NY)* **265**, 1098-1101.

- Nascimento-Carvalho, C. M., Ribeiro, C. T., Cardoso, M. R. & other authors (2008).** The Role of Respiratory Viral Infections among Children Hospitalized for Community-Acquired Pneumonia in a Developing Country. *The Pediatric infectious disease journal*.
- Nau, G. J., Richmond, J. F., Schlesinger, A., Jennings, E. G., Lander, E. S. & Young, R. A. (2002).** Human macrophage activation programs induced by bacterial pathogens. *Proceedings of the National Academy of Sciences of the United States of America* **99**, 1503-1508.
- Nelson-Rees, W. A., Daniels, D. W. & Flandermeyer, R. R. (1981).** Cross-contamination of cells in culture. *Science (New York, NY)* **212**, 446-452.
- Neutra, M. R., Mantis, N. J. & Kraehenbuhl, J. P. (2001).** Collaboration of epithelial cells with organized mucosal lymphoid tissues. *Nature immunology* **2**, 1004-1009.
- Niebuhr, K., Jouihri, N., Allaoui, A., Gounon, P., Sansonetti, P. J. & Parsot, C. (2000).** IpgD, a protein secreted by the type III secretion machinery of *Shigella flexneri*, is chaperoned by IpgE and implicated in entry focus formation. *Molecular microbiology* **38**, 8-19.
- Niedergang, F., Sirard, J. C., Blanc, C. T. & Kraehenbuhl, J. P. (2000).** Entry and survival of *Salmonella typhimurium* in dendritic cells and presentation of recombinant antigens do not require macrophage-specific virulence factors. *Proceedings of the National Academy of Sciences of the United States of America* **97**, 14650-14655.
- Niedergang, F., Didierlaurent, A., Kraehenbuhl, J. P. & Sirard, J. C. (2004).** Dendritic cells: the host Achilles' heel for mucosal pathogens? *Trends in microbiology* **12**, 79-88.
- Nishikawa, S. I., Nishikawa, S., Hirashima, M., Matsuyoshi, N. & Kodama, H. (1998).** Progressive lineage analysis by cell sorting and culture identifies FLK1+VE-cadherin+ cells at a diverging point of endothelial and hemopoietic lineages. *Development (Cambridge, England)* **125**, 1747-1757.
- Niyogi, S. K. (2005).** Shigellosis. *Journal of microbiology (Seoul, Korea)* **43**, 133-143.
- Nussenzweig, M. C., Steinman, R. M., Gutchinov, B. & Cohn, Z. A. (1980).** Dendritic cells are accessory cells for the development of anti-trinitrophenyl cytotoxic T lymphocytes. *The Journal of experimental medicine* **152**, 1070-1084.
- Odegaard, J. I., Vats, D., Zhang, L., Ricardo-Gonzalez, R., Smith, K. L., Sykes, D. B., Kamps, M. P. & Chawla, A. (2007).** Quantitative expansion of ES cell-derived myeloid progenitors capable of differentiating into macrophages. *Journal of leukocyte biology* **81**, 711-719.
- Ohl, M. E. & Miller, S. I. (2001).** *Salmonella*: a model for bacterial pathogenesis. *Annu Rev Med* **52**, 259-274.

- Ohnishi, K., Fan, F., Schoenhals, G. J., Kihara, M. & Macnab, R. M. (1997).** The FliO, FliP, FliQ, and FliR proteins of *Salmonella typhimurium*: putative components for flagellar assembly. *Journal of bacteriology* **179**, 6092-6099.
- Ohya, K., Handa, Y., Ogawa, M., Suzuki, M. & Sasakawa, C. (2005).** IpgB1 is a novel *Shigella* effector protein involved in bacterial invasion of host cells. Its activity to promote membrane ruffling via Rac1 and Cdc42 activation. *The Journal of biological chemistry* **280**, 24022-24034.
- Okoniewski, M. J. & Miller, C. J. (2008).** Comprehensive analysis of affymetrix exon arrays using BioConductor. *PLoS computational biology* **4**, e6.
- Oldach, D. W., Richard, R. E., Borza, E. N. & Benitez, R. M. (1998).** A mysterious death. *N Engl J Med* **338**, 1764-1769.
- Pal, C., Ganguly, D., Paul, K. & Pal, S. (2007).** Dendritic cells and antigen trapping technology--a revolution in vaccine/immunotherapy strategy. *Indian journal of experimental biology* **45**, 491-504.
- Park, S. J., Nakagawa, T., Kitamura, H. & other authors (2004).** IL-6 regulates in vivo dendritic cell differentiation through STAT3 activation. *J Immunol* **173**, 3844-3854.
- Parry, C. M. (2006).** Epidemiological and clinical aspects of human typhoid fever. In *Salmonella infections*. Edited by P. Mastroeni & D. Maskell: Cambridge University Press.
- Pascale Cossart, P. B., Staffan Normark, Rino Rappuoli (Second Edition 2005).** *Cellular Microbiology*.
- Pasquali, P. (2004).** HIV infections and zoonoses. *FAO Animal Production and Health* **163**.
- Patel, J. C. & Galan, J. E. (2006).** Differential activation and function of Rho GTPases during *Salmonella*-host cell interactions. *The Journal of cell biology* **175**, 453-463.
- Persson, J. & Vance, R. E. (2007).** Genetics-squared: combining host and pathogen genetics in the analysis of innate immunity and bacterial virulence. *Immunogenetics* **59**, 761-778.
- Petrovska, L., Aspinall, R. J., Barber, L. & other authors (2004).** *Salmonella enterica* serovar Typhimurium interaction with dendritic cells: impact of the *sifA* gene. *Cellular microbiology* **6**, 1071-1084.
- Pfaffl, M. W., Horgan, G. W. & Dempfle, L. (2002).** Relative expression software tool (REST) for group-wise comparison and statistical analysis of relative expression results in real-time PCR. *Nucleic acids research* **30**, e36.
- Plotkin, S. A. (2005).** Vaccines: past, present and future. *Nat Med* **11**, S5-11.

- Poltorak, A., He, X., Smirnova, I. & other authors (1998).** Defective LPS signaling in C3H/HeJ and C57BL/10ScCr mice: mutations in Tlr4 gene. *Science (New York, NY)* **282**, 2085-2088.
- Ponka, P. (1999).** Cell biology of heme. *The American journal of the medical sciences* **318**, 241-256.
- Purdy, G. E., Hong, M. & Payne, S. M. (2002).** Shigella flexneri DegP facilitates IcsA surface expression and is required for efficient intercellular spread. *Infection and immunity* **70**, 6355-6364.
- Rajeevan, M. S., Ranamukhaarachchi, D. G., Vernon, S. D. & Unger, E. R. (2001).** Use of real-time quantitative PCR to validate the results of cDNA array and differential display PCR technologies. *Methods (San Diego, Calif)* **25**, 443-451.
- Ramalho-Santos, M., Yoon, S., Matsuzaki, Y., Mulligan, R. C. & Melton, D. A. (2002).** "Stemness": transcriptional profiling of embryonic and adult stem cells. *Science* **298**, 597-600.
- Ramirez-Solis, R., Liu, P. & Bradley, A. (1995).** Chromosome engineering in mice. *Nature* **378**, 720-724.
- Ramsden, A. E., Holden, D. W. & Mota, L. J. (2007).** Membrane dynamics and spatial distribution of Salmonella-containing vacuoles. *Trends in microbiology* **15**, 516-524.
- Rescigno, M., Urbano, M., Valzasina, B., Francolini, M., Rotta, G., Bonasio, R., Granucci, F., Kraehenbuhl, J. P. & Ricciardi-Castagnoli, P. (2001).** Dendritic cells express tight junction proteins and penetrate gut epithelial monolayers to sample bacteria. *Nature immunology* **2**, 361-367.
- Rimoldi, M., Chieppa, M., Vulcano, M., Allavena, P. & Rescigno, M. (2004).** Intestinal epithelial cells control dendritic cell function. *Annals of the New York Academy of Sciences* **1029**, 66-74.
- Rosenberger, C. M., Scott, M. G., Gold, M. R., Hancock, R. E. & Finlay, B. B. (2000).** Salmonella typhimurium infection and lipopolysaccharide stimulation induce similar changes in macrophage gene expression. *J Immunol* **164**, 5894-5904.
- Rosenberger, C. M., Pollard, A. J. & Finlay, B. B. (2001).** Gene array technology to determine host responses to Salmonella. *Microbes and infection / Institut Pasteur* **3**, 1353-1360.
- Sansonetti, P. (2002).** Host-pathogen interactions: the seduction of molecular cross talk. *Gut* **50 Suppl 3**, III2-8.
- Sansonetti, P. J., Ryter, A., Clerc, P., Maurelli, A. T. & Mounier, J. (1986).** Multiplication of Shigella flexneri within HeLa cells: lysis of the phagocytic vacuole and plasmid-mediated contact hemolysis. *Infection and immunity* **51**, 461-469.

- Sansonetti, P. J., Mounier, J., Prevost, M. C. & Mege, R. M. (1994).** Cadherin expression is required for the spread of *Shigella flexneri* between epithelial cells. *Cell* **76**, 829-839.
- Sansonetti, P. J. (2004).** War and peace at mucosal surfaces. *Nat Rev Immunol* **4**, 953-964.
- Sansonetti, P. J. (2006).** Shigellosis: an old disease in new clothes? *PLoS medicine* **3**, e354.
- Santana, A., Ensenat-Waser, R., Arribas, M. I., Reig, J. A. & Roche, E. (2006).** Insulin-producing cells derived from stem cells: recent progress and future directions. *Journal of cellular and molecular medicine* **10**, 866-883.
- Schmitt, T. M., de Pooter, R. F., Gronski, M. A., Cho, S. K., Ohashi, P. S. & Zuniga-Pflucker, J. C. (2004).** Induction of T cell development and establishment of T cell competence from embryonic stem cells differentiated in vitro. *Nature immunology* **5**, 410-417.
- Schroeder, A., Mueller, O., Stocker, S. & other authors (2006).** The RIN: an RNA integrity number for assigning integrity values to RNA measurements. *BMC molecular biology* **7**, 3.
- Schuch, R., Sandlin, R. C. & Maurelli, A. T. (1999).** A system for identifying post-invasion functions of invasion genes: requirements for the Mxi-Spa type III secretion pathway of *Shigella flexneri* in intercellular dissemination. *Molecular microbiology* **34**, 675-689.
- Schulz, O., Edwards, A. D., Schito, M., Aliberti, J., Manickasingham, S., Sher, A. & Reis e Sousa, C. (2000).** CD40 triggering of heterodimeric IL-12 p70 production by dendritic cells in vivo requires a microbial priming signal. *Immunity* **13**, 453-462.
- Senju, S., Hirata, S., Matsuyoshi, H., Masuda, M., Uemura, Y., Araki, K., Yamamura, K. & Nishimura, Y. (2003).** Generation and genetic modification of dendritic cells derived from mouse embryonic stem cells. *Blood* **101**, 3501-3508.
- Shen, L., Sigal, L. J., Boes, M. & Rock, K. L. (2004).** Important role of cathepsin S in generating peptides for TAP-independent MHC class I crosspresentation in vivo. *Immunity* **21**, 155-165.
- Shin, J. W., Jin, P., Fan, Y. & other authors (2008).** Evaluation of gene expression profiles of immature dendritic cells prepared from peripheral blood mononuclear cells. *Transfusion* **48**, 647-657.
- Shotland, Y., Kramer, H. & Groisman, E. A. (2003).** The *Salmonella* SpiC protein targets the mammalian Hook3 protein function to alter cellular trafficking. *Molecular microbiology* **49**, 1565-1576.
- Siegemund, S., Schutze, N., Freudenberg, M. A., Lutz, M. B., Straubinger, R. K. & Alber, G. (2007).** Production of IL-12, IL-23 and IL-27p28 by bone marrow-derived

conventional dendritic cells rather than macrophages after LPS/TLR4-dependent induction by *Salmonella* Enteritidis. *Immunobiology* **212**, 739-750.

Singer, C. (1989). A history of biology to about the year 1900. Iowa State University Press.

Skoudy, A., Mounier, J., Aruffo, A., Ohayon, H., Gounon, P., Sansonetti, P. & Tran Van Nhieu, G. (2000). CD44 binds to the *Shigella* IpaB protein and participates in bacterial invasion of epithelial cells. *Cellular microbiology* **2**, 19-33.

Smilde, A. K., Jansen, J. J., Hoefsloot, H. C., Lamers, R. J., van der Greef, J. & Timmerman, M. E. (2005). ANOVA-simultaneous component analysis (ASCA): a new tool for analyzing designed metabolomics data. *Bioinformatics (Oxford, England)* **21**, 3043-3048.

Smith, A. C., Heo, W. D., Braun, V. & other authors (2007). A network of Rab GTPases controls phagosome maturation and is modulated by *Salmonella* enterica serovar Typhimurium. *The Journal of cell biology* **176**, 263-268.

Smith, A. G., Heath, J. K., Donaldson, D. D., Wong, G. G., Moreau, J., Stahl, M. & Rogers, D. (1988). Inhibition of pluripotential embryonic stem cell differentiation by purified polypeptides. *Nature* **336**, 688-690.

Smith, A. G. (2001). Embryo-derived stem cells: of mice and men. *Annu Rev Cell Dev Biol* **17**, 435-462.

Soilleux, E. J. (2003). DC-SIGN (dendritic cell-specific ICAM-grabbing non-integrin) and DC-SIGN-related (DC-SIGNR): friend or foe? *Clin Sci (Lond)* **104**, 437-446.

Sokol, C. L., Barton, G. M., Farr, A. G. & Medzhitov, R. (2008). A mechanism for the initiation of allergen-induced T helper type 2 responses. *Nature immunology* **9**, 310-318.

Solter, D. & Knowles, B. B. (1978). Monoclonal antibody defining a stage-specific mouse embryonic antigen (SSEA-1). *Proceedings of the National Academy of Sciences of the United States of America* **75**, 5565-5569.

Sparwasser, T. & Eberl, G. (2007). BAC to immunology--bacterial artificial chromosome-mediated transgenesis for targeting of immune cells. *Immunology* **121**, 308-313.

Stanford, W. L., Cohn, J. B. & Cordes, S. P. (2001). Gene-trap mutagenesis: past, present and beyond. *Nature reviews* **2**, 756-768.

Steinman, R. M. & Cohn, Z. A. (1973). Identification of a novel cell type in peripheral lymphoid organs of mice. I. Morphology, quantitation, tissue distribution. *The Journal of experimental medicine* **137**, 1142-1162.

- Steinman, R. M. & Cohn, Z. A. (1974).** Identification of a novel cell type in peripheral lymphoid organs of mice. II. Functional properties in vitro. *The Journal of experimental medicine* **139**, 380-397.
- Steinman, R. M., Lustig, D. S. & Cohn, Z. A. (1974).** Identification of a novel cell type in peripheral lymphoid organs of mice. 3. Functional properties in vivo. *The Journal of experimental medicine* **139**, 1431-1445.
- Steinman, R. M. & Witmer, M. D. (1978).** Lymphoid dendritic cells are potent stimulators of the primary mixed leukocyte reaction in mice. *Proceedings of the National Academy of Sciences of the United States of America* **75**, 5132-5136.
- Stevens, L. C. (1984).** Spontaneous and experimentally induced testicular teratomas in mice. *Cell differentiation* **15**, 69-74.
- Stober, D., Schirmbeck, R. & Reimann, J. (2001).** IL-12/IL-18-dependent IFN-gamma release by murine dendritic cells. *J Immunol* **167**, 957-965.
- Sukhan, A. (2000).** The invasion-associated type III secretion system of *Salmonella typhimurium*: common and unique features. *Cell Mol Life Sci* **57**, 1033-1049.
- Sundquist, M. & Wick, M. J. (2005).** TNF-alpha-dependent and -independent maturation of dendritic cells and recruited CD11c(int)CD11b+ Cells during oral *Salmonella* infection. *J Immunol* **175**, 3287-3298.
- Suzuki, T., Saga, S. & Sasakawa, C. (1996).** Functional analysis of *Shigella* VirG domains essential for interaction with vinculin and actin-based motility. *The Journal of biological chemistry* **271**, 21878-21885.
- Svensson, M., Johansson, C. & Wick, M. J. (2000).** *Salmonella enterica* Serovar Typhimurium-Induced Maturation of Bone Marrow-Derived Dendritic Cells. *Infect Immun* **68**, 6311-6320.
- Swenson, G. R., Patino, M. M., Beck, M. M., Gaffield, L. & Walden, W. E. (1991).** Characteristics of the interaction of the ferritin repressor protein with the iron-responsive element. *Biology of metals* **4**, 48-55.
- Syvanen, A. C. (2005).** Toward genome-wide SNP genotyping. *Nature genetics* **37** Suppl, S5-10.
- Tailleux, L., Waddell, S. J., Pelizzola, M. & other authors (2008).** Probing host pathogen cross-talk by transcriptional profiling of both *Mycobacterium tuberculosis* and infected human dendritic cells and macrophages. *PLoS ONE* **3**, e1403.
- Takeuchi, O. & Akira, S. (2007).** Toll-like receptor signaling. In *Dendritic cell interactions with bacteria*, pp. 25-50. Edited by M. Rescigno: Cambridge University Press.
- Tangri, S., Brossay, L., Burdin, N., Lee, D. J., Corr, M. & Kronenberg, M. (1998).** Presentation of peptide antigens by mouse CD1 requires endosomal localization and

- protein antigen processing. *Proceedings of the National Academy of Sciences of the United States of America* **95**, 14314-14319.
- Tarkowski, A. K. (1961).** Mouse chimaeras developed from fused eggs. *Nature* **190**, 857-860.
- Tartour, E. & Kadereit, S. (2006).** Immunogenicity of embryonic stem cells and future directions to improve transplantation tolerance. *Atelier de formation Inserm 171; 16-17 November 2006 Cellules souches: du concept a la clinique*.
- Terme, M., Tomasello, E., Maruyama, K. & other authors (2004).** IL-4 confers NK stimulatory capacity to murine dendritic cells: a signaling pathway involving KARAP/DAP12-triggering receptor expressed on myeloid cell 2 molecules. *J Immunol* **172**, 5957-5966.
- The Nobel Prize Assembly (Press Release 2007-10-08).** The Nobel Prize in Physiology or Medicine 2007 In *Principles for introducing specific gene modifications in mice by the use of embryonic stem cells*.
- Thomson, H. (2007).** Bioprocessing of embryonic stem cells for drug discovery. *Trends in biotechnology* **25**, 224-230.
- Torihashi, S. (2006).** Formation of gut-like structures in vitro from mouse embryonic stem cells. *Methods in molecular biology (Clifton, NJ)* **330**, 279-285.
- Tortorella, D., Gewurz, B. E., Furman, M. H., Schust, D. J. & Ploegh, H. L. (2000).** Viral subversion of the immune system. *Annual review of immunology* **18**, 861-926.
- Tran Van Nhieu, G., Caron, E., Hall, A. & Sansonetti, P. J. (1999).** IpaC induces actin polymerization and filopodia formation during Shigella entry into epithelial cells. *The EMBO journal* **18**, 3249-3262.
- Trinchieri, G. & Sher, A. (2007).** Cooperation of Toll-like receptor signals in innate immune defence. *Nat Rev Immunol* **7**, 179-190.
- Tsai, B., Ye, Y. & Rapoport, T. A. (2002).** Retro-translocation of proteins from the endoplasmic reticulum into the cytosol. *Nat Rev Mol Cell Biol* **3**, 246-255.
- Uchiya, K., Barbieri, M. A., Funato, K., Shah, A. H., Stahl, P. D. & Groisman, E. A. (1999).** A Salmonella virulence protein that inhibits cellular trafficking. *The EMBO journal* **18**, 3924-3933.
- Uchiya, K. & Nikai, T. (2005).** Salmonella pathogenicity island 2-dependent expression of suppressor of cytokine signaling 3 in macrophages. *Infection and immunity* **73**, 5587-5594.
- UNICEF (2003).** Malaria technical note #6.
- UNICEF (2005).** Joint press release: Global goal to reduce measles in children surpassed.

- Uthe, J. J., Royace, A., Lunney, J. K., Stabel, T. J., Zhao, S. H., Tuggle, C. K. & Bearson, S. M. (2007). Porcine differential gene expression in response to *Salmonella enterica* serovars Choleraesuis and Typhimurium. *Molecular immunology* **44**, 2900-2914.
- Vallon-Eberhard, A., Landsman, L., Yogev, N., Verrier, B. & Jung, S. (2006). Transepithelial pathogen uptake into the small intestinal lamina propria. *J Immunol* **176**, 2465-2469.
- van Helden, S. F., van Leeuwen, F. N. & Figdor, C. G. (2008). Human and murine model cell lines for dendritic cell biology evaluated. *Immunology letters* **117**, 191-197.
- van Steensel, B. (2005). Mapping of genetic and epigenetic regulatory networks using microarrays. *Nature genetics* **37 Suppl**, S18-24.
- Villadangos, J. A. & Schnorrer, P. (2007). Intrinsic and cooperative antigen-presenting functions of dendritic-cell subsets in vivo. *Nat Rev Immunol* **7**, 543-555.
- Vivekanandhana, A. & Klinman, D. M. (2007). Contribution of MAPAK and NF- κ B signaling to TLR mediated MCP-1 secretion. *Cytokine* **39**.
- Wagener, F. A., Volk, H. D., Willis, D., Abraham, N. G., Soares, M. P., Adema, G. J. & Figdor, C. G. (2003). Different faces of the heme-heme oxygenase system in inflammation. *Pharmacological reviews* **55**, 551-571.
- Walker, L., Levine, H. & Jucker, M. (2006). Koch's postulates and infectious proteins. *Acta neuropathologica* **112**, 1-4.
- Weinrauch, Y., Drujan, D., Shapiro, S. D., Weiss, J. & Zychlinsky, A. (2002). Neutrophil elastase targets virulence factors of enterobacteria. *Nature* **417**, 91-94.
- Werbrouck, S., Van Huylenbroeck, J., Finnie, J., Jäger, A., Van Staden, J. & Debergh, P. (1998). Tissue culture and biotechnology. Ghent: <http://users.ugent.be/~pdebergh/ind/content.htm>.
- Wheeler, D. B., Carpenter, A. E. & Sabatini, D. M. (2005). Cell microarrays and RNA interference chip away at gene function. *Nature genetics* **37 Suppl**, S25-30.
- WHO (2002). Foodborne diseases, emerging Fact Sheet N°124.
- WHO (Fact Sheet N 139 Revised April 2005). Drug-resistant *Salmonella*.
- Wick, M. J. (2002). The role of dendritic cells during *Salmonella* infection. *Current opinion in immunology* **14**, 437-443.
- Wiles, M. V. & Keller, G. (1991). Multiple hematopoietic lineages develop from embryonic stem (ES) cells in culture. *Development (Cambridge, England)* **111**, 259-267.

- Wiles, S., Hanage, W. P., Frankel, G. & Robertson, B. (2006).** Modelling infectious disease - time to think outside the box? *Nat Rev Microbiol* **4**, 307-312.
- Williams, R. L., Hilton, D. J., Pease, S. & other authors (1988).** Myeloid leukaemia inhibitory factor maintains the developmental potential of embryonic stem cells. *Nature* **336**, 684-687.
- Wu, Z., Irizarry, A. R., Gentleman, R., Murillo, F. M. & Spencer, F. (2004).** A model based background adjustment for oligonucleotide expression arrays. *John Hopkins University, Dept of Biostatistics Working Papers Working Paper 1 The Berkeley Electronic Press.*
- Yam, K. K., Pouliot, P., N'Diaye M, M., Fournier, S., Olivier, M. & Cousineau, B. (2008).** Innate inflammatory responses to the Gram-positive bacterium *Lactococcus lactis*. *Vaccine* **26**, 2689-2699.
- Yamazaki, S., Muta, T. & Takeshige, K. (2001).** A novel IkappaB protein, IkappaB-zeta, induced by proinflammatory stimuli, negatively regulates nuclear factor-kappaB in the nuclei. *The Journal of biological chemistry* **276**, 27657-27662.
- Yang, Y. & Wilson, J. M. (1996).** CD40 ligand-dependent T cell activation: requirement of B7-CD28 signaling through CD40. *Science (New York, NY)* **273**, 1862-1864.
- Yasukawa, H., Sasaki, A. & Yoshimura, A. (2000).** Negative regulation of cytokine signaling pathways. *Annual review of immunology* **18**, 143-164.
- Yoshida, H., Hayashi, S., Kunisada, T., Ogawa, M., Nishikawa, S., Okamura, H., Sudo, T., Shultz, L. D. & Nishikawa, S. (1990).** The murine mutation osteopetrosis is in the coding region of the macrophage colony stimulating factor gene. *Nature* **345**, 442-444.
- Yrliid, U. & Wick, M. J. (2002).** Antigen Presentation Capacity and Cytokine Production by Murine Splenic Dendritic Cell Subsets upon *Salmonella* Encounter. *J Immunol* **169**, 108-116.
- Yu, J. (1998).** Inactivation of DsbA, but not DsbC and DsbD, affects the intracellular survival and virulence of *Shigella flexneri*. *Infection and immunity* **66**, 3909-3917.
- Yu, J., Edwards-Jones, B., Neyrolles, O. & Kroll, J. S. (2000).** Key role for DsbA in cell-to-cell spread of *Shigella flexneri*, permitting secretion of Ipa proteins into interepithelial protrusions. *Infection and immunity* **68**, 6449-6456.
- Yu, X. J., Liu, M. & Holden, D. W. (2004).** SsaM and SpiC interact and regulate secretion of *Salmonella* pathogenicity island 2 type III secretion system effectors and translocators. *Molecular microbiology* **54**, 604-619.
- Zhang, L. & Guarente, L. (1995).** Heme binds to a short sequence that serves a regulatory function in diverse proteins. *The EMBO journal* **14**, 313-320.

Zhang, Y., Higashide, W., Dai, S., Sherman, D. M. & Zhou, D. (2005). Recognition and ubiquitination of Salmonella type III effector SopA by a ubiquitin E3 ligase, HsrMA1. *The Journal of biological chemistry* **280**, 38682-38688.

Zhou, D., Hardt, W. D. & Galan, J. E. (1999). Salmonella typhimurium encodes a putative iron transport system within the centisome 63 pathogenicity island. *Infection and immunity* **67**, 1974-1981.

8 Appendix A

8.1 Affymetrix QC report for Bioconductor analysis

Affymetrix arrays Quality Control (QC) report reported by Dr. Lefebvre using Bioconductor.

Array Index	Array Name
1	r12_1_2CRNA.CEL
2	r13_1_0_AB2_2_1st_bio_rep.CEL
3	r13_1_3CRNA_AB2_2.CEL
4	r13_2_5CRNA.CEL
5	r13_2_0_AB2_2_BA271_2h_1st_bio_rep.CEL
6	r13_2_0_cRNA_AB2_2_0ai.CEL
7	r13_3_0_AB2_2_BA271_4h_1st_bio_rep.CEL
8	r13_3_8CRNA.CEL
9	r13_3_9CRNA.CEL
10	r13_4_0_AB2_2_2nd_bio_rep.CEL
11	r13_4_2CRNA.CEL
12	r13_4_3CRNA.CEL
13	r13_5_0_AB2_2_BA271_2h_2nd_bio_rep.CEL
14	r13_5_M_cRNA_AB2_2_0ai.CEL
15	r13_5_N_cRNA_AB2_2_0ai.CEL
16	r13_5_0_AB2_2_BA271_4h_2nd_bio_rep.CEL
17	r13_5_P_cRNA_AB2_2_0ai.CEL
18	r13_5_R_cRNA_AB2_2_0ai.CEL
19	r13_7_0_AB2_2_3rd_bio_rep.CEL
20	r13_7_3CRNA.CEL
21	r13_7_AcRNA.CEL
22	r13_8_0_AB2_2_BA271_2h_3rd_bio_rep.CEL
23	r13_8_3CRNA.CEL
24	r13_8_CcRNA.CEL
25	r13_9_0_AB2_2_BA271_4h_3rd_bio_rep.CEL
26	r13_9_3CRNA.CEL
27	r13_9_EcRNA.CEL

Mon Dec 18 16:50:05 2006

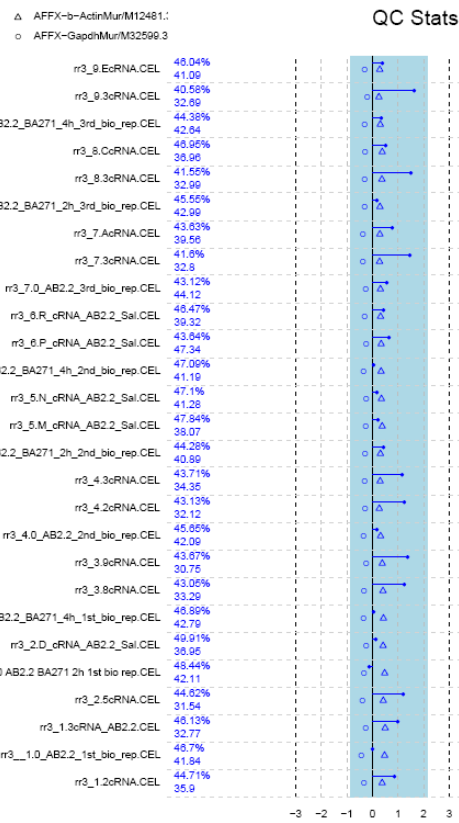
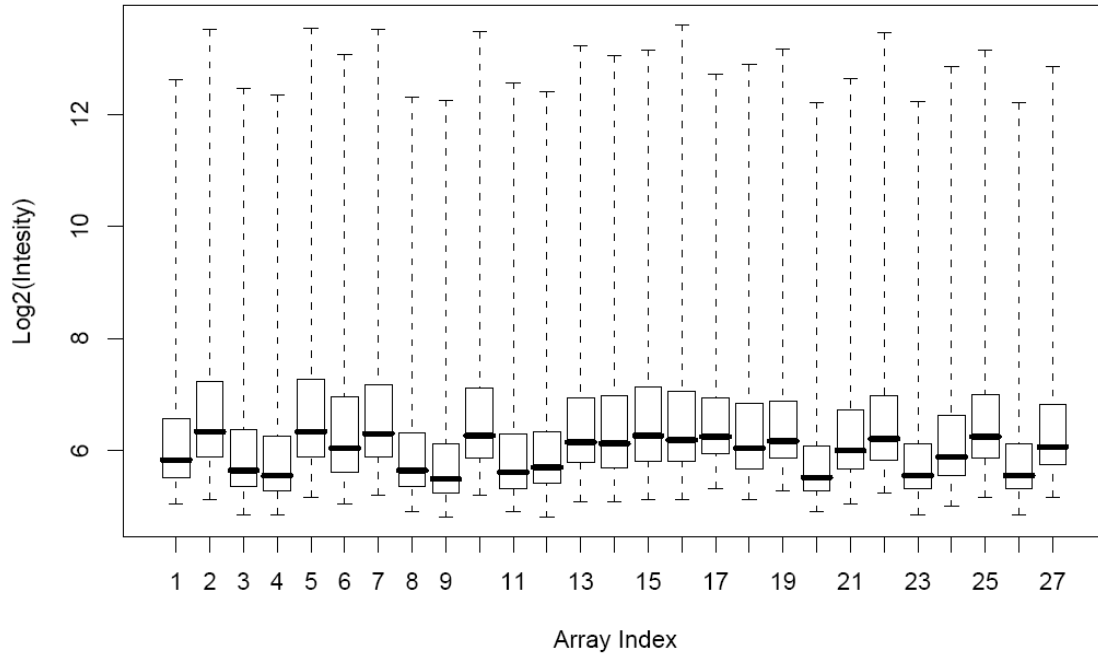


Figure 8.1 Affymetrix QC report

8.2 Gene Ontology analysis of the top GeneSpring annotated genes

The p-value is determined by:

- Number of entities in the entity list with the particular GO term and its children;
- The number of entities with the GO term in the experiment;
- The total number of entities in the entity list;
- The total number of entities in the experiment.

GeneSpring analysis of genes differentially expressed at 4 hours infection of murine AB2.2 ES cells are reported here divided by cellular component

8.2.1 GO description for cellular component of the top genes deriving from GeneSpring analysis

Table 8.1 GeneSpring data analyzed for GO term Cellular component

Filter on 1.5 fold change 4-0h (89 genes, 58 annotated) selected with GO:5575:cellular_component with p value< 0.05					
Category	Genes in Category	% of Genes in Category	Genes in List in Category	% of Genes in List in Category	p-Value
GO:5623: cell	14323	62.74	43	74.14	0.0457
GO:42598: vesicular fraction	136	0.596	3	5.172	0.00502
GO:5792: microsome	136	0.596	3	5.172	0.00502
GO:5622: intracellular	9415	41.24	37	63.79	0.00044
GO:5634: nucleus	4517	19.79	24	41.38	0.00013
GO:5783: endoplasmic reticulum	601	2.633	7	12.07	0.0008
GO:5789: endoplasmic reticulum membrane	71	0.311	2	3.448	0.0141
GO:5798: Golgi vesicle	3	0.0131	1	1.724	0.0076
GO:43229: intracellular organelle	8064	35.33	35	60.34	8.80E-05
GO:43231: intracellular membrane-bound organelle	7056	30.91	34	58.62	1.15E-05
GO:42175: nuclear envelope-endoplasmic reticulum network	74	0.324	2	3.448	0.0152
GO:43226: organelle	8064	35.33	35	60.34	8.80E-05
GO:43227: membrane-bound organelle	7056	30.91	34	58.62	1.15E-05

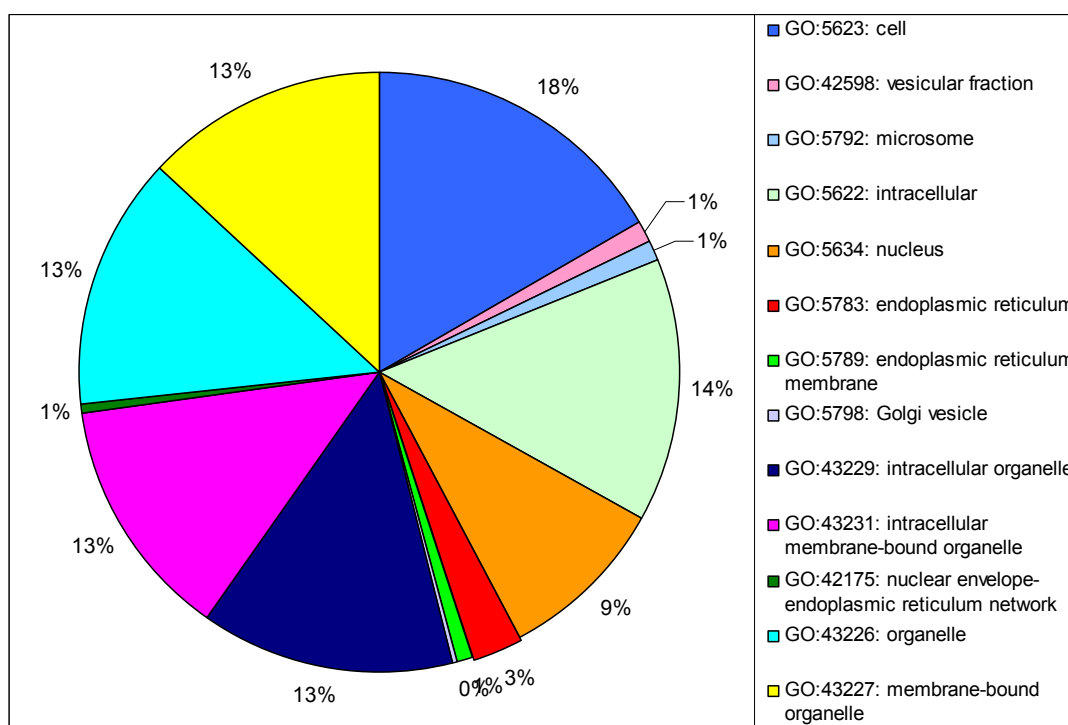


Figure 8.2 Pie chart of the GeneSpring data analyzed for GO term Cellular components

8.2.2 GO description for biological process of the top genes deriving from GeneSpring analysis

Table 8.2 GeneSpring pear-comparison data analyzed for GO term Biological Process

Filter on 1.5 Fold Change 4-0h (89genes, 59 annotated) selected with GO:8150: Biological_process					
Category	Genes in Category	% of Genes in Category	Genes in List in Category	% of Genes in List in Category	p-Value
GO:35112: genitalia morphogenesis	14	0.0613	1	1.724	0.035
GO:30539: male genitalia morphogenesis	14	0.0613	1	1.724	0.035
GO:19222: regulation of metabolism	1639	7.18	11	18.97	0.0025
GO:9892: negative regulation of metabolism	209	0.916	4	6.897	0.00197
GO:31324: negative regulation of cellular metabolism	172	0.753	4	6.897	0.000962
GO:45934: negative regulation of nucleobase, nucleoside, nucleotide and nucleic acid metabolism	161	0.705	4	6.897	0.000752
GO:16481: negative regulation of transcription	157	0.688	4	6.897	0.000684
GO:45892: negative regulation of transcription, DNA-dependent	97	0.425	2	3.448	0.0253
GO:122: negative regulation of transcription from RNA polymerase II promoter	83	0.364	2	3.448	0.0189
GO:31323: regulation of cellular metabolism	1582	6.93	11	18.97	0.00189
GO:19219: regulation of nucleobase, nucleoside, nucleotide and nucleic acid metabolism	1469	6.435	10	17.24	0.00362
GO:45449: regulation of transcription	1464	6.413	10	17.24	0.00353
GO:6355: regulation of transcription, DNA-dependent	1350	5.914	9	15.52	0.00667
GO:398: nuclear mRNA splicing, via spliceosome	98	0.429	2	3.448	0.0258

GO:8380: RNA splicing	110	0.482	2	3.448	0.0319
GO:375: RNA splicing, via transesterification reactions	98	0.429	2	3.448	0.0258
GO:377: RNA splicing, via transesterification reactions with bulged adenosine as nucleophile	98	0.429	2	3.448	0.0258
GO:6091: generation of precursor metabolites and energy	688	3.014	5	8.621	0.0303
GO:6118: electron transport	457	2.002	5	8.621	0.00603
GO:6350: transcription	1643	7.197	10	17.24	0.0079
GO:6351: transcription, DNA-dependent	1431	6.269	9	15.52	0.00962
GO:8632: apoptotic program	58	0.254	3	5.172	0.000435
GO:6919: caspase activation	33	0.145	3	5.172	8.04E-05
GO:43026: regulation of caspase activation	13	0.0569	3	5.172	4.37E-06
GO:43154: negative regulation of caspase activation	11	0.0482	3	5.172	2.53E-06
GO:1719: inhibition of caspase activation	11	0.0482	3	5.172	2.53E-06
GO:42981: regulation of apoptosis	229	1.003	3	5.172	0.0205
GO:43066: negative regulation of apoptosis	68	0.298	3	5.172	0.000694
GO:6916: anti-apoptosis	57	0.25	3	5.172	0.000413
GO:43067: regulation of programmed cell death	231	1.012	3	5.172	0.021
GO:43069: negative regulation of programmed cell death	68	0.298	3	5.172	0.000694
GO:50791: regulation of physiological process	2582	11.31	17	29.31	0.000159
GO:43118: negative regulation of physiological process	479	2.098	7	12.07	0.000204
GO:51243: negative regulation of cellular physiological process	445	1.949	7	12.07	0.00013
GO:51244: regulation of cellular physiological process	2460	10.78	17	29.31	8.75E-05
GO:41: transition metal ion transport	61	0.267	2	3.448	0.0105
GO:6829: zinc ion transport	12	0.0526	2	3.448	0.000412
GO:8333: endosome to lysosome transport	4	0.0175	1	1.724	0.0101
GO:6892: post-Golgi transport	11	0.0482	1	1.724	0.0276
GO:6893: Golgi to plasma membrane transport	4	0.0175	1	1.724	0.0101
GO:7034: vacuolar transport	14	0.0613	1	1.724	0.035
GO:7041: lysosomal transport	4	0.0175	1	1.724	0.0101
GO:7033: vacuole organization and biogenesis	19	0.0832	1	1.724	0.0472
GO:7040: lysosome organization and biogenesis	9	0.0394	1	1.724	0.0226
GO:50794: regulation of cellular process	2550	11.17	17	29.31	0.000137
GO:48523: negative regulation of cellular process	485	2.125	7	12.07	0.000221
GO:50789: regulation of biological process	2849	12.48	17	29.31	0.000517
GO:43085: positive regulation of enzyme activity	85	0.372	3	5.172	0.00133
GO:51345: positive regulation of hydrolase activity	33	0.145	3	5.172	8.04E-05
GO:43280: positive regulation of caspase activity	33	0.145	3	5.172	8.04E-05
GO:48519: negative regulation of biological process	559	2.449	7	12.07	0.000519
GO:50790: regulation of enzyme activity	143	0.626	3	5.172	0.00577
GO:51336: regulation of hydrolase activity	38	0.166	3	5.172	0.000123
GO:43281: regulation of caspase activity	33	0.145	3	5.172	8.04E-05
GO:50896: response to stimulus	1556	6.816	11	18.97	0.00166
GO:6950: response to stress	823	3.605	11	18.97	6.05E-06
GO:6986: response to unfolded protein	16	0.0701	4	6.897	6.67E-08
GO:9408: response to heat	50	0.219	4	6.897	7.92E-06
GO:9628: response to abiotic stimulus	363	1.59	9	15.52	3.16E-07
GO:9266: response to temperature stimulus	53	0.232	4	6.897	1.00E-05
GO:42221: response to chemical stimulus	251	1.1	5	8.621	0.00044

8.3 Genes analyzed by RT-PCR deriving from ASCA analysis

Table 8.3 Table Gene resulting from ASCA analysis which expression was confirmed by RT-PCR

cluster	Gene Symbol	Gene Title	Pathway	go biological process term
3	Bfar	bifunctional apoptosis regulator	---	apoptosis /// anti-apoptosis
3	Rhod	ras homolog gene family, member D	---	small GTPase mediated signal transduction
8; 8	Apaf1	apoptotic peptidase activating factor 1	Apoptosis	neural tube closure /// proteolysis /// apoptosis /// caspase activation /// defense response /// multicellular organismal development
9; 9	Socs3	suppressor of cytokine signaling 3		regulation of cell growth /// regulation of protein amino acid phosphorylation /// negative regulation of signal transduction /// negative regulation of insulin receptor signaling pathway
7; 5; 5	Lamp2	lysosomal-associated membrane protein 2	-	tRNA aminoacylation for protein translation
7; 5	Fst	follicle-stimulating hormone receptor 1	TGF_Beta_Signaling_Pathway	

9 Appendix B

9.1 Flow cytometric characterization of murine ES cells AB2.2, esDCs and BMDCs testing the expression of myeloid surface markers

In order to highlight the difference between the original murine ES cell line AB2.2 and the derived esDC we decided to test myeloid surface markers. We were able to highlight the expression of these markers when the cells were dislocated using a non enzymatic buffer. May be these buffer is been to mild and dislocate only those cells at the edge of the cells clusters which usually are the most differentiated one or our ES cell line has hematopoietic progenitor characteristic.

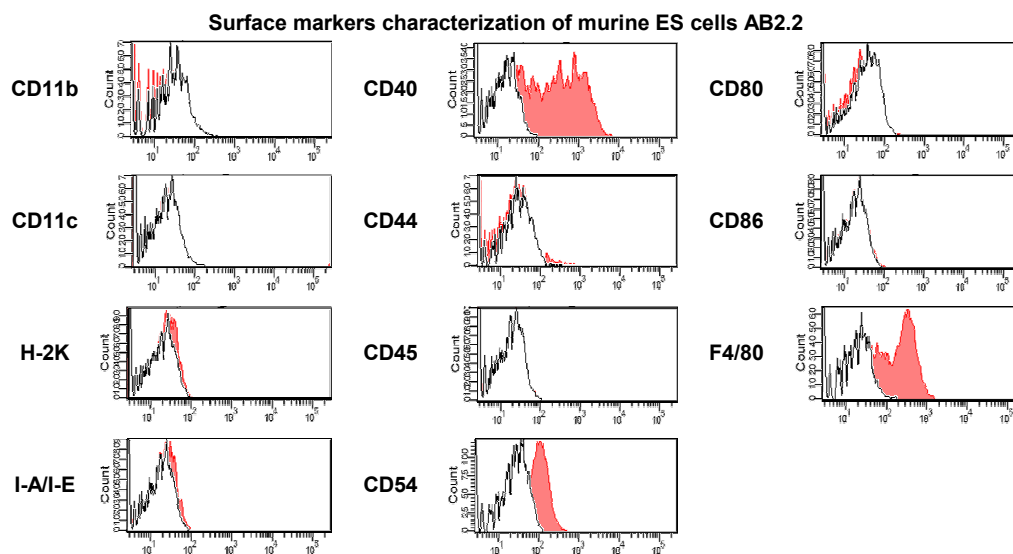


Figure 9.1 Flow cytometry characterization of murine AB2.2 ES cells

Murine ES cells were also stained for surface markers used to define esDC . Here are reported histograms representing a few target surface markers, red peaks, which expression was compared to their relative isotype control antibody, white peaks.

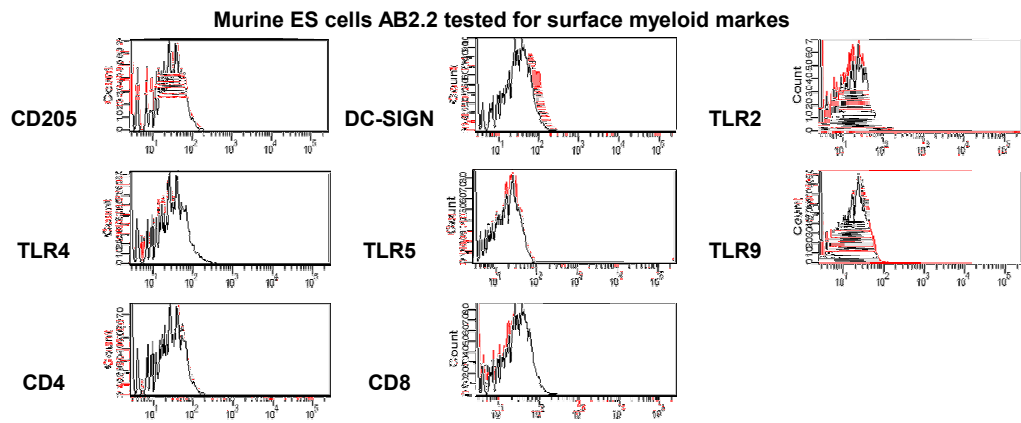


Figure 9.2 Murine ES cells characterization for myeloid markers

Figure 9.3 Flow cytometric characterization of immature and mature esDCs

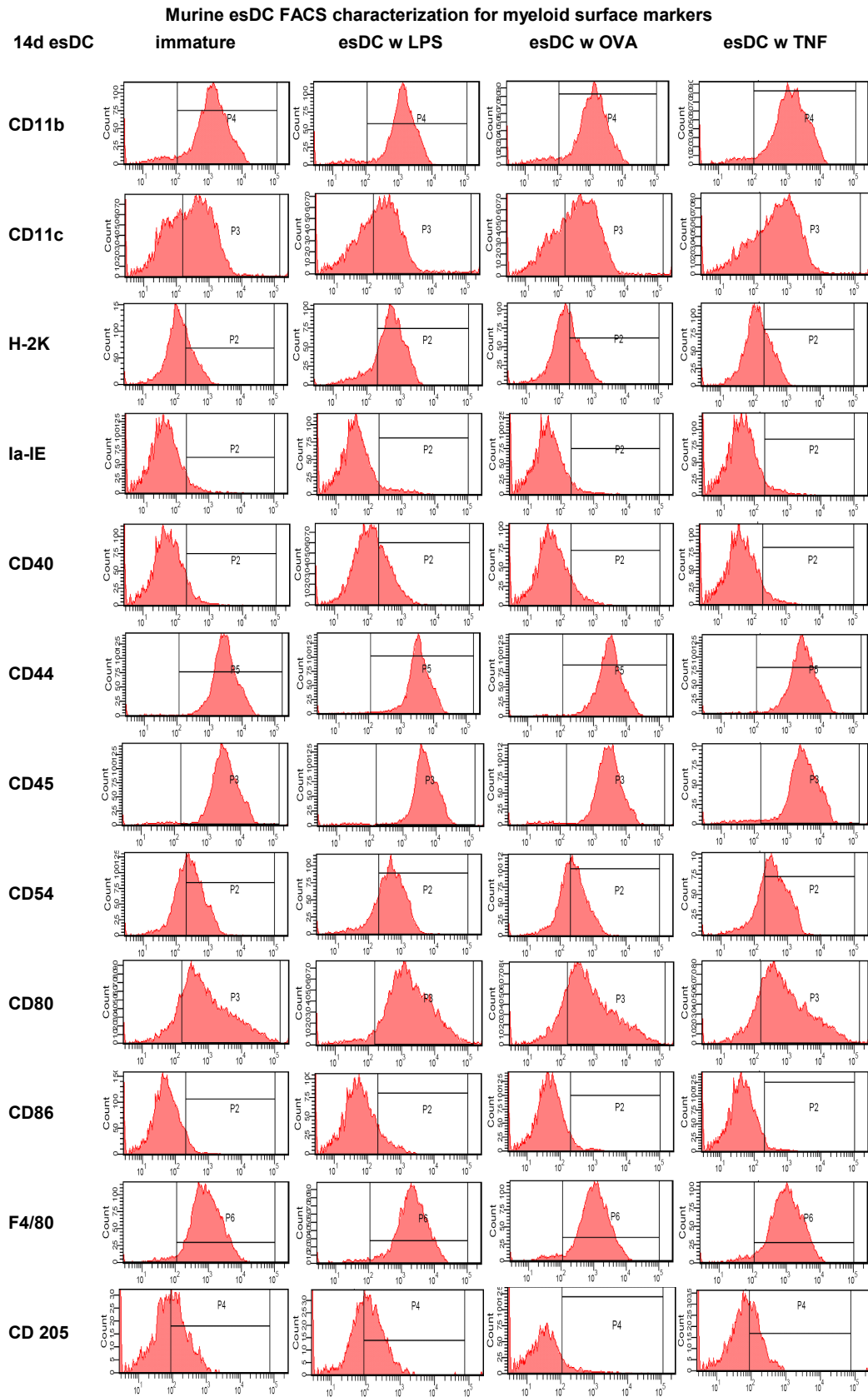


Figure 9.4 Flow cytometric characterization of immature and mature esDCs, number 2

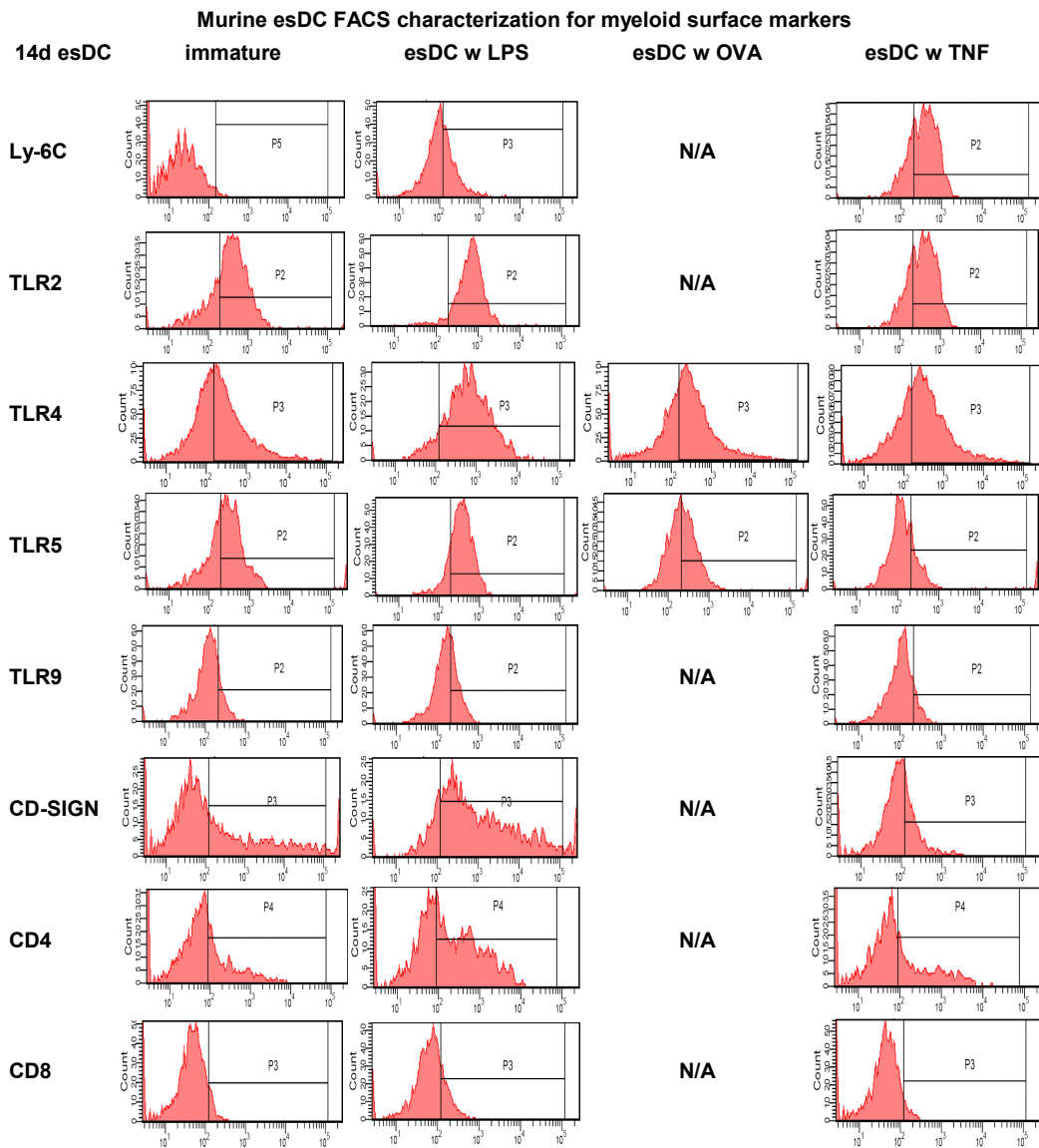


Figure 9.5 Flow cytometric characterization of BMDCs immature and mature

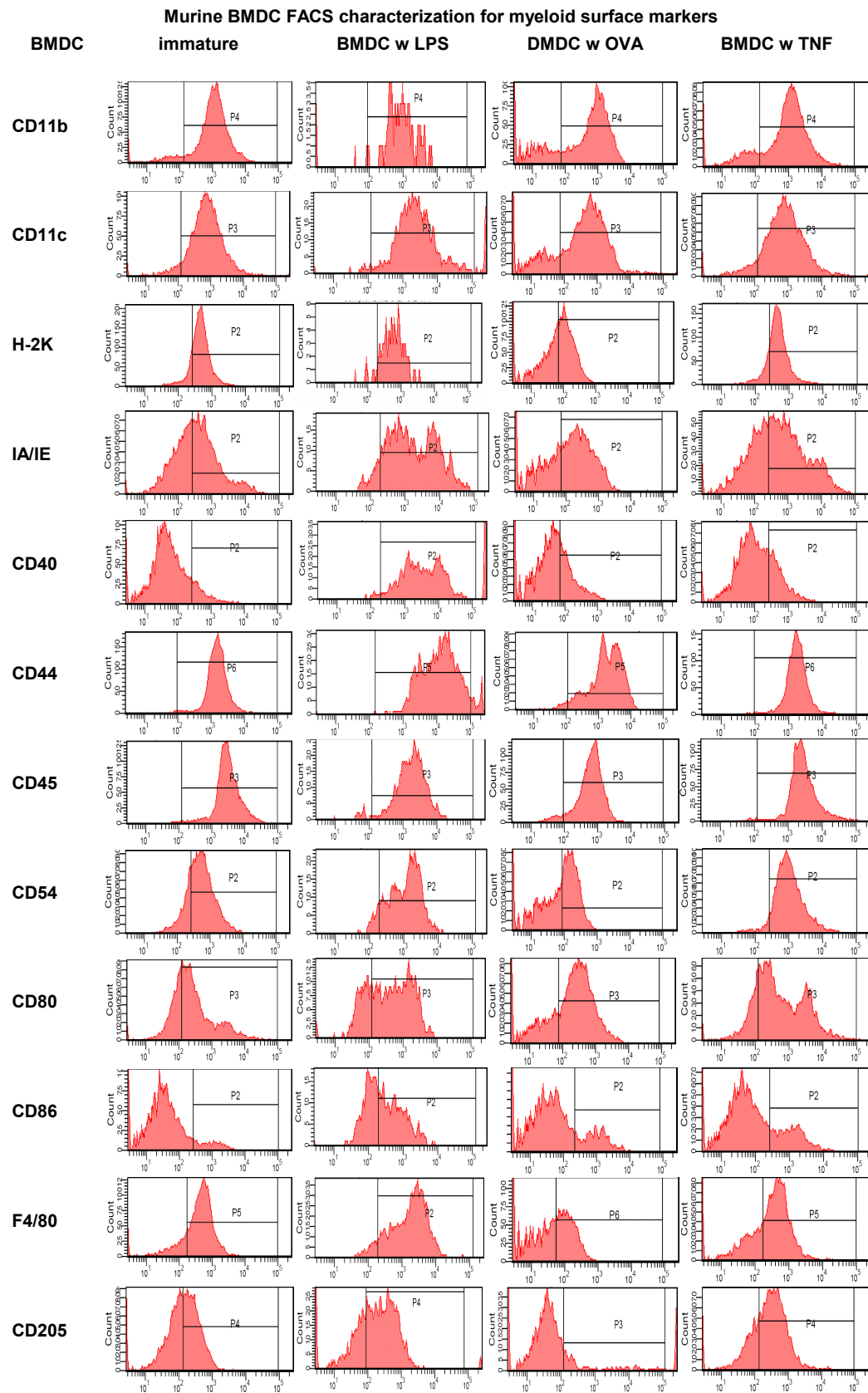


Figure 9.6 Flow cytometric characterization of immature and mature BMDCs, number 2